PH4442 Lecture Notes

Advanced Particle Physics

Glen D. Cowan

Physics Department
Royal Holloway, University of London

Last revised: April 1, 2026

Preface

These notes accompany the course PH4442 Advanced Particle Physics at Royal Holloway, University of London. The notes assume a familiarity with Particle Physics at a level of the third-year RHUL course PH3520 [1]. This includes knowledge of the particles of the Standard Model such as quarks, leptons and gauge bosons; their properties such charge and the interactions in which they take part; a qualitative understanding of Feynman diagrams; observable properties such as scattering cross sections and decay rates and some exposure to the important experimental tests.

The present course focuses on the theoretical tools needed to calculate cross sections and decay rates for high-energy processes in the Standard Model of Particle Physics. In the first instance this is done using the Feynman-Stückelberg interpretation of relativistic quantum mechanics. This leads directly to the rules for Feynman diagrams while avoiding the complicated formalism of Quantum Field Theory (QFT). Some ideas of field theory are introduced towards the end in connection with the electroweak Standard Model and the Higgs mechanism.

The notes focus on first-order approximations based on tree-level Feynman diagrams. Higher-order corrections and renormalisation are briefly mentioned, e.g., in the context of running couplings, but the intricate mathematics required for a rigorous treatment of these topics is beyond the scope of the course.

Roughly the first half of the notes are devoted to the developing the general framework of the Standard Model in the context of Quantum Electrodynamics (QED), i.e., the interactions of charged fermions and photons. The second half extends this to the weak interactions, then to the electroweak Standard Model, the Higgs mechanism and the strong interaction with Quantum Chromodynamics (QCD). Finally there is an introduction to partons and physics at the Large Hadron Collider.

These notes draw on many sources, in particular from the texts by Schmüser [2], Thomson [3] and Aitchison and Hey [4] and from the notes and valuable feedback of Asher Kaboth, Pedro Teixeira-Dias and Véronique Boisvert. Please send any corrections, suggestions and comments to `g.cowan@rhul.ac.uk`.

GDC
September, 2025

Contents

Chapter 1

Introduction and basic concepts

This course introduces the tools needed to make quantitative predictions for particle physics reactions such as cross sections and decay rates. It is intended to follow on from a course that provides a more qualitative overview of Particle Physics as in Ref. [1]. To make the present notes more self contained, in this chapter the most important concepts are reviewed.

1.1 Units

In Particle Physics it is convenient to use "natural units", which amounts to setting $\hbar = c = 1$. Thus when we write m for mass we really mean the rest mass energy mc^2. The physical energy, momentum and mass are all measured in units of energy, e.g., GeV. Time and space both have units of inverse energy, e.g., GeV^{-1}.

To convert between natural and the usual physical units it is sufficient to know the speed of light $c = 3.00 \times 10^8\,\text{m/s}$ and $\hbar c = 0.197\,\text{GeV fm}$. For example, a cross section in natural units has units of GeV^{-2}. To convert this to a usual unit of area such as fm^2, one multiplies by $(\hbar c)^2$.

1.2 The Standard Model of Particle Physics: cast of characters

In the Standard Model (SM), the particles of matter are spin-1/2 fermions that come in two types: leptons and quarks. These are listed in Tables 1.1 and 1.2 with their electric charges in units of the proton's charge e.[1]

In addition to the leptons and quarks there exist antiparticles with the same mass but opposite electrical charge. For the charged leptons these are denoted with a positive charge: e^+, μ^+, τ^+; for the others a bar is used, e.g., $\overline{\nu}_e$, $\overline{u}$.

In the Standard Model of Particle Physics, the fermions (leptons and quarks) in Tables 1.1 and 1.2 interact by exchanging the spin-1 gauge bosons shown in Table 1.3. The table also includes the spin-0 Higgs boson, which is related to the masses of particles.

[1] The symbol e for charge will always be taken to be positive, so that the electron's charge is $-e$.

Table 1.1: Leptons and their electrical charges (in units of e).

Lepton			Charge
ν_e	ν_μ	ν_τ	0
e^-	μ^-	τ^-	-1

Table 1.2: Quarks and their electrical charges (in units of e).

Quark			Charge
u	c	t	$2/3$
d	s	b	$-1/3$

Table 1.3: Bosons of the Standard Model, their spins, electrical charges, and the interaction that they mediate.

Boson	Spin	Charge	Interaction
Photon (γ)	1	0	Electromagnetic
$W^\pm$	1	± 1	Weak
Z	1	0	Weak
Gluon (g)	1	0	Strong
Higgs (H)	0	0	(Weak)

Although all particles should be subject to gravity, its effect is extremly small on the scale of the interactions that we can observe, so for now it is neglected. A brief sketch of the interactions of the Standard Model can be found in Sections 2.4-2.7 of the PH3520 lecture notes [1].

1.3 Theoretical framework of the Standard Model

The particles of the SM obey the rules of quantum mechanics and special relativity, and in high-energy reactions particles are created and destroyed. This can be described using the language of Quantum Field Theory (QFT), where particles emerge as quantised excitations of fields, analogous to the vibrations of a crystal lattice. In additional to obeying the mathematical symmetries required by special relativity, the fields of the Standard Model exhibit what is called *gauge symmetry*, which dictates what gauge bosons must be present and how they interact.

The mathematics needed to formulate the SM as a field theory is difficult and not strictly necessary if the goal is, as here, to calculate observables such as cross sections and decay rates. In this course we will develop the relativistic equations of quantum mechanics (the Klein-Gordon

and Dirac equations) and we will see that this results in negative-energy solutions. The Feynman-Stückelberg interpretation of the solutions then leads to a theory in which particles, including antiparticles, can be created and destroyed without the full machinery of QFT.

The SM particles are measured to have nonzero masses. Including masses into the SM in the simplest way would, however, break the gauge symmetry. This is circumvented by including an additional field corresponding to what we now call the Higgs boson. To describe this mechanism we will in Chapter 10 introduce the basics of Lagrangian-based Quantum Field Theory.

1.3.1 Feynman diagrams

A reaction characterised by given incoming and outgoing particles can be represented as a Feynman diagram. The particles of different types are usually drawn with different line styles as shown in Fig. 1.1.

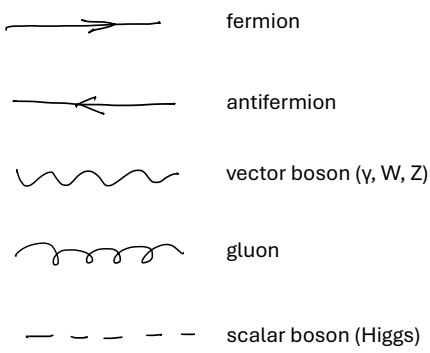

Figure 1.1: Lines representing different types of particles in Feynman diagrams.

In a theory such as the Standard Model, the particles are allowed to be emitted or absorbed as shown by a given set of vertices. For example, in the reaction $e^+e^- \to \mu^+\mu^-$ shown in Fig. 1.2, the electron and positron annihilate to form a photon, which dissociates into a $\mu^+\mu^-$ pair. The vertical direction represents particle separation and the horizontal direction gives the flow of time from left to right.

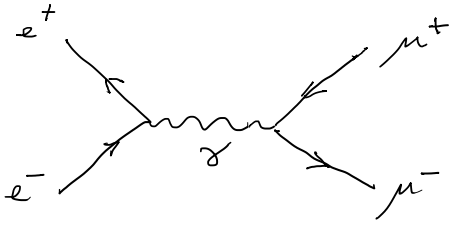

Figure 1.2: A Feynman diagram representing the reaction $e^+e^- \to \mu^+\mu^-$.

There is a quantum mechanical amplitude $\mathcal{M}$ associated with each diagram. If a reaction can proceed from given initial to final states through different intermediate states, then there is an amplitude for each and the total amplitude is given by their sum. One of the primary goals of this course is to develop and apply the rules for obtaining the amplitudes for different Feynman diagrams.

As an example of one of these rules, each vertex in the diagram corresponds to a numerical parameter called the coupling strength, which in the case of the diagram above is the electric

charge e. The amplitude for a diagram is proportional to the product of all the coupling strengths that appear. The diagram above, for example, is proportional to e^2.

The diagrams below show the same reaction, $e^+e^- \to \mu^+\mu^-$, but with different intermediate states.

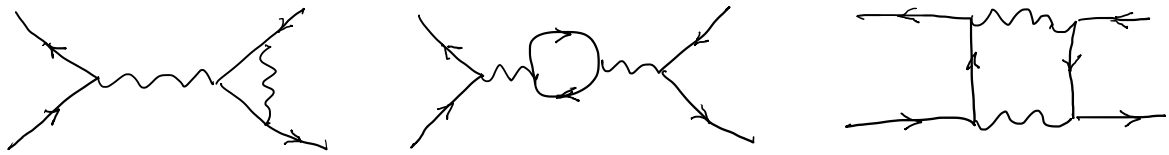

Figure 1.3: Higher-order Feynman diagrams for the reaction $e^+e^- \to \mu^+\mu^-$ showing several possible intermediate states.

In all cases these have four vertices that connect a photon to a charged fermion, and thus all of the diagrams below have amplitudes proportional to e^4. The total amplitude is the sum of the amplitudes for all possible intermediate states,

$$\mathcal{M} = \sum_i \mathcal{M}_i \ , \tag{1.1}$$

and following the usual rules of quantum mechanics, the probability for the reaction to occur is related to the absolute square of the amplitude:

$$P(\text{reaction occurs}) \propto |\mathcal{M}|^2 \ . \tag{1.2}$$

In practice this probability is expressed for as a cross section σ for a scattering reaction or as a decay rate Γ for the decay of an unstable particle. This will be presented in detail in Ch. 7.

When using Particle Physics units ($\hbar = c = 1$), the charge of the proton is related to the fine structure constant as $\alpha = e^2/4\pi \approx 1/137$ and so the charge $e \approx 0.303$ is dimensionless. By summing diagrams as described above, the total amplitude becomes a power series in e, or equivalently the observables such as cross sections are a series in α. As α is much less than unity, the series for electromagnetic processes are found to converge very quickly. In this course we will focus on amplitudes computed at "leading order" in perturbation theory. The corresponding diagrams have the minimum number of vertices and thus the smallest number of powers of e.

Chapter 2

Relativity

We want to develop a quantum mechanical theory that can describe particles moving with speeds comparable to the speed of light. To that end we present in this section the necessary ingredients from Einstein's special theory of relativity. We will spend some time developing the relativistic notation that allows one to see easily how certain mathematical objects transform if viewed in a different reference frame.

We will write a point in time t and space $\boldsymbol{r} = (x, y, z)$ as a four-dimensional space-time vector or *four-vector* $x = (t, x, y, z) = (x^0, x^1, x^2, x^3)$. That is, the components x^μ use upper Lorentz indices $\mu = 0, 1, 2, 3$ for the usual time and space coordinates and are said to form a *contravariant* four-vector. Although we will often refer to objects like x^μ as four-vectors, strictly speaking the four vector is x, and x^μ is its μ component.

For every contravariant (upper-index) four-vector, we define the corresponding *covariant* (lower-index) vector through

$$x_\mu = g_{\mu\nu} x^\nu \ . \tag{2.1}$$

Here it is understood that one sums over repeated upper and lower indices, i.e., $g_{\mu\nu}x^\nu = \sum_{\nu=0}^{3} g_{\mu\nu}x^\nu$, and the Minkowski metric tensor g is defined as

$$g = \begin{pmatrix} 1 & 0 & 0 & 0 \\ 0 & -1 & 0 & 0 \\ 0 & 0 & -1 & 0 \\ 0 & 0 & 0 & -1 \end{pmatrix} \ . \tag{2.2}$$

The components are given as above when written either with upper or lower indices: $g_{\mu\nu} = g^{\mu\nu}$. The contravariant and covariant indices are useful because they allow one to see easily how four-vectors and combinations of them change under Lorentz transformations.

In going back and forth between matrix notation and components, it can help to say that $g_{\mu\nu}$ are the components of g and $g^{\mu\nu}$ are the components of g^{-1}, even though the two matrices are in fact the same. Some references use the notation η for the Minkowski metric corresponding to flat space-time and reserve g for the more general metric of General Relativity. Here effects of GR and curved space-time do not enter our discussion so there we will always take $g = \mathrm{diag}(1, -1, -1, -1)$ as above.

One can always convert contravariant into a covariant four-vector or vice-versa by multiplying by the metric tensor $g_{\mu\nu}$ or $g^{\mu\nu}$ as appropriate and summing over the repeated index, e.g., $x^\mu = g^{\mu\nu}x_\nu$. Note that the contravariant form of x corresponds to the usual space-time components, i.e., $x = (x^0, x^1, x^2, x^3) = (t, x, y, z)$, whereas the lower-index spatial components get a minus sign: $x_i = -x^i$ for $i = 1, 2, 3$.

2.1 Lorentz transformations

A Lorentz transformation of a four-vector x^μ is a linear, homogeneous transformation that leaves the four-vector product $x_\mu x^\mu = (x^0)^2 - (x^1)^2 - (x^2)^2 - (x^3)^2 = t^2 - x^2 - y^2 - z^2$ unchanged. That is, starting from a four-vector x one defines a Lorentz-transformed four-vector $x' = \Lambda x$, where Λ is a constant (independent of space or time) 4×4 matrix. Written out in component form this is

$$x'^\mu = \Lambda^\mu{}_\nu x^\nu \ . \tag{2.3}$$

We define the indices of Λ such that the row (left) index is up and the column (right) index down, i.e., the elements of Λ are $\Lambda^\mu{}_\nu$. Starting from there, the indices of $\Lambda^\mu{}_\nu$ can be raised and lowered by contracting with $g_{\mu\nu}$ or $g^{\mu\nu}$ as appropriate. The transpose matrix is obtained by swapping row and column, but not changing whether an index is up or down, so that $(\Lambda^T)_\nu{}^\mu = \Lambda^\mu{}_\nu$.

For Eq. (2.3) to be a Lorentz transformation we require the four-vector product to be invariant, i.e., $x'_\mu x'^\mu = x_\mu x^\mu$. The primed quantity $x'_\mu x'^\mu$ is given in terms of the unprimed coordinates as

$$\begin{aligned} x'^2 &= x'_\mu x'^\mu = g_{\mu\nu} x'^\mu x'^\nu = g_{\mu\nu}\, \Lambda^\mu{}_\rho x^\rho\, \Lambda^\nu{}_\sigma x^\sigma \\ &= g_{\mu\nu}\, \Lambda^\mu{}_\rho\, \Lambda^\nu{}_\sigma\, x^\rho x^\sigma \ , \end{aligned} \tag{2.4}$$

and we want this to be equal to

$$x^2 = g_{\rho\sigma} x^\rho x^\sigma \ . \tag{2.5}$$

Comparing Eqs. (2.4) and (2.5), we see that for the transformation to leave $x'^2 = x^2$ for arbitrary x, one needs

$$g_{\mu\nu}\, \Lambda^\mu{}_\rho\, \Lambda^\nu{}_\sigma = g_{\rho\sigma} \ . \tag{2.6}$$

Equation (2.6) gives the general requirement on the matrix Λ for $x' = \Lambda x$ to be a Lorentz transformation.

To express Eq. (2.6) in matrix form we need to pay attention to whether summed indices represent rows or columns, i.e., whether the index is on the left or the right. Using $\Lambda^\mu{}_\rho = (\Lambda^T)_\rho{}^\mu$, we can rewrite it as

$$(\Lambda^T)_\rho{}^\mu g_{\mu\nu}\ \Lambda^\nu{}_\sigma = g_{\rho\sigma} \ . \tag{2.7}$$

Here the indices follow the usual conventions of matrix multiplication, e.g., the sum over μ combines elements of each column of Λ^T with corresponding rows of g. The defining property of a Lorentz transformation (2.6) can therefore be written as

$$\Lambda^T g \Lambda = g \ . \tag{2.8}$$

By multiplying (2.8) on the left by g^{-1} we find $g^{-1}\Lambda^T g\Lambda = I$, where I is the 4×4 identity matrix, and therefore the inverse of Λ is

$$\Lambda^{-1} = g^{-1}\Lambda^T g \ , \tag{2.9}$$

or written out in component form,

$$(\Lambda^{-1})^\mu{}_\nu = g^{\mu\rho}(\Lambda^T)_\rho{}^\sigma g_{\sigma\nu} = (\Lambda^T)^\mu{}_\nu \equiv \Lambda_\nu{}^\mu \ . \tag{2.10}$$

The first and third terms in Eq. (2.10) may seem to imply that $\Lambda^{-1} = \Lambda^T$ but this is not true in general (it is true for rotations but not for boosts). This is because the standard index position for Λ^T is with the row index lower and the column index upper, as in the second term, $(\Lambda^T)_\rho{}^\sigma$. As indicated by the final equality, $\Lambda_\nu{}^\mu$ is thus a synonym for $(\Lambda^{-1})^\mu{}_\nu$.

2.2 The Lorentz Group

We can show that two successive Lorentz transformations together are equivalent to a single Lorentz transformation. Suppose we apply Λ_1 to x and then apply Λ_2, i.e.,

$$x' = \Lambda_2(\Lambda_1 x) = (\Lambda_2\Lambda_1)x \ , \tag{2.11}$$

where the second equality follows from the associative property of matrix multiplication. That is, the transformation is equivalent to using $\Lambda = \Lambda_2\Lambda_1$ as a single transformation. To show that this is still a Lorentz transformation, we compute the left-hand side of Eq. (2.8), which gives

$$(\Lambda_2\Lambda_1)^T g(\Lambda_2\Lambda_1) = \Lambda_1^T\Lambda_2^T g\Lambda_2\Lambda_1 = \Lambda_1^T g\Lambda_1 = g \ , \tag{2.12}$$

where we used $\Lambda_1^T g\Lambda_1 = g$ and $\Lambda_2^T g\Lambda_2 = g$ since these are both individually Lorentz transformations.

The set of all transformations that satisfy Eq. (2.6) together with matrix multiplication define the Lorentz group.[1] Depending on the elements of Λ, a Lorentz transformation can correspond to boosts, rotations, parity or time reversal. Notice that because we have insisted that the transformation be homogeneous (it leaves the origin unchanged), Lorentz transformations do not include translations. The more general set of transformations that also includes translations is called the Poincaré group.

[1] Some basic concepts of group theory are given in Appendix A.

Although any number of successive Lorentz transformations results in a Lorentz transformation, the order in which they are applied matters in general. For example, a rotation of 90° about the x axis followed by one of 90° about the y axis leaves a system in a different configuration than if one carries out the rotations in the opposite order. And although Galilean boosts are independent of the order in which they are applied, this is no longer the case in special relativity. The Lorentz group is said to be non-Abelian.

The set of all possible Lorentz transformations can be separated into two distinct subsets, depending on the determinant of the transformation matrix Λ. We can take the determinant of both sides of Eq. (2.8),

$$\det(\Lambda^T g \Lambda) = \det(g) \ , \tag{2.13}$$

and use the fact that the determinant of a product of square matrices is the product of the determinants, so $\det(\Lambda^T g \Lambda) = \det(\Lambda^T)\det(g)\det(\Lambda)$. Furthermore $\det(\Lambda^T) = \det(\Lambda)$ and $\det(g) = -1$, so we find $[\det(\Lambda)]^2 = 1$ or

$$\det(\Lambda) = \pm 1 \ . \tag{2.14}$$

A Lorentz transformation with $\det(\Lambda) = 1$ is said to be proper; those with $\det(\Lambda) = -1$ are improper. When we derive explicit forms of the transformation matrices we will find that boosts and rotations correspond to $\det(\Lambda) = 1$ whereas parity and time reversal have $\det(\Lambda) = -1$. If a combination of Lorentz transformations is given by $\Lambda = \Lambda_1 \Lambda_2 \cdots \Lambda_n$, then because $\det(\Lambda) = \prod_{i=1}^n \det(\Lambda_i)$ we see that if all Λ_i are proper, then their combination is also proper. Thus an arbitrary combination of boosts and rotations results in an overall proper Lorentz transformation.

2.3 Examples of Lorentz transformations

We present here without proof some examples of Lorentz transformations. Suppose the transformed (primed) frame is boosted relative to the original one with a speed v along the z axis, so that $x' = \Lambda_B x$. The Lorentz transformation matrix is

$$\Lambda_B = \begin{pmatrix} \gamma & 0 & 0 & -\beta\gamma \\ 0 & 1 & 0 & 0 \\ 0 & 0 & 1 & 0 \\ -\beta\gamma & 0 & 0 & \gamma \end{pmatrix} \ , \tag{2.15}$$

where $\beta = v$ ($c = 1$) and $\gamma = 1/\sqrt{1-\beta^2}$. It is often convenient to express a boost by defining the rapidity ω as

$$\cosh\omega = \gamma \ , \tag{2.16}$$

or equivalently $\sinh\omega = \beta\gamma$, so that the Lorentz transformation (2.15) can be written

$$\Lambda_B = \begin{pmatrix} \cosh\omega & 0 & 0 & -\sinh\omega \\ 0 & 1 & 0 & 0 \\ 0 & 0 & 1 & 0 \\ -\sinh\omega & 0 & 0 & \cosh\omega \end{pmatrix} . \tag{2.17}$$

A Lorentz transformation that corresponds to a rotation of an angle θ about the z axis is

$$\Lambda_R = \begin{pmatrix} 1 & 0 & 0 & 0 \\ 0 & \cos\theta & \sin\theta & 0 \\ 0 & -\sin\theta & \cos\theta & 0 \\ 0 & 0 & 0 & 1 \end{pmatrix} . \tag{2.18}$$

The transformations for boosts and rotations can easily be generalised to refer to different directions in space. Notice that boosts and rotations have $\det\Lambda = +1$, i.e., they are proper Lorentz transformations.

The transformations that correspond to parity (space inversion) and time reversal are

$$\Lambda_P = \begin{pmatrix} 1 & 0 & 0 & 0 \\ 0 & -1 & 0 & 0 \\ 0 & 0 & -1 & 0 \\ 0 & 0 & 0 & -1 \end{pmatrix} \tag{2.19}$$

and

$$\Lambda_T = \begin{pmatrix} -1 & 0 & 0 & 0 \\ 0 & 1 & 0 & 0 \\ 0 & 0 & 1 & 0 \\ 0 & 0 & 0 & 1 \end{pmatrix} . \tag{2.20}$$

These are both improper, i.e., $\det\Lambda = -1$.

2.4 Four-vectors

A Lorentz four-vector $a = (a^0, a^1, a^2, a^3)$ is a collection of four components that transform under a Lorentz transformation in the same way as the space-time four-vector $x = (x^0, x^1, x^2, x^3)$. That is, in a transformed frame related to an original frame by $x' = \Lambda x$, the transformed four-vector a' should be $a' = \Lambda a$ or in component form

$$a'^{\mu} = \Lambda^{\mu}{}_{\nu} a^{\nu} , \tag{2.21}$$

By default, the term four-vector refers to the contravariant (upper-index) version. As with x, any contravariant four-vector a has a corresponding covariant form with components $a_\mu = g_{\mu\nu}a^\nu$, and one can transform between contra- and covariant forms by contracting with the appropriate factors of the metric g. Thus a covariant four-vector transforms under a Lorentz transformation as

$$a'_\mu = g_{\mu\rho} a'^\rho = g_{\mu\rho} \Lambda^\rho{}_\sigma g^{\sigma\nu} a_\nu = \Lambda_\mu{}^\nu a_\nu \ . \tag{2.22}$$

Given two four-vectors a and b, the four-vector product $a \cdot b$ is defined as

$$a \cdot b = a_\mu b^\mu = a^\mu b_\mu \ . \tag{2.23}$$

Since the Lorentz transformation was designed to leave $x^2 = x \cdot x = x_\mu x^\mu$ invariant, it is straightforward to show that the four-vector product of any two four-vectors is similarly invariant, since

$$\begin{aligned} a' \cdot b' &= a'_\mu b'^\mu = g_{\mu\nu} a'^\nu b'^\mu = g_{\mu\nu} \, \Lambda^\nu{}_\rho a^\rho \, \Lambda^\mu{}_\sigma b^\sigma & (2.24) \\ &= g_{\mu\nu} \, \Lambda^\nu{}_\rho \, \Lambda^\mu{}_\sigma \, a^\rho b^\sigma \ . & (2.25) \end{aligned}$$

We assert that this is equal to

$$a \cdot b = a_\mu b^\mu = g_{\rho\sigma} a^\rho b^\sigma \ . \tag{2.26}$$

Since by definition the Lorentz transformation satisfies $g_{\mu\nu} \, \Lambda^\nu{}_\rho \, \Lambda^\mu{}_\sigma = g_{\rho\sigma}$, we indeed find $a' \cdot b' = a \cdot b$.

One can show (see, e.g., Ref. [5] Vol. I, Ch. 17), that the energy E and three-dimensional vector momentum $\boldsymbol{p}$ transform such $p = (E, \boldsymbol{p})$ is a four-vector. An immediate consequence is that the four-vector product of p with itself is

$$p \cdot p = p_\mu p^\mu = g_{\mu\nu} p^\nu p^\mu = (p^0)^2 - (p^1)^2 - (p^2)^2 - (p^3)^3 = E^2 - |\boldsymbol{p}|^2 = m^2 \tag{2.27}$$

i.e., $p \cdot p$ (also written p^2) is the simply the rest mass squared, regardless of the reference frame used for the components of p.

2.5 Fields and four-vector derivatives

To derive the relativistic versions of quantum mechanical wave equations we will need to differentiate various fields, i.e., functions of the space-time coordinates x. To express these operations in a relativistic notation, we define the covariant four-vector derivative as

$$\partial_\mu = \frac{\partial}{\partial x^\mu} = \left(\frac{\partial}{\partial t}, \nabla \right) \ . \tag{2.28}$$

Notice that here that ∂_μ has a lower index despite being defined as the derivative with respect to the contravariant coordinate x^μ. The corresponding contravariant derivative is

$$\partial^\mu = \frac{\partial}{\partial x_\mu} = \left(\frac{\partial}{\partial t}, -\nabla \right) \ . \tag{2.29}$$

The motivation for this choice of notation becomes clear when we consider how derivatives of different quantities transform.

Consider first a Lorentz scalar field $\varphi(x)$, that is, a function of the space-time coordinate x that transforms such that the transformed function evaluated at the transformed coordinates is equal to the original function at the original coordinates of that point:[2]

$$\varphi'(x') = \varphi(x) \; . \tag{2.30}$$

Now consider the contravariant four-vector derivative $\partial^\mu \varphi$. Using the chain rule gives

$$\partial'^\mu \varphi'(x') = \frac{\partial \varphi'(x')}{\partial x'_\mu} = \frac{\partial x_\nu}{\partial x'_\mu} \frac{\partial \varphi'(x')}{\partial x_\nu} = \frac{\partial x_\nu}{\partial x'_\mu} \partial^\nu \varphi(x) \; . \tag{2.31}$$

We can use $x'^\mu = \Lambda^\mu{}_\nu x^\nu$ and its inverse relation $x^\nu = (\Lambda^{-1})^\nu{}_\mu x'^\mu$, and we can lower the index by contracting with g to find

$$x_\nu = g_{\nu\rho} (\Lambda^{-1})^\rho{}_\sigma g^{\sigma\mu} x'_\mu \; , \tag{2.32}$$

$$\frac{\partial x_\nu}{\partial x'_\mu} = g_{\nu\rho} (\Lambda^{-1})^\rho{}_\sigma g^{\sigma\mu} \; . \tag{2.33}$$

Using this together with Eq. (2.10) for Λ^{-1} in Eq. (2.31) gives

$$\partial'^\mu \varphi'(x') = (\Lambda^T)_\nu{}^\mu \partial^\nu \varphi(x) = \Lambda^\mu{}_\nu \partial^\nu \varphi(x) \; . \tag{2.34}$$

That is, if $\varphi(x)$ is a Lorentz scalar, then $\partial^\mu \varphi$ transforms as a (contravariant) four-vector. In a similar way, one can show that $\partial_\mu \varphi$ transforms as a covariant four-vector.

Suppose that $v(x)$ is a four-vector field, i.e., it transforms as $v'(x') = \Lambda v(x)$. One can then show that $\partial_\mu v^\mu = \partial^\mu v_\mu$ is a Lorentz scalar. A similar property can be derived for the four-dimensional d'Alembertian operator

$$\partial_\mu \partial^\mu = \frac{\partial^2}{\partial t^2} - \nabla^2 \; , \tag{2.35}$$

which is also written $\Box$ or sometimes $\Box^2$. One finds

$$\partial'_\mu \partial'^\mu = \partial_\mu \partial^\mu \; , \tag{2.36}$$

so that if $\varphi(x)$ is a Lorentz scalar, then $\partial_\mu \partial^\mu \varphi$ is as well.

[2] Note we are writing here the transformed function φ' in terms of the transformed coordinate x'. If we want to write it in terms of the original x, we can use $x = \Lambda^{-1} x'$ so that $\varphi'(x') = \varphi(\Lambda^{-1} x')$. This must hold for arbitrary x so we can drop the prime on x, i.e., $\varphi'(x) = \varphi(\Lambda^{-1} x)$.

2.6 Exponential form of Lorentz transformations

In this section we will extend the formalism of Lorentz transformations in a manner that will prove useful, later in Chapter 5, when we examine how relativistic wave equations appear in different reference frames. Specifically, we will show how the matrix for a continuous Lorentz transformation can be written as an exponential whose argument is a linear combination of another set of six matrices called the *generators* of the Lorentz group. Each of the generators corresponds to one of the three possible boost directions or rotation axes, and the coefficients in the linear combination determine the mixture of these operations to be carried out.

Consider a rotation of an angle θ in the (x_1, x_2) plane, and to simplify the equations we will suppress for now the x^0 and x^3 components, which remain unchanged. From Eq. (2.18) we see this can be written in the form $x' = Rx$ where $x = (x_1, x_2)^T$ and R is the 2×2 matrix

$$R = \begin{pmatrix} \cos\theta & \sin\theta \\ -\sin\theta & \cos\theta \end{pmatrix} . \tag{2.37}$$

We now claim that R can be written as the exponential of θ times another 2×2 matrix S, which is defined by its Taylor series as

$$R = e^{-\theta S} = 1 - \theta S + \frac{(-\theta S)^2}{2!} + \dots . \tag{2.38}$$

It is easy to verify that the matrix

$$S = \begin{pmatrix} 0 & -1 \\ 1 & 0 \end{pmatrix} \tag{2.39}$$

gives the Taylor expansion

$$e^{-\theta S} = \begin{pmatrix} 1 & 0 \\ 0 & 1 \end{pmatrix} - \theta \begin{pmatrix} 0 & -1 \\ 1 & 0 \end{pmatrix} + \frac{(-\theta)^2}{2!} \begin{pmatrix} 0 & -1 \\ 1 & 0 \end{pmatrix} \begin{pmatrix} 0 & -1 \\ 1 & 0 \end{pmatrix} + \dots \tag{2.40}$$

$$= \begin{pmatrix} 1 - \frac{\theta^2}{2} + \dots & \theta - \frac{\theta^3}{3!} + \dots \\ -\theta + \frac{\theta^3}{3!} + \dots & 1 - \frac{\theta^2}{2} + \dots \end{pmatrix} \quad \to \quad \begin{pmatrix} \cos\theta & \sin\theta \\ -\sin\theta & \cos\theta \end{pmatrix} , \tag{2.41}$$

which confirms that $e^{-\theta S}$ has the same form as the matrix R of Eq. (2.37).

In a similar way one can show (see, e.g., Ref. [6]) that a general combination of rotations and boosts corresponds to the Lorentz transformation

$$\Lambda = \exp\left(-\boldsymbol{\theta} \cdot \boldsymbol{S} - \boldsymbol{\zeta} \cdot \boldsymbol{K}\right) , \tag{2.42}$$

where

$$\boldsymbol{\theta} = \theta \boldsymbol{n} \ , \tag{2.43}$$

gives a rotation of angle θ about the unit vector $\boldsymbol{n}$ and

$$\boldsymbol{\zeta} = \frac{\boldsymbol{\beta}}{\beta} \tanh^{-1} \beta \tag{2.44}$$

corresponds to a boost with rapidity of magnitude $\zeta = |\boldsymbol{\zeta}|$ in the direction of the velocity vector $\boldsymbol{\beta}$, and $\boldsymbol{S} = (S_1, S_2, S_3)$ and $\boldsymbol{K} = (K_1, K_2, K_3)$ are vectors whose components are 4×4 matrices, given by

$$S_1 = \begin{pmatrix} 0 & 0 & 0 & 0 \\ 0 & 0 & 0 & 0 \\ 0 & 0 & 0 & -1 \\ 0 & 0 & 1 & 0 \end{pmatrix} \ , \quad S_2 = \begin{pmatrix} 0 & 0 & 0 & 0 \\ 0 & 0 & 0 & 1 \\ 0 & 0 & 0 & 0 \\ 0 & -1 & 0 & 0 \end{pmatrix} \ , \quad S_3 = \begin{pmatrix} 0 & 0 & 0 & 0 \\ 0 & 0 & -1 & 0 \\ 0 & 1 & 0 & 0 \\ 0 & 0 & 0 & 0 \end{pmatrix} \tag{2.45}$$

and

$$K_1 = \begin{pmatrix} 0 & 1 & 0 & 0 \\ 1 & 0 & 0 & 0 \\ 0 & 0 & 0 & 0 \\ 0 & 0 & 0 & 0 \end{pmatrix} \ , \quad K_2 = \begin{pmatrix} 0 & 0 & 1 & 0 \\ 0 & 0 & 0 & 0 \\ 1 & 0 & 0 & 0 \\ 0 & 0 & 0 & 0 \end{pmatrix} \ , \quad K_3 = \begin{pmatrix} 0 & 0 & 0 & 1 \\ 0 & 0 & 0 & 0 \\ 0 & 0 & 0 & 0 \\ 1 & 0 & 0 & 0 \end{pmatrix} \ . \tag{2.46}$$

That is, the matrices $\boldsymbol{S}$ and $\boldsymbol{K}$ "generate" different rotations and boosts, and the parameters $\boldsymbol{\theta}$ and $\boldsymbol{\zeta}$ encode which of the operations is included and with what magnitude.

The formalism introduced here illustrates a special case of what are called *Lie groups*, which are indexed as in this case by a set of continuous parameters. One finds that the generators satisfy commutation relations

$$[S_i, S_j] = \epsilon_{ijk} S_k \ , \tag{2.47}$$

$$[S_i, K_j] = \epsilon_{ijk} K_k \ , \tag{2.48}$$

$$[K_i, K_j] = -\epsilon_{ijk} S_k \ , \tag{2.49}$$

where $i, j, k = 1, 2, 3$ and ϵ_{ijk} is the Levi-Cevita symbol (i.e., the fully anti-symmetric tensor: $\epsilon_{123} = 1$, $\epsilon_{ijk} = 0$ if any of i, j, k are equal, and ϵ_{ijk} changes sign upon interchange of any two adjacent indices). The commutation relations (2.47)-(2.49) constitute the group's *Lie algebra*. Some further information on Lie groups can be found in Appendix A.

We will find it useful to make one further modification to our expression for the Lorentz transformation, by rewriting the six matrices $\boldsymbol{S}$ and $\boldsymbol{K}$ as an array of matrices $L^{\alpha\beta}$, with each matrix labelled by two indices $\alpha, \beta = 0, \ldots 3$ defined as

$$L^{12} = S_3 , \quad L^{13} = -S_2 , \quad L^{23} = S_1 , \tag{2.50}$$

$$L^{01} = K_1 , \quad L^{02} = K_2 , \quad L^{03} = K_3 , \tag{2.51}$$

and the other combinations of indices are defined so that L is antisymmetric, i.e., $L^{\alpha\beta} = -L^{\beta\alpha}$ and therefore $L^{\alpha\alpha} = 0$ (a 4×4 matrix of zeros) for all $\alpha = 0, \ldots, 3$.

Thus although Eqs. (2.54) and (2.55) really only define six new matrices in place of the six original ones, we include ten more so that L is itself a 4×4 matrix, each component of which is a 4×4 matrix. One can verify that with $\boldsymbol{S}$ and $\boldsymbol{K}$ as defined in Eqs. (2.45) and (2.46), the (μ, ν) element of the matrix $L^{\alpha\beta}$ is [3]

$$(L^{\alpha\beta})^{\mu}{}_{\nu} = g^{\alpha\mu}\delta^{\beta}{}_{\nu} - g^{\beta\mu}\delta^{\alpha}{}_{\nu} . \tag{2.52}$$

In this way, the Lorentz transformation (2.42) can be rewritten as

$$\Lambda = \exp\left(-\frac{1}{2}\omega_{\alpha\beta}L^{\alpha\beta}\right) , \tag{2.53}$$

where the matrix of numbers $\omega_{\alpha\beta}$ contains the boost and rotation coefficients $\boldsymbol{\zeta} = (\zeta_1, \zeta_2, \zeta_3)$ and $\boldsymbol{\theta} = (\theta_1, \theta_2, \theta_3)$. For Eq. (2.53) to correspond to Eq. (2.42), the elements of ω are found to be

$$\omega_{12} = \theta_3 , \quad \omega_{13} = -\theta_2 , \quad \omega_{23} = \theta_1 , \tag{2.54}$$

$$\omega_{01} = \zeta_1 , \quad \omega_{02} = \zeta_2 , \quad \omega_{03} = \zeta_3 , \tag{2.55}$$

and the rest are defined to make ω fully antisymmetric, i.e., $\omega_{\alpha\beta} = -\omega_{\beta\alpha}$. Thus there are only six independent values of the matrix ω, just as there are only six independent matrices in S. The factor of $1/2$ in Eq. (2.53) appears because the sum is carried out over all combinations of α and β, and thus each product of coefficient and matrix is included twice, once for each order of the indices.

We will return to the Lorentz transformation as expressed by Eq. (2.53) in Ch. 5 when we investigate the covariance of the Dirac equation.

[3] Here $\delta^{\mu}{}_{\nu} = \delta_{\mu}{}^{\nu} = 1$ for $\mu = \nu$ and 0 otherwise. If both indices are in the upper or lower positions, then one finds, e.g., $\delta_{\mu\nu} = g_{\mu\rho}\delta^{\rho}{}_{\nu} = g_{\mu\nu}$.

Chapter 3

Maxwell, Schrödinger and Klein-Gordon Equations

In this chapter we first recap Maxwell's theory of electromagnetism and non-relativistic quantum mechanics, and then develop the first important equation of relativistic quantum mechanics, the Klein-Gordon equation.

3.1 Review of Maxwell's equations

In Heaviside-Lorentz units ($\varepsilon_0 = \mu_0 = 1$), Maxwell's equations for the electric and magnetic fields are

$$\nabla \cdot \boldsymbol{B} = 0 \,, \tag{3.1}$$

$$\nabla \times \boldsymbol{E} + \frac{\partial \boldsymbol{B}}{\partial t} = 0 \,, \tag{3.2}$$

$$\nabla \cdot \boldsymbol{E} = \rho \,, \tag{3.3}$$

$$\nabla \times \boldsymbol{B} - \frac{\partial \boldsymbol{E}}{\partial t} = \boldsymbol{j} \,. \tag{3.4}$$

Because $\boldsymbol{B}$ has zero divergence it can be written as the curl of a vector potential $\boldsymbol{A}$,

$$\boldsymbol{B} = \nabla \times \boldsymbol{A} \,. \tag{3.5}$$

Substituting this into Eq. (3.2) and swapping the order of the derivatives gives

$$\nabla \times \left(\boldsymbol{E} + \frac{\partial \boldsymbol{A}}{\partial t} \right) = 0 \,. \tag{3.6}$$

Since $\boldsymbol{E} + \frac{\partial \boldsymbol{A}}{\partial t}$ has zero curl it can be written as the (negative) gradient of a scalar potential ϕ, so the electric field $\boldsymbol{E}$ is

$$\boldsymbol{E} = -\frac{\partial \boldsymbol{A}}{\partial t} - \nabla\phi \; . \tag{3.7}$$

The scalar and vector potentials can be put together as a four-vector $A^\mu = (\phi, \boldsymbol{A})$, and the charge and current density ρ and $\boldsymbol{j}$ form a four-vector $j^\mu = (\rho, \boldsymbol{j})$.

The potentials thus determine the $\boldsymbol{E}$ and $\boldsymbol{B}$ fields, but they are not unique. If they are changed by a *gauge transformation*,

$$A'^\mu = A^\mu - \partial^\mu \chi \; , \tag{3.8}$$

where $\chi(x)$ is an arbitrary (Lorentz) scalar function, then one finds the same $\boldsymbol{E}$ and $\boldsymbol{B}$. This gauge symmetry of electromagnetism, when generalised to the weak and strong interactions, will turn out to be a key principle in constructing the Standard Model.

We can write Maxwell's equations in a form equivalent to Eqs. (3.1)-(3.4) by defining the field strength tensor $F^{\mu\nu}$ as

$$F^{\mu\nu} = \partial^\mu A^\nu - \partial^\nu A^\mu \; , \tag{3.9}$$

which is antisymmetric in the two indices, i.e., $F^{\mu\nu} = -F^{\nu\mu}$. Its components give the electric and magnetic fields as

$$F^{\mu\nu} = \begin{pmatrix} 0 & -E_x & -E_y & -E_z \\ E_x & 0 & -B_z & B_y \\ E_y & B_z & 0 & -B_x \\ E_z & -B_y & B_x & 0 \end{pmatrix} \; . \tag{3.10}$$

The two homogeneous Maxwell equations (3.1) and (3.2) are then contained in the single equation

$$\partial^\lambda F^{\mu\nu} + \partial^\mu F^{\nu\lambda} + \partial^\nu F^{\lambda\mu} = 0 \; , \tag{3.11}$$

and the two equations with source terms (3.3) and (3.4) can be expressed as

$$\partial_\mu F^{\mu\nu} = j^\nu \; . \tag{3.12}$$

Differentiating Eq. (3.12) with ∂_ν gives

$$\partial_\nu j^\nu = \partial_\nu \partial_\mu F^{\mu\nu} = 0 \; , \tag{3.13}$$

where the final equality follows because $\partial_\nu \partial_\mu$ is symmetric in μ and ν, and it is contracted with $F^{\mu\nu}$ which is antisymmetric. Thus the four-vector current satisfies the continuity equation

$$\partial_\nu j^\nu = \frac{\partial \rho}{\partial t} + \nabla \cdot \boldsymbol{j} = 0 \; . \tag{3.14}$$

Returning to Eq. (3.12), by inserting the definition of $F^{\mu\nu}$ from Eq. (3.9) one obtains

$$(\partial_\mu \partial^\mu) A^\nu - \partial^\nu (\partial_\mu A^\mu) = j^\nu \ . \tag{3.15}$$

By applying ∂_μ to the gauge transformation expressed by Eq. (3.8), however, we see that for an appropriate choice of the function χ such that $\partial_\mu A^\mu = \partial_\mu \partial^\mu \chi$, one can fix

$$\partial_\mu A^\mu = 0 \ , \tag{3.16}$$

which is called the *Lorenz* gauge.[1] In this gauge, Eq. (3.12) takes on the form

$$(\partial_\mu \partial^\mu) A^\nu = j^\nu \ . \tag{3.17}$$

To solve this in a region with no electric charge we can use the trial solution

$$A^\mu = N \varepsilon^\mu e^{-ik\cdot x} \ , \tag{3.18}$$

where the four-vector polarisation ε^μ will be a function of the four-momentum k^μ to be determined and N is a normalisation constant. Using this in Eq. (3.17) with $j^\mu = 0$ gives

$$(\partial_\mu \partial^\mu) A^\nu = -k^2 A^\nu \ . \tag{3.19}$$

Equation (3.18) is thus a solution provided $k^2 = k_\mu k^\mu = 0$. This allows one to interpret an excitation of the electromagnetic field as a photon with zero mass. Using Eq. (3.18) with the Lorenz gauge condition (3.16) therefore gives

$$\partial_\mu A^\mu \propto k_\mu \varepsilon^\mu = k^0 \varepsilon^0 - \boldsymbol{k} \cdot \boldsymbol{\varepsilon} = 0 \ , \tag{3.20}$$

and thus in this gauge the four-momentum is orthogonal, in the sense of the four-vector product, to the polarisation vector. The polarisation vector ε^μ has four components but with the constraint of Eq. (3.20) only three of them are independent.

The Lorenz condition $\partial_\mu A^\mu = 0$ does not completely fix A^μ, since one could still add to it the four-vector gradient of a scalar function λ, i.e.,

$$A'^\mu = A^\mu + \partial^\mu \lambda \tag{3.21}$$

provided λ satisfies

$$(\partial_\nu \partial^\nu) \lambda = \left(\frac{\partial^2}{\partial t^2} - \nabla^2 \right) \lambda = 0 \ . \tag{3.22}$$

In this way the Lorenz condition continues to hold, since

[1] Danish physicist Ludvig Lorenz, 1829-1891, not to be confused with Dutch physicist Hendrik Antoon Lorentz, 1853-1928.

$$\partial_\mu A'^\mu = \partial_\mu A^\mu + \partial_\mu \partial^\mu \lambda = \partial_\mu A^\mu + 0 = 0 \; . \tag{3.23}$$

Suppose in a given Lorenz gauge, the vector potential has some nonzero divergence, say, $\nabla \cdot \boldsymbol{A} = g(x)$. Then we can carry out a further gauge transformation according to Eq. (3.21) with a function λ that satisfies $\nabla^2 \lambda = g(x)$, so that by construction the transformed vector potential has $\nabla \cdot \boldsymbol{A'} = 0$. That is, since $\partial^\mu = (\partial/\partial t, -\nabla)$, one obtains for the transformation of the spatial components $\boldsymbol{A'} = \boldsymbol{A} - \nabla \cdot \boldsymbol{A}$ and therefore $\nabla \cdot \boldsymbol{A'} = \nabla \cdot \boldsymbol{A} - \nabla^2 \lambda = g(x) - g(x) = 0$. This is called the Coulomb gauge.

The further requirement of zero divergence of the vector potential represents one more constraint, so in the Coloumb gauge the polarisation vector $(\varepsilon^0, \boldsymbol{\varepsilon})$ has only two independent components. From $\nabla \cdot \boldsymbol{A} = -iN\boldsymbol{k} \cdot \boldsymbol{\varepsilon} e^{-ik\cdot x} = 0$ one has

$$\boldsymbol{k} \cdot \boldsymbol{\varepsilon} = 0 \; , \tag{3.24}$$

and from the Lorenz gauge condition (3.20) it then follows that $\varepsilon^0 = 0$. That is, the three-dimensional polarisation vector vector $\boldsymbol{\varepsilon}$ is perpendicular to the direction of the momentum vector $\boldsymbol{k}$. For example, for $\boldsymbol{k}$ along the z axis we can take the two independent basis vectors to be

$$\boldsymbol{\varepsilon}_1 = (1, 0, 0) \; , \tag{3.25}$$

$$\boldsymbol{\varepsilon}_2 = (0, 1, 0) \; . \tag{3.26}$$

The normalisation is set such that $\boldsymbol{\varepsilon}_r \cdot \boldsymbol{\varepsilon}_s = \delta_{rs}$, where $r, s = 1, 2$ label the two independent polarisation states.

3.2 Review of non-relativistic Quantum Mechanics

In quantum mechanics, a free particle of energy E and momentum $\boldsymbol{p}$ is associated with a wave function,[2]

$$\Psi(\boldsymbol{r}, t) = \frac{1}{\sqrt{V}} e^{i(\boldsymbol{k}\cdot\boldsymbol{r} - \omega t)} \; , \tag{3.27}$$

where ω and $\boldsymbol{k}$ are related to the energy and momentum by $E = \hbar\omega$ and $\boldsymbol{p} = \hbar\boldsymbol{k}$. The wave function can be normalised to unity inside a volume V, i.e.,

$$\int_V |\Psi(\boldsymbol{r}, t)|^2 \, d^3\boldsymbol{r} = 1 \; , \tag{3.28}$$

where the spatial extent of V is large compared to the particle's de Broglie wavelength $\lambda = 2\pi/|\boldsymbol{k}|$. In the limit where the volume is large, the factor V drops out of predictions for physical observables and in some calculations it will be convenient to simply set $V = 1$.

[2] In this section we retain the usual factors of $\hbar$ and c.

Observable quantities such as energy and momentum are associated with operators, written here with hats, that act on the wave functions. The possible outcomes of a measurement are given by the eigenvalues of the corresponding operator, e.g.,

$$\hat{E}\Psi = E\Psi = \hbar\omega\Psi \ , \tag{3.29}$$

$$\hat{\boldsymbol{p}}\Psi = \boldsymbol{p}\Psi = \hbar\boldsymbol{k}\Psi \ . \tag{3.30}$$

Using the wave function Eq. (3.27) in Eqs. (3.29) and (3.30), we find for the energy and momentum operators,

$$\hat{E} = i\hbar\frac{\partial}{\partial t} \ , \tag{3.31}$$

$$\hat{\boldsymbol{p}} = -i\hbar\nabla \ . \tag{3.32}$$

A non-relativistic particle of momentum p and mass m in a potential $V(\boldsymbol{r},t)$ has an energy

$$E = \frac{p^2}{2m} + V(\boldsymbol{r},t) \ . \tag{3.33}$$

Using the momentum operator (3.32) we can form the total energy operator or Hamiltonian

$$H = \frac{\hat{p}^2}{2m} + V(\boldsymbol{r},t) = -\frac{\hbar^2}{2m}\nabla^2 + V(\boldsymbol{r},t) \ . \tag{3.34}$$

Operating with H on the wave function and using Eq. (3.31) gives the time-dependent Schrödinger equation,

$$\left(-\frac{\hbar^2}{2m}\nabla^2 + V(\boldsymbol{r},t)\right)\Psi = i\hbar\frac{\partial}{\partial t}\Psi \ . \tag{3.35}$$

Often the potential V is time independent. In this case the wave function can be separated into space and time dependent parts as

$$\Psi(\boldsymbol{r},t) = \psi(\boldsymbol{r})e^{-iEt/\hbar} \ , \tag{3.36}$$

which results in the time-independent Schrödinger equation,

$$H\psi(\boldsymbol{r}) = E\psi(\boldsymbol{r}) \ . \tag{3.37}$$

One postulates that the probability density ρ to measure the particle's position at $\boldsymbol{r}$ is given by the absolute square of the wave function. We can define as well a probability current $\boldsymbol{j}$ that will, together with ρ, obey a continuity equation so that probability is locally conserved. To do this, we write first the Schrödinger equation and its complex conjugate,

$$H\Psi = \imath\hbar\frac{\partial}{\partial t}\Psi \,, \tag{3.38}$$

$$H^*\Psi^* = -i\hbar\frac{\partial}{\partial t}\Psi^* = H\Psi^* \,, \tag{3.39}$$

where $H^* = H$ provided the potential V is real, which we will assume to hold. Subtracting Ψ times Eq. (3.39) from Ψ^* times Eq. (3.38) gives

$$\Psi^* H\Psi - \Psi H\Psi^* = i\hbar\left(\Psi^*\frac{\partial\Psi}{\partial t} + \Psi\frac{\partial\Psi^*}{\partial t}\right) \,. \tag{3.40}$$

Using the Hamiltonian defined by Eq. (3.35), Eq. (3.40) can be rewritten as

$$\frac{\partial}{\partial t}\left(\Psi^*\Psi\right) + \frac{\hbar}{2im}\left(\Psi^*\nabla^2\Psi - \Psi\nabla^2\Psi^*\right) = 0 \,. \tag{3.41}$$

It is easy to verify that this can be written as a continuity equation

$$\frac{\partial\rho}{\partial t} + \nabla\cdot\boldsymbol{j} = 0 \,, \tag{3.42}$$

where the probability density ρ and probability current $\boldsymbol{j}$ are

$$\rho = \Psi^*\Psi \,, \tag{3.43}$$

$$\boldsymbol{j} = \frac{\hbar}{2im}\left[\Psi^*\nabla\Psi - (\nabla\Psi)^*\Psi\right] \,. \tag{3.44}$$

The corresponding electric charge density and current are given by $\rho_{\text{e.m.}} = q\rho$ and $\boldsymbol{j}_{\text{e.m.}} = q\boldsymbol{j}$, i.e., they include a factor of the particle's charge q. The symbols ρ and $\boldsymbol{j}$ may refer to either charge or probability density and one may need to infer from context which is meant.

For the free-particle wave function (3.27), $\Psi(\boldsymbol{r},t) = \frac{1}{\sqrt{V}}e^{i(\boldsymbol{k}\cdot\boldsymbol{r}-\omega t)}$, the probability density and current are found to be

$$\rho = \Psi^*\Psi = \frac{1}{V} \,, \tag{3.45}$$

$$\boldsymbol{j} = \frac{\hbar}{2im}\left[i\boldsymbol{k}\Psi^*\Psi - (-i\boldsymbol{k})\Psi^*\Psi\right] = \frac{\hbar\boldsymbol{k}}{2m}2\Psi^*\Psi = \frac{\boldsymbol{p}}{m}\rho = \boldsymbol{v}\rho \,. \tag{3.46}$$

As expected for a free particle, ρ and $\boldsymbol{j}$ are independent of space and time.

3.3 The Klein-Gordon Equation

The Schrödinger equation was based on the non-relativistic relation between energy and momentum given by Eq. (3.33). To develop a relativistic equation it seems natural to replace this by the corresponding relativistic relation, which for a free particle of mass m is (here again with $c = \hbar = 1$)

$$E^2 = |\boldsymbol{p}|^2 + m^2 \; . \tag{3.47}$$

We assume as before that energy and momentum correspond to differential operators,

$$\hat{E} \;=\; i\frac{\partial}{\partial t} \; , \tag{3.48}$$

$$\hat{\boldsymbol{p}} \;=\; -i\nabla \; , \tag{3.49}$$

that act on a wave function $\varphi(x)$, where $x = (t, x, y, z)$. Using these in Eq. (3.47) gives

$$\left(\frac{\partial^2}{\partial t^2} - \nabla^2 + m^2\right)\varphi = 0 \; , \tag{3.50}$$

or in the four-vector notation from Ch. 2,

$$(\partial_\mu \partial^\mu + m^2)\varphi = 0 \; , \tag{3.51}$$

which is the Klein-Gordon equation for a free particle of mass m.

The solutions to the free-particle Klein-Gordon equation are plane waves,

$$\varphi(x) = Ne^{\pm ip\cdot x} = Ne^{\pm i(Et - \boldsymbol{p}\cdot\boldsymbol{r})} \; , \tag{3.52}$$

where N is a normalisation factor that we will set later.

The solutions must include both the plus and minus signs in the exponents of Eq.(3.52). Depending on which sign we choose, the solutions have positive or negative energy, which we label as φ_+ and φ_-:

$$\varphi_+ \;=\; Ne^{-ip\cdot x} \qquad \rightarrow \qquad i\frac{\partial}{\partial t}\varphi_+ = +E\varphi_+ \; , \tag{3.53}$$

$$\varphi_- \;=\; Ne^{ip\cdot x} \qquad \rightarrow \qquad i\frac{\partial}{\partial t}\varphi_- = -E\varphi_- \; . \tag{3.54}$$

We take "energy" to always mean the eigenvalue of the energy operator $i\partial/\partial t$, whereas here the quantity E is an abbreviation for $\sqrt{|\boldsymbol{p}|^2 + m^2}$ and is always positive. In the exponents of Eqs. (3.53) and (3.54), the product $p \cdot x$ is understood to mean $Et - \boldsymbol{p} \cdot \boldsymbol{r}$.

When these solutions were first considered, it was not clear how to interpret those with negative energy. It is tempting to simply ignore them as unphysical, but this would leave one without a complete system of eigenfunctions. Later on we will see that they are used, in a nontrivial way, to describe antiparticles.

Problematic as negative energies may seem, matters get worse when we try to interpret the solutions of the Klein-Gordon equation in terms of probability. Whatever its interpretation, we want to regard $\varphi(x)$ as a Lorentz scalar, i.e., in a Lorentz-transformed frame we should find $\varphi'(x') = \varphi(x)$. Therefore we cannot simply identify $|\varphi^2|$ with a probability density. The probability content of a volume element $|\varphi^2|\,dV$ should be Lorentz invariant, but dV would undergo contraction under a boost.

In a manner similar to what was done with the Schrödinger equation, we can define a probability density ρ and current $\boldsymbol{j}$ as

$$j^\mu = (\rho, \boldsymbol{j}) = \frac{i}{2m}(\varphi^* \partial^\mu \varphi - \varphi \partial^\mu \varphi^*) \; . \tag{3.55}$$

The factor of $i/2m$ is included here to make the probability density and current coincide with the corresponding quantities from the Schrödinger Eqs. (3.45) and (3.46) in the nonrelativistic limit. The fact that we can identify $(\rho, \boldsymbol{j})$ with the components of a four-vector is more than just a matter of notation; since φ is a Lorentz scalar, the fact that we have formed j^μ with the four-vector derivative ∂^μ as above guarantees that it will transform as a four-vector. It will be left as an exercise to verify explicitly that

$$\partial_\mu \boldsymbol{j}^\mu = \frac{\partial \rho}{\partial t} + \nabla \cdot \boldsymbol{j} = 0 \; , \tag{3.56}$$

which is to say, the probability density and current satisfy a continuity equation.

By substituting the positive solution φ_+ into Eq. (3.61), one finds

$$\rho = \frac{i}{2m}\left[(-iE)\varphi_+^* \varphi_+ - (+iE)\varphi_+^* \varphi_+\right] = \frac{E}{m}|N|^2 \tag{3.57}$$

$$\boldsymbol{j} = -i\left[(i\boldsymbol{p})\varphi_+^* \varphi_+ - (-i\boldsymbol{p})\varphi_+^* \varphi_+\right] = \frac{\boldsymbol{p}}{m}|N|^2 \; . \tag{3.58}$$

In the non-relativistic limit we have $p^0 \to m$ and therefore $\rho \to |N|^2$, so if we take $N = 1/\sqrt{V}$ for some normalising volume V, then $\rho \to 1/V$, the same as we had earlier with the Schrödinger equation.

The interpretation of the solution in terms of probabilities has, however, a more serious problem. For the negative energy solution one finds

$$\rho = i\left[(iE)\varphi_-^* \varphi_- - (-iE)\varphi_-^* \varphi_-\right] = -\frac{E}{m}|N|^2 \; , \tag{3.59}$$

i.e., a negative probability. At this point Klein, Gordon and Schrödinger abandoned the Klein-Gordon equation as a physically meaningful description of matter.

We will resurrect it later, however, by using the negative-energy solutions to describe antiparticles. It is then more convenient to define the current without the normalising factor of $2m$ so that

$$j^\mu = (\rho, \boldsymbol{j}) = i(\varphi^* \partial^\mu \varphi - \varphi \partial^\mu \varphi^*) \; . \tag{3.60}$$

The continuity relation $\partial_\mu j^\mu$ still holds, and with the plane-wave solution (3.52) the current is

$$j^\mu = 2p^\mu |N|^2 \; . \tag{3.61}$$

Chapter 4

The Dirac Equation

In this chapter we introduce the Dirac equation and find its solutions for a free particle. We will see how the equation reduces in the non-relativistic limit to something like the Schrödinger equation but with a two-component solution, which we can use to describe spin. Finally we will see how the negative energy solutions of relativistic wave equations can be reinterpreted to describe antiparticles as well as interactions that involve creation and destruction of particles.

4.1 Deriving the Dirac Equation

The negative energy solutions found from the Klein-Gordon equation arose because it was based on the relativistic relation between energy, momentum and mass,

$$E^2 = |\boldsymbol{p}|^2 + m^2 \, . \tag{4.1}$$

The two roots $E = \pm\sqrt{|\boldsymbol{p}|^2 + m^2}$ led to positive and negative energy solutions φ_+ and φ_-, and the negative probability density from $|\varphi_-|^2$ made it impossible to interpret the solution as a probability.

To circumvent this difficulty, Dirac proposed an equation that is first order in $\partial/\partial t$, corresponding to a single power of the energy. To be consistent with special relativity it should therefore treat space coordinates on the same footing and also contain only first-order derivatives $\partial/\partial x_i$. When we follow this through we find, first, that the solutions are not scalar functions but rather they must contain at least four components, and second, that the solutions still include negative energies. In this case, however, the solutions lead to a *positive* probability density. Furthermore, following the approach of Stückelberg [12] and Feynman [13, 14], the negative energy solutions can be re-interpreted to describe antiparticles. This can be applied as well to the Klein-Gordon equation, and the theory then allows for creation and destruction of particles, which we will see in greater detail in Ch. 6. The Dirac and Klein-Gordon Equations are thus found to provide a meaningful relativistic theory of quantum mechanics.

In constructing a relativistic wave equation, Dirac retained the ideas of de Broglie and Einstein that the free-particle solutions should correspond to plane waves,

$$\psi \sim e^{\pm ip\cdot x} = e^{\pm i(Et - \boldsymbol{p}\cdot\boldsymbol{x})} \,, \tag{4.2}$$

and that these should satisfy the relativistic relation between energy, momentum and mass $E^2 = |\boldsymbol{p}|^2 + m^2$. Thus the energy and momentum operators are as before $\hat{E} = i\partial/\partial t$ and $\hat{\boldsymbol{p}} = -i\nabla$. Dirac proposed that the relativistic wave equation for a particle of mass m should have the form

$$i\frac{\partial\psi}{\partial t} = -i\left(\alpha_1\frac{\partial\psi}{\partial x_1} + \alpha_2\frac{\partial\psi}{\partial x_2} + \alpha_3\frac{\partial\psi}{\partial x_3}\right) + \beta m\psi \equiv H\psi \,. \tag{4.3}$$

The right-hand side defines the Dirac Hamiltonian $H = -i\boldsymbol{\alpha}\cdot\nabla + m = \boldsymbol{\alpha}\cdot\hat{\boldsymbol{p}} + m$ for a free particle for some appropriately chosen $\boldsymbol{\alpha} = (\alpha_1,\, \alpha_2,\, \alpha_3)$ and β. We will see below that α_1, α_2, α_3 and β cannot be interpreted as scalars but rather as 4×4 matrices, so for the moment with no loss of generality we will not assume that they commute.

We want to see if Eq. (4.3) is compatible with $E^2 = |\boldsymbol{p}|^2 + m^2$, so we apply once again the energy operator $i\partial/\partial t$ on the left and the Dirac Hamiltonian on the right, retaining the order of all factors of α_i and β. This gives

$$-\frac{\partial^2\psi}{\partial t^2} = -\sum_{i=1}^{3}\alpha_i^2\frac{\partial^2\psi}{\partial x_i^2} + m^2\beta^2\psi - \sum_{i\neq j}\frac{1}{2}(\alpha_i\alpha_j + \alpha_j\alpha_i)\frac{\partial^2\psi}{\partial x_i\,\partial x_j} - im\sum_{i=1}^{3}(\alpha_i\beta + \beta\alpha_i)\frac{\partial\psi}{\partial x_i} \,. \tag{4.4}$$

For a free particle we want to find plane-wave solutions (4.2) that give the correct relativistic relationship between momentum and energy. Suppose we take

$$\alpha_i^2 = \beta^2 = I \,, \quad i = 1,2,3 \,, \tag{4.5}$$

$$\alpha_i\alpha_j + \alpha_j\alpha_i = 0 \,, \quad i \neq j \,, \tag{4.6}$$

$$\alpha_i\beta + \beta\alpha_i = 0 \,, \quad i = 1,2,3 \,, \tag{4.7}$$

where for now we can think of I as unity. Using Eqs. (4.5), (4.6) and (4.7) together with Eq. (4.4) and the plane-wave solution (4.2) gives

$$E^2 = -\sum_{i=1}^{3}(ip_i)^2 + m^2 + 0 - im0 \,, \tag{4.8}$$

which is to say $E^2 = |\boldsymbol{p}|^2 + m^2$.

Our approach appears to give the desired result, but Eqs. (4.5), (4.6) and (4.7) clearly cannot be satisfied by real or complex numbers for α_i and β. They could, however, be fulfilled if α_i and β are matrices. To see what properties these matrices must have, recall that the Hamiltonian $H = \boldsymbol{\alpha}\cdot\hat{\boldsymbol{p}} + m$ must be Hermitian, and since $\hat{\boldsymbol{p}}$ and m are Hermitian, the matrices α_i and β must therefore be as well, and therefore they have real eigenvalues.

From the relation (4.5) $\alpha_i^2 = \beta^2 = I$ one has

$$\alpha_i^2\psi = \psi \,, \tag{4.9}$$

$$\beta^2\psi = \psi \,. \tag{4.10}$$

That is, the eigenvalues of α_i^2 and β^2 are 1, and so the eigenvalues of α_i and β are ± 1.

Furthermore, we can show in the following way that all of the matrices must have zero trace. Using $\beta^2 = I$ and $\beta\alpha_i = -\alpha_i\beta$ plus the fact that the trace of a product of matrices is invariant under cyclic permutation one has, e.g.,

$$\mathrm{Tr}(\alpha_i) = \mathrm{Tr}(\beta^2\alpha_i) = \mathrm{Tr}(-\beta\alpha_i\beta) = -\mathrm{Tr}(\alpha_i\beta^2) = -\mathrm{Tr}(\alpha_i) \tag{4.11}$$

and therefore $\mathrm{Tr}(\alpha_i) = 0$, $i = 1, 2, 3$. In a similar way one finds $\mathrm{Tr}(\beta) = 0$ as well.

Next, we can exploit the fact that the trace of a matrix is equal to the sum of its eigenvalues, so the sum of the eigenvalues of the α_i and β are all zero. Since we have just seen the eigenvalues are ± 1, this means that the dimension of these matrices must be even.

One could try a dimension $N = 2$, but there are only three linearly independent 2×2 traceless Hermitian matrices, e.g., the Pauli matrices,

$$\sigma_1 = \begin{pmatrix} 0 & 1 \\ 1 & 0 \end{pmatrix} \,, \qquad \sigma_2 = \begin{pmatrix} 0 & -i \\ i & 0 \end{pmatrix} \,, \qquad \sigma_3 = \begin{pmatrix} 1 & 0 \\ 0 & -1 \end{pmatrix} \,. \tag{4.12}$$

The next smallest dimension one can try is $N = 4$. One possible choice of four linearly independent 4×4 Hermitian matrices is

$$\alpha_i = \begin{pmatrix} 0 & \sigma_i \\ \sigma_i & 0 \end{pmatrix} \,, \qquad \beta = \begin{pmatrix} I_2 & 0 \\ 0 & -I_2 \end{pmatrix} \,, \tag{4.13}$$

for $i = 1, 2, 3$, where I_2 is the 2×2 identity matrix. These matrices used in Eq. (4.3), which we can write as

$$i\frac{\partial\psi}{\partial t} = -i\sum_{i=1}^{3}\alpha_i\frac{\partial\psi}{\partial x_i} + \beta m\psi \,, \tag{4.14}$$

give the wave equation originally proposed by Dirac in 1928 [7]. Since the Dirac Hamiltonian is a 4×4 matrix, the wave function ψ on which it operates must be a four-component (column) vector called a Dirac *spinor*,

$$\psi = \begin{pmatrix} \psi_1 \\ \psi_2 \\ \psi_3 \\ \psi_4 \end{pmatrix} \,. \tag{4.15}$$

4.2 Probability Density and Current from the Dirac Equation

We will now show that the solution to the Dirac equation satisfies a continuity equation of the same form as those found earlier for the Schrödinger and Klein-Gordon equations. Since the Dirac spinor (4.15) is a column vector, its Hermitian conjugate (i.e., complex conjugate transpose or adjoint) $\psi^\dagger$ is the row vector

$$\psi^\dagger = (\psi_1^*, \psi_2^*, \psi_3^*, \psi_4^*) \; , \tag{4.16}$$

which satisfies the Hermitian conjugate of the Dirac equation,

$$-i\frac{\partial \psi^\dagger}{\partial t} = i\sum_{i=1}^{3} \frac{\partial \psi^\dagger}{\partial x_i}\alpha_i + m\psi^\dagger\beta \; . \tag{4.17}$$

Note that in taking the Hermitian conjugate, the order of the spinor and the matrices α_i and β gets reversed.

To derive the continuity relation, we follow the same path as used with the Schrödinger and Klein-Gordon equations, namely, we compute $\psi^\dagger$ times the Dirac equation for ψ and subtract the Hermitian conjugate equation for $\psi^\dagger$ multiplied on the right by ψ. This gives

$$i\psi^\dagger\frac{\partial \psi}{\partial t} - \left(-i\frac{\partial \psi^\dagger}{\partial t}\,\psi\right) = -i\left(\sum_{i=1}^{3}\psi^\dagger\alpha_i\frac{\partial \psi}{\partial x_i}\right) + m\psi^\dagger\beta\psi - \left[i\left(\sum_{i=1}^{3}\frac{\partial \psi^\dagger}{\partial x_i}\alpha_i\psi\right) + m\psi^\dagger\beta\psi\right] \tag{4.18}$$

which after canceling the terms with $m\psi^\dagger\beta\psi$ and rearranging the derivatives can be written

$$i\frac{\partial}{\partial t}\left(\psi^\dagger\psi\right) = -i\sum_{i=}^{3}\frac{\partial}{\partial x_i}\left(\psi^\dagger\alpha_i\psi\right) \; . \tag{4.19}$$

This can then be written with the usual form of a continuity equation

$$\frac{\partial \rho}{\partial t} + \nabla\cdot\boldsymbol{j} = 0 \; , \tag{4.20}$$

where the Dirac probability density ρ and current $\boldsymbol{j}$ are

$$\rho = \psi^\dagger\psi \; , \tag{4.21}$$

$$\boldsymbol{j} = \psi^\dagger\boldsymbol{\alpha}\psi \; , \tag{4.22}$$

and where $\boldsymbol{\alpha} = (\alpha_1, \alpha_2, \alpha_3)$ is a vector whose components are matrices. Note that the quantity ρ,

$$\rho = \psi^\dagger\psi = \sum_{a=1}^{4}|\psi_a|^2 \geq 0 \; , \tag{4.23}$$

is never negative, so the difficulty of negative probabilities encountered earlier with the Klein-Gordon equation is avoided.

4.3 Non-relativistic limit of the Dirac equation

Consider an electron at rest, i.e., $\boldsymbol{p} = 0$ and therefore $\nabla\psi = 0$. The Dirac equation (4.14) becomes

$$i\frac{\partial\psi}{\partial t} = m\beta\psi \,, \tag{4.24}$$

or written out in components,

$$i\begin{pmatrix} \frac{\partial\psi_1}{\partial t} \\ \frac{\partial\psi_2}{\partial t} \\ \frac{\partial\psi_3}{\partial t} \\ \frac{\partial\psi_4}{\partial t} \end{pmatrix} = m\begin{pmatrix} 1 & 0 & 0 & 0 \\ 0 & 1 & 0 & 0 \\ 0 & 0 & -1 & 0 \\ 0 & 0 & 0 & -1 \end{pmatrix}\begin{pmatrix} \psi_1 \\ \psi_2 \\ \psi_3 \\ \psi_4 \end{pmatrix} \,. \tag{4.25}$$

These are four differential equations with four linearly independent solutions. Two have positive energy, which we can take as

$$\psi^{(1)} = e^{-imt}\begin{pmatrix} 1 \\ 0 \\ 0 \\ 0 \end{pmatrix} \,, \qquad \psi^{(2)} = e^{-imt}\begin{pmatrix} 0 \\ 1 \\ 0 \\ 0 \end{pmatrix} \,. \tag{4.26}$$

Here the superscripts label to the solution, and should not be confused with the subscripts, which refer to the components of the spinor. Applying $\hat{E} = i\partial/\partial t$ to these solutions gives for both energies $E_1 = E_2 = m$. Two further linearly independent solutions can be taken as

$$\psi^{(3)} = e^{imt}\begin{pmatrix} 0 \\ 0 \\ 1 \\ 0 \end{pmatrix} \,, \qquad \psi^{(4)} = e^{imt}\begin{pmatrix} 0 \\ 0 \\ 0 \\ 1 \end{pmatrix} \,. \tag{4.27}$$

These have negative energy: $E_3 = E_4 = -m$.

Now consider the positive energy solutions in a case where the momentum is nonzero but still nonrelativistic: $|\boldsymbol{p}| \ll m$. We can guess that the solution will be of the form

$$\psi(t, \boldsymbol{x}) = e^{-imt}\begin{pmatrix} \varphi(t, \boldsymbol{x}) \\ \chi(t, \boldsymbol{x}) \end{pmatrix} \,, \tag{4.28}$$

where φ and χ are two-component spinors that vary in time slowly compared to e^{-imt}. The full time dependence should be e^{-iEt} where E is the total energy. In the nonrelativistic limit, this

is approximately $E \approx m + |\boldsymbol{p}|^2/2m$ and so the spinors φ and χ should both depend on time as $e^{-i\omega t}$, where

$$\omega = \frac{|\boldsymbol{p}|^2}{2m} \ll m \; . \tag{4.29}$$

Inserting the Ansatz (4.28) into the Dirac equation (4.14) gives

$$i\left[e^{-imt}\begin{pmatrix}\dot{\varphi}\\ \dot{\chi}\end{pmatrix} + (-im)e^{-imt}\begin{pmatrix}\varphi\\ \chi\end{pmatrix}\right] = -ie^{-imt}\sum_{i=1}^{3}\alpha_i\frac{\partial}{\partial x_i}\begin{pmatrix}\varphi\\ \chi\end{pmatrix} + \beta m e^{-imt}\begin{pmatrix}\varphi\\ \chi\end{pmatrix} \; . \tag{4.30}$$

Canceling the factors of e^{-imt} and using Eqs. (4.13) for the matrices α_i and β gives

$$i\begin{pmatrix}\dot{\varphi}\\ \dot{\chi}\end{pmatrix} - im\begin{pmatrix}\varphi\\ \chi\end{pmatrix} = \sum_{i=1}^{3}\begin{pmatrix}0 & \sigma_i\\ \sigma_i & 0\end{pmatrix}\begin{pmatrix}\partial\varphi/\partial x_i\\ \partial\chi/\partial x_i\end{pmatrix} + m\begin{pmatrix}I_2 & 0\\ 0 & -I_2\end{pmatrix}\begin{pmatrix}\varphi\\ \chi\end{pmatrix} \; . \tag{4.31}$$

Now using the momentum operators $p_i = -i\partial/\partial x_i$ (here for simplicity of notation written without hats)

$$m\begin{pmatrix}\varphi\\ \chi\end{pmatrix} + i\begin{pmatrix}\dot{\varphi}\\ \dot{\chi}\end{pmatrix} = \begin{pmatrix}\boldsymbol{\sigma}\cdot\boldsymbol{p} & 0\\ 0 & \boldsymbol{\sigma}\cdot\boldsymbol{p}\end{pmatrix}\begin{pmatrix}\chi\\ \varphi\end{pmatrix} + m\begin{pmatrix}\varphi\\ -\chi\end{pmatrix} \; , \tag{4.32}$$

where $\boldsymbol{\sigma} = (\sigma_1, \sigma_2, \sigma_3)$ is a vector whose elements are the Pauli matrices. For the lower equation,

$$m\chi + i\dot{\chi} = (\boldsymbol{\sigma}\cdot\boldsymbol{p})\varphi - m\chi \; , \tag{4.33}$$

we can try the Ansatz $\varphi, \chi \sim e^{-i\omega t}$ with $\omega = |\boldsymbol{p}|^2/2m$. Using this gives

$$i\dot{\chi} = \omega\chi = (\boldsymbol{\sigma}\cdot\boldsymbol{p})\varphi - 2m\chi \; . \tag{4.34}$$

But since $\omega \ll m$ we find

$$\chi \approx \frac{1}{2m}(\boldsymbol{\sigma}\cdot\boldsymbol{p})\varphi \; . \tag{4.35}$$

By using the Pauli matrices (4.12) we can find

$$\boldsymbol{\sigma}\cdot\boldsymbol{p} = \begin{pmatrix}p_z & px - ip_y\\ p_x + ip_y & -p_z\end{pmatrix} \tag{4.36}$$

and squaring this gives

$$(\boldsymbol{\sigma}\cdot\boldsymbol{p})^2 = |\boldsymbol{p}|^2\begin{pmatrix}1 & 0\\ 0 & 1\end{pmatrix} \; . \tag{4.37}$$

Using this with Eq. (4.35) we find in the nonrelativistic limit that

$$\chi^\dagger\chi = \frac{1}{4m^2}\varphi^\dagger(\boldsymbol{\sigma}\cdot\boldsymbol{p})\cdot(\boldsymbol{\sigma}\cdot\boldsymbol{p})\varphi = \frac{|\boldsymbol{p}|^2}{4m^2}\varphi^\dagger\varphi = \frac{|\boldsymbol{p}|^2/2m}{2m}\varphi^\dagger\varphi\ . \tag{4.38}$$

Thus we find $\chi^\dagger\chi \ll \varphi^\dagger\varphi$ as long as we are in the nonrelativistic regime with $|\boldsymbol{p}|^2/2m \ll m$. The components φ are referred to as the "large" components of the four-component spinor ψ and χ give the "small" components.

From the upper part of Equation (4.32) for φ, one has

$$i\dot{\varphi} = (\boldsymbol{\sigma}\cdot\boldsymbol{p})\chi \approx \frac{(\boldsymbol{\sigma}\cdot\boldsymbol{p})^2}{2m}\varphi\ . \tag{4.39}$$

Now using $(\boldsymbol{\sigma}\cdot\boldsymbol{p})^2 = |\boldsymbol{p}|^2 I_2$ and then identifying the momentum with the operator $\boldsymbol{p} = -i\nabla$ we obtain in the nonrelativistic limit

$$i\frac{\partial\varphi}{\partial t} = -\frac{1}{2m}\nabla^2\varphi\ . \tag{4.40}$$

This of course has the same form as the Schrödinger equation for a free particle, with the difference that the quantity φ is a two-component spinor. As we will see below, the two components can be identified with the two spin states of the electron.

4.4 Dirac equation for particle in an electromagnetic potential

In this section we will extend the Dirac equation for a free-particle to the case of a particle in an electromagnetic field. Suppose the field is determined by a scalar potential ϕ and vector potential $\boldsymbol{A}$. In classical mechanics, one includes an electromagnetic potential into the Hamiltonian for a particle of charge q by making the "minimal substitution" to the potential energy V and momentum $\boldsymbol{p}$ (see, e.g., Ref. [8])

$$V \ \rightarrow\ V + q\phi\ , \tag{4.41}$$

$$\boldsymbol{p} \ \rightarrow\ \boldsymbol{p} - q\boldsymbol{A}\ . \tag{4.42}$$

From Eq. (4.3) we have the free-particle Dirac Hamiltonian

$$H = \boldsymbol{\alpha}\cdot\boldsymbol{p} + m\beta\ , \tag{4.43}$$

where the momentum operator $\boldsymbol{p}$ is $-i\nabla$ and the potential energy is $V = 0$. Making the substitutions (4.41) and (4.42) one obtains the Dirac equation for a particle of charge q in a electromagnetic potentials $(\phi, \boldsymbol{A})$,

$$i\frac{\partial\psi}{\partial t} = H\psi = \left[\boldsymbol{\alpha}\cdot(\boldsymbol{p} - q\boldsymbol{A}) + m\beta + q\phi\right]\psi\ . \tag{4.44}$$

Using the substitutions (4.41) and (4.42) and using the operator $-i\nabla$ for $\boldsymbol{p}$ in Eq. (4.39) for the large component φ gives

$$\begin{aligned} i\dot{\varphi} &= \frac{1}{2m}\left[\boldsymbol{\sigma}\cdot(\boldsymbol{p}-q\boldsymbol{A})\right]^2\varphi + q\phi\varphi \\ &= \frac{1}{2m}\left[\boldsymbol{\sigma}\cdot(-i\nabla - q\boldsymbol{A})\right]\left[\boldsymbol{\sigma}\cdot(-i\nabla - q\boldsymbol{A})\right]\varphi + q\phi\varphi\ . \end{aligned} \tag{4.45}$$

The differential operators inside ∇ act on everything to the right, so that the first one acts on both the vector potential $\boldsymbol{A}$ in the second pair of brackets as well as on φ. After a complicated but straightforward application of the product rule, one finds that these derivatives conspire to give $\nabla\times\boldsymbol{A}$, which is the magnetic field $\boldsymbol{B}$. For an electron with charge $q=-e$ the resulting equation for φ is found to be

$$i\frac{\partial\varphi}{\partial t} = \left[\frac{1}{2m}(-i\nabla + e\boldsymbol{A})^2 - e\phi + \frac{e}{2m}\boldsymbol{\sigma}\cdot\boldsymbol{B}\right]\varphi\ , \tag{4.46}$$

which is called the *Pauli equation* and the term in brackets is the Pauli Hamiltonian. We can identify $H_B = \frac{e}{2m}\boldsymbol{\sigma}\cdot\boldsymbol{B}$ as the term in the Hamiltonian corresponding to the potential energy of the electron's magnetic moment in a magnetic field.

We can compare the Pauli equation to the Schrödinger equation for an electron in an electromagnetic potential,

$$i\frac{\partial\psi_{\rm S}}{\partial t} = \left[\frac{1}{2m}(-i\nabla + e\boldsymbol{A})^2 - e\phi\right]\psi_{\rm S}\ . \tag{4.47}$$

The two equations have a very similar form, but Schrödinger wave function $\psi_{\rm s}$ is a scalar, whereas the Pauli equation is for spinor φ, whose two components can be identified with the two spin states of the electron.

The concept of electron spin had in fact already been introduced in 1925 by Uhlenbeck and Goudsmit [9] to explain the anomalous Zeeman effect. They had described the electron with two-component spinor like φ and its spin was modeled as $\boldsymbol{S} = \frac{1}{2}\boldsymbol{\sigma}$ (in units of $\hbar$), where $\boldsymbol{\sigma}$ are the Pauli matrices. Classically, if a body with mass m and charge $-e$, both distributed in space proportionally, rotates such that it has angular momentum $\boldsymbol{L}$, then this generates a magnetic moment $\boldsymbol{\mu}$ given by (see, e.g., [8])

$$\boldsymbol{\mu} = -\frac{e}{2m}\boldsymbol{L}\ . \tag{4.48}$$

In a magnetic field $\boldsymbol{B}$, this gives a potential energy $V_B = -\boldsymbol{\mu}\cdot\boldsymbol{B}$.

Since the electron is not classical, one would not expect exactly these relations to work in quantum mechanics simply by replacing $\boldsymbol{L}$ with the spin $\boldsymbol{S}$ and including the potential energy term $-\boldsymbol{\mu}\cdot\boldsymbol{B}$ in the Hamiltonian. But it is reasonable to guess that the magnetic momentum of the electron is

$$\boldsymbol{\mu}_{\rm e} = -g\frac{e}{2m}\boldsymbol{S} = -g\frac{e}{2m}\,\tfrac{1}{2}\boldsymbol{\sigma}\ , \tag{4.49}$$

where the dimensionless factor g parametrises our ignorance about how quantum particles behave.

Using these ingredients for $H_B = -\boldsymbol{\mu}_{\rm e} \cdot \boldsymbol{B}$ and comparing with the Pauli equation (4.46), we see that Dirac's relativistic theory of the electron predicts $g = 2$. (Uhlenbeck and Goudsmit and had also arrived at $g = 2$ using different arguments.) Experimentally, the g-factor of the electron can be determined to extremely high accuracy to be (see [10])

$$g_{\rm exp} = 2.00231930436118 \pm 0.00000000000026 \; . \tag{4.50}$$

That the prediction of $g = 2$ agrees with experiment to 1 part in 1000 is in itself a remarkable success, which Dirac had not anticipated. By including higher-order QED effects, the small discrepancy from the measured value is understood to almost perfect precision.

4.5 Covariant form of the Dirac equation

It is possible to rewrite the Dirac equation so that its properties under Lorentz transformations are more transarent by defining the 4×4 *gamma matrices* as

$$\gamma^0 \;=\; \beta = \begin{pmatrix} I_2 & 0 \\ 0 & -I_2 \end{pmatrix} \; , \tag{4.51}$$

$$\gamma^i \;=\; \beta\alpha_i = \begin{pmatrix} 0 & \sigma_i \\ -\sigma_i & 0 \end{pmatrix} \; , \qquad i = 1, 2, 3 \; , \tag{4.52}$$

where I_2 is the 2×2 unit matrix and the σ_i are the Pauli matrices (4.12). These matrices are written with the same notation as a four-vector γ^μ with $\mu = 0, 1, 2, 3$. Furthermore one defines the corresponding lower-index versions by contracting with the metric tensor $g_{\mu\nu}$:

$$\gamma_\mu = g_{\mu\nu}\gamma^\nu \; , \tag{4.53}$$

which gives $\gamma_0 = \gamma^0$ and $\gamma_i = -\gamma^i$, $i = 1, 2, 3$. Despite the similarity with four-vectors, the matrices γ^μ do not change under a Lorentz transformation, but rather have the same form in all reference frames.

It is straightforward to show that the matrices γ^μ satisfy the anticommutation relation

$$\{\gamma^\mu, \gamma^\nu\} \equiv \gamma^\mu\gamma^\nu + \gamma^\nu\gamma^\mu = 2g^{\mu\nu} I_4 \; , \tag{4.54}$$

where I_4 is the 4×4 unit matrix. Note here that $g^{\mu\nu}$ is the (μ, ν) element of g, i.e., it is a number, not a matrix. The relations (4.54) say in effect that $(\gamma^0)^2 = 1$, $(\gamma^i)^2 = -1$ where often we will use 1 to mean a unit matrix of the appropriate dimension and the index i is understood to indicate the components $1, 2, 3$. Some useful properties of gamma matrices are given in Sec. 4.6.

Consider the Dirac equation (4.44) for a particle of mass m and charge q in electromagnetic scalar and vector potentials $(\phi, \boldsymbol{A})$, which we can write as

$$i\left(\frac{\partial\psi}{\partial t}+\boldsymbol{\alpha}\cdot\nabla\psi\right)-m\beta\psi=q(\boldsymbol{\alpha}\cdot\boldsymbol{A}-\phi)\psi\ . \tag{4.55}$$

By multiplying on the left by γ^0 and using the fact that $(\gamma^0)^2=I_4$, one finds

$$\left[i\left(\gamma^0\frac{\partial}{\partial x^0}+\gamma^1\frac{\partial}{\partial x^1}+\gamma^2\frac{\partial}{\partial x^2}+\gamma^3\frac{\partial}{\partial x^3}\right)-mI_4\right]\psi=-q(\gamma^0\phi-\gamma^1A^1-\gamma^2A^2-\gamma^3A^3)\psi\ . \tag{4.56}$$

Defining the contravariant four-vector potential $A^\mu=(\phi,\boldsymbol{A})$, so that the corresponding covariant vector is $A_\mu=(\phi,-\boldsymbol{A})$, the Dirac equation becomes

$$(i\gamma^\mu\partial_\mu-m)\psi(x)=q\gamma^\mu A_\mu\ , \tag{4.57}$$

where $\partial_\mu=\left(\frac{\partial}{\partial t},\nabla\right)$ as introduced in Sec. 2.5.

To write the Dirac equation in an even more compact way we can use the Feynman "slash" notation, where for any four-vector-like quantity a^μ we define

$$\not{a}=\gamma_\mu a^\mu=\gamma^\mu a_\mu\ . \tag{4.58}$$

This notation also works for the differential operators ∂_μ, so that $\not{\partial}=\gamma^\mu\partial_\mu$. In this way the Dirac equation for particle in an electromagnetic potential becomes

$$(i\not{\partial}-m)\psi(x)=q\not{A}\psi(x)\ . \tag{4.59}$$

4.6 Properties of gamma matrices

We will encounter many calculations that involve combinations of gamma matrices γ^μ. These can be simplified using relations that follow from the defining anticommutation relations (4.54) (an example of a *Clifford algebra*),

$$\{\gamma^\mu,\gamma^\nu\}=2g^{\mu\nu}I_4\ . \tag{4.60}$$

Often one encounters combinations of gamma matrices contracted with others, a simple example being $\gamma^\mu\gamma_\mu$. To put this in a form that can be directly related to the anticommutation relations we raise the lowered index by inserting a factor of the metric tensor and then express $\gamma^\mu\gamma^\nu$ as the sum of symmetric and antisymmetric parts:

$$\gamma^\mu\gamma_\mu=g_{\mu\nu}\gamma^\mu\gamma^\nu=g_{\mu\nu}\left[\frac{1}{2}(\gamma^\mu\gamma^\nu+\gamma^\nu\gamma^\mu)+\frac{1}{2}(\gamma^\mu\gamma^\nu-\gamma^\nu\gamma^\mu)\right]\ . \tag{4.61}$$

Next we use the general result that a symmetric tensor contracted with an antisymmetric one is zero. To see this, suppose $s^{\mu\nu}$ is symmetric ($s^{\mu\nu}=s^{\nu\mu}$) and $a^{\mu\nu}$ is antisymmetric ($a^{\mu\nu}=-a^{\nu\mu}$). Then

$$\begin{aligned} s_{\mu\nu}a^{\mu\nu} &= -s_{\nu\mu}a^{\nu\mu} \\ &= -s_{\mu\nu}a^{\mu\nu} \\ &= 0 \,, \end{aligned} \tag{4.62}$$

where in going from the first to the second line we simply relabeled the indices by swapping μ and ν.

Returning to Eq. (4.61), we see that $g_{\mu\nu}$ is symmetric, and thus contracting with the antisymmetric piece $(\gamma^\mu\gamma^\nu - \gamma^\nu\gamma^\mu)$ gives zero. We therefore find

$$\gamma^\mu\gamma_\mu = g_{\mu\nu}\frac{1}{2}(\gamma^\mu\gamma^\nu + \gamma^\nu\gamma^\mu) = g_{\mu\nu}g^{\mu\nu}I_4 = 4I_4 \,, \tag{4.63}$$

where the second equality follows from the anticommutation relation (4.54) and the final one from $g_{\mu\nu}g^{\mu\nu} = \delta_\mu{}^\mu = 4$.

In many calculations we will need the adjoint (complex-conjugate transpose) matrices $\gamma^{\mu\dagger} \equiv (\gamma^\mu)^{*T}$. For these one finds

$$\gamma^{0\dagger} = \gamma^0 \,, \tag{4.64}$$

$$\gamma^{i\dagger} = -\gamma^i \,, \qquad i = 1,2,3 \,. \tag{4.65}$$

The adjoints can be summarised with the useful relation

$$\gamma^{\mu\dagger} = \gamma^0\gamma^\mu\gamma^0 \,. \tag{4.66}$$

This can be derived from the specific representation of the matrices in Eqs. (4.51) and (4.52), but one can show that it holds in general for any set of four matrices that obey the anticommutation relations (4.54).

Here we provide without proof several important properties of gamma matrices:

$$\gamma^\mu\gamma_\mu = 4I_4 \,, \tag{4.67}$$

$$\gamma^\mu\gamma^\nu\gamma_\mu = -2\gamma^\nu \,, \tag{4.68}$$

$$\gamma^\mu\gamma^\nu\gamma^\rho\gamma_\mu = 4g^{\nu\rho}I_4 \,, \tag{4.69}$$

$$\gamma^\mu\gamma^\nu\gamma^\rho\gamma^\sigma\gamma_\mu = -2\gamma^\sigma\gamma^\rho\gamma^\nu \,. \tag{4.70}$$

In our discussion of weak interactions we will encounter the matrix γ^5, defined as

$$\gamma^5 = i\gamma^0\gamma^1\gamma^2\gamma^3 \,. \tag{4.71}$$

Its important properties include

$$\gamma^{5\,\dagger} = \gamma^5 \,, \tag{4.72}$$

$$(\gamma^5)^2 = I_4 \,, \tag{4.73}$$

$$\{\gamma^5, \gamma^\mu\} = 0 \,. \tag{4.74}$$

4.7 Solving the Dirac Equation for a free particle

The goal is to find the solutions to the Dirac equation for a free particle of mass m,

$$(i\partial\!\!\!/ - m)\psi(x) = 0 \,, \tag{4.75}$$

where the slash notation is $\partial\!\!\!/ = \gamma^\mu \partial_\mu$, γ^μ are the 4×4 Dirac gamma matrices and $\psi(x)$ is a four-component Dirac spinor.

4.7.1 Components of Dirac equation as solutions to the Klein-Gordon equation

As a first step, we will show that all components of ψ individually satisfy the Klein-Gordon equation. To do this we apply $(i\partial\!\!\!/ + m)$ to Eq. (4.75),

$$(i\partial\!\!\!/ + m)(i\partial\!\!\!/ - m)\psi(x) = 0 \,, \tag{4.76}$$

which gives

$$(\partial\!\!\!/\partial\!\!\!/ + m^2)\psi(x) = (\gamma^\mu\gamma^\nu\partial_\mu\partial_\nu + m^2)\psi(x) = 0 \,. \tag{4.77}$$

The derivatives $\partial_\mu\partial_\nu$ are symmetric under interchange of μ and ν, and this is contracted with $\gamma^\mu\gamma^\nu$, which can written as a sum of symmetric and antisymmetric parts as

$$\gamma^\mu\gamma^\nu = \frac{1}{2}(\gamma^\mu\gamma^\nu + \gamma^\nu\gamma^\mu) + \frac{1}{2}(\gamma^\mu\gamma^\nu - \gamma^\nu\gamma^\mu) = \frac{1}{2}\{\gamma^\mu, \gamma^\nu\} + \frac{1}{2}[\gamma^\mu, \gamma^\nu] \,. \tag{4.78}$$

The commutator is antisymmetric in μ and ν, and so contracting with the symmetric $\partial_\mu\partial_\nu$ gives zero. For the anticommutator we can use $\{\gamma^\mu, \gamma^\nu\} = 2g^{\mu\nu}I$. We therefore find

$$\left[\tfrac{1}{2}(\gamma^\mu\gamma^\nu + \gamma^\nu\gamma^\mu)\partial_\mu\partial_\nu + m^2\right]\psi = (g^{\mu\nu}\partial_\mu\partial_\nu + m^2)\psi = (\partial_\mu\partial^\mu + m^2)\psi = 0 \,. \tag{4.79}$$

This actually represents four equations, i.e., a 4×4 matrix multiplying the four-component spinor ψ. Thus each component of ψ individually satisfies the Klein-Gordon equation:

$$(\partial_\mu\partial^\mu + m^2)\psi_i = 0 \,, \quad i = 1, \ldots 4 \,. \tag{4.80}$$

4.7.2 Dirac spinors u and v

Since each component of the solution to the Dirac equation satisfies the Klein-Gordon equation (4.80), we will have four linearly independent plane-wave solutions for $\psi(x)$ that can be written

$$\psi_+(x) = u_s(p)e^{-ip\cdot x} , \tag{4.81}$$

$$\psi_-(x) = v_s(p)e^{ip\cdot x} , \tag{4.82}$$

where $s = 1, 2$ is an index that we will later associate with the spin state and as usual $p \cdot x = Et - \boldsymbol{p} \cdot \boldsymbol{x}$. The solutions have eigenvalues of the energy and momentum operators $\hat{E} = i\partial/\partial t$ and $\hat{\boldsymbol{p}} = -i\nabla$

$$\hat{E}\psi_+ = E\psi_+ , \qquad \hat{\boldsymbol{p}}\psi_+ = \boldsymbol{p}\psi_+ , \tag{4.83}$$

$$\hat{E}\psi_- = -E\psi_- , \qquad \hat{\boldsymbol{p}}\psi_- = -\boldsymbol{p}\psi_- . \tag{4.84}$$

In Sec. 4.8 we will see that the solutions ψ_- can be interpreted as antiparticles after the replacement $(E, \boldsymbol{p}) \to (-E, -\boldsymbol{p})$. Therefore we will take two of the four solutions to represent particles having the space-time dependence of $\psi_+ \sim e^{-ip\cdot x}$, and two others representing antiparticles to follow $\psi_- \sim e^{ip\cdot x}$. We will then find corresponding functions of p that multiply the exponentials: $u_1(p)$ and $u_2(p)$ for ψ_+ and $v_1(p)$ and $v_2(p)$ for ψ_-. In all cases we treat $p = (E, \boldsymbol{p})$ as representing the physical energy and momentum of the particle or antiparticle. The symbol E is thus always positive and for a free particle means $E = +\sqrt{|\boldsymbol{p}|^2 + m^2}$.

By substituting ψ_+ into the Dirac equation and temporarily suppressing the spin index we find

$$(i\partial\!\!\!/ - m)u(p)e^{-ip\cdot x} = 0 , \tag{4.85}$$

which gives

$$(i(-ip\!\!\!/) - m)u(p)e^{-ip\cdot x} = 0 , \tag{4.86}$$

The exponential term can be canceled and the analogous procedure carried out for ψ_-, leading to the equations for $u(p)$ and $v(p)$,

$$(p\!\!\!/ - m)u(p) = 0 , \tag{4.87}$$

$$(p\!\!\!/ + m)v(p) = 0 . \tag{4.88}$$

In a similar way one finds for the Dirac adjoint spinors $\overline{u} = u^\dagger\gamma^0$ and $\overline{v} = v^\dagger\gamma^0$

$$\overline{u}(p\!\!\!/ - m) = 0 , \tag{4.89}$$

$$\overline{v}(p\!\!\!/ + m) = 0 . \tag{4.90}$$

4.7.3 Rest-frame solutions

First consider the rest frame, where the particle's four-momentum is $p^\mu = (p^0, 0, 0, 0) = (m, \mathbf{0})$. In this frame we want to solve Eqs. (4.87) and (4.88). Using $\not{p} = \gamma^\mu p_\mu = m\gamma^0$ and canceling a factor of m we obtain

$$(\gamma^0 - I)u(m, \mathbf{0}) = 0 \,, \tag{4.91}$$

$$(\gamma^0 + I)v(m, \mathbf{0}) = 0 \,. \tag{4.92}$$

In the Dirac representation for the gamma matrices, γ^0 is

$$\gamma^0 = \begin{pmatrix} 1 & 0 & 0 & 0 \\ 0 & 1 & 0 & 0 \\ 0 & 0 & -1 & 0 \\ 0 & 0 & 0 & -1 \end{pmatrix} \,, \tag{4.93}$$

so that equation (4.91) becomes

$$\begin{pmatrix} 0 & 0 & 0 & 0 \\ 0 & 0 & 0 & 0 \\ 0 & 0 & -2 & 0 \\ 0 & 0 & 0 & -2 \end{pmatrix} \begin{pmatrix} a \\ b \\ c \\ d \end{pmatrix} = 0 \,, \tag{4.94}$$

where a, b, c and d are the four components of u that we want to find. Equation (4.94) is solved for arbitrary a and b with $c = d = 0$. We thus can choose two linearly independent solutions to be

$$u_s(m, \mathbf{0}) = \begin{pmatrix} a \\ b \\ c \\ d \end{pmatrix} = N \begin{pmatrix} \varphi_s \\ 0 \end{pmatrix} \,, \tag{4.95}$$

where N is a normalization constant and the index $s = 1, 2$ labels the two independent two-component *Weyl* spinors. These are chosen to be orthogonal and normalized to unity, i.e., $\varphi_r^\dagger \varphi_s = \delta_{rs}$. We can take φ_1 and φ_2 to be, for example,

$$\varphi_1 = \begin{pmatrix} 1 \\ 0 \end{pmatrix} \,, \qquad \varphi_2 = \begin{pmatrix} 0 \\ 1 \end{pmatrix} \,. \tag{4.96}$$

In a similar way one can find the rest-frame solution for the spinor v_s to be

$$v_s(m, \mathbf{0}) = N \begin{pmatrix} 0 \\ \chi_s \end{pmatrix} \,, \tag{4.97}$$

where the two-component spinors χ_s can be taken as

$$\chi_1 = \begin{pmatrix} 0 \\ 1 \end{pmatrix} , \qquad \chi_2 = \begin{pmatrix} 1 \\ 0 \end{pmatrix} . \tag{4.98}$$

For χ_s the order of the 1 and 0 in the upper and lower elements is reversed compared to φ_s; this is so that we can identify later the solutions u_1 and v_1 as representing particles with spin parallel to the z axis. Note that fixing the normalization of the Weyl spinors such that $\varphi_r^\dagger \varphi_s = \chi_r^\dagger \chi_s = \delta_{rs}$ does not fix the normalization of u_s or v_s.

4.7.4 Solutions for four-momentum p

Before dealing with the normalization, we can first work out the solutions in a reference frame where the particle has four-momentum p. That is, we want to find the solutions $u_s(p)$ and $v_s(p)$ to Eqs. (4.87) and (4.88). These can be derived from the rest-frame solutions as

$$u_s(p) = (\not{p} + m) u_s(m, \mathbf{0}) , \tag{4.99}$$

$$v_s(p) = (\not{p} - m) v_s(m, \mathbf{0}) . \tag{4.100}$$

To see that this actually gives the correction solutions, we can apply $(\not{p} - m)$ to the left-hand side of Eq. (4.99):

$$(\not{p} - m) u_s(p) = (\not{p} - m)(\not{p} + m) u_s(m, \mathbf{0}) \tag{4.101}$$

$$= (\not{p}\not{p} - m^2) u_s(m, \mathbf{0}) \tag{4.102}$$

$$= (p^2 - m^2) u_s(m, \mathbf{0}) \tag{4.103}$$

$$= 0 . \tag{4.104}$$

Here we used $\not{p}\not{p} = p_\mu p_\nu \gamma^\mu \gamma^\nu = p^2$, which can be easily verified by using the anticommutation properties of the gamma matrices. The final equality above follows from the fact that $p^2 = m^2$ for a free on-shell particle. The analogous result follows for $v_s(p)$ and thus Eqs. (4.99) and (4.100) allow one to obtain the solutions for a particle with four-momentum p directly from the rest-frame solutions.

To write down the solutions explicitly we can use the Dirac representation of the gamma matrices, where

$$\gamma^0 = \begin{pmatrix} I_2 & 0 \\ 0 & -I_2 \end{pmatrix} , \qquad \gamma^i = \begin{pmatrix} 0 & \sigma_i \\ -\sigma_i & 0 \end{pmatrix} , \quad i = 1, 2, 3 , \tag{4.105}$$

and therefore $\not{p} = \gamma^\mu p_\mu$ is

$$\not{p} = \begin{pmatrix} p^0 & -\boldsymbol{\sigma}\cdot\mathbf{p} \\ \boldsymbol{\sigma}\cdot\mathbf{p} & -p^0 \end{pmatrix} . \tag{4.106}$$

The *unnormalized* solutions are thus found from Eqs. (4.99) and (4.100) to be

$$u_s(p) = \begin{pmatrix} p^0+m & -\boldsymbol{\sigma}\cdot\mathbf{p} \\ \boldsymbol{\sigma}\cdot\mathbf{p} & -p^0+m \end{pmatrix} \begin{pmatrix} \varphi_s \\ 0 \end{pmatrix} = \begin{pmatrix} (p^0+m)\varphi_s \\ (\boldsymbol{\sigma}\cdot\mathbf{p})\varphi_s \end{pmatrix} , \tag{4.107}$$

$$v_s(p) = \begin{pmatrix} p^0-m & -\boldsymbol{\sigma}\cdot\mathbf{p} \\ \boldsymbol{\sigma}\cdot\mathbf{p} & -p^0-m \end{pmatrix} \begin{pmatrix} 0 \\ \chi_s \end{pmatrix} = \begin{pmatrix} (\boldsymbol{\sigma}\cdot\mathbf{p})\chi_s \\ (p^0+m)\chi_s \end{pmatrix} . \tag{4.108}$$

4.7.5 Normalization of spinors

To choose the normalization of the Dirac spinors we recall that $\rho = \psi^\dagger\psi$ will be interpreted as a probability density, and furthermore this density is the zeroth component of the four-vector current $j^\mu = (\rho, \mathbf{j})$. We need the probability to find the particle inside a specified volume to be Lorentz invariant. This probability is

$$P = \int d^3x\, j^0(x) = \int d^3x\, \psi^\dagger(x)\psi(x) = \begin{cases} \int d^3x\, u^\dagger u & \text{for } \psi_+ \\ \int d^3x\, v^\dagger v & \text{for } \psi_- \end{cases} . \tag{4.109}$$

One can show (see, e.g., Ref. [79]) that this will be Lorentz invariant if $\psi^\dagger\psi$ transforms like the zeroth component of a four-vector. And the only four-vector on which this can depend is $p = (p^0, \mathbf{p})$, i.e., the four-momentum of the particle. We therefore take $u^\dagger u \propto v^\dagger v \propto p^0$. A widely used convention that we will follow is to choose the the normalization such that

$$u_r^\dagger u_s = v_r^\dagger v_s = 2E\delta_{rs} , \tag{4.110}$$

where $E = +\sqrt{|\mathbf{p}|^2 + m^2}$ is positive. (The convention $u_r^\dagger u_s = v_r^\dagger v_s = (E/m)\delta_{rs}$ is also used.)

The normalization condition also takes on a simple form when expressed in terms of the Dirac adjoint spinors $\overline{u} = u^\dagger\gamma^0$ and $\overline{v} = v^\dagger\gamma^0$. One can easily show that (4.110) implies

$$\overline{u}_r u_s = 2m\delta_{rs} , \tag{4.111}$$

$$\overline{v}_r v_s = -2m\delta_{rs} . \tag{4.112}$$

Using this normalization and the Pauli matrices for the terms involving $\boldsymbol{\sigma}\cdot\mathbf{p}$ allows us to write the complete solutions for the spinors u and v as

$$u_1(p) = \sqrt{E+m}\begin{pmatrix} 1 \\ 0 \\ \frac{p_z}{E+m} \\ \frac{p_x+ip_y}{E+m} \end{pmatrix} , \qquad u_2(p) = \sqrt{E+m}\begin{pmatrix} 0 \\ 1 \\ \frac{p_x-ip_y}{E+m} \\ \frac{-p_z}{E+m} \end{pmatrix} , \tag{4.113}$$

$$v_1(p) = \sqrt{E+m}\begin{pmatrix} \frac{p_x - ip_y}{E+m} \\ \frac{-p_z}{E+m} \\ 0 \\ 1 \end{pmatrix}, \qquad v_2(p) = \sqrt{E+m}\begin{pmatrix} \frac{p_z}{E+m} \\ \frac{p_x + ip_y}{E+m} \\ 1 \\ 0 \end{pmatrix}. \tag{4.114}$$

The full solutions to the Dirac equation are obtained by combining the spinors u_s or v_s with the exponential term $e^{-ip\cdot x}$ or $e^{ip\cdot x}$, respectively, according to Eqs. (4.81) and (4.82). The solutions also implicitly contain a factor $1/\sqrt{V}$ to be normalized in a volume V. For now it is convenient to drop this factor, i.e., we take $V = 1$.

4.8 Interpretation of negative energy solutions

As seen above, the Dirac equation for a free particle has solutions

$$\psi_+(x) = u(p)e^{-ip\cdot x}, \tag{4.115}$$

$$\psi_-(x) = v(p)e^{ip\cdot x}, \tag{4.116}$$

with energy greater than m for ψ_+ and less than $-m$ for ψ_-, where $p \cdot x = Et - \boldsymbol{p}\cdot\boldsymbol{x}$ with $E = \sqrt{|\boldsymbol{p}|^2 + m^2}$ always positive. Dirac's first attempt to interpret the solutions was to say that all negative energy energy states were filled, forming what he called the *sea*, as illustrated in Fig. 4.1. Because of the Pauli exclusion principle, no transition would be possible to a negative energy state. If a negative energy level were to be free it would constitute a "hole", whose motion through the sea would result in net motion of positive charge, namely, an antiparticle.

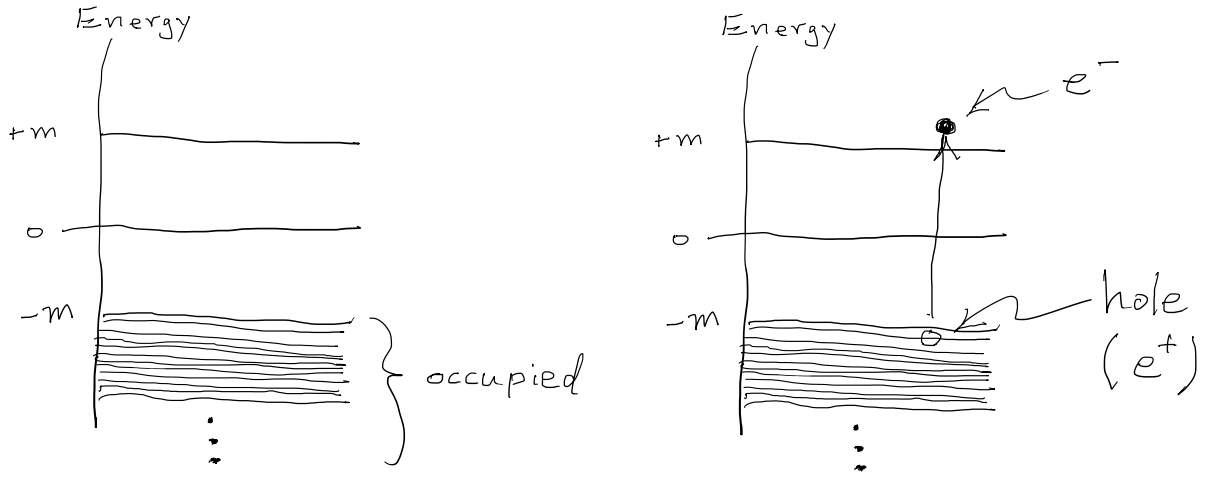

Figure 4.1: Energy levels corresponding to the solutions of the Dirac equation with (left) all negative energy states are filled and (right) a particle in a negative energy state promoted to a positive energy electron by adding energy $E \geq 2m$, leaving behind a hole.

Transition of a positive energy electron to an empty negative energy state would be accompanied by emission of photons with total energy at least twice the electron's rest mass energy $2m_{\mathrm{e}}$. This would correspond to annihilation of an antiparticle (a positron) with an electron, which we recognise as the experimentally observed reaction $e^+e^- \to \gamma\gamma$. Creation of an open negative energy state would require addition of an energy $2m_{\mathrm{e}}$, resulting in a positive energy electron along with a positive energy positron, i.e., the reaction $\gamma\gamma \to e^+e^-$.

The Dirac sea picture was, however, unable to explain the negative energy solutions for bosons, which we also found from the Klein-Gordon equation. This view has therefore been abandoned in particle physics, although its analog is used successfully to describe electron/hole pairs in a semiconductor.

The next attempt to interpret negative energy solutions is due to Stückelberg [12] and Feynman [13, 14]. In their view, a negative energy solution is seen as propagating backwards in time and interpreted as positive-energy antiparticle propagating forwards in time. This emerges naturally from the time dependence of plane-wave solutions, since

$$\psi_- \sim e^{iEt} = e^{i(-E)(-t)} \ . \tag{4.117}$$

This interpretation also works for bosons, and provides a consistent description of scattering processes including pair creation and annihilation. More precisely, the Feynman-Stückelberg interpretation postulates:

- Emission of an antiparticle with four-momentum p^μ is equivalent to absorption of a particle with $-p^\mu$.
- Absorption of an antiparticle with p^μ is equivalent to emission of a particle with $-p^\mu$.

It was subsequently shown by Dyson [15] that this view is mathematically equivalent to that of Quantum Field Theory, whereby particles are viewed as quantised excitations of a field, which can be created and destroyed. Although QFT is now usually taken as the more fundamental starting point, the Feynman-Stückelberg picture allows a fast route to the basic rules for Feynman diagrams and predictions for observable cross sections and decay rates.

Chapter 5

Covariance of Relativistic Wave Equations

In this chapter we will examine how the solutions to the relativistic wave equations change under a Lorentz transformation. We will find that after the transformation they are solutions to an equation that has the same form as the original one. They are in this sense said to be *covariant*.

5.1 Covariance of Maxwell's equations

The inhomogeneous Maxwell equations (3.12), can be expressed as

$$\partial_\mu F^{\mu\nu}(x) = j^\nu(x) \,, \tag{5.1}$$

where the field-strength tensor is $F^{\mu\nu} = \partial^\mu A^\nu - \partial^\nu A^\mu$ and $j^\nu = (\rho, \mathbf{j})$ is the four-vector current. We can see by inspection that both sides of the equation transform as Lorentz four-vectors and therefore it must be that the equation has the same form under a Lorentz transformation. Nevertheless it is interesting to see this explicitly. Two Lorentz frames are related by $x'^\mu = \Lambda^\mu{}_\nu x^\nu$ and therefore $x^\mu = (\Lambda^{-1})^\mu{}_\alpha x'^\alpha$. We can write down Eq. (5.1) in the primed frame, for which we need

$$\partial'_\mu = \frac{\partial}{\partial x'^\mu} = \frac{\partial x^\alpha}{\partial x'^\mu}\frac{\partial}{\partial x^\alpha} = (\Lambda^{-1})^\alpha{}_\mu \partial_\alpha \,. \tag{5.2}$$

Using this and the fact that the potential A^μ transforms as a four-vector, i.e., $A'^\mu(x') = \Lambda^\mu{}_\nu A^\nu(x)$, one can find that the field strength tensor transforms as

$$F'^{\mu\nu}(x') = \Lambda^\mu{}_\rho \Lambda^\nu{}_\sigma F^{\rho\sigma}(x) \,. \tag{5.3}$$

The left-hand side of Eq. (5.1) written in the primed frame becomes

$$\partial'_\mu F'^{\mu\nu}(x') = (\Lambda^{-1})^\alpha{}_\mu \partial_\alpha \left(\Lambda^\mu{}_\rho \Lambda^\nu{}_\sigma F^{\rho\sigma}(x)\right) \,. \tag{5.4}$$

The Lorentz transformation matrices are constants and so can be brought outside the derivative to give

$$\partial'_\mu F'^{\mu\nu}(x') = \delta^\alpha{}_\rho \Lambda^\nu{}_\sigma \partial_\alpha F^{\rho\sigma}(x) = \Lambda^\nu{}_\sigma \partial_\rho F^{\rho\sigma}(x) \,, \tag{5.5}$$

where the first equality follows from contracting Λ^{-1} and Λ. Then using the inhomogeneous Maxwell equation (5.1) in the right-hand side of Eq. (5.5) gives

$$\partial'_\mu F'^{\mu\nu}(x') = \Lambda^\nu{}_\sigma j^\sigma(x) = j'^\nu(x') \,, \tag{5.6}$$

where final equality follows from the fact that the electromagnetic current transforms as a four-vector. This confirms that the inhomogeneous Maxwell equation has the same form in the primed and unprimed frames, provided the potential A^μ and current j^μ transform as four-vectors. In an analogous manner, covariance can also be demonstrated for the homogeneous Maxwell equation (3.11).

5.2 Covariance of the Klein-Gordon equation

Consider two reference frames related by a Lorentz transformation $x' = \Lambda x$. In the original frame, the Klein-Gordon equation for a particle of mass m is

$$(\partial_\mu \partial^\mu + m^2)\varphi(x) = 0 \,. \tag{5.7}$$

We assume that the solution $\varphi(x)$ is a Lorentz scalar, i.e., in the primed frame, the coordinates and solution transform such that

$$\varphi'(x') = \varphi(x) \,. \tag{5.8}$$

Here proof of covariance of the equation is made almost trivial by the relativistic invariance of the differential operator $\partial_\mu \partial^\mu$. Following Sec. 2.5 one can show $\partial'_\mu \partial'^\mu = \partial_\mu \partial^\mu$, and therefore in the primed frame one finds

$$(\partial'_\mu \partial'^\mu + m^2)\varphi'(x') = 0 \,. \tag{5.9}$$

Thus we say that the Klein-Gordon equation is covariant, and this statement has two parts: first, we have a relation between the solution in the original and primed frames; here it is simply $\varphi'(x') = \varphi(x)$, and second, the equation in the primed frame has the same form as the one in the original frame.

5.3 Covariance of the Dirac equation

Consider two reference frames related by a Lorentz transformation of the coordinates $x' = \Lambda x$. In the original frame, consider a free particle described by the Dirac equation:

$$(i\gamma^\mu \partial_\mu - m)\psi(x) = 0 \; . \tag{5.10}$$

In the primed frame, both the coordinates and ψ will transform, but we want them to satisfy an equation of the same form, i.e.,

$$(i\gamma^\mu \partial'_\mu - m)\psi'(x') = 0 \; . \tag{5.11}$$

Notice that the γ^μ do not transform. They are coefficients that determine the coupled differential equations for the components of ψ, and we do not change them in the transformed frame.[1]

We will say that the Dirac equation is covariant provided we can find the rule that relates $\psi(x)$ to $\psi'(x')$, where $x' = \Lambda x$ for an arbitrary Lorentz transformation Λ. We suppose that this relation is of the form

$$\psi'(x') = S(\Lambda)\psi(x) = S(\Lambda)\psi(\Lambda^{-1}x') \; , \tag{5.12}$$

where $S(\Lambda)$ is a 4×4 matrix that multiplies the four-component spinor $\psi(x)$.

Since the Lorentz transformation is reversible with $x = \Lambda^{-1}x'$, the inverse of the transformation matrix S must be what one would find by transforming from primed frame to the original one, and therefore

$$S^{-1}(\Lambda) = S(\Lambda^{-1}) \; . \tag{5.13}$$

The question is, then, how do we find S for an arbitrary Lorentz transformation Λ? In the original frame, the Dirac equation (5.10) holds. We can insert $\psi(x) = S^{-1}(\Lambda)\psi'(x')$ and express ∂_μ in terms of the primed coordinates as

$$\partial_\mu = \frac{\partial}{\partial x^\mu} = \frac{\partial x'^\nu}{\partial x^\mu}\frac{\partial}{\partial x'^\nu} = \Lambda^\nu{}_\mu \partial'_\nu \tag{5.14}$$

to find

$$(i\gamma^\mu \Lambda^\nu{}_\mu \partial'_\nu - m)S^{-1}(\Lambda)\psi'(x') = 0 \; . \tag{5.15}$$

Next, multiply Eq. (5.15) on the left by $S(\Lambda)$ and use the fact that $\gamma^\mu \Lambda^\nu{}_\mu = \Lambda^\nu{}_\mu \gamma^\mu$, since γ^μ is a 4×4 matrix but $\Lambda^\nu{}_\mu$ is a number (the (μ, ν) element of the matrix Λ). This gives

$$(iS\Lambda^\nu{}_\mu \gamma^\mu S^{-1}\partial'_\nu - m)\psi'(x') = 0 \; , \tag{5.16}$$

where S means $S(\Lambda)$. This will have the same form as the original Dirac equation (5.10) provided

$$S\Lambda^\nu{}_\mu \gamma^\mu S^{-1} = \gamma^\nu \; . \tag{5.17}$$

If this condition holds, then Eq. (5.16) becomes

[1] There is an equivalent way of looking at the problem taken by some texts whereby the γ^μ do transform but we here we will take the more commonly used approach whereby the γ^μ remain unchanged.

$$(i\gamma^\nu \partial'_\nu - m)\psi'(x') = 0 \ , \tag{5.18}$$

and the Dirac equation is thus said to be Lorentz covariant. Note that the gamma matrices themselves do not transform; there is no prime on γ^ν in Eq. (5.18). By multiplying on the left and right by S^{-1} and S, respectively, and relabeling the indices, Eq. (5.17) can be written in an equivalent and sometimes more useful form as

$$S^{-1}\gamma^\mu S = \Lambda^\mu{}_\nu \gamma^\nu \ . \tag{5.19}$$

To find the matrix S that corresponds to a given Λ, we can make use of the exponential form of the Lorentz transformation derived in Sec. 2.6. We found that a Lorentz transformation can be written

$$\Lambda = \exp\left(-\frac{1}{2}\omega_{\alpha\beta}L^{\alpha\beta}\right) \ , \tag{5.20}$$

where each element of $L^{\alpha\beta}$ is a 4×4 matrix corresponding to a rotation or boost and the constants $\omega_{\alpha\beta}$ encode what mixture of these matrices is included. We claim that the spinor transformation S corresponding to a Lorentz transformation Λ is

$$S = \exp\left(-\frac{1}{2}\omega_{\alpha\beta}\Sigma^{\alpha\beta}\right) \ , \tag{5.21}$$

where the constants $\omega_{\alpha\beta}$ are the same as those that define the Lorentz transformation through Eq. (5.20) and each element of $\Sigma^{\alpha\beta}$ is a 4×4 matrix proportional to the commutator of Dirac gamma matrices given by

$$\Sigma^{\alpha\beta} = \frac{1}{4}[\gamma^\alpha, \gamma^\beta] \ . \tag{5.22}$$

To prove this result, one can first show that

$$[\Sigma^{\alpha\beta}, \gamma^\mu] = \gamma^\alpha g^{\beta\mu} - \gamma^\beta g^{\mu\alpha} \ . \tag{5.23}$$

For $\alpha = \beta$ both the left- and right-hand sides reduce to zero; for $\alpha \neq \beta$ the result follows after expanding the commutator and commuting gamma matrices using $\{\gamma^\alpha, \gamma^\beta\} = 2g^{\alpha\beta}I_4$.

Next, suppose the coefficients $\omega_{\alpha\beta}$ are infinitesimal and so we can expand

$$\Lambda = \exp\left(\frac{1}{2}\omega_{\alpha\beta}L^{\alpha\beta}\right) \approx 1 + \frac{1}{2}\omega_{\alpha\beta}L^{\alpha\beta} \ , \tag{5.24}$$

$$S = \exp\left(\frac{1}{2}\omega_{\alpha\beta}\Sigma^{\alpha\beta}\right) \approx 1 + \frac{1}{2}\omega_{\alpha\beta}\Sigma^{\alpha\beta} \ . \tag{5.25}$$

Using these in the requirement for Lorentz covariance (5.19) gives

$$-[\Sigma^{\alpha\beta}, \gamma^\mu] = (L^{\alpha\beta})^\mu{}_\nu \gamma^\nu = (g^{\alpha\mu}\delta^\beta{}_\nu - g^{\beta\mu}\delta^\alpha{}_\nu)\gamma^\nu \ , \tag{5.26}$$

where the second equality follows from Eq. (2.52) for the generators of a Lorentz transformation. But from Eq. (5.23) we see that the final expression in Eq. (5.26) is none other than $-[\Sigma^{\alpha\beta}, \gamma^\mu]$, and so the equality is confirmed to hold. Extension of the result to the case of non-infinitesimal $\omega_{\alpha\beta}$ follows from the group property of the Lorentz transformations, whereby a finite transformation is found from repeated application of infinitesimal ones.

5.3.1 Rotations and spin

Using Eqs. (5.21) for S together with Eqs. (2.54) and (2.55) for the coefficients $\omega_{\alpha\beta}$ we can easily write down the transformation for a spinor corresponding to an arbitrary rotation or boost. For example, consider a rotation of the coordinate system by an angle θ about the x^3 axis. The Lorentz transformation $\Lambda_{\rm R}$ was given in Eq. (2.18) and can also be written in the exponential form of Eq. (5.20) using the parameters $\omega_{12} = -\omega_{21} = \theta$ and all other $\omega_{\alpha\beta} = 0$. Thus the argument of the exponential in the equation for S contains only

$$\Sigma^{12} = \frac{1}{4}(\gamma^1\gamma^2 - \gamma^2\gamma^1) = \frac{1}{2}\gamma^1\gamma^2 \tag{5.27}$$

and $\Sigma^{21} = -\Sigma^{12}$. The spinor transformation matrix is therefore

$$S_R(\theta) = \exp\left(-\frac{1}{2}(\omega_{12}\Sigma^{12} + \omega_{21}\Sigma^{21})\right) = \exp\left(-\frac{\theta}{2}\gamma^1\gamma^2\right) \ . \tag{5.28}$$

The product of matrices $\gamma^1\gamma^2$ has the interesting property

$$(\gamma^1\gamma^2)^2 = \gamma^1\gamma^2\gamma^1\gamma^2 = -\gamma^1\gamma^1\gamma^2\gamma^2 = -I_4 \ , \tag{5.29}$$

where in the second equality we used $\gamma^2\gamma^1 = -\gamma^1\gamma^2$, and for the final one $(\gamma^1)^2 = (\gamma^2)^2 = I_4$. Thus the matrix $\gamma^1\gamma^2$ behaves like the imaginary number i in that its square gives the negative of unity. As a result one finds

$$S_R(\theta) = I_4 \cos\frac{\theta}{2} - \gamma^1\gamma^2 \sin\frac{\theta}{2} \ . \tag{5.30}$$

This result can be confirmed by substituting the Taylor series expansions for sine and cosine on the right-hand side, whose combination leads to the exponential of Eq. (5.28). It is left as an exercise to show the following useful property for the inverse matrix:

$$S_R^{-1} = \gamma^0 S_R^\dagger \gamma^0 \ . \tag{5.31}$$

For the rotation by θ about x^3 one finds therefore that the inverse satisfies as expected

$$S_R^{-1}(\theta) = S_R(-\theta) \ . \tag{5.32}$$

Note that for a rotation by $\theta = 2\pi$ one finds $S(2\pi) = -I_4$ and thus the spinor acquires a minus sign. Only upon rotation $\theta = 4\pi$ does the spinor return to the original.

Using the transformation matrix S_R from Eq. (5.28) we can demonstrate that a particle described by the Dirac equation corresponds to spin of 1/2. Consider carrying out an infinitesimal rotation $\delta\theta$ about the x^3 axis. We can express the original coordinates x in terms of the rotated ones x' by replacing $\delta\theta \to -\delta\theta$ in the rotation matrix, which gives

$$\begin{pmatrix} x^0 \\ x^1 \\ x^2 \\ x^3 \end{pmatrix} = \begin{pmatrix} 1 & 0 & 0 & 0 \\ 0 & \cos\delta\theta & -\sin\delta\theta & \\ 0 & \sin\delta\theta & \cos\delta\theta & 0 \\ 0 & 0 & 0 & 1 \end{pmatrix} \begin{pmatrix} x'^0 \\ x'^1 \\ x'^2 \\ x'^3 \end{pmatrix} \approx \begin{pmatrix} 1 & 0 & 0 & 0 \\ 0 & 1 & -\delta\theta & 0 \\ 0 & \delta\theta & 1 & 0 \\ 0 & 0 & 0 & 1 \end{pmatrix} \begin{pmatrix} x'^0 \\ x'^1 \\ x'^2 \\ x'^3 \end{pmatrix} . \tag{5.33}$$

The transformation matrix $S_R(\delta\theta)$ from Eq. (5.28) is

$$S_R(\delta\theta) = \exp\left(-\frac{\delta\theta}{2}\gamma^1\gamma^2\right) \approx I - \frac{\delta\theta}{2}\gamma^1\gamma^2 = I + i\frac{\delta\theta}{2}\begin{pmatrix} \sigma_3 & 0 \\ 0 & \sigma^3 \end{pmatrix} , \tag{5.34}$$

where σ_3 is a Pauli matrix, and therefore to first order in $\delta\theta$,

$$\psi'(x') = \left[I + i\frac{\delta\theta}{2}\begin{pmatrix} \sigma_3 & 0 \\ 0 & \sigma_3 \end{pmatrix}\right]\psi(x) . \tag{5.35}$$

Furthermore we can express $\psi(x)$ in terms of the transformed coordinates using Eqs. (5.33) and then expand in a Taylor series about x' to first order to find

$$\begin{aligned} \psi(x) &= \psi(x'^0, x'^1 - x'^2\delta\theta, x'^1\delta\theta + x'^2, x'^3) \\ &= \psi(x') + \left(x'^1\frac{\partial\psi}{\partial x'^2} - x'^2\frac{\partial\psi}{\partial x'^1}\right)\delta\theta + \mathcal{O}(\delta\theta^2) . \end{aligned} \tag{5.36}$$

Using Eq. (5.36) in Eq. (5.35) gives

$$\psi'(x') = \left[I + i\frac{\delta\theta}{2}\begin{pmatrix} \sigma_3 & 0 \\ 0 & \sigma_3 \end{pmatrix}\right]\left(\psi(x') + \left(x'^1\frac{\partial\psi}{\partial x'^2} - x'^2\frac{\partial\psi}{\partial x'^1}\right)\delta\theta\right) + \mathcal{O}(\delta\theta^2) . \tag{5.37}$$

This holds for all values of the coordinates so we can relabel $x' \to x$ and write

$$\psi'(x) = [I + i\delta\theta(L_3 + S_3)]\,\psi(x) , \tag{5.38}$$

where

$$L_3 = -i\left(x^1\frac{\partial}{\partial x^2} - x^2\frac{\partial}{\partial x^1}\right) \tag{5.39}$$

is the third component of the orbital angular momentum operator $\boldsymbol{L} = \boldsymbol{r}\times\boldsymbol{p}$ with $\boldsymbol{p} = -i\nabla$ and S_3 is the third component of the spin operator for a spin-$\frac{1}{2}$ particle,

$$\boldsymbol{S} = \frac{1}{2}\begin{pmatrix}\boldsymbol{\sigma} & 0\\ 0 & \boldsymbol{\sigma}\end{pmatrix} . \tag{5.40}$$

The infinitesimal rotation by $\delta\theta$ can be extended to a finite θ by repeating N times the transformation by $\delta\theta = \theta/N$ and letting $N\to\infty$. This gives

$$\psi'(x) = \lim_{N\to\infty}\left[I + i\frac{\theta}{N}(L_3+S_3)\right]^N\psi(x) = \exp\left[i\theta(L_3+S_3)\right]\psi(x) . \tag{5.41}$$

We recognize the exponential as the unitary operator that generates a (passive) rotation of coordinates[2] $U(\theta) = e^{i\theta J_3}$ where J_3 is the third component of the *total* angular momentum, $\boldsymbol{J} = \boldsymbol{L} + \boldsymbol{S}$. In this way we arrive at the important result that the Dirac equation describes particles with spin 1/2.

5.3.2 Lorentz boosts

In an manner analogous to what we did above for rotations, one finds that the spinor transformation corresponding to a boost with rapidity ω along the x^3 axis is

$$S_{\rm B}(\omega) = \exp\left(-\frac{\omega}{2}\gamma^0\gamma^3\right) . \tag{5.42}$$

This corresponds to the Lorentz transformation $\Lambda_{\rm B}$ given by Eq. (2.15). By expanding the exponential one can show that Eq. (5.42) can be written equivalently as

$$S_{\rm B}(\omega) = I_4\cosh\frac{\omega}{2} - \gamma^0\gamma^3\sinh\frac{\omega}{2} . \tag{5.43}$$

One can show that S_B is self adjoint ($S_B^\dagger = S_B$) and that the inverse matrix satisfies

$$S_{\rm B}^{-1} = \gamma^0 S_{\rm B}^\dagger\gamma^0 , \tag{5.44}$$

which gives $S_{\rm B}^{-1}(\omega) = S_{\rm B}(-\omega)$. Thus for both rotations and boosts one has

$$S^{-1}(\Lambda) = \gamma^0 S^\dagger(\Lambda)\gamma^0 , \tag{5.45}$$

and it can be shown this holds for any Lorentz transformation Λ that does not involve time reversal [11].

[2]For the *active* rotation of the system, $\theta\to-\theta$

To illustrate application of the boost from Eq. (5.42), consider the spinor for an electron at rest,

$$u_1(0) = \sqrt{2m} \begin{pmatrix} 1 \\ 0 \\ 0 \\ 0 \end{pmatrix} . \tag{5.46}$$

Suppose we view this electron in a reference frame boosted with velocity $v_z = -\beta$ in the z (i.e., x^3) direction. That is, the electron is moving in the lab frame with velocity β . In this frame, the spinor u_1 becomes

$$u_1(p) = S_B u_1(0) = \left(I_4 \cosh \frac{\omega}{2} + \gamma^0 \gamma^3 \sinh \frac{\omega}{2} \right) u_1(0) , \tag{5.47}$$

where here ω refers to the rapidity of the electron in the lab frame, which is the negative of the rapidity of the boosted frame relative to the electron at rest. This can be related to the energy E and momentum p_z using

$$\cosh \frac{\omega}{2} = \sqrt{\frac{E+m}{2m}} , \qquad \sinh \frac{\omega}{2} = \sqrt{\frac{E+m}{2m}} \frac{p_z}{E+m} . \tag{5.48}$$

Further one finds for $\gamma^0\gamma^3$,

$$\gamma^0 \gamma^3 = \begin{pmatrix} 0 & 0 & 1 & 0 \\ 0 & 0 & 0 & -1 \\ 1 & 0 & 0 & 0 \\ 0 & -1 & 0 & 0 \end{pmatrix} . \tag{5.49}$$

Assembling the ingredients gives

$$u_1(p) = \sqrt{E+m} \begin{pmatrix} 1 \\ 0 \\ \frac{p_z}{E+m} \\ 0 \end{pmatrix} , \tag{5.50}$$

which agrees with the result found in Eq. (4.113) for the special case of $p_x = p_y = 0$.

5.3.3 Parity

Parity or space-inversion is the Lorentz transformation defined by $x' = \Lambda_P x$ with

$$\Lambda_P = \begin{pmatrix} 1 & 0 & 0 & 0 \\ 0 & -1 & 0 & 0 \\ 0 & 0 & -1 & 0 \\ 0 & 0 & 0 & -1 \end{pmatrix} , \tag{5.51}$$

which is to say, $\Lambda^{\mu}_{P\nu}$ is the same as the Minkowski metric tensor $g_{\mu\nu}$. Here $\det \Lambda_P = -1$ and thus parity is an improper Lorentz transformation. In the transformed reference frame, the Dirac equation

$$(i\gamma^{\mu}\partial_{\mu} - m)\psi(x) = 0 \tag{5.52}$$

becomes

$$(i\gamma^{\mu}\partial'_{\mu} - m)\psi'(x') = 0 \tag{5.53}$$

where the differentials appearing above are $\partial_{\mu} = (\frac{\partial}{\partial t}, \nabla)$ and $\partial'_{\mu} = (\frac{\partial}{\partial t}, -\nabla)$.

We want to find the matrix S_P such that $\psi'(x') = S_P\psi(x)$. But the parity operation is not characterised by continuous parameters as in the case of rotations or boosts and so Eq. (5.21) cannot be used. Nevertheless, we claim that the spinor transformation is given, up to an arbitrary complex phase, by

$$S_P = \gamma^0 = \begin{pmatrix} 1 & 0 & 0 & 0 \\ 0 & 1 & 0 & 0 \\ 0 & 0 & -1 & 0 \\ 0 & 0 & 0 & -1 \end{pmatrix} . \tag{5.54}$$

This follows directly from the requirement on S from Eq. (5.17) applied to the special case of parity,

$$S_P \Lambda^{\nu}_{P\mu} \gamma^{\mu} S_P^{-1} = \gamma^{\nu} . \tag{5.55}$$

Using Eq. (5.51) for Λ_P, $S_P = \gamma^0$ and $S_P^{-1} = \gamma^0$ (since $(\gamma^0)^2 = I$), the left-hand side of Eq. (5.55) becomes

$$S_P \Lambda^{\nu}_{P\mu} \gamma^{\mu} S_P^{-1} = \Lambda^{\nu}_{P\mu} \gamma^0 \gamma^{\mu} \gamma^0 = \gamma^{\nu} , \tag{5.56}$$

where the final equality follows since $\gamma^0\gamma^{\mu}\gamma^0 = \gamma^0$ for $\mu = 0$ and $\gamma^0\gamma^i\gamma^0 = -\gamma^i$ for $\mu = i = 1, 2, 3$. The requirement on S_P remains satisfied if it is multiplied by an arbitrary complex phase factor, which by convention we can set to unity.

Since the Dirac spinors therefore transform using $S_P = \gamma^0$, we find (see Eq. (5.54) that

$$S_P u_s(p) = +u_s(p) \tag{5.57}$$

$$S_P v_s(p) = -v_s(p) \tag{5.58}$$

and therefore a Dirac particle and its antiparticle have opposite parity; this holds regardless of the choice of the arbitrary phase.

5.4 Bilinear covariants

We will find that Lorentz invariant amplitudes for particle reactions contain products of Dirac wave functions called bilinear covariants, which can be classified according to how they transform. These terms are also building blocks of a Lagrangian density, which we will encounter with Quantum Field Theory in Ch. 10. To express these terms in a way that reveals clearly their properties, we define

$$\overline{\psi} = \psi^\dagger \gamma^0 = (\psi_1^*, \psi_2^*, -\psi_3^*, -\psi_4^*) \; , \tag{5.59}$$

where $\psi^\dagger = (\psi_1^*, \psi_2^*, \psi_3^*, \psi_4^*)$ is the adjoint (complex conjugate transpose). Sometimes $\overline{\psi}$ is called the Dirac adjoint but to avoid confusion with $\psi^\dagger$ it is usually just called "psi bar".

The bilinear covariants are terms of the form $\overline{\psi}\Gamma\psi$, where Γ represents an arbitrary 4×4 matrix. Such a matrix can be written as a linear combination of 16 independent basis matrices. By choosing these as shown in Table 5.1, one obtains bilinear covariants that transform under a Lorentz transformation in the manner indicated. The terms in the table are explained further below.

Table 5.1: Basis combinations of γ matrices, the number of indepedent matrices, and their Lorentz transformation properties (see below).

Matrix	N_{indep}	Lorentz transformation
I_4	1	scalar
γ^5	1	pseudoscalar
γ^μ	4	vector
$\gamma^\mu\gamma^5$	4	axial vector
$\sigma^{\mu\nu}$	6	tensor

Consider first the scalar combination corresonding to $\Gamma = I_4$. Under an arbitrary Lorentz transformation matrix Λ, the spinors ψ and $\psi^\dagger$ transform as

$$\psi'(x') = S\psi(x) \tag{5.60}$$

$$\psi'^\dagger(x') = \psi^\dagger(x) S^\dagger \; , \tag{5.61}$$

where $S = S(\Lambda)$ is the corresponding transformation of ψ from Eq. (5.21). We can now demonstrate that $\overline{\psi}\psi$ transforms as a Lorentz scalar. To see this, compute

$$\begin{aligned} \overline{\psi}'(x')\psi'(x') &= \psi'^\dagger(x')\gamma^0\psi'(x') = \psi^\dagger(x) S^\dagger \gamma^0 S \psi(x) \\ &= \psi^\dagger(x)\gamma^0\gamma^0 S^\dagger \gamma^0 S \psi(x) = \overline{\psi}(x)\, \gamma^0 S^\dagger \gamma^0 S\, \psi(x) \\ &= \overline{\psi}(x)\psi(x) \; , \end{aligned} \tag{5.62}$$

where to go to the second line we inserted $\gamma^0\gamma^0 = I$ and to arrive at the final equality we used $\gamma^0 S^\dagger \gamma^0 = S^{-1}$ (see Eq. (5.45)).

Next, we can show that under a Lorentz transformation Λ, the quantity $\overline{\psi}\gamma^\mu\psi$ transforms as

$$\begin{aligned} \overline{\psi}'(x')\gamma^\mu\psi'(x') &= \psi'^\dagger(x')\gamma^0\gamma^\mu\psi'(x') = \psi^\dagger(x)S^\dagger\gamma^0\gamma^\mu S\psi(x) \\ &= \psi^\dagger(x)\gamma^0 S^{-1}\gamma^\mu S\psi(x)\ , \end{aligned} \tag{5.63}$$

where for the final equality we used $S^\dagger\gamma^0 = \gamma^0 S^{-1}$, which follows directly from Eq. (5.45). Then using the fundamental requirement $S^{-1}\gamma^\mu S = \Lambda^\mu{}_\nu\gamma^\nu$ between S and Λ (see Eq. (5.19) one finds

$$\overline{\psi}'(x')\gamma^\mu\psi'(x') = \Lambda^\mu{}_\nu\overline{\psi}(x)\gamma^\nu\psi(x) \tag{5.64}$$

and we therefore see that $\overline{\psi}\gamma^\mu\psi$ transforms as a four-vector.

As an example of such a quantity, recall from Eqs. (4.21) and (4.22) that the probability density and current corresponding to the Dirac wave function ψ are

$$\rho = \psi^\dagger\psi = \psi^\dagger\gamma^0\gamma^0\psi = \overline{\psi}\gamma^0\psi\ , \tag{5.65}$$

$$\boldsymbol{j} = \psi^\dagger\boldsymbol{\alpha}\psi = \psi^\dagger\gamma^0\gamma^0\boldsymbol{\alpha}\psi = \overline{\psi}\gamma^i\psi\ , \qquad i = 1,2,3\ . \tag{5.66}$$

These can be written as the the four-vector (probability) current

$$\boldsymbol{j}^\mu = (\rho, \boldsymbol{j}) = \overline{\psi}\gamma^\mu\psi\ . \tag{5.67}$$

The corresponding electromagnetic four-vector current for a particle of charge q is $\boldsymbol{j}^\mu_{\rm EM} = q\boldsymbol{j}^\mu$.

In a similar way, we can show that

$$P = \overline{\psi}\gamma^5\psi \tag{5.68}$$

$$A^\mu = \overline{\psi}\gamma^\mu\gamma^5\psi \tag{5.69}$$

transform as a pseudoscalar and axial vector, respectively. That is, for boosts and rotations, P transforms as a scalar and A^μ as a four-vector. But for the parity transformation $\psi' = S_P\psi$ with $S_P = \gamma^0$ (see Eq. 5.54)) and $\{\gamma^5, \gamma^\mu\} = 0$ (see Eq.4.74), one finds for the pseudoscalar P,

$$P' = \overline{\psi}'\gamma^5\psi' = \overline{\psi}\gamma^0\gamma^5\gamma^0\psi = -\overline{\psi}\gamma^5\psi = -P\ . \tag{5.70}$$

For the axial vector A^μ the parity transformation gives

$$A'^\mu = \overline{\psi}'\gamma^\mu\gamma^5\psi' = \overline{\psi}\gamma^0\gamma^\mu\gamma^5\gamma^0\psi = \begin{cases} -\overline{\psi}\gamma^0\gamma^5\psi & \mu = 0\ , \\ \overline{\psi}\gamma^i\gamma^5\psi & \mu = i = 1,2,3. \end{cases} \tag{5.71}$$

That is, the time component of the axial vector picks up a minus sign under parity but the spatial components do not change.

Finally we have the tensor covariant, which carries two Lorentz indices. First we define the collection of 4×4 matrices

$$\sigma^{\mu\nu} = \frac{i}{2}[\gamma^\mu, \gamma^\nu] \,, \tag{5.72}$$

with $\mu = 0, 1, 2, 3$. There are thus 16 combinations of the labels μ and ν, but because it is fully antisymmetric, the diagonal combinations must be zero, and further $\sigma^{\nu\mu} = -\sigma^{\nu\mu}$. There are therefore only six independent matrices. A tensor current has the form

$$T^{\mu\nu} = \overline{\psi}\sigma^{\mu\nu}\psi \,. \tag{5.73}$$

Under a Lorentz transformation Λ it becomes

$$T'^{\mu\nu} = \Lambda^\mu{}_\rho \Lambda^\nu{}_\sigma T^{\rho\sigma} \,. \tag{5.74}$$

Chapter 6

Calculating Amplitudes

In this chapter we will solve the Dirac equation using perturbation theory, whereby each term in the perturbation series can be visualised as a Feynman diagram. This will give a set of "Feynman rules" that can be used to write down the amplitude for a reaction almost by inspection.[1]

6.1 Green functions and propagators

Our goal is to solve the Dirac equation for an electron with mass m and charge $q = -e$ in an electromagnetic potential $A^\mu(x)$, namely,

$$(i\partial\!\!\!/ - m)\psi(x) = -eA\!\!\!/(x)\psi(x) \; . \tag{6.1}$$

If the right-hand side were zero then we obtain plane-wave solutions, but in a nonzero potential we cannot solve in general for $\psi(x)$ in closed form. To recast the problem into a form that will allow us to use perturbation theory we can first solve

$$(i\partial\!\!\!/ - m)K(x - x') = \delta^4(x - x')I_4 \; , \tag{6.2}$$

where $K(x - x')$ is called the *Green function* corresponding to the operator $(i\partial\!\!\!/ - m)$. Note that $K(x - x')$ is a 4×4 matrix. It represents the solution where the source term on the right-hand side is a delta function $\delta^4(x - x')$ and therefore K itself must depend only on the difference $x - x'$. An introduction to Green functions as a general tool for solving inhomogeneous differential equations can be found in Appendix B.

Once we have found $K(x - x')$, it is easy to show that the general solution to Eq. (6.1) is

$$\psi(x) = \phi(x) - e \int K(x - x')A\!\!\!/(x')\psi(x') \, d^4x' \; , \tag{6.3}$$

where $\phi(x)$ is a free-particle solution, i.e., $(i\partial\!\!\!/ - m)\phi(x) = 0$. To check that this works we apply $(i\partial\!\!\!/ - m)$ to both sides of Eq. (6.3), which gives

[1] This chapter mainly follows the treatment of Schmüser [2].

$$\begin{aligned}(i\partial\!\!\!/ - m)\psi(x) &= (i\partial\!\!\!/ - m)\phi(x) - e\int (i\partial\!\!\!/ - m)K(x-x')A\!\!\!/(x')\psi(x')\,d^4x' \\ &= -e\int \delta^4(x-x')A\!\!\!/(x')\psi(x')\,d^4x' \\ &= -eA\!\!\!/(x)\psi(x)\ . \end{aligned} \tag{6.4}$$

Here we have assumed that the limits of integration do not depend on x so we can bring the operator $(i\partial\!\!\!/ - m)$ inside the integral. Its derivatives are with respect to x, not x', so it only acts on K resulting in the delta function $\delta^4(x-x')$.

We cannot regard the $\psi(x)$ from Eq. (6.3) as providing the desired solution, however, since ψ also appears on the right-hand side of the equation. Rather, we have simply converted the original differential equation into an integral equation. Nevertheless, this leads to an iterative method to find the solution by regarding the right-hand side as a small perturbation. The resulting amplitudes will be a perturbation series in powers of the electric charge e. After squaring amplitudes to find observable cross sections or decay rates, the effective expansion parameter will be the fine structure constant $\alpha = e^2/4\pi \approx 1/137$. Because this is a small number, a highly accurate prediction can be obtained by summing terms to a fairly low order.

6.2 Electron propagator

We can solve Eq. (6.3) by regarding the term proportional to e on the right-hand side as a small perturbation. That is, to leading (zeroth) order, we have the free-particle solution

$$\psi^{(0)}(x) = \phi(x)\ . \tag{6.5}$$

This can be used on the right-hand side of Eq. (6.3) to find the first-order solution,

$$\psi^{(1)}(x) = \phi(x) - e\int d^4x'\, K(x-x')A\!\!\!/(x')\phi(x')\ , \tag{6.6}$$

and $\psi^{(1)}$ can again be used on the right-hand side of Eq. (6.3) to find $\psi^{(2)}$, where we need to relabel the parameters of integration to x' and x'' as appropriate,

$$\psi^{(2)}(x) = \phi(x) - e\int d^4x'\, K(x-x')A\!\!\!/(x')\left[\phi(x') - e\int d^4x''\, K(x'-x'')A\!\!\!/(x'')\phi(x'')\right]\ . \tag{6.7}$$

That is, in general we find the solution to order $n+1$ from the nth order one by using

$$\psi^{(n+1)}(x) = \phi(x) - e\int d^4x'\, K(x-x')A\!\!\!/(x')\psi^{(n)}(x')\ . \tag{6.8}$$

To find $K(x-x')$, consider its Fourier transform

$$\tilde{K}(p) = \int d^4x\, e^{ip\cdot x} K(x - x') \tag{6.9}$$

and the inverse

$$K(x - x') = \frac{1}{(2\pi)^4} \int d^4p\, e^{-ip\cdot(x-x')} \tilde{K}(p)\ . \tag{6.10}$$

The defining equation (6.2) for $K(x - x')$ can therefore be written

$$\begin{aligned} (i\partial\!\!\!/ - m)K(x - x') &= \frac{1}{(2\pi)^4} \int d^4p\, e^{-ip\cdot(x-x')} (p\!\!\!/ - m)\tilde{K}(p) \\ &= \delta^4(x - x')I_4 = \frac{1}{(2\pi)^4} \int d^4p\, e^{-ip\cdot(x-x')}\, I_4\ . \end{aligned} \tag{6.11}$$

Here in the first line we applied the operator $(i\partial\!\!\!/ - m)$ to the integrand of Eq. (6.10), which brings down the factor $(p\!\!\!/ - m)$. The second line sets this equal to an integral representation of the delta function $\delta^4(x - x')$ (see, e.g., Ref. [77] Sec. 10.3.3). Since the integrals in the first and second lines of Eq. (6.11) are equal, so are their respective inverse Fourier transforms, i.e.,

$$(p\!\!\!/ - m)\tilde{K}(p) = I_4\ . \tag{6.12}$$

We can solve for $\tilde{K}(p)$ by multiplying both sides of Eq. (6.12) by $(p\!\!\!/ + m)$, which gives

$$(p\!\!\!/ + m)(p\!\!\!/ - m)\tilde{K}(p) = (p^2 - m^2)\tilde{K}(p) = p\!\!\!/ + m\ . \tag{6.13}$$

where we used the fact that $p\!\!\!/p\!\!\!/ = p^2 I_4$. We therefore find for the Fourier transform of the Green function

$$\tilde{K}(p) = \frac{p\!\!\!/ + m}{p^2 - m^2}\ , \qquad (p^2 \neq m^2)\ , \tag{6.14}$$

which is called the electron *propagator*. Note that in this form it is defined only for virtual electrons, i.e., with $p^2 \neq m^2$.

We can invert the Fourier transform to obtain the Green function as

$$\begin{aligned} K(x - x') &= \frac{1}{(2\pi)^4} \int d^4p\, e^{-ip\cdot(x-x')} \tilde{K}(p) \\ &= \frac{1}{(2\pi)^4} \int d^3\boldsymbol{p}\, e^{i\boldsymbol{p}\cdot(\boldsymbol{x}-\boldsymbol{x}')} \int_{-\infty}^{\infty} dp^0\, \frac{e^{-ip^0(t-t')}(p\!\!\!/ + m)}{(p^0 - E)(p^0 + E)}\ . \end{aligned} \tag{6.15}$$

The integral over the energy p^0 requires methods of complex contour integration. A brief introduction to this mathematical technique is given in Appendix C.

If we treat p^0 as complex, the integral has poles at $p^0 = \pm E$. We cannot integrate directly over the pole, so we use a contour that avoids the divergence by an infinitesimal amount above or below. One arrives at the Feynman-Stückelberg interpretation of negative-energy solutions propagating backwards in time by choosing a particular path of integration that avoids the poles. This is shown in Fig. 6.1(a) for $t > t'$ and Fig. 6.1(b) for $t < t'$. For, e.g., the case of $t > t'$ we close in the lower half-plane where p^0 is negative imaginary, which means that the factor $e^{-ip^0(t-t')}$ goes to zero for large $|p^0|$. In a similar way, closing the contour in the upper half-plane gives $e^{-ip^0(t-t')} \to 0$ if $t > t'$. In both cases, one integrates below the pole at $p^0 = -E$ and above the pole at $p^0 = +E$.

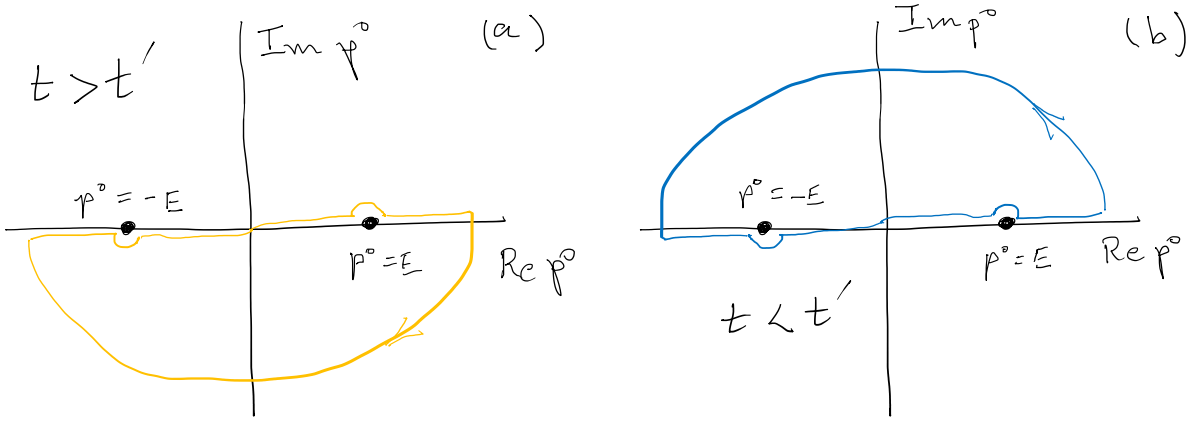

Figure 6.1: Integration contours in the complex p^0 plane that avoid the poles at $p^2 = m^2$ (a) for $t > t'$ and (b) for $t < t'$.

Consider first $t > t'$. The contour of integration contains only the simple pole at $p^0 = E$. Using the residue theorem, the integral over p^0 is

$$\int dp^0 \, \frac{1}{p^0 - E} \left[\frac{(\not{p} + m) e^{-ip^0(t-t')}}{p^0 + E} \right] = -2\pi i \left[\frac{\gamma^0 E - \boldsymbol{\gamma} \cdot \boldsymbol{p} + m}{2E} e^{-iE(t-t')} \right] , \tag{6.16}$$

where the term in square brackets on the right is the residue of the integrand at $p^0 = E$ and the minus sign enters because the contour is follows a clockwise direction. The Green function is therefore

$$K(x - x') = -\frac{i}{(2\pi)^3} \int d^3\boldsymbol{p} \exp\left[i\boldsymbol{p} \cdot (\boldsymbol{x} - \boldsymbol{x}') - iE(t - t') \right] \left(\frac{\gamma^0 E - \boldsymbol{\gamma} \cdot \boldsymbol{p} + m}{2E} \right) , \qquad t > t' . \tag{6.17}$$

For $t < t'$, closing the contour in the upper half-plane gives

$$K(x - x') = -\frac{i}{(2\pi)^3} \int d^3\boldsymbol{p} \exp\left[i\boldsymbol{p} \cdot (\boldsymbol{x} - \boldsymbol{x}') - iE(t - t') \right] \left(\frac{-\gamma^0 E - \boldsymbol{\gamma} \cdot \boldsymbol{p} + m}{2E} \right) , \qquad t < t' . \tag{6.18}$$

In both expressions for $K(x-x')$, E is positive, and the functions differ only in the sign in front of γ^0.

Here we have chosen the contour of integration to miss the poles in such a way as to give the propagator of Eqs. (6.17) and (6.18). We could achieve the same result by adding a small imaginary part to the position of the pole, as shown in Fig. 6.2. This corresponds to taking the electron propagator to be

$$\tilde{K}(p) = \frac{\not{p} + m}{p^2 - m^2 + i\varepsilon} \tag{6.19}$$

with $\varepsilon > 0$. In the limit $\varepsilon \to 0$, Eq. (6.19) results in the Green function given by Eqs.(6.17) and (6.18).

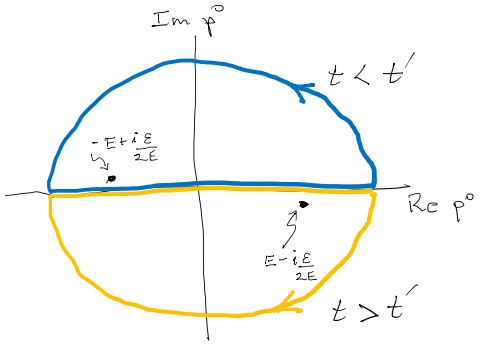

Figure 6.2: Contours of integration that move the poles at $p^2 = m^2$ away from the real axis by $\pm i\varepsilon/2E$.

6.3 Propagator and time evolution

We will now show that the Green function found in the previous section results in the desired behaviour of the solutions, namely, positive energy waves propagate only forwards in time and negative energy states only backwards. Consider a free electron with four-momentum $k = (k^0, \boldsymbol{k})$ with $k^0 > 0$. Suppressing for now the spin index, the Dirac wave function is

$$\phi_+(x') = \phi_+(t', \boldsymbol{x}') = u(k) \exp[-ik^0 t' + i\boldsymbol{k} \cdot \boldsymbol{x}'] \,. \tag{6.20}$$

We claim that at a later time $t > t'$ the wave function is given by the integral over the spatial coordinates $\boldsymbol{x}'$ of ϕ_+ at the earlier time t', i.e.,

$$\phi_+(x) = \phi_+(t, \boldsymbol{x}) = i \int d^3\boldsymbol{x}' \, K(x - x') \gamma^0 \phi_+(t', \boldsymbol{x}') \,. \tag{6.21}$$

To prove this result, use Eq. (6.17) for the Green function $K(x-x')$ at $t > t'$ and Eq. (6.20) for $\phi_+(t', \boldsymbol{x}')$ in Eq. (6.21). This gives

$$\begin{aligned}\phi_+(t,\boldsymbol{x}) &= i\int d^3\boldsymbol{x}'\left[\frac{-i}{(2\pi)^3}\int d^3\boldsymbol{p}\,\exp\left[i\boldsymbol{p}\cdot(\boldsymbol{x}-\boldsymbol{x}')-iE(t-t')\right]\right.\\ &\times \left.\left(\frac{\gamma^0E-\boldsymbol{\gamma}\cdot\boldsymbol{p}+m}{2E}\right)\gamma^0u(k)\exp[-ik^0t'+i\boldsymbol{k}\cdot\boldsymbol{x}']\right]\,. \end{aligned} \tag{6.22}$$

We can then collect together the terms containing $\boldsymbol{x}'$ and move terms involving $\boldsymbol{x}$ outside the integral over $\boldsymbol{x}'$, which gives

$$\begin{aligned}\phi_+(t,\boldsymbol{x}) &= \int d^3\boldsymbol{p}\left[\frac{1}{(2\pi)^3}\int d^3\boldsymbol{x}'\,\exp(i(\boldsymbol{k}-\boldsymbol{p})\cdot\boldsymbol{x}')\right]\left(\frac{\gamma^0E-\boldsymbol{\gamma}\cdot\boldsymbol{p}+m}{2E}\right)\\ &\times \exp(i(E-k^0)t')\gamma^0u(k)\exp(i\boldsymbol{p}\cdot\boldsymbol{x}-iEt)\end{aligned} \tag{6.23}$$

The term in square brackets containing the integral over $\boldsymbol{x}'$ is none other than the delta function $\delta^3(\boldsymbol{k}-\boldsymbol{p})$. Using this allows us to carry out the integral over $\boldsymbol{p}$, which gives

$$\phi_+(t,\boldsymbol{x}) = \exp(-ik^0t+i\boldsymbol{k}\cdot\boldsymbol{x})\frac{(\gamma^0k^0-\boldsymbol{\gamma}\cdot\boldsymbol{k}+m)\gamma^0u(k)}{2k^0}\,. \tag{6.24}$$

To arrive at this expression we used the fact that $E=\sqrt{|\boldsymbol{p}|^2+m^2}$. When integrating over $\boldsymbol{p}$ the delta function causes $\boldsymbol{p}$ to be set equal to $\boldsymbol{k}$ and thus also E to be replaced by k^0.

Now we can exploit the fact that $u(k)$ is a solution of the free-particle Dirac equation,

$$(\not{k}-m)u(k) = (\gamma^0k_0-\boldsymbol{\gamma}\cdot\boldsymbol{k}-m)u(k) = 0\,. \tag{6.25}$$

The term $(\gamma^0k^0-\boldsymbol{\gamma}\cdot\boldsymbol{k}+m)\gamma^0u(k)$ appearing in Eq. (6.24) can therefore be written

$$(\gamma^0k^0-\boldsymbol{\gamma}\cdot\boldsymbol{k}+m)\gamma^0u(k) = \gamma^0(\gamma^0k_0+\boldsymbol{\gamma}\cdot\boldsymbol{k}+m)u(k) = 2k_0u(k)\,, \tag{6.26}$$

where to arrive at the first equality we used $\gamma^i\gamma^0=-\gamma^0\gamma^i$ and for the final equality we used $(\boldsymbol{\gamma}\cdot\boldsymbol{k}+m)u(k)=\gamma^0k_0u(k)$, which results from Eq. (6.25). Using this in Eq. (6.24) then gives

$$\phi_+(t,\boldsymbol{x}) = u(k)\exp(-ik^0t+i\boldsymbol{k}\cdot\boldsymbol{x})\,,\qquad t>t'\,, \tag{6.27}$$

which agrees with Eq. (6.20) and thus proves the result for $t>t'$.

For times $t<t'$, we need to use the Green function $K(x-x')$ from Eq. (6.18). Recall this only differs from the Green function for $t>t'$ in the sign of the factor γ^0E. Thus the calculation for $\phi_+(t,\boldsymbol{x})$ is the same as before except the term shown in Eq. (6.26) is now instead

$$(-\gamma^0k^0-\boldsymbol{\gamma}\cdot\boldsymbol{k}+m)\gamma^0u(k) = -\gamma^0(\not{k}-m)u(k) = 0\,. \tag{6.28}$$

Combining the results for $t<t'$ and $t>t'$ we therefore have

$$i\int d^3\boldsymbol{x}'\, K(x-x')\gamma^0\phi_+(t',\boldsymbol{x}') = \begin{cases} \phi_+(t,\boldsymbol{x}) & t>t'\,, \\ 0 & t<t'\,. \end{cases} \tag{6.29}$$

That is, the solution $\phi_+(t,\boldsymbol{x})$ for $k^0>0$ can be given as an integral over $\boldsymbol{x}'$ at a given time t' in the *past* ($t>t'$).

Consider now a negative energy solution, so instead of Eq. (6.20) we use

$$\phi_-(x') = v(k)e^{ik\cdot x'}\,. \tag{6.30}$$

Here k^0 is still positive so that the energy is $-k^0$. The calculation for the integral of ϕ_- times the Green function proceeds along the same lines as above, and the result is exactly the same except with the two conditions on the time exchanged, i.e., $t>t' \leftrightarrow t<t'$, i.e.,

$$i\int d^3\boldsymbol{x}'\, K(x-x')\gamma^0\phi_-(t',\boldsymbol{x}') = \begin{cases} 0 & t>t'\,, \\ \phi_-(t,\boldsymbol{x}) & t<t'\,. \end{cases} \tag{6.31}$$

We therefore arrive at the crucial result, namely, positive energy solutions spread out into the future, but negative energy solutions spread out into the past.

The same calculations can be carried out for the Dirac adjoint solutions $\overline{\phi}_+$ and $\overline{\phi}_-$, for example,

$$i\int d^3\boldsymbol{x}\, \overline{\phi}_+(t,\boldsymbol{x})\gamma^0 K(x-x') = \begin{cases} 0 & t'>t\,, \\ \overline{\phi}_+(t',\boldsymbol{x}') & t'<t\,. \end{cases} \tag{6.32}$$

That is, the Dirac adjoint of the positive energy solution at time t' is given by an integral over $\boldsymbol{x}$ at a later time t. This equation will be useful in the following section for computing a scattering amplitude.

6.4 Amplitude for e^- scattering by a potential

To see how to compute the quantum mechanical amplitude for a scattering reaction, suppose an electron is incident on a region with an electromagnetic potential $A^\mu(x)$ produced, .e.g, by another particle. At a time long before the interaction we will describe the incoming particle as a plane wave ϕ_i with four-momentum p_i, and the scattered wave will spread out in all directions corresponding to the solution $\psi_{\rm s}$. We define the operator S (for "scattering matrix") as evolving the initial state at time t_i to the final scattered one at t_f,

$$\psi_{\rm s}(t_f,\boldsymbol{x}) = S\phi_i(t_i,\boldsymbol{x})\,. \tag{6.33}$$

Using Eq. (6.6) we can write $\psi_{\rm s}$ to second order as

$$\begin{aligned}\psi_{\rm s}^{(2)}(x) &= \phi_i(x) - e\int d^4x'\, K(x-x')\not{A}(x')\phi_i(x') \\ &+ e^2\int\int d^4x'\, d^4x''\, K(x-x'')\not{A}(x'')K(x''-x')\not{A}(x')\phi_i(x')\ . \end{aligned} \tag{6.34}$$

If we look far enough away from the interaction in the direction of a momentum vector $\boldsymbol{p}_f$ then there will be a component of $\psi_{\rm s}$ that is approximately a plane wave ϕ_f with some momentum $\boldsymbol{p}_f$. The S-matrix element S_{fi} is defined by the projection of $\psi_{\rm s}$ onto ϕ_f, i.e.,

$$S_{fi} = \langle \boldsymbol{p}_f, t_f|\psi_{\rm s}\rangle = \langle \boldsymbol{p}_f, t_f|S|\boldsymbol{p}_i, t_i\rangle\ , \tag{6.35}$$

where the initial and final times are taken as $t_i \to -\infty$ and $t_f \to \infty$. The inner product represented by Eq. (6.35) is therefore an integral over the spatial coordinate only,

$$S_{fi} = \int d^3\boldsymbol{x}\, \phi_f^\dagger(t_f,\boldsymbol{x}) S\phi_i(t_i,\boldsymbol{x})\ , \tag{6.36}$$

or using the solution (6.34) to second order for $\psi_{\rm s}$,

$$\begin{aligned} S_{fi} &= \int d^3\boldsymbol{x}\, \phi_f^\dagger(x)\phi_i(x) \\ &- e\int d^3\boldsymbol{x}\, \phi_f^\dagger(x)\int d^4x'\, K(x-x')\not{A}(x')\phi_i(x') \\ &+ e^2\int d^3\boldsymbol{x}\, \phi_f^\dagger(x)\int d^4x'\, d^4x'' K(x-x'')\not{A}(x'')K(x''-x')\not{A}(x')\phi_i(x')\ , \end{aligned} \tag{6.37}$$

where x in the integrals means the four-vector $(t_f, \boldsymbol{x})$.

To evaluate the integrals we can take the initial and final plane waves to be

$$\phi_i(x) = u(p_i)e^{-ip_i\cdot x} = u(p_i)e^{-i(p_i^0 t_f - \boldsymbol{p}_i\cdot\boldsymbol{x})} \tag{6.38}$$

$$\phi_f(x) = u(p_f)e^{-ip_f\cdot x} = u(p_f)e^{-i(p_f^0 t_f - \boldsymbol{p}_f\cdot\boldsymbol{x})} \tag{6.39}$$

and therefore for the adjoint of ϕ_f,

$$\phi_f^\dagger(x) = \overline{u}(p_f)\gamma^0 e^{ip_f\cdot x} = \overline{u}(p_f)\gamma^0 e^{i(p_f^0 t_f - \boldsymbol{p}_f\cdot\boldsymbol{x})} \tag{6.40}$$

The zero-order term in the perturbation series (6.37) is therefore

$$S_{fi}^{(0)} = \int d^3\boldsymbol{x}\, \phi_f^\dagger(x)\phi_i(x) = \int d^3\boldsymbol{x}\, e^{i(\boldsymbol{p}_i-\boldsymbol{p}_f)\cdot\boldsymbol{x}} e^{-i(p_i^0-p_f^0)t_f}\overline{u}(p_f)\gamma^0 u(p_i)\ . \tag{6.41}$$

The integral over $\boldsymbol{x}$ is a delta function,

$$\int d^3\boldsymbol{x}\, e^{i(\boldsymbol{p}_i-\boldsymbol{p}_f)\cdot\boldsymbol{x}} = (2\pi)^3\delta^3(\boldsymbol{p}_i-\boldsymbol{p}_f)\;, \tag{6.42}$$

and so $S_{fi}^{(0)}$ will be zero unless $\boldsymbol{p}_f = \boldsymbol{p}_i$ and thus also $p_f^0 = p_i^0 \equiv E_i$. If we were to enforce these equalities in anticipation of carrying out the integral over $\boldsymbol{x}$ over the (large) volume V we would find

$$\int d^3\boldsymbol{x}\, e^0 \to V\;. \tag{6.43}$$

This would then cancel the two implicit normalisation factors of $1/\sqrt{V}$ which we had dropped from the plane-wave solutions (6.38) and (6.39). Referring to Eq. (4.110) for the normalisation of the Dirac spinors we therefore find

$$S_{fi}^{(0)} = \overline{u}(p_i)\gamma^0 u(p_i) = u^\dagger(p_i)u(p_i) = 2E_i\delta_{fi}\;, \tag{6.44}$$

where the Kronecker delta δ_{fi} reflects the fact that this term is only present when the initial and final momenta are equal. The term $2E_i\delta_{fi}$ thus represents the case of no scattering and will not actually enter into our prediction for scattering cross sections. The perturbative expansion for the S-matrix therefore has the form

$$S_{fi} = 2E_i\delta_{fi} + S_{fi}^{(1)} + S_{fi}^{(2)} + \cdots\;. \tag{6.45}$$

Using Eq. (6.37), the first-order matrix element is

$$S_{fi}^{(1)} = -e\int d^4x' \int d^3\boldsymbol{x}\, \phi_f^\dagger(x)K(x-x')\not{A}(x')\phi_i(x')\;, \tag{6.46}$$

where as above $x = (t_f, \boldsymbol{x})$ and $t_f \to \infty$. For the integral over $\boldsymbol{x}$ we can use Eq. (6.32) to write

$$\int d^3\boldsymbol{x}\, \phi_f^\dagger(t,\boldsymbol{x})K(x-x') = \int d^3\boldsymbol{x}\, \overline{\phi}_f(t,\boldsymbol{x})\gamma^0 K(x-x') = -i\overline{\phi}_f(t',\boldsymbol{x}')\;, \qquad t'<t\;, \tag{6.47}$$

and the integral is zero for $t' > t$. Equation (6.45) is therefore

$$S_{fi}^{(1)} = ie\int d^4x'\, \overline{\phi}_f(x')\not{A}(x')\phi_i(x')\;. \tag{6.48}$$

Note that the propagator K no longer appears as it was related to $\overline{\phi}$ through Eq. (6.47). The four-dimensional integral over x' is indicated schematically in Fig. 6.3.

Again using Eqs. (6.37) and (6.47), we find the second-order contribution to be

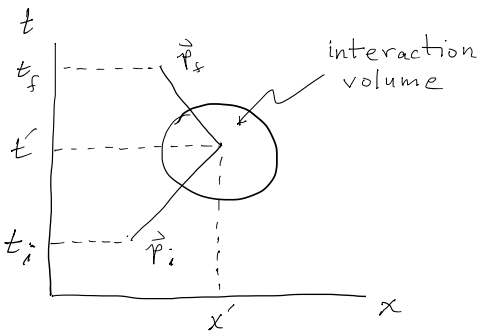

Figure 6.3: Illustration of the contribution to scattering at first order.

$$
\begin{aligned}
S_{fi}^{(2)} &= e^2 \int\int d^4x'\, d^4x'' \int d^3\boldsymbol{x}\, \phi_f^\dagger(x) K(x-x'') \not{A}(x'') K(x''-x') \not{A}(x') \phi_i(x') \\
&= -ie^2 \int\int d^4x'\, d^4x'' \overline{\phi}_f(x'') \not{A}(x'') K(x''-x') \not{A}(x') \phi_i(x') \; . \qquad (6.49)
\end{aligned}
$$

The regions of space-time that contribute to the second-order matrix element are illustrated in Fig. 6.4. By integrating over all possible values of t' and t'' within the interaction region, both orderings, $t' < t''$ and $t' > t''$ are included. For $t' < t''$, the electron scatters at t' and then continues to propagate and scatters again at t'', as shown in Fig. 6.4(a). If $t' > t''$, the electron is scattered at t', then the negative energy solution contributes from that point back to the earlier time t'', where the electron is scattered into its final state. This is equivalent to saying that an electron-positron pair is created at t'', and the positron then annihilates with the incident electron at t', as shown in Fig. 6.4(b). Both time orderings are needed for the final amplitude to be Lorentz invariant.

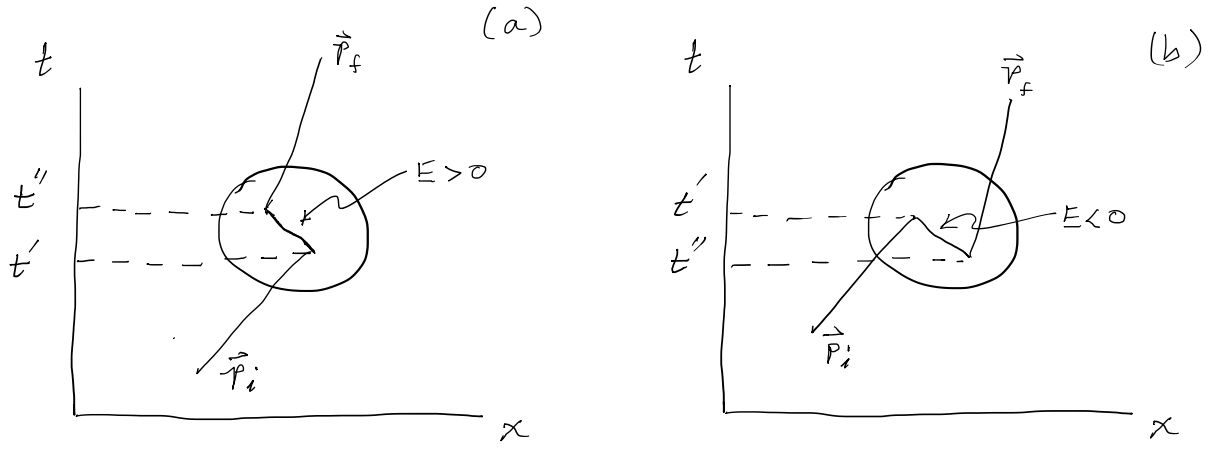

Figure 6.4: Illustration of the contribution to scattering at second order: (a) a double scatter and (b) pair annihilation and creation.

6.5 Photon propagator

In this section we will find the Green function for the electromagnetic potential $A^\mu(x)$ and the corresponding Fourier transform, i.e., the photon propagator. This is the analog of the electron propagator found in Sec. 6.2 and will allow us to compute amplitudes for reactions involving the scattering of charged particles.

In the scattering of two charged particles, we can take one of them as a target that creates an electromagnetic potential and the other as a projectile that scatters off of this potential. Of course we obtain the same result if the roles of target and projectile are reversed. Consider, for example, the scattering of an electron by a point-like proton, i.e., a proton that we model using the Dirac equation and having no internal structure. Treating the proton as the target, it gives rise to a potential $A^\mu(x)$ that is a solution to Maxwell's equations, for which we can choose the Lorenz gauge (cf. Eq. (3.17)),

$$\partial_\alpha \partial^\alpha A^\mu(x) = eJ^\mu(x) \; . \tag{6.50}$$

Here J^μ is the probability current density of the proton and eJ^μ is the corresponding charge current density. For the moment suppose this is given and we want to find $A^\mu(x)$. To do this we first solve the corresponding equation for the Green function $D^{\mu\nu}(x-x')$,

$$\partial_\alpha \partial^\alpha D^{\mu\nu}(x-x') = g^{\mu\nu}\delta^4(x-x') \; . \tag{6.51}$$

If we can find $D^{\mu\nu}(x-x')$, then the desired potential can be obtained from

$$A^\mu(x) = e\int d^4x' \, D^{\mu\nu}(x-x')J_\nu(x') \; . \tag{6.52}$$

Substituting this back into Eq. (6.50), we find

$$\begin{aligned} \partial_\alpha \partial^\alpha A^\mu(x) &= e\int d^4x' \, \partial_\alpha \partial^\alpha D^{\mu\nu}(x-x')J_\nu(x') \\ &= e\int d^4x' \, \delta^4(x-x')g^{\mu\nu}J_\nu(x') \\ &= eJ^\mu(x) \; , \end{aligned} \tag{6.53}$$

as required. The Green function $D^{\mu\nu})(x-x')$ is related to its Fourier transform $\tilde{D}^{\mu\nu}(q)$ by

$$D^{\mu\nu}(x-x') = \int \frac{d^4q}{(2\pi)^4} \, \tilde{D}^{\mu\nu}(q)e^{-iq\cdot(x-x')} \; . \tag{6.54}$$

Using this in the differential equation for the Green function (6.51) gives

$$\begin{aligned}\partial_\alpha\partial^\alpha D^{\mu\nu}(x-x') &= \int \frac{d^4q}{(2\pi)^4}\,\tilde{D}^{\mu\nu}(q)\,(-q^2)e^{-iq\cdot(x-x')} \\ &= g^{\mu\nu}\delta^4(x-x') \qquad (6.55)\\ &= g^{\mu\nu}\int \frac{d^4q}{(2\pi)^4}\,e^{-iq\cdot(x-x')}\,. \qquad (6.56)\end{aligned}$$

The second line follows from Eq. (6.51) by definition of the Green function and the integral in the third line is a representation of a delta function. Comparison of the first and third lines therefore gives for

$$\tilde{D}^{\mu\nu}(q) = -\frac{g^{\mu\nu}}{q^2}\,, \qquad (6.57)$$

which is the photon propagator. Following arguments similar to what was done in Sec. 6.2, in when integrating over the pole at $q^2 = 0$ one replaces $q^2 \to q^2 + i\varepsilon$ and takes the limit $\varepsilon \to 0$.

6.6 Amplitude for electron-proton scattering

We can now return to the problem of scattering an electron by a point-like proton. Suppose the initial-state electron and proton have four-momenta p_1 and p_2, and the final-state ones p_3 and p_4, respectively. To find the electromagnetic potential created by the proton, we need the photon propagator from the previous section and in addition we need to know the proton's current density eJ^μ. Recall (cf. Eq. (5.67)) that the probability current for a particle with Dirac wave function ψ is $j^\mu = \overline{\psi}\gamma^\mu\psi$. But now we have two different wave functions for the proton: $\psi_2(x) = u(p_2)e^{-ip_2\cdot x}$ for the intial-state and $\psi_4(x) = u(p_4)e^{-ip_4\cdot x}$ for the final state. A reasonable guess, therefore, is

$$J^\mu(x) = \overline{\psi}_4(x)\gamma^\mu\psi_2(x)\,, \qquad (6.58)$$

which is called the *transition current*. This guess can be rigorously justified by requiring the same result if the proton is treated as the projectile and the electron as the target. The electromagnetic current of the proton is therefore

$$eJ^\mu(x) = e\overline{u}(p_4)\gamma^\mu u(p_2)e^{i(p_4-p_2)\cdot x}\,. \qquad (6.59)$$

Using this in Eq. (6.52) for the electromagnetic potential gives

$$\begin{aligned}A^\mu(x) &= e\int d^4x'\,D^{\mu\nu}(x-x')J_\nu(x') \\ &= e\int d^4x'\int \frac{d^4q}{(2\pi)^4}\,\frac{-g^{\mu\nu}}{q^2+i\varepsilon}e^{-i(p_4-p_2+q)\cdot x'}e^{-iq\cdot x}\overline{u}(p_4)\gamma_\nu u(p_2) \\ &= e\int d^4q\,\delta^4(p_4-p_2+q)\frac{-g^{\mu\nu}}{q^2+i\varepsilon}e^{-iq\cdot x}\overline{u}(p_4)\gamma_\nu u(p_2)\,. \qquad (6.60)\end{aligned}$$

This gives the potential that we can use for the S-matrix element $S_{fi}^{(1)}$. For the electron wave functions in the intial and final states we have

$$\begin{aligned} \phi_1(x) &= u(p_1)e^{-ip_1\cdot x} \,, \\ \phi_3(x) &= u(p_3)e^{-ip_3\cdot x} \,, \end{aligned} \tag{6.61}$$

in Eq. (6.48) and we use the photon propagator from Eq. (6.57). Carrying out the integrals results in two delta functions and one obtains for $S_{fi}^{(1)}$

$$S_{fi}^{(1)} = ie^2 \int d^4q\, \delta^4(p_4 - p_2 + q)\delta^4(p_3 - p_1 + q)(2\pi)^4 \overline{u}(p_3)\gamma_\mu u(p_1)\frac{-g^{\mu\nu}}{q^2 + i\varepsilon}\overline{u}(p_4)\gamma_\nu u(p_2) \,. \tag{6.62}$$

This result can be depicted using the Feynman diagram shown in Fig. 6.5. A more complete list of the conventions for the diagrams is given in following section. For now, notice that each external fermion line is associated with the corresponding Dirac spinor. The wavey line connecting the electron and photon represents an exchanged photon. Each vertex is characterised by a coupling strength, in this case the electric charge e, and charge is strictly conserved at every vertex. The vertices also each have a delta function that represents conservation of four-momentum, in this case,

$$q = p_3 - p_1 = p_2 - p_4 \,. \tag{6.63}$$

As a consequence, one will necessarily have $q^2 \neq 0$ and the photon is therefore said to be virtual, as opposed to real. The photon line is associated with the propagator $-ig^{\mu\nu}/q^2$, which includes by convention a factor of i.

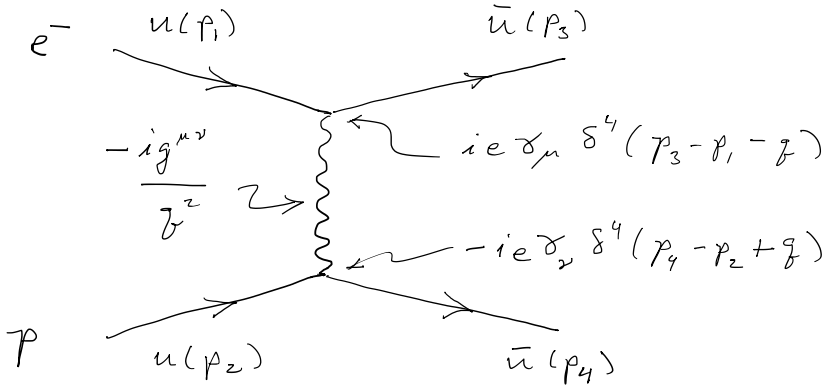

Figure 6.5: Feynman diagram for the reaction $e^- p \to e^- p$.

Carrying out the final integral over q enforces overall four-momentum conservation, i.e.,

$$\int d^4q\, \delta^4(p_4 - p_2 + q)\delta^4(p_3 - p_1 - q) = \delta^4(p_3 + p_4 - p_1 - p_2) \,, \tag{6.64}$$

so that $p_1 + p_2 = p_3 + p_4$. The expression for the first-order matrix element can therefore be written

$$S_{fi}^{(1)} = (2\pi)^4 \delta^4(p_3 + p_4 - p_1 - p_2) \; [\overline{u}(p_3)(ie\gamma_\mu)u(p_1)] \; \frac{-i}{q^2} \; [\overline{u}(p_4)(-ie\gamma^\mu)u(p_2)] \; . \tag{6.65}$$

In general for a reaction with total initial- and final-state four-momenta P_i and P_f, one defines the (Lorentz) invariant amplitude $\mathcal{M}$ by

$$S_{fi} = (2\pi)^4 \delta^4(P_f - P_i)\mathcal{M} \; . \tag{6.66}$$

Thus in the present example we find the first-order invariant amplitude for electron-proton scattering to be

$$\mathcal{M} = \frac{-ie^2}{(p_3 - p_1)^2} \; [\overline{u}(p_3)\gamma_\mu u(p_1)] \; [\overline{u}(p_4)\gamma^\mu u(p_2)] \; , \tag{6.67}$$

where we used $q^2 = (p_3 - p_1)^2$. Sometimes different conventions are used for the factor of i that appears in the amplitudes; some references define the above expression as $i\mathcal{M}$ or $-i\mathcal{M}$ instead of $\mathcal{M}$. As long as this is done consistently for all terms that summed into the total amplitude, these factors appear as an overall phase that goes away when taking the absolute square.

Notice that Eq. (6.63) gives $p_3 = q + p_1$, and $p_2 = q + p_4$, so conservation of four-momentum implies that the photon is emitted by the proton and then absorbed by the electron. In fact, the integrations over the space-time variables that lead to Eq. (6.67) could be expressed in an equivalent manner by taking $q = p_1 - p_3 = p_4 - p_2$. In the diagram, the photon line has been draw vertically and both time orderings of the vertices are implied.

6.7 Rules for Feynman diagrams in QED

The electron-proton scattering example from the previous section has shown how to derive the invariant amplitude using perturbation theory and that the result can be depicted using a Feynman diagram. If we consider different reactions we can get their amplitudes in a similar way and write down the corresponding diagrams. What should now be plausible is that we can write down a set of "Feynman rules" that allows us to write down the amplitude for any of the possible diagrams. We present these rules here for the theory of Quantum Electrodynamics (QED), which describes the interaction of charged fermions (electron, muon, tau lepton, quarks) with photons. The full set of rules for the Standard Model are summarised in App. D.

For QED, the allowed vertices always connect two fermions of the same type with a photon so as to conserve charge, e.g., $e^- \to e^-\gamma$, $\gamma \to e^- + \gamma$, $e^+e^- \to \gamma$, and the corresponding vertices obtained by exchange of e^+ and e^- or exchange of initial and final states. For now we will concentrate on "tree-level" diagrams, i.e., those that do not contain loops. The Feynman rules for tree-level diagrams in QED are as follows.

- For a given reaction, write down all topologically distinct diagrams for that connect the initial and final state particles using the allowed vertices of the theory. Assign four-momenta to each particle so that it is conserved at each vertex.

- The conventions for lines were shown in Fig. 1.1. For fermions, the arrow points forward in time and for antifermions it points backwards. Photons are drawn with wavey lines.
- For each external fermion line, start at the tip of the arrow and write a Dirac spinor $\overline{u}$ for a particle and $\overline{v}$ for an antiparticle, evaluated with the particle's four-momentum.
- At a fermion-photon vertex, write down the factor $-iq\gamma_\mu$, where q is the charge of the particle, e.g., $ie\gamma_\mu$ for an electron.
- After the vertex factor, if the tail of the fermion line is in the initial or final state, write down a Dirac spinor u for a particle or v for antiparticle.
- For a photon in an initial or final state, include a factor of the polarisation vector ε^μ or $\varepsilon^{\mu\,*}$, respectively. Its Lorentz index is contracted with that of the gamma matrix at the vertex to which the photon is coupled.
- For an internal photon, include the propagator $-ig^{\mu\nu}/q^2$. The Lorentz indices are contracted with those of the gamma matrices of the vertices at each end of the photon.
- For an internal electron, include the propagator $i(\not{p} + m)/(p^2 - m^2)$.
- For a diagram that differs from another by exchange of an identical fermion, include a minus sign.

The resulting combination of factors gives the invariant amplitude $\mathcal{M}$. The rules are summarised in Fig. 6.6.

The delta functions at each vertex do not need to be included explicitly for tree-level diagrams, since all four-momenta are fixed by momentum conservation. In diagrams with loops, one must include the delta function and integrate over the undetermine four-momentum.

6.8 Example: amplitude for $e^+e^- \to \mu^+\mu^-$ in QED

As an example of application of the Feynman rules, consider the reaction $e^+e^- \to \mu^+\mu^-$ as shown in Fig. 6.7. Here we are only considering QED processes so at leading order we only include the diagram with where the e^+ and e^- annihilate into a virtual photon.

Following the fermon lines backwards for both the electron and muon and including the photon propagator gives the amplitude

$$\mathcal{M} = [\overline{v}(p_2, s_2)(ie\gamma_\mu)u(p_1, s_1)] \frac{-ig^{\mu\nu}}{q^2} [\overline{u}(p_3, s_3)(ie\gamma_\nu)v(p_4, s_4)] \tag{6.68}$$

We can then contract $g^{\mu\nu}\gamma_\nu = \gamma^\mu$, collect together the constants and replace $q^2 = (p_1 + p_2)^2 \equiv s$, where $s = E_{\rm cm}^2$ is the centre-of-mass energy squared, to find

$$\mathcal{M} = i\frac{e^2}{s} [\overline{v}(p_2, s_2)\gamma_\mu u(p_1, s_1)] [\overline{u}(p_3, s_3)\gamma^\mu v(p_4, s_4)] \ . \tag{6.69}$$

Notice this has the form $\mathcal{M} \sim j_\mu J^\mu$, i.e., the product of two vector currents, and therefore the amplitude is a Lorentz scalar.

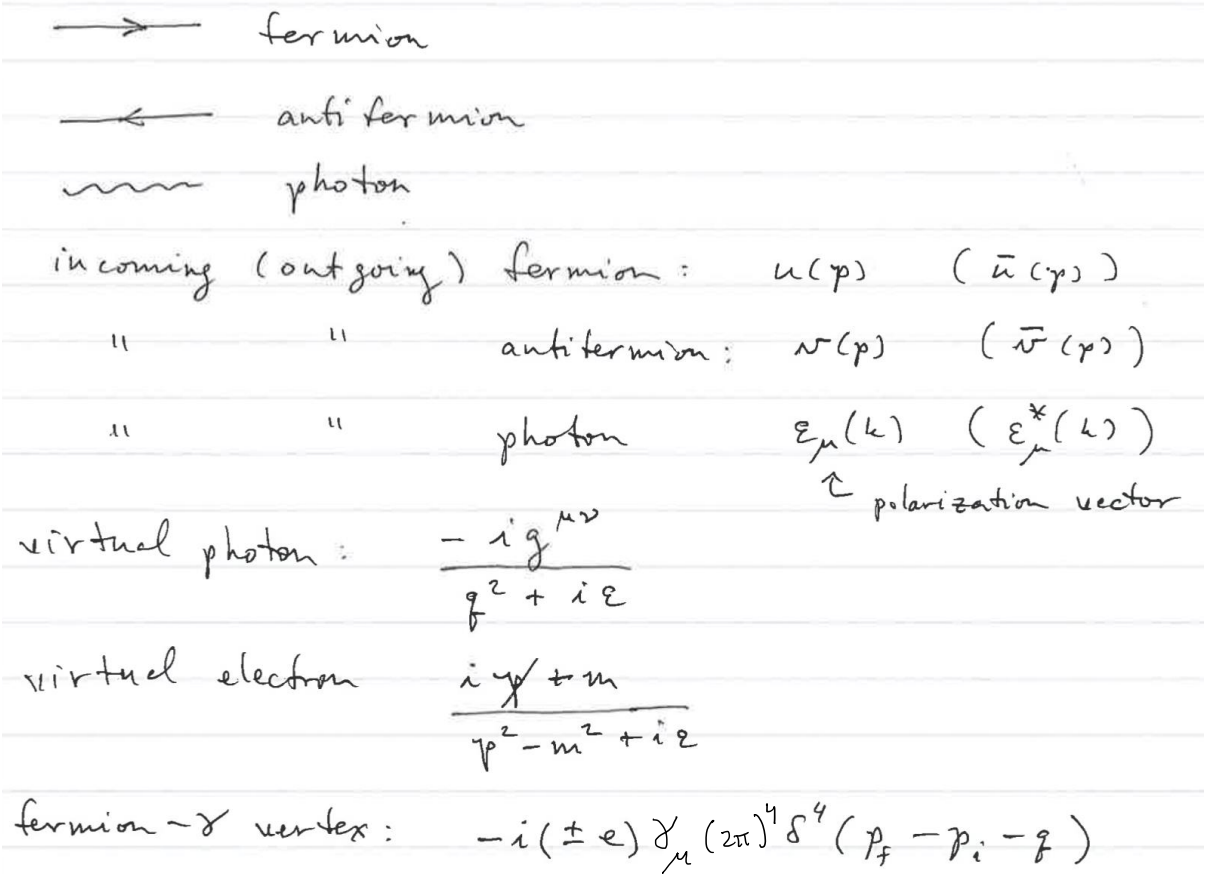

Figure 6.6: Summary of Feynman rules for QED.

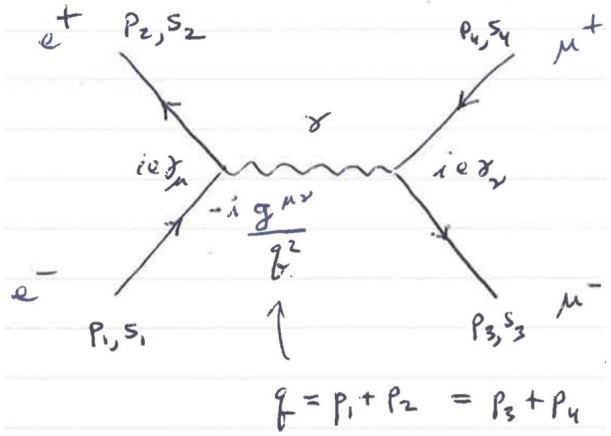

Figure 6.7: A Feynman diagram representing the reaction $e^+e^- \to \mu^+\mu^-$ in QED.

Chapter 7

From Amplitudes to Cross Sections and Decay Rates

Once the Lorentz invariant amplitude $\mathcal{M}$ for a scattering or decay process has been obtained, e.g., from Feynman diagrams and the relevant Feynman rules, one can use this to find the corresponding cross section or decay rate. This involves a formula called Fermi's Golden Rule, which we derive in its Lorentz invariant form in Sec. 7.1. The ingredients of the rule include the amplitude $\mathcal{M}$ and a term called "Lorentz invariant phase space" dLIPS that depends on the number of particles in the final state (Sec. 7.2). These are assembled in Sec. 7.3 to find a differential decay rate of a particle of mass M,

$$d\Gamma = \frac{|\mathcal{M}|^2}{2M}\, d\text{LIPS} \,, \tag{7.1}$$

and in Sec. 7.4 we find the formula for a cross section

$$d\sigma = \frac{|\mathcal{M}|^2}{F}\, d\text{LIPS} \,. \tag{7.2}$$

After deriving these equations, they will be illustrated by computing the differential cross section for $e^+e^- \to \mu^+\mu^-$.

7.1 Fermi's Golden Rule

The starting point for this stage of a calculation is the Lorentz invariant amplitude $\mathcal{M}$, which is related to the unnormalized transition amplitude T_{fi} by

$$T_{fi} = (2\pi)^4 \delta^4(P_f - P_i)\mathcal{M} \,, \tag{7.3}$$

where P_f and P_i are the total four-momenta of the final and initial states. The transition matrix T_{fi} is equivalent the scattering matrix S_{fi} but excludes the term representing no interaction.

It is not quite correct to obtain the transition probability from the square of Eq. (7.3), however, because the wave functions used in the amplitude $\mathcal{M}$ are not normalized to unity.

Rather, up to now we have written the wave function for a fermion of mass m and four-momentum p as

$$\psi(x) = u(p)e^{-ip\cdot x} \,, \tag{7.4}$$

with the Dirac spinors normalized as $u^\dagger(p)u(p) = 2E$, where $E = \sqrt{|\mathbf{p}|^2 + m^2}$. If we integrate $\psi^\dagger\psi$ over the normalizing volume V we get

$$\int_V \psi^\dagger(x)\psi(x)\, d^3\mathbf{x} = u^\dagger(p)u(p) \int_V e^{i(p-p)\cdot x}\, d^3\mathbf{x} = 2EV \,. \tag{7.5}$$

To have all wave functions normalized to unity we should divide $\mathcal{M}$ by a factor of $\sqrt{2EV}$ for every wave function that it contains. So Eq. (7.3) should be modified to read

$$T_{fi} = (2\pi)^4\delta^4(P_f - P_i)\frac{\mathcal{M}}{\prod_{i=1}^N \sqrt{2E_iV}} \,, \tag{7.6}$$

where $N = N_i + N_f$ is the total number of particles in the entering or leaving the interaction, including N_i in the initial and N_f in the final state. This includes boson wave functions, which we have also normalized to $2EV$, but excludes particles in intermediate states.

According to the rules of quantum mechanics, the probability of a transition from initial state i to final state f is given by

$$P_{fi} = |T_{fi}|^2 = \frac{|\mathcal{M}|^2}{\prod_{i=1}^N 2E_iV} \left|(2\pi)^4\delta^4(P_f - P_i)\right|^2 \,. \tag{7.7}$$

The square of a delta function may appear mysterious but it is easy to deal with by representing one of the two factors as an integral over the large normalizing volume V and a correspondingly long time T:

$$(2\pi)^4\delta^4(P_f - P_i) = \int_{V,T} e^{i(P_f - P_i)\cdot x}\, d^4x \to \int_{V,T} e^0\, d^4x = VT \,, \tag{7.8}$$

where we can set $P_f = P_i$ in the integral as this will be enforced by the other delta function. In this way the transition probability becomes

$$P_{fi} = \frac{|\mathcal{M}|^2}{\prod_{i=1}^N 2E_iV}(2\pi)^4\delta^4(P_f - P_i)VT \,, \tag{7.9}$$

and the probability per unit time is therefore

$$\frac{P_{fi}}{T} = \frac{|\mathcal{M}|^2(2\pi)^4\delta^4(P_f - P_i)}{V^{N-1}\prod_{i=1}^N 2E_i} \,. \tag{7.10}$$

Equation (7.10) represents the probability per unit time for a transition between a specific initial state i and final state f, in which the momentum vectors and spins of all particles entering and leaving the reaction are given. The particles' momenta are, however, continuous variables.

We can consider fixed initial-state momenta, but the fact that the final-state momenta take on values selected out of a continuum leads to a complication when assigning a probability to the transition. To get the correct probability we need to integrate over all values for the final-state momenta, and the delta function $\delta^4(P_f - P_i)$ in Eq. (7.10) will automatically select those that are consistent with energy and momentum conservation.

We are considering the system to be in a box of volume $V = L^3$. Imposing periodic boundary conditions on a particle's wave function in the box limits the values of a component of momentum to

$$p = \frac{2\pi n}{L} \,, \tag{7.11}$$

where n is an integer (recall we are setting $\hbar = 1$). The states thus have a spacing $\Delta p = 2\pi/L$ for each of the three directions. There is therefore one allowed state per six-dimensional phase-space volume

$$\left(\frac{2\pi}{L}\right)^3 V = (2\pi)^3 \,. \tag{7.12}$$

If we consider a small element of momentum space $d^3\mathbf{p}_j$ for particle j, the number of states in the phase-space element $V d^3\mathbf{p}_j$ is

$$dn_j = \frac{V\, d^3\mathbf{p}_j}{(2\pi)^3} \,. \tag{7.13}$$

By including a factor like dn_j for all of the N_f final-state particles in the reaction and rearranging various terms, the transition probability per unit time becomes

$$\frac{dP}{T} \equiv dW = \frac{|\mathcal{M}|^2 (2\pi)^4 \delta^4(P_f - P_i)}{V^{N_i - 1} \prod_{j=1}^{N_i} 2E_j} \prod_{k=1}^{N_f} \frac{d^3\mathbf{p}_k}{(2\pi)^3 2E_k} \,, \tag{7.14}$$

where the product of terms $2E_j$ in the denominator is over the N_i initial state particles, and the product over terms $\frac{d^3p_k}{(2\pi)^3 2E_k}$ is over the N_f particles in the final state. Equation (7.14) is called Fermi's Golden Rule. Although the volume V still appears in the formula, this cancels once we convert the probability into a cross section or decay rate.

7.2 Lorentz invariant phase space

The terms in Eq. (7.14) containing $\frac{d^3p_k}{(2\pi)^3 2E_k}$ together with the delta function are often called the *Lorentz invariant phase space* factor

$$d\text{LIPS} = (2\pi)^4 \delta^4(P_f - P_i) \prod_{k=1}^{N_f} \frac{d^3\mathbf{p}}{(2\pi)^3 2E_k} \,. \tag{7.15}$$

Here the term "phase space" takes on a meaning different from the six-dimensional single-particle $d^3\mathbf{x}\ d^3\mathbf{p}$ phase space mentioned previously. The phase space of dLIPS refers to the subspace of the total $3N_f$-dimensional momentum space of the final-state particles that satisfies the four constraints of total energy and momentum conservation, as reflected by $\delta^4(P_f - P_i)$. One can show that dLIPS is, as the name implies, invariant under a Lorentz transformation.

The formula for the differential rate dW represents the joint distribution of all of the final-state momenta $\mathbf{p}_1, \ldots \mathbf{p}_{N_f}$ given the initial-state momenta. Usually we need to integrate this over all but one or two of the final-state momentum components to obtain a differential rate with respect to the remaining kinematic variables. In general both the invariant amplitude squared $|\mathcal{M}|^2$ and dLIPS depend on the momentum vectors so their product must be integrated together. For more than two particles in the final state, the integral cannot in general be expressed in closed form and must be carried out numerically.

For the special case of two final-state particles, however, the dLIPS factor can written in a simple form in a given reference frame, which we choose to be the centre-of-momentum frame. Here the momentum space of the final-state particles has $3N_f = 6$ dimensions, and energy/momentum conservation provide four constraints. Therefore the final state is characterized by two values, which we can take to be the angles θ and ϕ of one of the two particles in the c.m. frame (the other particle's momentum vector is the negative of the first).

For the two final-state four-momenta $p_1 = (E_1, \mathbf{p}_1)$ and $p_2 = (E_2, \mathbf{p}_2)$, dLIPS is

$$d\text{LIPS} = (2\pi)^4 \delta^4(P_f - P_i) \frac{d^3\mathbf{p}_1}{(2\pi)^3 2E_1} \frac{d^3\mathbf{p}_2}{(2\pi)^3 2E_2} \ . \tag{7.16}$$

Although one must first combine dLIPS with the other factors before integrating over $\mathbf{p}_1$ and $\mathbf{p}_2$, the delta function $\delta^4(P_f - P_i)$ will enforce $\mathbf{p}_1 = -\mathbf{p}_2 \equiv \mathbf{p}$. So even if $|\mathcal{M}|^2$ depends on the magnitudes of $\mathbf{p}_1$ and $\mathbf{p}_2$, these values are held constant by the delta function and so $|\mathcal{M}|^2$ can be treated as a constant.

The four-momenta of the two final-state particles are therefore $p_1 = (E_1, \mathbf{p})$ and $p_2 = (E_2, -\mathbf{p})$, where $E_i = \sqrt{|\mathbf{p}|^2 + m_i^2}$ with $i = 1, 2$. The total four-momentum of the final state is $P_f = (E_f, \mathbf{P}_f) = (E_1 + E_2, 0)$, and $P_i = (E_{\rm cm}, 0)$ where $E_{\rm cm}$ is the centre-of-mass energy. Having now integrated over $d^3\mathbf{p}_2$, the Lorentz invariant phase space element can therefore be written

$$d\text{LIPS} = \frac{(2\pi)^4 \delta(E_1 + E_2 - E_{\rm cm})\, d^3\mathbf{p}}{(2\pi)^3 2E_1\, (2\pi)^3 2E_2} \ . \tag{7.17}$$

The final state is now determined by direction of the single momentum vector $\mathbf{p} = \mathbf{p}_1$. Using spherical polar coordinates, we can express $d^3\mathbf{p}$ as

$$d^3\mathbf{p} = p^2\, dp \sin\theta\, d\theta\, d\phi \ , \tag{7.18}$$

where here and below p means $|\mathbf{p}|$. The final remaining delta function in Eq. (7.17) is $\delta(E_1(p) + E_2(p) - E_{\rm cm})$, where $E_i(p) = \sqrt{p_i^2 + m_i^2}$ for $i = 1, 2$. The particle rest masses m_1 and m_2 as well as the centre-of-mass energy $E_{\rm cm}$ are fixed constants, so the argument of the delta function is a given function of p, namely, $f(p) = E_1(p) + E_2(p) - E_{\rm cm}$.

To carry out an integral of a delta function of another function, we can use the property (see, e.g., Ref. [78])

$$\delta(f(x)) = \sum_i \frac{\delta(x - x_i)}{|f'(\alpha_i)|} \,, \tag{7.19}$$

where α_i is the ith zero of $f(x)$. The function

$$f(p) = \sqrt{p^2 + m_1^2} + \sqrt{p^2 + m_2^2} - E_{\rm cm} \tag{7.20}$$

has a zero when $E_1(p) + E_2(p) = E_{\rm cm}$, which happens when p is the magnitude of the momentum of each of the two final-state particles. After some calculation one finds this at

$$p = \frac{\lambda^{1/2}(s, m_1^2, m_2^2)}{2\sqrt{s}} \equiv p^* \,, \tag{7.21}$$

where $s = E_{\rm cm}^2$ and

$$\lambda(s, m_1^2, m_2^2) = (s - m_1^2 - m_2^2)^2 - 4m_1^2 m_2^2 \tag{7.22}$$

is called the Källén triangle function. The delta function over p therefore becomes

$$\delta(E_1(p) + E_2(p) - E_{\rm cm}) = \frac{\delta(p - p^*)}{\left| \frac{\partial E_1}{\partial p}\Big|_{p^*} + \frac{\partial E_2}{\partial p}\Big|_{p^*} \right|} = \frac{E_1(p^*)E_2(p^*)}{(E_1(p^*) + E_2(p^*))p^*} \delta(p - p^*) \,. \tag{7.23}$$

After integrating Eq. (7.17) over p, the Lorentz invariant phase space factor in the c.m. frame for a two-body final state therefore becomes

$$d\text{LIPS} = \frac{1}{(2\pi)^2} \frac{1}{2E_1\, 2E_2} p^2 \, d\Omega \frac{E_1 E_2}{(E_1 + E_2)p}\bigg|_{p=p^*} = \frac{1}{16\pi^2} \frac{p^*}{E_{\rm cm}} \, d\Omega \,, \tag{7.24}$$

where $d\Omega = \sin\theta \, d\theta \, d\phi$ is an element of solid angle that points in the direction of $\mathbf{p}$.

7.3 Decay rates

Returning to Fermi's Golden Rule (7.14), we see that for the case of a single initial-state particle, i.e., $N_i = 1$, the factor of $V^{N_i - 1}$ disappears. If we use the rest frame of the particle of mass M, we have $E_j = M$ and so the transition rate dW, here called the *decay rate* $d\Gamma$, is

$$d\Gamma = \frac{1}{2M} |\mathcal{M}|^2 \, (2\pi)^4 \delta^4(P_f - P_i) \prod_{k=1}^{N_f} \frac{d^3\mathbf{p}_k}{(2\pi)^3 2E_k} = \frac{|\mathcal{M}|^2 \, d\text{LIPS}}{2M} \,. \tag{7.25}$$

If the particle of mass M decays into two particles with masses m_1 and m_2, then using the formula (7.24) for dLIPS in the c.m. frame gives

$$d\Gamma = \frac{1}{32\pi^2 M^2} |\mathcal{M}|^2 p^* \, d\Omega \, . \tag{7.26}$$

If the amplitude squared is independent of the angles θ and ϕ, which is to say the decay is isotropic, then from $\int d\Omega = 4\pi$ one finds the total decay rate

$$\Gamma = \frac{p^*}{8\pi M^2} |\mathcal{M}|^2 \, . \tag{7.27}$$

Equation (7.27) holds in the particle's rest frame and its inverse $\tau = 1/\Gamma$ gives the mean lifetime of the particle. In a boosted reference frame the lifetime is multiplied by the time dilation factor $\gamma = 1/\sqrt{1-\beta^2}$, i.e. $\Gamma \to \Gamma/\gamma$.

7.4 Cross sections

The rate for the scattering of two particles A and B is characterized by the cross section

$$d\sigma = \frac{dW}{J} \, , \tag{7.28}$$

where dW is given by Fermi's Golden Rule (7.14) and J is the incident flux, which we can take to refer to particle A. This can be expressed as

$$J = \rho |\mathbf{v}_{\rm rel}| = \frac{|\mathbf{v}_A - \mathbf{v}_B|}{V} \tag{7.29}$$

where $\rho = 1/V$ is the incident particle density, namely, one per unit volume V. The factors of V therefore cancel in the formula for the cross section,

$$d\sigma = \frac{|\mathcal{M}|^2 (2\pi)^4 \delta^4(P_f - P_i)}{4E_A E_B |\mathbf{v}_A - \mathbf{v}_B|} \prod_{k=1}^{N_f} \frac{d^3\mathbf{p}_k}{(2\pi)^3 2E_K} \equiv \frac{|\mathcal{M}|^2 \, d\text{LIPS}}{F} \, , \tag{7.30}$$

where

$$F = 4E_A E_B |\mathbf{v}_A - \mathbf{v}_B| \tag{7.31}$$

is the *flux factor*. In the rest frame of particle B (the "lab" frame), we have $\mathbf{p}_B = 0$ and $E_B = m_B$. Using $\mathbf{v}_A = \mathbf{p}_A/E_A$ and $\mathbf{v}_B = 0$, the flux factor in the lab frame is $F = 4|\mathbf{p}_A| m_B$.

The terms $d\sigma$, $|\mathcal{M}|^2$ and dLIPS are Lorentz invariant and therefore the factor F should be as well. This can be achieved by taking the general formula for the flux factor to be

$$F = 4((p_A \cdot p_B)^2 - m_A^2 m_B^2)^{1/2} \, . \tag{7.32}$$

The right-hand side depends only on the four-vector product of the four-momenta p_A and p_B and rest masses m_A and m_B and therefore must be Lorentz invariant. Furthermore one can easily show that Eq. (7.32) reduces to the previous formula (7.31) when the four-momenta are evaluated in the lab frame. And since it is a Lorentz invariant it has this value in all frames.

For a scattering process that results in two final-state particles $A+B \to 1+2$, we can combine the amplitude squared, Lorentz invariant phase space and flux factors to find the differential cross section. In the c.m. frame we have for the initial-state particles $\mathbf{p}_A = -\mathbf{p}_B \equiv \mathbf{p}_i^*$ and for the final state $\mathbf{p}_1 = -\mathbf{p}_2 \equiv \mathbf{p}_f^*$. Therefore the flux factor becomes

$$F = 4((p_A \cdot p_B)^2 - m_A^2 m_B^2)^{1/2} \ = 4|\mathbf{p}_i^*|E_{\rm cm} \ . \tag{7.33}$$

Using this in the formula for the cross section with $p^* = |\mathbf{p}_f^*|$ gives for the c.m. frame

$$\frac{d\sigma}{d\Omega} = \frac{1}{64\pi^2 E_{\rm cm}^2}\frac{|\mathbf{p}_f^*|}{|\mathbf{p}_i^*|}|\mathcal{M}|^2 \ . \tag{7.34}$$

If, as is often the case, the initial and final-state particles are ultra-relativistic, then the factor $|\mathbf{p}_f^*|/|\mathbf{p}_i^*| \to 1$. And if, as is the case for a collision of unpolarized particles, $|\mathcal{M}|^2$ is independent of the azimuthal angle ϕ, then one can integrate over ϕ which gives a factor $\int d\phi = 2\pi$, and the differential cross section with respect to the variable $\cos\theta$ is found to be

$$\frac{d\sigma}{d\cos\theta} = \frac{1}{32\pi E_{\rm cm}^2}|\mathcal{M}|^2 \ . \tag{7.35}$$

Equations (7.34) and (7.35) apply in the c.m. frame. To find differential cross sections in other frames it is useful to find the corresponding formula in terms of Lorentz invariant kinematic variables. For a reaction with incoming particles 1 and 2 going to outgoing ones 3 and 4 one defines the Mandelstam variables s, t and u as

$$s = (p_1 + p_2)^2 \ , \tag{7.36}$$
$$t = (p_1 - p_3)^2 \ , \tag{7.37}$$
$$u = (p_1 - p_4)^2 \ . \tag{7.38}$$

One can show that s, t and u are not independent, but rather satisfy the constraint $s + t + u = m_1^2 + m_2^2 + m_3^2 + m_4^2$. One finds $s = E_{\rm cm}^2$ and t can be related to the scattering angle of particle 3. Using for now the c.m. frame this relation is

$$\begin{aligned} t &= (p_1 - p_3)^2 \\ &= p_1^2 + p_3^2 - 2p_1 \cdot p_3 \\ &= m_1^2 + m_3^2 - 2E_1E_3 + 2|\mathbf{p}_1||\mathbf{p}_3|\cos\theta \ , \end{aligned} \tag{7.39}$$

where the scattering angle θ is defined as the angle between $\mathbf{p}_1$ and $\mathbf{p}_3$ in the c.m. frame. After some algebra one finds the c.m.-frame energies and momenta for particles 1 and 3,

$$
\begin{aligned}
E_1 &= \frac{s+m_1^2-m_2^2}{2\sqrt{s}}\,, & E_2 &= \frac{s+m_2^2-m_1^2}{2\sqrt{s}}\,, \\
E_3 &= \frac{s+m_3^2-m_4^2}{2\sqrt{s}}\,, & E_4 &= \frac{s+m_4^2-m_3^2}{2\sqrt{s}}\,, \\
|\mathbf{p}_1| &= |\mathbf{p}_2| = \frac{\lambda^{1/2}(s,m_1^2,m_2^2)}{2\sqrt{s}}\,, & |\mathbf{p}_3| &= |\mathbf{p}_4| = \frac{\lambda^{1/2}(s,m_3^2,m_4^2)}{2\sqrt{s}}\,,
\end{aligned}
\tag{7.40}
$$

where λ is the Källén triangle function defined in Eq. (7.22). Note these depend only on the total centre-of-mass energy and on the rest masses of the initial and final-state particles. Using these these in Eq. (7.39) for t gives

$$
t = m_1^2 + m_3^2 - \frac{(s-m_1^2+m_2^2)(s-m_3^2+m_4^2)}{2s} + \frac{\lambda^{1/2}(s,m_1^2,m_2^2)\lambda^{1/2}(s,m_3^2,m_4^2)}{2s}\cos\theta \tag{7.41}
$$

and therefore

$$
\frac{dt}{d\cos\theta} = \frac{\lambda^{1/2}(s,m_1^2,m_2^2)\lambda^{1/2}(s,m_3^2,m_4^2)}{2s}\,. \tag{7.42}
$$

Provided the amplitude squared has no dependence on the azimuthal angle ϕ we can use Eq. (7.34) for $d\sigma/d\Omega$, integrate over ϕ giving a factor of 2π, and divide by $dt/d\cos\theta$ to find

$$
\frac{d\sigma}{dt} = \frac{|\mathcal{M}|^2}{16\pi\lambda(s,m_1^2,m_2^2)}\,. \tag{7.43}
$$

Although we have used ingredients in the c.m. frame to derive this expression, everything in the final formula is Lorentz invariant and thus it holds in all frames.

7.5 Spin averages

To compute amplitudes with the Feynman rules as outlined in Ch. 6 we need to specify the momenta of the initial- and final-state particles as well as their spins. For example, Eq. (6.69) gives the amplitude for annihilation of e^- and e^+ with four-momenta and spin indices (p_1, s_1) and (p_2, s_2) into a μ^- and μ^+ with (p_3, s_3) and (p_4, s_4). In most experiments we set the incoming and measure the outgoing momenta, but we do not set or measure the spins of the particles. Usually the initial-state particles come with equal probability in any of the possible spin states and the final-state particles appear the same regardless of their spins. In some experiments it is possible to set the spin state with a polarised beam and/or target, and in principle final-state spins could be measured, e.g., in some analog of a Stern-Gerlach apparatus. But for now we will assume the far more usual case where we have no experimental control over the particle spin.

To make a theoretical prediction for the quantity that we actually measure, therefore, we need to sum over the final-state and average over the initial-state spins. Thus the square of the amplitude $|\mathcal{M}|^2$ in the equations for the cross section or decay rate gets replaced by the

corresponding quantity averaged over initial-state and summed over final-state spins, which we will simply call the spin-averaged (squared) matrix element, often written $\langle|\mathcal{M}|^2\rangle$. In practice this is rarely done by literally summing all of the possible terms, but rather by exploiting some clever tricks that involve traces of products of gamma matrices.

Let us suppose that the amplitude for a reaction has the general form

$$\mathcal{M} \sim \overline{u}_1 \Gamma u_2 \ , \tag{7.44}$$

where the subscripts on $\overline{u}$ and u indicate both the momentum and spin state, i.e., (p_i, s_i) for $i = 1, 2$, and Γ is some combination of gamma matrices, e.g., simply γ^μ in the example of $e^+e^- \to \mu^+\mu^-$ (see Eq. (6.69)). If some of the particles are in fact antiparticles then the spinor u is replaced with the corresponding v, and we will see later that this possibility is easy to include. The absolute square of the amplitude is therefore

$$\begin{aligned} |\mathcal{M}|^2 &\sim [\overline{u}_1 \Gamma u_2][\overline{u}_1 \Gamma u_2]^* \\ &= [\overline{u}_1 \Gamma u_2][u_1^\dagger \gamma^0 \Gamma u_2]^\dagger \\ &= [\overline{u}_1 \Gamma u_2][u_2^\dagger \Gamma^\dagger \gamma^{0\,\dagger} u_1] \\ &= [\overline{u}_1 \Gamma u_2][u_2^\dagger \gamma^0 \gamma^0 \Gamma^\dagger \gamma^{0\,\dagger} u_1] \\ &= [\overline{u}_1 \Gamma u_2][\overline{u}_2 \overline{\Gamma} u_1] \ , \end{aligned} \tag{7.45}$$

where

$$\overline{\Gamma} = \gamma^0 \Gamma^\dagger \gamma^0 \ . \tag{7.46}$$

The second line in Eq. (7.45) follows from the definition of $\overline{u}_1$ and because the term in brackets is a scalar, hence its complex conjugate is the same as its adjoint; the third line follow because when taking the adjoint of a product the order is reversed, i.e., $(ABC)^\dagger = C^\dagger B^\dagger A^\dagger$; to reach the fourth line we inserted a factor $\gamma^0\gamma^0 = I_4$ and used $\gamma^{0\,\dagger} = \gamma^0$, and the final line uses the definition of $\overline{\Gamma}$ from Eq. (7.46).

In using the bar notation of Eq. (7.46) one can take advantage of results for combinations of gamma matrices that come up in practice, for example,

$$\begin{aligned} \overline{\gamma^\mu} &= \gamma^\mu \\ \overline{\gamma^5} &= -\gamma^5 \\ \overline{\gamma^\mu \gamma^5} &= \gamma^\mu \gamma^5 \\ \overline{\not{a}\not{b}\not{c} \cdots \not{p}} &= \not{p} \cdots \not{c}\not{b}\not{a} \ . \end{aligned} \tag{7.47}$$

When Eq. (7.45) is summed over the possible values of the spin indices s_1 and s_2, it will lead to terms such as $\sum_{s_2} \overline{u}_2 u_2$. These can be evaluated using the completeness relation for Dirac spinors. Let $A(p)$ be

$$A(p) = \sum_s u(p,s)\overline{u}(p,s) \ , \tag{7.48}$$

where $s = 1, 2$ labels the spin. Multiplying on the right by $u(p,r)$ gives

$$\begin{aligned} A(p)u(p,r) &= \sum_s u(p,s)\overline{u}(p,s)u(p,r) \\ &= \sum_s u(p,s)2m\delta_{rs} \\ &= u(p,r)2m \ , \end{aligned} \tag{7.49}$$

where the second line follows from the normalisation of the spinors given by Eqs. (4.111). But from the free-particle solutions to the Dirac equation (cf. Eqs. (4.87) and (4.88)) we have $(\not{p} - m)u(p,r) = 0$ so $(A - 2m)u = (\not{p} - m)u$ and therefore

$$A = \not{p} + m \tag{7.50}$$

The corresponding calculation can also be carried out for a v spinor by using $\overline{v}(p,s)v(p,r) = -2m\delta_{rs}$, and one thus arrives at the completeness relations

$$\sum_s u(p,s)\overline{u}(p,s) = \not{p} + m \ , \tag{7.51}$$

$$\sum_s v(p,s)\overline{v}(p,s) = \not{p} - m \ . \tag{7.52}$$

Returning to Eq. (7.45) and carrying out the sum over s_2 gives

$$\sum_{s_2} |\mathcal{M}|^2 = [\overline{u}_1 \Gamma u_2][\overline{u}_2 \overline{\Gamma} u_1] = \overline{u}_1 \Gamma (\not{p}_2 + m_2)\overline{\Gamma} u_1 \ . \tag{7.53}$$

To carry out the sum over s_1, let $Q = \Gamma(\not{p} + m_2)\overline{\Gamma}$ and write

$$\overline{u}_1 Q u_1 = \sum_{a,b=1}^{4} (\overline{u}_1)_a Q_{ab} (u_1)_b = \sum_{a,b=1}^{4} Q_{ab}(u_1\overline{u}_1)_{ba} = \sum_{a=1}^{4} [Q u_1 \overline{u}_1]_{aa} = \mathrm{Tr}[Q u_1 \overline{u}_1] \ . \tag{7.54}$$

We can again use the completeness relation with respect to the spin index s_1,

$$\sum_{s_1} \overline{u}_1 Q u_1 = \mathrm{Tr}[Q(\not{p}_1 + m_1)] \ , \tag{7.55}$$

so that the sum over both s_1 and s_2 gives

$$\sum_{s_1,s_2} |\mathcal{M}|^2 = \mathrm{Tr}[\Gamma(\not{p}_2 + m_2)\overline{\Gamma}(\not{p}_1 + m_1)] \; . \tag{7.56}$$

The general result

$$\sum_{s_1,s_2} [\overline{u}_1 \Gamma_A u_2][\overline{u}_1 \Gamma_B u_2]^* = \mathrm{Tr}[(\not{p}_1 + m_1)\Gamma_A(\not{p}_2 + m_2)\overline{\Gamma}_B] \tag{7.57}$$

is sometimes called *Casimir's trick*. Here the term $(\not{p}_1 + m_1)$ has been cyclically permuted to the beginning of the trace to provide an easier mnemonic for the order. If any of the terms involve the spinor v instead of u, then the mass m is replaced by $-m$ (cf. Eq. (7.52)). In sufficiently high-energy reactions one can neglect the mass terms and use

$$\sum_{s_1,s_2} [\overline{u}_1 \Gamma_A u_2][\overline{u}_1 \Gamma_B u_2]^* \approx \mathrm{Tr}[\not{p}_1 \Gamma_A \not{p}_2 \overline{\Gamma}_B] \; . \tag{7.58}$$

Carrying out the sum over spins is thus reduced to evaluating traces of gamma matrices that are contracted with four-momenta. To do this final step one can refer to the following trace theorems (see also properties of gamma matrices given in Sec. 4.6 as well as, e.g., App. J of Aitchison and Hey [4]):

$$\begin{aligned}
\mathrm{Tr}(\gamma^\mu) &= \mathrm{Tr}(\text{any product of odd number of } \gamma \text{ matrices}) = 0 \; , && (7.59)\\
\mathrm{Tr}(\gamma^\mu \gamma^\nu) &= 4g^{\mu\nu} \; , && (7.60)\\
\mathrm{Tr}(\gamma^\mu \gamma^\nu \gamma^\rho \gamma^\sigma) &= 4\left[g^{\mu\nu}g^{\rho\sigma} + g^{\mu\sigma}g^{\nu\rho} - g^{\mu\rho}g^{\nu\sigma}\right] \; , && (7.61)\\
\mathrm{Tr}(\gamma^5) &= 0 \; , && (7.62)\\
\mathrm{Tr}(\gamma^\mu \gamma^\nu \gamma^\rho \gamma^\sigma \gamma^5) &= -4i\epsilon^{\mu\nu\rho\sigma} \; , && (7.63)
\end{aligned}$$

where $\epsilon^{\mu\nu\rho\sigma}$ is the totally antisymmetric tensor with $\epsilon^{0123} = 1$.[1] Useful variants of Eq. (7.61) are

$$\begin{aligned}
\mathrm{Tr}(\not{p}\gamma^\mu \not{k}\gamma^\nu) &= 4\left[p^\mu k^\nu + p^\nu k^\mu - (p\cdot k)g^{\mu\nu}\right] \; , && (7.64)\\
\mathrm{Tr}(\not{a}\not{b}\not{c}\not{d}) &= 4\left[(a\cdot b)(c\cdot d) + (a\cdot d)(b\cdot c) - (a\cdot c)(b\cdot d)\right] \; . && (7.65)
\end{aligned}$$

7.6 Spin-averaged cross section for $e^+e^- \to \mu^+\mu^-$

Returning to the example of $e^+e^- \to \mu^+\mu^-$ from Sec. 6.8, we had found the amplitude

[1] By lowering the Lorentz indices in Eq. (7.63) one finds the same sign: $\mathrm{Tr}(\gamma_\mu\gamma_\nu\gamma_\rho\gamma_\sigma\gamma^5) = -4i\epsilon_{\mu\nu\rho\sigma}$, although for the antisymmetric tensor itself one has $\epsilon_{\mu\nu\rho\sigma} = -\epsilon^{\mu\nu\rho\sigma}$. In some references one finds the opposite sign convention: $\mathrm{Tr}(\gamma^\mu\gamma^\nu\gamma^\rho\gamma^\sigma\gamma^5) = 4i\epsilon^{\mu\nu\rho\sigma}$ with ϵ^{0123} defined as -1 and thus $\epsilon_{0123} = +1$.

$$\mathcal{M} = i\frac{e^2}{s}\left[\overline{v}(p_2, s_2)\gamma_\mu u(p_1, s_1)\right]\left[\overline{u}(p_3, s_3)\gamma^\mu v(p_4, s_4)\right] \ . \tag{7.66}$$

Taking its absolute square and rearranging the terms gives

$$|\mathcal{M}|^2 = \frac{e^4}{s^2}\left[\overline{v}_2\gamma_\mu u_1\right]\left[\overline{v}_2\gamma_\nu u_1\right]^*\left[\overline{u}_3\gamma^\mu v_4\right]\left[\overline{u}_3\gamma^\nu v_4\right]^* , \tag{7.67}$$

where u_i is shorthand for $u(p_i, s_i)$. We can then apply Casimir's trick to the pair of square brackets with $\overline{v}_2$ and u_1 and also to the one with $\overline{u}_3$ and v_4. Assuming the energies are all high enough so that rest masses can be neglected, Eq. (7.58) gives

$$\langle|\mathcal{M}|^2\rangle = \frac{1}{4}\sum_{s_1,s_2,s_3,s_4}|\mathcal{M}|^2 = \frac{e^4}{4s^2}\mathrm{Tr}[\not{p}_2\gamma_\mu\not{p}_1\gamma_\nu]\,\mathrm{Tr}[\not{p}_3\gamma^\mu\not{p}_4\gamma^\nu] , \tag{7.68}$$

where the factor of $1/4$ comes from averaging over the four possible spin combinations of the initial state.

To evaluate the traces we can use the theorem from Eq. (7.61) to find

$$\begin{aligned}\langle|\mathcal{M}|^2\rangle &= \frac{4e^4}{s^2}[p_{1\mu}p_{2\nu} + p_{2\mu}p_{1\nu} - g_{\mu\nu}(p_1\cdot p_2)][p_3^\mu p_4^\nu + p_4^\mu p_3^\nu - g^{\mu\nu}(p_3\cdot p_4)] \qquad (7.69)\\ &= \frac{4e^4}{s^2}[2(p_1\cdot p_3)(p_2\cdot p_4) + 2(p_1\cdot p_4)(p_2\cdot p_3) + (g_{\mu\nu}g^{\mu\nu} - 4)(p_1\cdot p_2)(p_3\cdot p_4)] \ .\end{aligned}$$

The final term disappears since $g_{\mu\nu}g^{\mu\nu} - 4 = 0$. The charge e can be expressed using the fine structure constant $\alpha = e^2/4\pi$ to find

$$\langle|\mathcal{M}|^2\rangle = \frac{128\pi^2\alpha^2}{s^2}[(p_1\cdot p_3)(p_2\cdot p_4) + (p_1\cdot p_4)(p_2\cdot p_3)] \ . \tag{7.70}$$

Now let us consider the reaction in the centre-of-momentum frame, with the scattering angle θ defined as shown in Fig. 7.1.

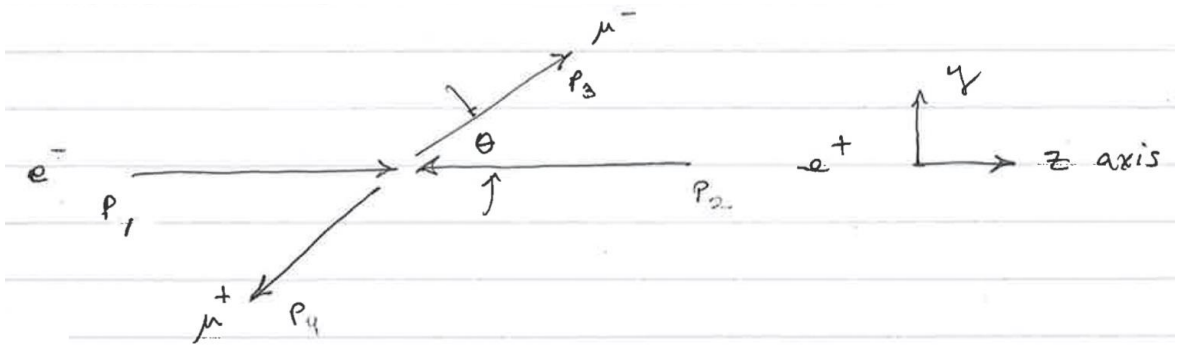

Figure 7.1: The reaction $e^+e^- \to \mu^+\mu^-$ in the c.m. frame.

In the c.m. frame, the four-momenta of the incoming and outgoing particles are

$$p_1 = (E, 0, 0, E) \tag{7.71}$$

$$p_2 = (E, 0, 0, -E) \tag{7.72}$$

$$p_3 = (E, 0, E\sin\theta, E\cos\theta) \tag{7.73}$$

$$p_4 = (E, 0, -E\sin\theta, -E\cos\theta)\ . \tag{7.74}$$

where $E = \sqrt{s}/2$ is the energy of the incoming electron (and of the positron) and we have taken the outgoing muon pair to lie in the (y, z) plane. The dot products of four-vectors are found to be

$$p_1 \cdot p_3 = p_2 \cdot p_4 = E^2(1 + \cos\theta)\ , \tag{7.75}$$

$$p_1 \cdot p_4 = p_2 \cdot p_3 = E^2(1 - \cos\theta)\ , \tag{7.76}$$

$$p_1 \cdot p_2 = p_3 \cdot p_4 = 2E^2\ . \tag{7.77}$$

Combining all the ingredients one finds that the terms simplify to

$$\langle|\mathcal{M}|^2\rangle = 16\pi^2\alpha^2(1 + \cos^2\theta)\ . \tag{7.78}$$

This can now be used in place of $|\mathcal{M}|^2$ in the formula (7.34) for the differential cross section to give

$$\frac{d\sigma}{d\Omega} = \frac{\langle|\mathcal{M}|^2\rangle}{64\pi^2E_{\rm cm}^2} = \frac{\alpha^2}{4E_{\rm cm}^2}(1 + \cos^2\theta)\ , \tag{7.79}$$

where $E_{\rm cm} = \sqrt{s} = 2E$ is the centre-of-mass energy. The cross section does not depend on the azimuthal angle ϕ so we can use Eq. (7.35) to express the result as the differential cross section with respect to $\cos\theta$ as

$$\frac{d\sigma}{d\cos\theta} = \frac{\alpha^2\pi}{2E_{\rm cm}^2}(1 + \cos^2\theta)\ . \tag{7.80}$$

That is, the distribution of $\cos\theta$ has the parabolic shape shown in Fig. 7.2.

To find the total cross section for the reaction we integrate the differential cross section (7.80) over $\cos\theta$ from -1 to 1. Letting $x = \cos\theta$, we find

$$\sigma = \int_{-1}^{1}\frac{d\sigma}{d\cos\theta}\,d\cos\theta = \frac{\pi\alpha^2}{2E_{\rm cm}^2}\int_{-1}^{1}(1 + x^2)\,dx = \frac{4\pi\alpha^2}{3E_{\rm cm}^2}\ . \tag{7.81}$$

In this formula we are using $\hbar = c = 1$, so the cross section has units of inverse energy squared. Inserting the appropriate factors to obtain units of area gives

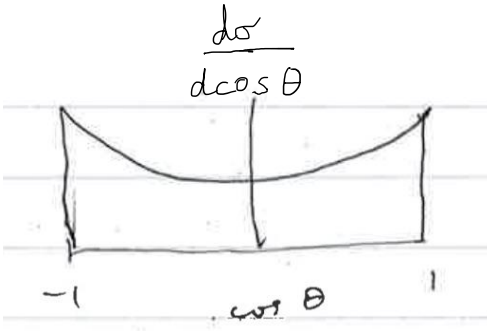

Figure 7.2: Sketch of the differential cross section of $e^+e^- \to \mu^+\mu^-$.

$$\sigma = \frac{4\pi\alpha^2\hbar^2c^2}{3E_{\rm cm}^2} \ . \tag{7.82}$$

For example, at the PEP accelerator at SLAC the centre-of-mass energy was 29 GeV, giving a cross section for $e^+e^- \to \mu^+\mu^-$ of $\sigma = 0.103\,\text{nb}$, where a nanobarn (nb) is $10^{-33}\,\text{cm}^2$. From 1984-86, the TPC/2γ Experiment collected at PEP data corresponding to an integrated luminosity of $\int \mathcal{L}\,dt = 60\,\text{pb}^{-1}$. The number of $e^+e^- \to \mu^+\mu^-$ events was therefore

$$N = \sigma \int \mathcal{L}\,dt = 0.103\,\text{nb} \ \times \ 60\,\text{pb}^{-1} \times \frac{1000\,\text{nb}^{-1}}{1\,\text{pb}^{-1}} = 6\,180 \text{ events} \ . \tag{7.83}$$

Because of the form of the differential cross section (7.80), one has a significant probability for the muon pair to be emitted with a small angle relative to the incoming beams, and as a result they cannot be detected and identified as muons. The number of events within angles covered by the detector, roughly $|\cos\theta| \leq 0.8$ was correspondingly less.

At a centre-of-mass energy of $E_{\rm cm} \sim 14\,\text{GeV}$, treating $e^+e^- \to \mu^+\mu^-$ as a pure QED process is a good approximation. At higher energies the differential cross section becomes sensitive to the amplitude in which the intermediate photon is replaced by a Z. Both diagrams are present at the same order and their interference leads to a forwards-backwards asymmetry, so that $\frac{d\sigma}{d\cos\theta} \sim 1 + B\cos\theta + \cos^2\theta$, where B depends on the mass and couplings of the Z boson. Measurements of this angular distribution at the PETRA accelerator at DESY (Hamburg) were an important early test of the Standard Model. Data from the JADE Experiment are shown in Fig. 7.3 (from Ref. [16]).

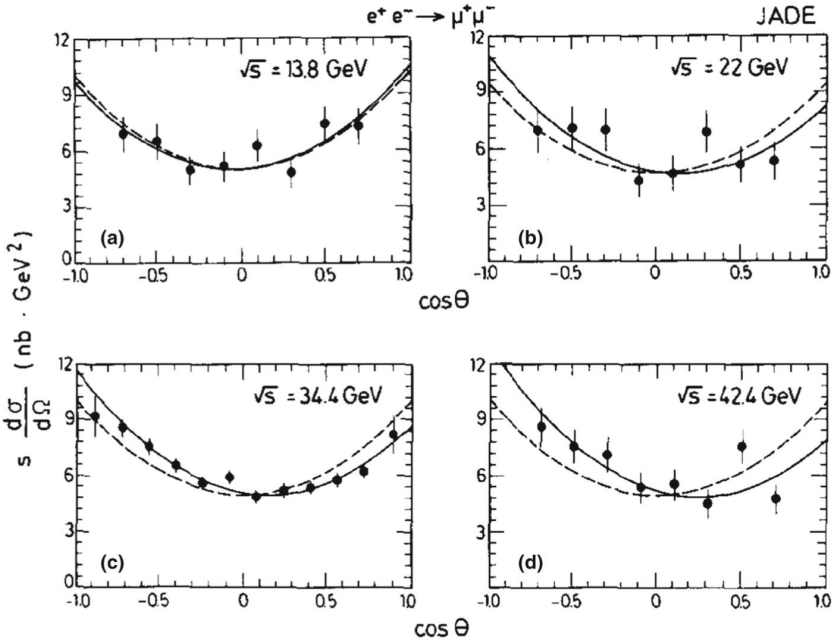

Figure 7.3: Differential cross sections for $e^+e^- \to \mu^+\mu^-$ at four centre-of-mass energies measured by the JADE Experiment [16] at PETRA. The dashed curves are the predictions of QED; the solid curves include the interference from the Z boson.

Chapter 8

The Weak Interaction

In this chapter we look at the weak interaction, starting with Fermi's theory of beta decay through to the $V-A$ theory including parity violation and the concept of quark-flavour mixing. As an example of weak reactions we look at neutrino scattering experiments, which also provide an introduction into the structure of the nucleon.

8.1 Introduction and history of the theory of weak interactions

The theory of weak interactions grew out of studies of radioactivity, specifically, β-decay of nuclei whereby an electron is emitted and the atomic number of the nucleus increases by one. From considerations of conservation of energy and angular momentum, Pauli proposed in 1930 that the decay must be accompanied by a spin-1/2, neutral and very weakly interacting particle, the neutrino [17]. These are now understood to arise from the transition of a neutron into a proton, electron and anti-electron neutrino, as shown in Fig. 8.1.[1]

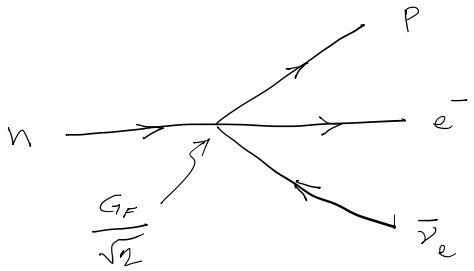

Figure 8.1: Nuclear beta decay modeled as proceeding via $n \to pe^-\overline{\nu}_e$.

In 1934, Fermi proposed a theory of weak interactions that used Pauli's neutrino and was patterned after Quantum Electrodynamics [18]. In analogy with QED, the amplitude for the decay $n \to pe^-\overline{\nu}$ was expressed as the product of two currents, initially taken to be Lorentz vectors: one representing the transition of neutron to proton (the hadron current", $J^\mu_{\rm had}$) and one for the production of the electron and antineutrino (the lepton current, $j^\mu_{\rm lep}$). The coupling strength is called the Fermi constant $G_{\rm F}$ (replaced in later versions of the theory by $G_{\rm F}/\sqrt{2}$):

[1] This section follows Sec. 9 of [1].

$$\mathcal{M} = G_{\mathrm{F}}\, J_{\mu}^{\mathrm{had}}\, j_{\mathrm{lep}}^{\mu} = G_{\mathrm{F}}[\overline{u}_p \gamma_\mu u_n][\overline{u}_e \gamma^\mu v_\nu] \,. \tag{8.1}$$

In contrast to QED, both the hadron and lepton currents result in a change of the particle's charge. Since Fermi's initial guess was that both currents were Lorentz vectors, the amplitude $\mathcal{M}$ is a scalar, and thus conserves parity.

Fermi's theory could be generalised to describe other phenomena such as muon decay, now understood to proceed as $\mu^- \to e^- \overline{\nu}_e \nu_\mu$, as shown in Fig. 8.2(a). Measurements of the muon's decay rate result in the current best determination of the Fermi constant [19]

$$G_{\mathrm{F}} = 1.66\,378\,8(6) \times 10^{-5}\,\mathrm{GeV}^{-2} \,. \tag{8.2}$$

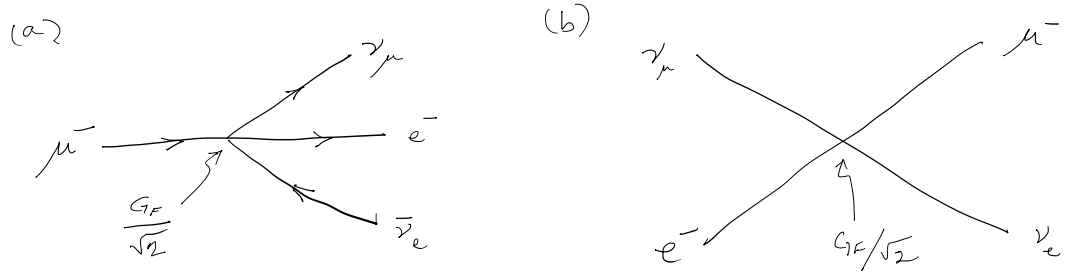

Figure 8.2: Weak-interaction processes in Fermi's theory: (a) the decay $\mu^- \to e^- \nu_\mu \overline{\nu}_e$ and (b) the scattering reaction $\nu_\mu e^- \to \mu^- \nu_e$.

Closely related to muon decay is the scattering reaction $\nu_\mu e^- \to \mu^- \nu_e$ as shown in Fig. 8.2(b). Even before this process was observed experimentally, it pointed to an important problem with Fermi's theory. The amplitude for the reaction is proportional to G_{F}, so the cross section goes as G_{F}^2. The cross section has units of area, or $1/E^2$ in particle physics units. At sufficiently high energies, the only relevant energy scale is the centre-of-mass energy of the reaction E_{cm}. Therefore on dimensional grounds we expect

$$\sigma(\nu_\mu e^- \to \mu^- \nu_e) \sim G_{\mathrm{F}}^2 E_{\mathrm{cm}}^2 \,. \tag{8.3}$$

Thus the cross section grows as E_{cm}^2 and at a high enough energy, found to be around $E_{\mathrm{cm}} \sim 300$ GeV, the corresponding reaction probability exceeds unity and is said to violate the unitarity bound.

Before the theory of weak interactions was finally reformulated as the electroweak Standard Model, it underwent several modifications, which we describe briefly in the following sections: First, it was proposed that the interaction proceeds by exchange of a massive intermediate vector boson, now called the $W^\pm$, which prevents cross sections from violating the unitarity bound. In addition, in accordance with experimental discoveries, the theory was modified to include parity violation. Our current picture of weak interactions includes "neutral current" processes corresponding to the exchange of the neutral Z boson, but these were only seen experimentally after being predicted by the Glashow-Weinberg-Salam electroweak model, which we will see in Ch. 9.

8.1.1 Unitarity and the Intermediate Vector Boson

One might try to explain the violation of the unitarity bound as a deficiency of using only the lowest-order contribution to the amplitude. In principle there should be higher order graphs such as the one shown in Fig. 8.3. These contain additional factors of the coupling strength $G_{\rm F}$ and loops of particles, whose momenta must be integrated over all possible values. Ideally one expects higher-order terms in perturbation theory to represent small corrections, but in this case the integrals from the loops turn out to diverge, i.e., their contribution appeared to be not small, but infinite.

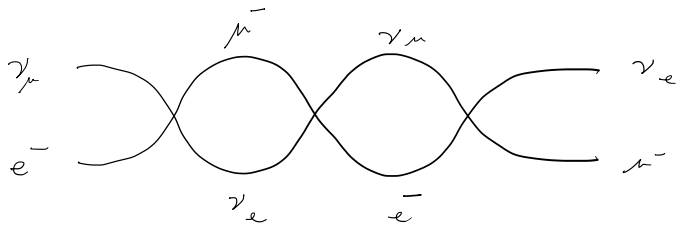

Figure 8.3: A possible higher-order Feynman diagram for the reaction $\nu_\mu e^- \to \mu^- \nu_e$.

In fact, divergent integrals from higher-order amplitudes arise not only in Fermi's theory but also in QED. In the 1940s, Tomonaga, Feynman and Schwinger succeeded in developing a procedure called *renormalisation*, where by appropriate redefinition of the measurable parameters one could separate the infinite integrals from a well-defined finite contribution. This was highly successful in QED, but could not be applied to Fermi's theory of weak interactions. The coupling strength $G_{\rm F}$ of the four-fermion interaction has dimension of inverse energy squared, in contrast to the dimensionless charge e of QED, and as a consequence Fermi's theory turns out to be non-renormalisable.

To reformulate Fermi's theory in closer correspondence with QED, it was proposed to replace the four-fermion interaction with the exchange of an Intermediate Vector (spin-one) Boson or IVB, which is what we now identify as the $W^\pm$. This particle should interact with fermions with a weak coupling $g/\sqrt{2}$ (the factor of $\sqrt{2}$ is a historical convention). The Feynman diagrams for muon decay and muon-neutrino scattering in the new theory are shown in Fig. 8.4.

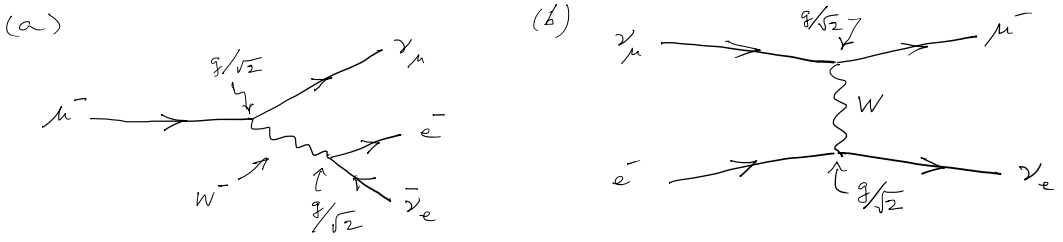

Figure 8.4: Weak-interaction processes with an Intermediate Vector Boson like the $W^\pm$ of the Standard Model: (a) the decay $\mu^- \to e^- \nu_\mu \overline{\nu}_e$ and (b) the scattering reaction $\nu_\mu e^- \to \nu_e \mu^-$.

The low reaction probability of the weak interaction can be explained by assuming that the IVB has a large mass. One can show that the wave equation (3.15) for the electromagnetic

potential A^μ for the photon is generalised to a spin-1 particle of mass M_W by using a field W^μ found from the *Proca equation*,

$$[(\partial_\nu \partial^\nu) + M_W^2]W^\mu - \partial^\mu(\partial_\nu W^\nu) = J^\mu \ . \tag{8.4}$$

By following a procedure analogous to what was done with A^μ, one finds that the propagator (6.57) for a photon with four-momentum q generalises to that of a spin-1 boson with mass M_W as

$$\frac{-ig^{\mu\nu}}{q^2 + i\varepsilon} \quad \to \quad \frac{-i\left(g^{\mu\nu} - \frac{q^\mu q^\nu}{M_W^2}\right)}{q^2 - M_W^2 + i\varepsilon} \ . \tag{8.5}$$

In muon decay, q^2 is the invariant mass of the $(e^- \overline{\nu}_e)$ pair. This is maximum when the ν_μ inherits a vanishingly small energy, in which case $q^2 = m_\mu^2$ with $m_\mu = 0.105\,\mathrm{GeV}$ being the muon mass. This is far less than what we eventually find for the W-boson's mass (80.4 GeV). For processes where $q^2 \ll M_W^2$, the propagator can be approximated

$$\frac{-i\left(g^{\mu\nu} - \frac{q^\mu q^\nu}{M_W^2}\right)}{q^2 - M_W^2 + i\varepsilon} \quad \to \quad \frac{ig^{\mu\nu}}{M_W^2} \ . \tag{8.6}$$

The amplitude for muon decay thus goes as g^2/M_W^2, which was proportional to G_F in Fermi's theory. By comparing the two predictions one obtains

$$G_\mathrm{F} = \frac{\sqrt{2}}{8}\frac{g^2}{M_W^2} \ , \tag{8.7}$$

where the factor $\sqrt{2}/8$ emerges after the interaction is modified from the original vector-current form to the parity-violating one that replaced it in 1957, as described in Sec. 8.4. From the measured value of G_F and using $M_\mathrm{W} = 80.4\,\mathrm{GeV}$ one finds for the weak coupling constant $g = 0.653$, the same order of magnitude as the electric charge $e = 0.303$. Thus the weakness of the weak interaction is explained by the large mass of the exchanged boson, not from the size of the coupling strength.

In the scattering reaction $\nu_\mu e^- \to \nu_e \mu^-$, the q^2 of the W boson has a magnitude proportional to the centre-of-mass energy squared (for a given scattering angle). When we consider sufficiently high energy with $E_\mathrm{cm} \gg M_\mathrm{W}$, the amplitude goes as

$$\mathcal{M} \sim g^2 \, \frac{g^{\mu\nu} - \frac{q^\mu q^\nu}{M_W^2}}{q^2 - M_W^2} \ \to \frac{g^2}{E_\mathrm{cm}^2} \ . \tag{8.8}$$

It is not so obvious is that the term $q^\mu q^\nu / M_W^2$ can be neglected; in fact one can show it makes only a small contribution to the amplitude. Provided this holds we have $\mathcal{M} \sim g^2/E_\mathrm{cm}^2$. Using again dimensional arguments we see that the cross section eventually falls as $\sigma \sim g^4/E_\mathrm{cm}^2$, thereby avoiding the unitarity bound. Furthermore, once the IVB theory is reformulated using gauge symmetry, as we will see in Ch. 9, one finds it is renormalisable and therefore the higher-order corrections result in accurate predictions.

8.1.2 Non-conservation of parity

By expressing the amplitude for weak interaction processes as the product of two vector currents as in Eq. (8.1), the amplitude is Lorentz invariant, which implies conservation of parity. In 1956 Lee and Yang [21] proposed that parity violation was a real possibility and that this hypothesis should be tested experimentally. This was done by Wu and collaborators [20] using β-decay of polarised ^{60}Co nuclei, as illustrated in Fig. 8.5.

The ^{60}Co nucleus has a nonzero magnetic moment and undergoes the decay

$$^{60}\mathrm{Co} \rightarrow ^{60}\mathrm{Ni} + \mathrm{e}^- + \overline{\nu}_\mathrm{e} \; .$$

Suppose we produce a magnetic field by running a current through a coil as shown in Fig. 8.5(a). The spins of the nuclei will then line up with the magnetic field, and we can measure the number of electrons emitted as a function of the angle θ as shown in the figure.

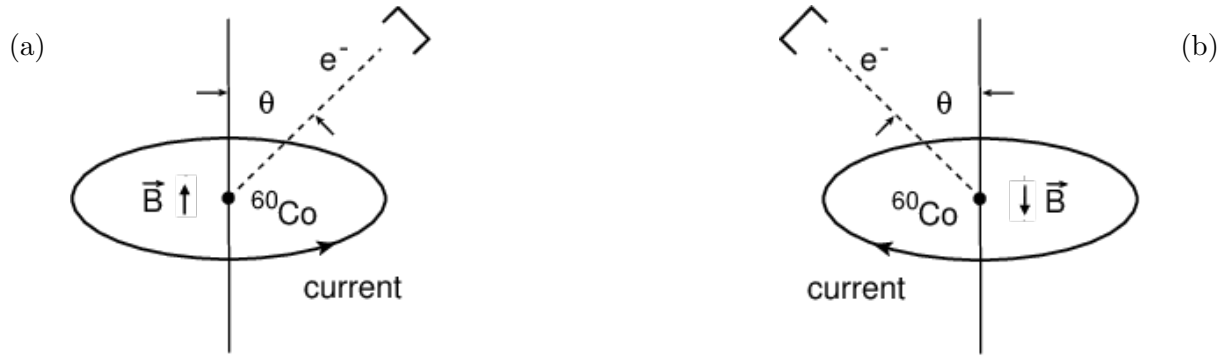

Figure 8.5: (a) An experiment in which nuclear spins are aligned parallel to a magnetic field created by a current loop, and the number of beta electrons is measured at the angle θ. (b) The mirror image experiment.

The mirror image experiment is shown in Fig. 8.5(b). If parity is conserved, we should expect the same numbers of electrons to be found in the two detectors. Note however, that in constructing the mirror image experiment, the current in the coil runs in the opposite direction. This means that the magnetic field in this experiment will point downwards, and the nuclear spins therefore also point down. In the mirror image experiment, the angle between the detector and the magnetic field is therefore not θ but rather $\pi - \theta$. That is, the mirror image experiment at $\pi - \theta$ is identical to the original experiment at θ, but with the entire apparatus rotated top for bottom.

We do not literally build the mirror image experiment, but simply measure the number of electrons $N(\theta)$ as a function of θ. If parity is conserved, we should find

$$N(\theta) = N(\pi - \theta) \; . \tag{8.9}$$

Wu found that equation (8.9) did *not* hold, and therefore that parity was not conserved.

Parity violation was subsequently measured to high precision in a number of weak interaction processes and this led to a modification of Fermi's original theory, in which the vector currents in the amplitudes such as Eq. (8.1) are replaced by a difference of vector and axial-vector currents,

which we will see in Sec. 8.4. This change to the theory is made entirely in response to the experimental evidence and does not emerge from any deeper theoretical considerations; parity violation must be put into the theory "by hand".

The measurements that showed parity violation such as the β-decay experiment by Wu could be explained if one assumed that neutrinos always have their spin antiparallel and antineutrinos always parallel to their direction of motion. To define these concepts more precisely and incorporate them into Fermi's theory we need to define *helicity* and *chirality*.

8.2 Helicity

The weak interactions have a particular dependence on the spin states of the particles involved. This is easiest to bring into the theory using the *helicity*, defined as the projection of a particle's spin along its direction of momentum $\boldsymbol{p}$. The helicity operator $\hat{\lambda}$ is

$$\hat{\lambda} = \frac{\boldsymbol{S}\cdot\boldsymbol{p}}{|\boldsymbol{p}|}\,, \tag{8.10}$$

where

$$\boldsymbol{S} = \frac{1}{2}\begin{pmatrix}\boldsymbol{\sigma} & 0\\ 0 & \boldsymbol{\sigma}\end{pmatrix} \tag{8.11}$$

is the spin operator for a Dirac particle. The helicity is not defined for a particle at rest. Furthermore it is not Lorentz invariant, since one can always reverse a particle's direction of motion by boosting to a reference frame moving in the opposite direction. In doing so, $\boldsymbol{p}$ changes sign but the spin is unchanged, so the helicity changes sign.

The spin index $s = 1, 2$ in the Dirac spinors u_s and v_s that we have seen in Eqs. (4.113) and (4.114) give the particle's spin as up or down relative to the z axis. Here we must recall that the negative energy solutions $\psi_- = v_s e^{ip\cdot x}$ describe physical antiparticles for which the four-momentum has the opposite sign. Under the replacement $(E, \boldsymbol{p}) \to (-E, -\boldsymbol{p})$, the orbital angular momentum $\boldsymbol{L} = \boldsymbol{r}\times\boldsymbol{p}$ changes to $-\boldsymbol{r}\times\boldsymbol{p}$. Therefore, when acting on antiparticle states, the spin operator must be taken as

$$\boldsymbol{S}^{(v)} = -\boldsymbol{S}\,, \tag{8.12}$$

so that its eigenvalue reflects the physical spin and the total angular momentum $\boldsymbol{L}+\boldsymbol{S}$ remains conserved.

If, for example, we have a particle with physical momentum along the z axis, $\boldsymbol{p} = \hat{z}p_z$, the spinors u_1, u_2, v_1 and v_2 are found from Eqs. (4.113) and (4.114) to be

$$u_1(p) = \sqrt{E+m}\begin{pmatrix}1\\ 0\\ \frac{p_z}{E+m}\\ 0\end{pmatrix}\,, \qquad u_2(p) = \sqrt{E+m}\begin{pmatrix}0\\ 1\\ 0\\ \frac{-p_z}{E+m}\end{pmatrix}\,, \tag{8.13}$$

$$v_1(p) = \sqrt{E+m}\begin{pmatrix} 0 \\ \frac{-p_z}{E+m} \\ 0 \\ 1 \end{pmatrix}, \qquad v_2(p) = \sqrt{E+m}\begin{pmatrix} \frac{p_z}{E+m} \\ 0 \\ 1 \\ 0 \end{pmatrix}. \tag{8.14}$$

The helicities for the particle spinors u_1 and u_2 with $\boldsymbol{p} = \hat{z}|\boldsymbol{p}|$ are found to be

$$\hat{\lambda}u_1 = \frac{1}{2}u_1\,, \qquad \hat{\lambda}u_2 = -\frac{1}{2}u_2\,. \tag{8.15}$$

For an antiparticle with physical momentum $\boldsymbol{p} = \hat{z}|\boldsymbol{p}|$, one finds for the *physical* spin,

$$S_z^{(v)}v_1 = -S_z v_1 = \frac{1}{2}v_1\,, \qquad S_z^{(v)}v_2 = -S_z v_2 = -\frac{1}{2}v_2\,. \tag{8.16}$$

The corresponding physical helicity operator that acts on v_1 and v_2 is therefore

$$\hat{\lambda}^{(v)} = -\hat{\lambda} = -\frac{1}{2}\frac{\boldsymbol{\sigma}\cdot\boldsymbol{p}}{|\boldsymbol{p}|}\,. \tag{8.17}$$

Suppose as above the particle is moving in the $+\hat{z}$ direction, i.e., $\boldsymbol{p} = \hat{z}|\boldsymbol{p}|$. Then the $\lambda^{(v)} = 1/2$ helicity state corresponds to v_1 and the $\lambda^{(v)} = -1/2$ helicity state to v_2:

$$\hat{\lambda}^{(v)}v_1 = \frac{1}{2}v_1\,, \qquad \hat{\lambda}^{(v)}v_2 = -\frac{1}{2}v_2\,. \tag{8.18}$$

One can show (see, e.g., Ref. [3] Sec. 4.8) that for a particle with momentum vector $\boldsymbol{p} = (p\sin\theta\cos\phi, p\sin\theta\sin\phi, p\cos\theta))$ the u spinors of positive and negative helicity are

$$u_+(p) = \sqrt{E+m}\begin{pmatrix} \cos\frac{\theta}{2} \\ \sin\frac{\theta}{2}e^{i\phi} \\ \frac{p}{E+m}\cos\frac{\theta}{2} \\ \frac{p}{E+m}\sin\frac{\theta}{2}e^{i\phi} \end{pmatrix}, \qquad u_-(p) = \sqrt{E+m}\begin{pmatrix} -\sin\frac{\theta}{2} \\ \cos\frac{\theta}{2}e^{i\phi} \\ \frac{p}{E+m}\sin\frac{\theta}{2} \\ -\frac{p}{E+m}\cos\frac{\theta}{2}e^{i\phi} \end{pmatrix}, \tag{8.19}$$

and the corresponding antiparticle v spinors with physical + and − helicity are

$$v_+(p) = \sqrt{E+m}\begin{pmatrix} \frac{p}{E+m}\sin\frac{\theta}{2} \\ -\frac{p}{E+m}\cos\frac{\theta}{2}e^{i\phi} \\ -\sin\frac{\theta}{2} \\ \cos\frac{\theta}{2}e^{i\phi} \end{pmatrix}, \qquad v_-(p) = \sqrt{E+m}\begin{pmatrix} \frac{p}{E+m}\cos\frac{\theta}{2} \\ \frac{p}{E+m}\sin\frac{\theta}{2}e^{i\phi} \\ \cos\frac{\theta}{2} \\ \sin\frac{\theta}{2}e^{i\phi} \end{pmatrix}. \tag{8.20}$$

For a nonzero momentum $\boldsymbol{p}$ these satisfy

$$\hat{\lambda} u_+(p) = \frac{1}{2} u_+(p), \quad \hat{\lambda} u_-(p) = -\frac{1}{2} u_-(p), \tag{8.21}$$

$$\hat{\lambda}^{(v)} v_+(p) = \frac{1}{2} v_+(p), \quad \hat{\lambda}^{(v)} v_-(p) = -\frac{1}{2} v_-(p) \; . \tag{8.22}$$

Positive and negative helicity solutions are usually called right- and left-handed, respectively. This can lead to some confusion with the related property of chirality, which also employs the same terms in a different sense, as explained in the following section. To avoid confusion we will usually therefore refer to the two helicity states as positive and negative. For ultra-relativistic particles like neutrinos, helicity and chirality coincide and so one may then use the terms left- and right-handed without risk of misunderstanding.

8.3 Chirality

The chirality of a particle relates to the representation of the Lorentz group under which its field transforms, and in particular distinguishes left- and right-handed components. It can be defined for particles of any spin, but we will only use it here in connection with fermions. Acting on a Dirac spinor, the chirality operator is defined as the matrix γ^5,

$$\gamma^5 = i\gamma^0\gamma^1\gamma^2\gamma^3 = \begin{pmatrix} 0 & 0 & 1 & 0 \\ 0 & 0 & 0 & 1 \\ 1 & 0 & 0 & 0 \\ 0 & 1 & 0 & 0 \end{pmatrix} \; , \tag{8.23}$$

which has the properties mentioned in Sec. 4.6, namely, $(\gamma^5)^2 = I_4$, $(\gamma^5)^\dagger = \gamma^5$ and $\gamma^5\gamma^\mu = -\gamma^\mu\gamma^5$. Since $(\gamma^5)^2 = I_4$, it follows that the eigenvalues of γ^5 are ± 1. Spinors $u(p)$ with chirality eigenvalues $+1$ and -1 are said to be right- and left-handed (or right- and left-chiral), respectively:

$$\gamma^5 u_R = +u_R, \qquad \gamma^5 u_L = -u_L \; . \tag{8.24}$$

Since the 4×4 matrix γ^5 has only two unique eigenvalues (± 1), the components u_R and u_L are not uniquely determined functions of p. We will see below, however, that the helicity eigenstates $u_+(p)$ and $u_-(p)$ become equal to their right- and left-chiral components, respectively, in the ultra-relativistic limit.

For v spinors, the naming convention is the opposite of what is used for u, namely,

$$\gamma^5 v_R = -v_R, \qquad \gamma^5 v_L = +v_L \; . \tag{8.25}$$

This unexpected notation is related to the connection between chirality and helicity in the ultra-relativistic limit, where v_+ and v_- become purely right- and left-chiral, respectively.

The left- and right-handed chirality projection operators are defined as

$$P_L = \frac{1}{2}(1-\gamma^5)\ , \qquad P_R = \frac{1}{2}(1+\gamma^5)\ , \tag{8.26}$$

where the number 1 here means the 4×4 identity matrix I_4. One can readily verify that these have the usual properties of quantum mechanical projection operators, i.e.,

$$\begin{aligned} P_L + P_R &= 1\ , & (8.27)\\ P_L^2 &= P_L\ , & (8.28)\\ P_R^2 &= P_R\ , & (8.29)\\ P_L P_R &= P_R P_L = 0\ . & (8.30) \end{aligned}$$

Using the projection operators, any Dirac spinor can be written as a sum of its left- and right-chiral components, e.g., $u = (P_R + P_L)u = P_R u + P_L u \equiv u_R + u_L$. One defines

$$\begin{aligned} u_L &= P_L u\ , \qquad u_R = P_R u\ , & (8.31)\\ v_L &= P_R v\ , \qquad v_R = P_L v\ . & (8.32) \end{aligned}$$

Notice again that the subscripts used for v_L and v_R are the opposite of what one may expect, and correspond to $\gamma^5 v_R = -v_R$, $\gamma^5 v_L = +v_L$. Using Eqs. (8.27) - (8.30) one finds

$$\begin{array}{llll} P_L u_R = 0\ , & P_R u_R = u_R\ , & P_L u_L = u_L\ , & P_R u_L = 0\ . \\ P_L v_R = v_R\ , & P_R v_R = 0\ , & P_L v_L = 0\ , & P_R v_L = v_L\ . \end{array} \tag{8.33}$$

Although one sometimes writes, as above, u_R or u_L with no other indices or arguments, it is important to note that the chiral components are not uniquely determined by the four-momentum, but depend also on the spin state. For example, the right-chiral component of $u_1(p)$ is not the same as that of $u_2(p)$. We will show below, however, that in the ultrarelativistic limit, the chiral components coincide with states of definite helicity.

Except in the ultrarelativistic limit, the chiral components u_R and u_L do not themselves represent physical states (eigenstates of the Hamiltonian), since they are not solutions of the Dirac equation. A solution must satisfy $(\not{p} - m)u(p) = 0$, and $u = u_R + u_L$, so one has

$$\not{p}(u_R + u_L) = m(u_R + u_L)\ . \tag{8.34}$$

Because $\gamma^5\gamma^\mu = -\gamma^\mu\gamma^5$ it follows that $P_L\not{p} = \not{p}P_R$. By applying P_R or P_L to both sides of Eq. (8.34) one finds

$$\not{p}u_R = m u_L\ , \qquad \not{p}u_L = m u_R\ . \tag{8.35}$$

Thus for $m \neq 0$ the two chiral components are not independent, and they do not solve the Dirac equation. Their importance derives from the fact that the left- and right-chiral components

play different roles in the weak interaction. In particular, only the left-chiral components of a fermion ($u_L = P_L u$) and right-chiral components of an antifermion ($v_R = P_L v$) couple to the W boson.

The connection between helicity and chirality comes in the ultra-relativistic limit ($E \gg m$) where the right- and left-chiral components become equal to postive and negative helicity eigenstates, respectively. Consider an electron with momentum $\boldsymbol{p} = \hat{z}|\boldsymbol{p}|$ and positive physical helicity, $\lambda = 1/2$. It is described by the spinor u_1 from Eq. (8.13). The right- and left-handed chiral operators P_R and P_L can written out as

$$P_R = \tfrac{1}{2}(1+\gamma^5) = \frac{1}{2}\begin{pmatrix} 1 & 0 & 1 & 0 \\ 0 & 1 & 0 & 1 \\ 1 & 0 & 1 & 0 \\ 0 & 1 & 0 & 1 \end{pmatrix} , \qquad P_L = \tfrac{1}{2}(1-\gamma^5) = \frac{1}{2}\begin{pmatrix} 1 & 0 & -1 & 0 \\ 0 & 1 & 0 & -1 \\ -1 & 0 & 1 & 0 \\ 0 & -1 & 0 & 1 \end{pmatrix} . \quad (8.36)$$

Operating with these on u_1 gives

$$P_R u_1 = \tfrac{1}{2}\sqrt{E+m}\left(1 + \frac{p_z}{E+m}\right)\begin{pmatrix} 1 \\ 0 \\ 1 \\ 0 \end{pmatrix} , \quad (8.37)$$

$$P_L u_1 = \tfrac{1}{2}\sqrt{E+m}\left(1 - \frac{p_z}{E+m}\right)\begin{pmatrix} 1 \\ 0 \\ -1 \\ 0 \end{pmatrix} . \quad (8.38)$$

Thus we find for $\boldsymbol{p} = z|\boldsymbol{p}|$ and $E \gg m$ that $P_L u_1 \to 0$, and for an arbitrary direction the left-chiral component of the positive-helicity spinor u_1 goes to zero. Amplitudes that contain spinors that go to zero in this way in the relativistic limit are said to be helicity suppressed. In the same limit, $P_R u_1 \to u_1$, and the positive-helicity spinor becomes entirely right-chiral. In a similar way, for $\boldsymbol{p} = \hat{z}|\boldsymbol{p}|$ in the relativistic limit, $P_R u_2 = 0$ and $P_L u_2 = u_2$.

For the antiparticle solutions one finds the effect of P_R and P_L on the two helicity states is the reverse. For example, for a positive helicity antiparticle moving in the z direction one has

$$P_R v_1 = \tfrac{1}{2}\sqrt{E+m}\left(1 - \frac{p_z}{E+m}\right)\begin{pmatrix} 0 \\ -1 \\ 0 \\ 1 \end{pmatrix} , \quad (8.39)$$

$$P_L v_1 = \tfrac{1}{2}\sqrt{E+m}\left(1 + \frac{p_z}{E+m}\right)\begin{pmatrix} 0 \\ -1 \\ 0 \\ 1 \end{pmatrix} . \quad (8.40)$$

That is, in the ultra-relativistic limit with momentum along the z axis, one finds $P_R v_1 = 0$, $P_L v_1 = v_1$ and similarly $P_R v_2 = v_2$, $P_L v_2 = 0$.

Since we are free to choose the z axis in any direction, for an arbitrary relativistic momentum, the positive and negative helicity states of a particle correspond to $u_+ \to u_R = P_R u$ and $u_- \to u_L = P_L u$, i.e., they coincide with their right- and left-chiral components, respectively. For a relativistic antiparticle, positive and negative helicity states correspond to $v+ \to v_R = P_L v$ and $v_- \to v_L = P_R v$, respectively.

8.4 The $V - A$ theory of weak interactions

In Fermi's original theory of weak interactions, the amplitude for β-decay was the product of two vector currents, i.e., $\mathcal{M} \sim J^{\rm had}_\mu j^\mu_{\rm lep}$ (cf. Eq. (8.1)). After the discovery of parity violation in 1957, the model had to be modified to allow for this while remaining consistent with all other space-time symmetries (i.e., boosts, rotations, translations and time reversal). In principle one can allow the currents to be combinations of any of the bilinear covariants mentioned in Sec. 5.4: scalar, pseudoscalar, vector, axial vector, and tensor, referred to here as S, P, V, A and T. It was soon realised that to make the theory agree with the data one could assume that the currents used to construct the amplitudes are not Lorentz vectors but rather a difference between vector and axial vector, hence the name "$V - A$ theory of weak interactions" [22, 23]. For example, the vector current $V^\mu = \overline{\psi}_e \gamma^\mu \psi_\nu$ is replaced by

$$V^\mu - A^\mu = \overline{\psi}_e \gamma^\mu \psi_\nu - \overline{\psi}_e \gamma^\mu \gamma^5 \psi_\nu \; . \tag{8.41}$$

If our amplitude were written in terms of u and d quarks rather than the proton and neutron, then the quark current would undergo a similar replacement, namely $J^\mu_q = \overline{\psi}_u \gamma_\mu (1-\gamma^5)\psi_d$. But because the neutron and proton are not point particles, but rather collections of quarks subject to constraints related to spin, the Pauli exclusion principle as well as strong-interaction effects, the corresponding hadronic current becomes $J^\mu_{\rm had} = \overline{\psi}_p \gamma_\mu (1 - g_A \gamma^5)\psi_n$, where $g_A = 1.2753 \pm 0.0013$ [19] is called the axial coupling constant and must be measured from experiment. The amplitude for β-decay, Eq. (8.1) becomes

$$\mathcal{M} = \frac{G_{\rm F}}{\sqrt{2}} [\overline{u}_p \gamma_\mu (1 - g_A \gamma^5) u_n][\overline{u}_e \gamma^\mu (1 - \gamma^5) v_\nu] \; . \tag{8.42}$$

The factor of $\sqrt{2}$ is included in the amplitude so that the numerical value of the Fermi constant $G_{\rm F}$ stays the same.

The combination of a vector minus axial-vector currents for the leptons can be written

$$V^\mu - A^\mu = 2\overline{\psi}_e \gamma^\mu P_L \psi_\nu \; , \tag{8.43}$$

where $P_L = \frac{1}{2}(1 - \gamma^5)$ is the left-chiral projection operator. Thus the consequence of the $V - A$ structure is that only the left-chiral component of the neutrino enters into the amplitude. Since its mass is being treated here as zero it is always relativistic, so a left-chiral neutrino $u_L = P_L u$ is always negative helicity. The antineutrino enters into amplitudes through the spinor v, and the right-chiral component $v_R = P_L v$ coincides with the positive helicity antiparticle. So the

theory only contains neutrinos with spin antiparallel to their momentum, and antineutrinos with (physical) spin parallel to the momentum. That is, neutrinos are always left-handed and antineutrinos right-handed.

Because of the $V-A$ structure of the interaction, we saw that only the left-chiral component of the neutrino participates, and as a consequence this also holds for the charged lepton. To see this, recall $P_L^2 = P_L$, $\{\gamma^\mu, \gamma^5\} = 0$, $(\gamma^5)^\dagger = \gamma^5$, and consider the amplitude for β-decay. This includes the current

$$\begin{aligned} \overline{\psi}_e \gamma^\mu P_L \psi_\nu &= \overline{\psi}_e \gamma^\mu P_L^2 \psi_\nu \\ &= \overline{\psi}_e \gamma^\mu \tfrac{1}{2}(1-\gamma^5) P_L \psi_\nu \\ &= [\tfrac{1}{2}(1-\gamma^5)\psi_e]^\dagger \gamma^0 \gamma^\mu P_L \psi_\nu \\ &= \overline{(\psi_e)}_L \gamma^\mu (\psi_\nu)_L \ . \end{aligned} \tag{8.44}$$

That is, the amplitude only contains the left-chiral component of the charged lepton, $(\psi_e)_L = \frac{1}{2}(1-\gamma^5)\psi_e$.

8.5 Charged pion decay

The decay of the charged π meson gives a clear illustration of helicity suppression and a resounding confirmation of the $V-A$ theory. The charged pion can decay into an electron or a muon plus the corresponding (anti)neutrino. The measured ratio of decay rates is found to be [19]

$$\frac{\Gamma(\pi \to e\nu)}{\Gamma(\pi \to \mu\nu)} = (1.2344 \pm 0.0023) \times 10^{-4} \ . \tag{8.45}$$

The effect of rest masses should tend to make the ratio large, not small, since the muon mass of 105.7 MeV is comparable to that of the pion's 139.6 MeV, both of which are far greater than the electron's 0.511 MeV. Nevertheless, charged pions decay to muons far more often than to electrons. First we will show how this arises as a consequence of conservation of angular momentum and the $V-A$ structure of the weak amplitude, and then we will compute the amplitude and decay rates explicitly.

From the angular distributions of production and decay, the spin of the charged pion is zero. The spins of the neutrino and lepton are each 1/2, so they could combine to form a total spin of 0 or 1. The orbital angular momentum L of the two decay products could therefore in principle be 0 or 1, but $L = 1$ is suppressed by the centrifugal barrier $\sim \ell(\ell+1)/r^2$ since the muon and neutrino are in effect produced at a point. Therefore one has $L = 0$ and the spins of the outgoing charged lepton (e or μ) and the antineutrino must be opposite and orientated as shown in Fig. 8.6.

As we have seen in Sec. 8.3, antineutrinos are only produced in the positive-helicity ("right-handed") state, as shown in Fig. 8.6. Therefore by conservation of angular momentum, the charged lepton ℓ must also have positive helicity ($\lambda = 1/2$) so that the final state has angular

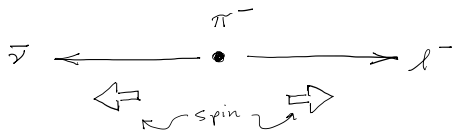

Figure 8.6: Orientation of spins (open arrows) in the decay $\pi^- \to \ell^- \overline{\nu}$, where the lepton ℓ^- is an electron or a muon.

momentum of zero. If we define the coordinate system such that the charged lepton is emitted in the $+\hat{z}$ direction, it is therefore described by the spinor u_1. But the weak interaction only uses $P_L u = u_L$, so the amplitude should contain

$$P_L u_1 = \tfrac{1}{2}(1-\gamma^5)u_1 = \tfrac{1}{2}\sqrt{E+m}\left(1 - \frac{p}{E+m}\right)\begin{pmatrix}1\\0\\-1\\0\end{pmatrix}\ , \tag{8.46}$$

which goes to zero for $E \gg m$. In the decay of the pion to $e^-\overline{\nu}$, the electron is highly relativistic since its energy is roughly half the pion mass, i.e., $\sim 70\,\mathrm{MeV}$, which is much greater than its rest mass of $0.511\,MeV$, and it gets a speed $\beta = 0.99997$. For the decay to muon and antineutrino, the muon's mass of 105.7 MeV is not much less than that of the pion, and it winds up with a speed of $\beta = 0.271$, only marginally relativistic. The corresponding factor that enters Eq. (8.46) is

$$1 - \frac{p}{E+m} = \begin{cases} 0.0073 & m = m_e, \\ 0.86 & m = m_\mu. \end{cases} \tag{8.47}$$

This suppression explains why the pion decays far more frequently to a muon rather than an electron, as we can show quantitatively by calculating in the $V-A$ theory the ratio of the two decay rates.

The decay $\pi^- \to \ell^-\overline{\nu}$ where $\ell = e$ or μ can be viewed roughly as proceeding through the Feynman diagram in Fig. (8.7).

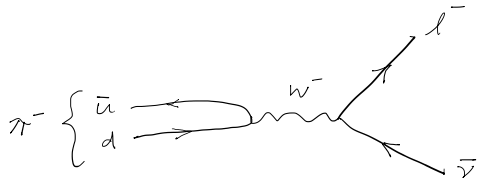

Figure 8.7: Feynman diagram for the decay $\pi^- \to \ell^-\overline{\nu}$, where the pion is modeled as a bound quark-antiquark pair and the lepton ℓ^- is an electron or a muon.

In the $V-A$ theory, the amplitude for the decay should have the general form

$$\mathcal{M} = \frac{G_{\rm F}}{\sqrt{2}} j_\mu^\pi \overline{u}_\ell \gamma^\mu (1-\gamma^5) v_\nu \ . \tag{8.48}$$

We assume that the lepton current is $\overline{u}_\ell \gamma^\mu (1-\gamma^5) v_\nu$, as appropriate for a $V-A$ interaction of charged leptons and neutrinos. If the initial quark-antiquark pair were to be free particles that collide, then we could take the hadronic current to be $j_\mu^\pi = \overline{v}_u \gamma_\mu (1-\gamma^5) u_d$. But the pair begins as a bound state involving complicated strong-interaction effects. These influence the probability of finding the quark and antiquark close enough to interact weakly. This cannot be computed easily, but we can constrain its form by the requirement that the amplitude itself be invariant under proper Lorentz transformations, so j_μ^π must be a combination of a Lorentz vector and axial vector. The only relevant four-vector on which it can depend is the four-momentum of the pion, q^μ, which is the same as the total four-momentum of the outgoing particles. We therefore take

$$j_\mu^\pi = f_\pi q_\mu \ , \tag{8.49}$$

where f_π is a constant whose value is eventually determined by experiment to be 130 MeV.

In the rest frame of the pion, we have $q_\mu = (m_\pi, 0, 0, 0)$. The decay amplitude therefore includes only the $\mu = 0$ components of the currents:

$$\mathcal{M} = \frac{G_{\rm F}}{\sqrt{2}} f_\pi m_\pi \overline{u}_\ell \gamma^0 (1-\gamma^5) v_\nu \ . \tag{8.50}$$

We can assign the coordinate system such that the momentum of the outgoing electron is along the z axis, $\boldsymbol{p} = \hat{z} p$ The antineutrino has momentum $\boldsymbol{k} = -\boldsymbol{p} = -\hat{z} p$. Since it must have positive helicity ("right-handed"), its spin points in the $-\hat{z}$ direction. Therefore it is described by the spinor v_2,

$$v_2(p) = \sqrt{E+m} \begin{pmatrix} \frac{p_z}{E+m} \\ \frac{p_x + i p_y}{E+m} \\ 1 \\ 0 \end{pmatrix} = \sqrt{k} \begin{pmatrix} -1 \\ 0 \\ 1 \\ 0 \end{pmatrix} \ , \tag{8.51}$$

where we set $m \to 0$ for neutrinos and $k \equiv |\boldsymbol{k}|$. The outgoing charged lepton also has positive helicity, so its spin is in the $\hat{z}$ direction. It is therefore described by the spinor u_1. So only u_1 and v_2 contribute. The amplitude is

$$\mathcal{M} = \frac{G_{\rm F}}{\sqrt{2}} f_\pi m_\pi \overline{u}_{1,\ell} \gamma^0 (1-\gamma^5) v_{2,\nu} = \frac{2 G_{\rm F}}{\sqrt{2}} f_\pi m_\pi u_{1,\ell}^\dagger v_{2,\nu} \ , \tag{8.52}$$

where the second equality follows from $\overline{u}_{1,\ell} \gamma^0 = u_{1,e}^\dagger \gamma^0 \gamma^0 = u_{1,\ell}^\dagger$ and $(1-\gamma^5) v_{2,\nu} = 2 P_L v_{2,\nu} = 2 v_{2,\nu}$. This can be further simplified by using the explicit forms of the spinors u_1 and v_2 to be

$$\begin{aligned}\mathcal{M} &= \frac{2G_{\rm F}}{\sqrt{2}} f_\pi m_\pi \sqrt{E+m_\ell}\left(1,0,\frac{p}{E+m_\ell},0\right)\sqrt{k}\begin{pmatrix}-1\\0\\1\\0\end{pmatrix} \\ &= \frac{2G_{\rm F}}{\sqrt{2}} f_\pi m_\pi \sqrt{p}\left(\sqrt{E-m_\ell}-\sqrt{E+m_\ell}\right) , \end{aligned} \tag{8.53}$$

where the last line used $k = p$. The absolute square of the amplitude is found to be

$$|\mathcal{M}|^2 = 4G_{\rm F}^2 f_\pi^2 m_\pi^2 E(E-p) = 2G_{\rm F}^2 f_\pi^2 m_\ell^2 (m_\pi^2 - m_\ell^2)^2 . \tag{8.54}$$

The squared amplitude is thus a constant independent of angle, as expected for decay of a spin-0 particle.

Recall from Eq. (7.27) that for an isotropic two-body decay, the total rate is given by

$$\Gamma = \frac{p}{8\pi m_\pi^2}|\mathcal{M}|^2 , \tag{8.55}$$

where here $p^* = p$ is the magnitude of the momentum of either of the two outgoing particles. We therefore find the decay rate for $\pi \to \ell\overline{\nu}$

$$\Gamma = \frac{G_{\rm F}^2}{8\pi m_\pi^3} f_\pi^2 m_\ell^2 (m_\pi^2 - m_\ell^2)^2 . \tag{8.56}$$

This gives the result for both choices for the charged lepton, $\ell = e$ or μ. Here it is important to note that the pion decay constant f_π is assumed to the same in both decays, and that the two rates differ only through the mass of the charged lepton. We therefore find the ratio of decay rates

$$\frac{\Gamma(\pi^- \to e^-\overline{\nu})}{\Gamma(\pi^- \to \mu^-\overline{\nu})} = \frac{m_e^2}{m_\mu^2}\frac{(m_\pi^2 - m_e^2)^2}{(m_\pi^2 - m_\mu^2)^2} = 1.28 \times 10^{-4} . \tag{8.57}$$

The small discrepancy between this prediction and the measured value shown above can be understood by taking into account higher-order corrections. This represents therefore a major success of the $V - A$ theory.

Examining this result further, we found above that the squared amplitude depended on the masses of the problem as

$$|\mathcal{M}|^2 \sim \frac{m_\ell^2}{m_\pi^3}(m_\pi^2 - m_\ell^2)^2 \tag{8.58}$$

and this multiplied a phase-space factor that is proportional to the momentum of the outgoing lepton,

$$p_\ell = \frac{m_\pi^2 - m_\ell^2}{2m_\pi} \tag{8.59}$$

The ratio of squared amplitudes is therefore

$$\frac{|\mathcal{M}(\pi^- \to e^-\overline{\nu})|^2}{|\mathcal{M}(\pi^- \to \mu^-\overline{\nu})|^2} = 5 \times 10^{-5} \; . \tag{8.60}$$

The final state with the electron has, however, a larger phase-space factor than for the muon,

$$\frac{p_e}{p_\mu} = \frac{m_\pi^2 - m_e^2}{m_\pi^2 - m_\mu^2} = 2.4 \; , \tag{8.61}$$

and the product of these factors gives the ratio of decay rates in Eq. (8.57). We see therefore that it is the amplitude squared that carries responsibility for the small ratio of decay rates. This results from the fact that the amplitude only couples to the left-chiral component of the electron, but from conservation of angular momentum, only a positive helicity electron can be produced. The positive helicity state is a mixture of the left-chiral and right-chiral states, and in the limit where the mass goes to zero it is entirely right-chiral, i.e., the wrong state to couple to the weak interaction. Thus for the electron's very small but nonzero mass, the amplitude is greatly suppressed.

8.6 The CKM matrix

By the mid-1960s, the weak interactions were understood in terms of the $V-A$ theory in which an effective current-current interaction arose from the exchange of a massive boson, which we now identify as the $W^\pm$. In 1964, Gell-Mann and Zweig proposed that nucleons are composed of point-like fermions called quarks [24, 25]. The diagram used to illustrate the decay $\pi^- \to \mu^-\overline{\nu}$ from Fig. 8.7 anticipated the modelling of the pion as a $\overline{u}d$ quark-antiquark pair.

Already in the early 1950s it was known that the charged kaon undergoes the corresponding decay $K^- \to \mu^-\overline{\nu}$, and by replacing the d quark by the heavier s ("strange") quark one should have the same diagram for kaon decay and one might therefore expect that the predicted decay rate for $K^- \to \ell^-\overline{\nu}$, with $\ell^- = \mu^-$ or e^- should be given by the result for $\pi^- \to \ell^-\overline{\nu}$ from Eq. (8.56) simply by replacing $m_\pi = 139.6\,\mathrm{MeV}$ by $m_K = 493.7\,\mathrm{MeV}$. This would predict

$$R_\ell \equiv \frac{\Gamma(K \to \ell\nu)}{\Gamma(\pi \to \ell\nu)} = \frac{f_K^2}{f_\pi^2}\frac{m_\pi^3}{m_K^3}\frac{(m_K^2 - m_\ell^2)^2}{(m_\pi^2 - m_\ell^2)^2} \; . \tag{8.62}$$

At the time it was not known what to assume for the ratio of decay constants so provisionally let us take $f_K/f_\pi = 1$. Evaluating the ratio of decay rates with the relevant masses gives predicted values of $R_e = 3.54$ for the electron- and $R_\mu = 17.7$ for the muon decay channel. To compare these with measured values we need the branching fractions for the relevant initial to final states $B(X \to f) = \Gamma(X \to f)/\Gamma_X$ and the mean lifetimes $\tau_X = 1/\Gamma_X$ with $X = \pi$ or K and $f = e\nu$ or $\mu\nu$:

$$\frac{\Gamma(K \to \ell\nu)}{\Gamma(\pi \to \ell\nu)} = \frac{B(K \to \ell\nu)\Gamma_K}{B(\pi \to \ell\nu)\Gamma_\pi} = \frac{B(K \to \ell\nu)}{B(\pi \to \ell\nu)} \frac{\tau_\pi}{\tau_K} \ . \tag{8.63}$$

Substituting measured values of the branching ratios and lifetimes from Ref. [19] gives $R_e = 0.270$ and $R_\mu = 1.34$. Thus the measured ratios of kaon to pion decay rates are for both the $e\nu$ and $\mu\nu$ final states is a factor of 13 smaller than the predicted ones.

In 1963, Cabibbo proposed that this arose because of a mixing of the states relevant for the weak interaction. If one translates his arguments into the present-day language of quarks, the coupling strength g applies not to the $\overline{u}Wd$ vertex, but rather to $\overline{u}Wd'$, where d' is a superposition of d and s states,

$$d' = d\,\cos\theta_{\rm C} + s\,\sin\theta_{\rm C} \ . \tag{8.64}$$

The superposition is parameterized by the mixing angle $\theta_{\rm C}$, called the Cabibbo angle, such that the normalisation of the state vectors is preserved. The state orthogonal to d' is

$$s' = -d\,\sin\theta_{\rm C} + s\,\cos\theta_{\rm C} \ , \tag{8.65}$$

and the $\overline{u}s'$ pair has a coupling to the W of zero. The amplitudes for pion and kaon decay, however, involve the d and s states,

$$d = d'\,\cos\theta_{\rm C} - s'\,\sin\theta_{\rm C} \ , \tag{8.66}$$

$$s = d'\,\sin\theta_{\rm C} + s'\,\cos\theta_{\rm C} \ . \tag{8.67}$$

This means that for the coupling of u, d and W^-, g is replaced by $g\cos\theta_{\rm C}$, and for $\overline{u}$, s and W^-, g changes into $g\sin\theta_{\rm C}$. The predicted decay rate $\Gamma(\pi \to \ell\nu)$ therefore gets multiplied by a factor of $\cos^2\theta_{\rm C}$ and $\Gamma(K \to \ell\nu)$ gets a factor $\sin^2\theta_{\rm C}$. Including these modifications to the ratio of decay rates gives therefore

$$\frac{\Gamma(K \to \ell\nu)}{\Gamma(\pi \to \ell\nu)} = \tan^2\theta_{\rm C}\,\frac{f_K^2}{f_\pi^2}\,\frac{m_\pi^3}{m_K^3}\,\frac{(m_K^2 - m_\ell^2)^2}{(m_\pi^2 - m_\ell^2)^2} \ . \tag{8.68}$$

To bring the measured and predicted ratios into agreement one needs a Cabibbo angle of 15.4°. A more refined analysis including an estimate from lattice QCD for the ratio of decay constants $f_K/f_\pi = 1.19$ gives $\theta_{\rm C} = 12.8°$, or equivalently $\sin\theta_{\rm C} = 0.221$ ($\cos\theta_{\rm C} = 0.975$) [19].

Even before the experimental discovery of the charmed quark in 1974, this picture was generalised to include charm using the state orthogonal to s',

$$c' = s\,\cos\theta_{\rm C} + d\,\sin\theta_{\rm C} \ . \tag{8.69}$$

When the charm and bottom quarks were discovered in the 1970s, Cabibbo's picture had to be extended. In doing so the existence of the t quark was assumed, although it was not observed directly until the mid 1990s. One defines the states d', s' and b' to be the ones that couple to u,

c and t, respectively, with the coupling strength g. The new states are related to the old ones, d, s and b, by a unitary transformation which can be represented by a 3×3 matrix V, called the *Cabibbo–Kobayashi–Maskawa (CKM) matrix* [26]

$$\begin{pmatrix} d' \\ s' \\ b' \end{pmatrix} = \begin{pmatrix} V_{ud} & V_{us} & V_{ub} \\ V_{cd} & V_{cs} & V_{cb} \\ V_{td} & V_{ts} & V_{tb} \end{pmatrix} \begin{pmatrix} d \\ s \\ b \end{pmatrix} . \tag{8.70}$$

At a vertex containing a W boson, a charge 2/3 quark of type $i = u, c, t$ and a charge $-1/3$ quark of type $j = d, s, b$, the coupling strength is therefore not g but rather gV_{ij}.

The magnitudes of the CKM matrix elements $|V_{ij}|$ have the following measured values [19]:

$$V_{\rm CKM} = \begin{pmatrix} 0.97435 \pm 0.00016 & 0.22500 \pm 0.00067 & 0.00369 \pm 0.00011 \\ 0.22486 \pm 0.00067 & 0.97349 \pm 0.00016 & 0.04182^{+0.00085}_{-0.00074} \\ 0.00857^{+0.00020}_{-0.00018} & 0.04110^{+0.00083}_{-0.00072} & 0.999118^{+0.000031}_{-0.000036} \end{pmatrix} .$$

Note that the diagonal elements are close to unity. That is, the coupling strength for vertices containing a W and ud, cs, or tb is close to g. The coupling strength for us and cd vertices is reduced by a factor of 0.22 (in the two-family model this was $\sin\theta_{\rm C}$). Naively one expected the suppression of the couplings for c with b to be of a similar magnitude, but in fact it turned out to be significantly smaller, namely, $|V_{cb}| \approx 0.04$. Transitions between the 1st and 3rd families are suppressed even further, with $|V_{ub}| \approx 0.003$ and $|V_{td}| \approx 0.008$.

In order for d', s' and b' to form an orthonormal set of states, the CKM matrix V must be unitary, i.e., $VV^\dagger = I$. An arbitrary complex 3×3 matrix contains 18 numbers, but requiring unitarity gives 9 constraints. Furthermore one can show that 5 more constraints can be obtained from the freedom to redefine the phases of the quark states. Therefore the most general form of V consistent with unitarity can be represented by 4 real parameters. A commonly used parameterization of the CKM matrix due to Wolfenstein [27] is

$$V = \begin{pmatrix} 1 - \lambda^2/2 & \lambda & A\lambda^3(\rho - i\eta) \\ -\lambda & 1 - \lambda^2/2 & A\lambda^2 \\ A\lambda^3(1 - \rho - i\eta) & -A\lambda^2 & 1 \end{pmatrix} . \tag{8.71}$$

One can show that this form of V is not exactly unitary, but that $VV^\dagger \approx I$ plus corrections of order λ^4. To the extent that λ is small, this is a good enough approximation. The measured values of all four parameters are [19]

$$\lambda = 0.22500 \pm 0.00067, \quad A = 0.826^{+0.018}_{-0.015}, \quad \bar{\rho} = 0.159 \pm 0.010, \quad \bar{\eta} = 0.348 \pm 0.01 , \tag{8.72}$$

where $\overline{\rho} = \rho(1 - \lambda^2/2)$ and $\overline{\eta} = \eta(1 - \lambda^2)$ are related to ρ and η but include some higher order corrections to make V closer to being unitary.

8.7 Neutrino scattering

In this section we turn to neutrino scattering, which will provide a platform to explore both the $V - A$ theory, the CKM matrix and to introduce the quark structure of the nucleon. We start with a basic overview of the experimental set-up, then look at the neutrino scattering reaction $\nu_\mu d \to \mu^- u$, and then at the corresponding antineutrino reaction $\overline{\nu}_\mu u \to \mu^+ d$.

8.7.1 Experimental set-up

The basic experimental set-up of neutrino scattering experiments is illustrated in Fig. 8.8 [28]. Starting from the left-hand side of the figure, high-energy protons collide with a target producing pions and kaons. These traverse a system of magnets which selects pions (or kaons) of a given momentum and charge. These then pass through a decay tunnel where, as seen in the previous section, the pions almost all decay as $\pi \to \mu\nu_\mu$. Therefore the neutrinos produced are almost all of the muon type. The muons are absorbed in a thick shield, and the neutrinos proceed to the detector. The kinematics of the pion decay are such that the neutrino energy depends on the angle of the neutrino relative to the central axis, so that the mean energy of the neutrino beam can be selected.

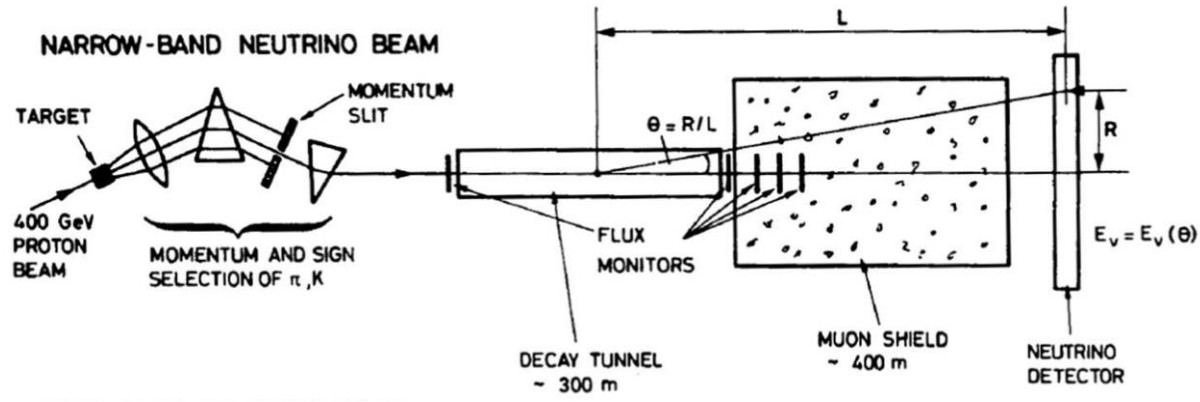

Figure 8.8: Set-up of a neutrino beam [28].

To have any appreciable event rate, a neutrino detector must have a large mass. A schematic view of neutrino interaction in the CDHS detector at CERN is shown in Fig. 8.9. A muon-type neutrino enters from the left and undergoes a charged-current interaction with a nucleon to produce a muon plus hadrons. The muon is identified as the long track that exits the detector on the right.

8.8 Neutrino-nucleon scattering

As a first example of neutrino scattering, consider a muon-type neutrino incident on a nucleon (proton or neutron). The proton is modeled as 3 quarks of types uud and the neutron has udd. To the extent that the target contains equal numbers of protons and neutrons, one has therefore

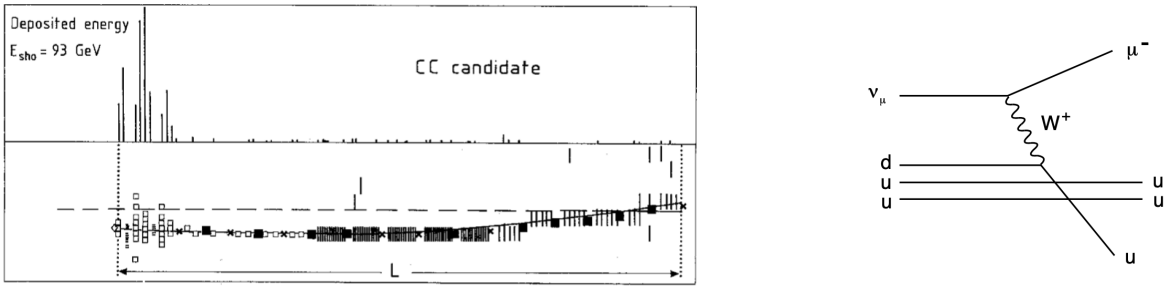

Figure 8.9: Display of a charged-current event in the CDHS neutrino experiment at CERN [29] with the corresponding Feynman diagram shown on the right.

equal numbers of u and d quarks, or what is called an "isoscalar" target. This is a reasonable first approximation for the targets used in practice (e.g., iron with 26 protons and 30 neutrons).

The relevant interaction for an incident neutrino is $\nu_\mu d \to \mu^- u$. Notice that $\nu_\mu u$ scattering is not possible, since the final state $\mu^- d$ would not conserve charge, and $\mu^+ d$ would not conserve lepton number. At tree level, $\nu_\mu d \to \mu^- u$ is described by the single Feynman diagram shown in Fig. 8.10. The incoming and outgoing particles are assigned four-momenta p_1, p_2, p_3, p_4 as shown, and the four-momentum of the exchanged W boson is $q = p_3 - p_1$.

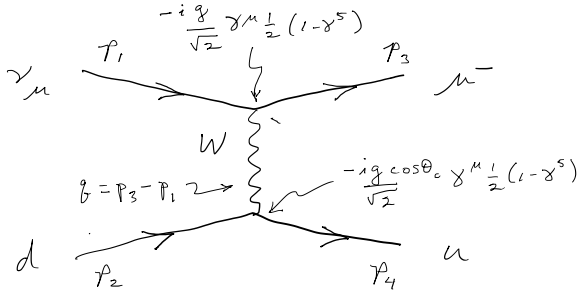

Figure 8.10: Feynman diagram for $\nu_\mu d \to \mu^- u$.

The Feynman rules for the diagram of Fig. 8.10 follow along the same lines as for QED (cf. Sec. 6.7) but use the propagator for a massive W boson shown in Eq. (8.6). For vertices between fermions and the W we now have $-i\frac{g}{\sqrt{2}}\gamma^\mu P_L = -i\frac{g}{\sqrt{2}}\gamma^\mu \frac{1}{2}(1-\gamma^5)$, with an additional factor $\cos\theta_{\rm c}$ at the vertex joining the d and u quarks. The extra factor of $\sqrt{2}$ in the definition of the coupling is included for reasons related to how the interaction is formulated in the full electroweak Standard Model. Using the extended set of rules, the amplitude for Fig. 8.10 is

$$\mathcal{M} = \overline{u}_\mu(p_3)\left[-i\frac{g}{\sqrt{2}}\gamma^\mu\tfrac{1}{2}(1-\gamma^5)\right]u_{\nu_\mu}(p_1)\left[\frac{-i\left(g_{\mu\nu}-\frac{q_\mu q_\nu}{M_W^2}\right)}{q^2-M_W^2}\right]\overline{u}_u(p_4)\left[-i\frac{g\cos\theta_{\rm C}}{\sqrt{2}}\gamma^\nu\tfrac{1}{2}(1-\gamma^5)\right]u_d(p_2)\,. \tag{8.73}$$

Suppose the four-momentum transfer is small in magnitude compared to the mass of the W,

i.e. $|q^2| \ll M_W^2$ so that the propagator can be approximated as $ig_{\mu\nu}/M_W^2$. By contracting the Lorentz indices so that $\gamma^\mu g_{\mu\nu}\gamma^\nu \to \gamma_\mu\gamma^\mu$, the amplitude can be written

$$\mathcal{M} = \frac{-iG_{\rm F}\cos\theta_{\rm C}}{\sqrt{2}}\left[\overline{u}(p_3)\gamma_\mu(1-\gamma^5)u(p_1)\right]\left[\overline{u}(p_4)\gamma^\mu(1-\gamma^5)u(p_2)\right] \ , \tag{8.74}$$

where we have replaced the couplings g using the Fermi constant $G_{\rm F} = \frac{\sqrt{2}g^2}{8M_W^2}$ and to simplify the notation we are identifying the particle of each Dirac spinor through its argument.

To compute the reaction's cross section we need to square the amplitude, average over the two spin states of the d quark and sum over final-state spins. There is no factor of 1/2 for the initial neutrino spins since they are always produced with negative helicity. The spin-averaged amplitude squared can be written

$$\langle|\mathcal{M}|^2\rangle = \frac{G_{\rm F}^2\cos^2\theta_{\rm C}}{2}L_{\mu\nu}W^{\mu\nu} \ , \tag{8.75}$$

where $L_{\mu\nu}$ involves the momenta of the ν_μ and μ^- and $W^{\mu\nu}$ contains the momenta of the d and u quarks. The lepton tensor $L_{\mu\nu}$ is

$$\begin{aligned} L_{\mu\nu} &= \sum_{s_1,s_3}\left[\overline{u}(p_3)\gamma_\mu(1-\gamma^5)u(p_1)\right]\left[\overline{u}(p_3)\gamma_\nu(1-\gamma^5)u(p_1)\right]^* \\ &= \sum_{s_1,s_3}\left[\overline{u}(p_3)\gamma_\mu(1-\gamma^5)u(p_1)\right]\left[\overline{u}(p_1)\overline{\gamma_\nu(1-\gamma^5)}u(p_3)\right] \ , \end{aligned} \tag{8.76}$$

where

$$\begin{aligned} \overline{\gamma_\nu(1-\gamma^5)} &= \gamma^0\left[\gamma_\nu(1-\gamma^5)\right]^\dagger\gamma^0 \\ &= \gamma^0(1-\gamma^5)^\dagger\gamma_\nu^\dagger\gamma^0 \\ &= \gamma^0(1-\gamma^5)\gamma^0\gamma_\nu\gamma^0\gamma^0 \\ &= \gamma_\nu(1-\gamma^5) \ . \end{aligned} \tag{8.77}$$

To arrive at the last result we used $(\gamma^5)^\dagger = \gamma^5$ and $(\gamma_\nu)^\dagger = \gamma^0\gamma_\nu\gamma^0$, along with the usual anticommutation relations. Then using Casimir's trick (Eq. 7.57) we have

$$\begin{aligned} L_{\mu\nu} &= {\rm Tr}\left[(\not{p}_3 + m_\mu)\gamma_\mu(1-\gamma^5)\not{p}_1\gamma_\nu(1-\gamma^5)\right] \\ &= 2{\rm Tr}\left[(\not{p}_3 + m_\mu)\gamma_\mu(1-\gamma^5)\not{p}_1\gamma_\nu\right] \ , \end{aligned} \tag{8.78}$$

where to arrive at the second line, the factor of $(1-\gamma^5)$ was moved passed both $\not{p}_1$ and γ_ν, resulting in two minus signs which cancel. Then recall $P_L^2 = P_L$ and thus $(1-\gamma^5)^2 = 2(1-\gamma^5)$.

When multiplying out the terms in the square brackets, those containing a factor of m_μ appear with an odd number of gamma matrices and so their trace vanishes, so that one obtains

$$L_{\mu\nu} = 2\mathrm{Tr}(\not{p}_3\gamma_\mu\not{p}_1\gamma_\nu) + 2\mathrm{Tr}(\gamma^5\gamma_\mu\not{p}_1\gamma_\nu\not{p}_3) \; . \tag{8.79}$$

The traces can be evaluated using Eqs. (7.61) and (7.63) to give

$$L_{\mu\nu} = 8\left([p_{1\,\mu}p_{3\,\nu} + p_{1\,\nu}p_{3\,\mu} - (p_1\cdot p_3)g_{\mu\nu}] - i\epsilon_{\mu\alpha\nu\beta}p_1^\alpha p_3^\beta\right) \; . \tag{8.80}$$

By making the replacements $p_1 \to p_2$ and $p_3 \to p_4$ one finds for the hadron tensor

$$W_{\mu\nu} = 4\left([p_{2\,\mu}p_{4\,\nu} + p_{2\,\nu}p_{4\,\mu} - (p_2\cdot p_4)g_{\mu\nu}] - i\epsilon_{\mu\alpha\nu\beta}p_2^\alpha p_4^\beta\right) \; , \tag{8.81}$$

which has a factor of 4 rather than 8 because of the average over the two possible spin states of the d quark.

To compute the product $L_{\mu\nu}W^{\mu\nu}$, one can exploit the fact that the terms containing only a single factor of the antisymmetric tensor $\epsilon_{\mu\alpha\nu\beta}$ are zero, since the term that multiplies it is symmetric under interchange of μ and ν. The result of contraction of the terms in square brackets gives

$$[\,]_{\mu\nu}\,[\,]^{\mu\nu} = 2(p_1\cdot p_2)(p_3\cdot p_4) + 2(p_1\cdot p_4)(p_2\cdot p_3) \; , \tag{8.82}$$

and the contraction of the two antisymmetric tensors gives

$$\epsilon\cdot\epsilon = 2(p_1\cdot p_2)(p_3\cdot p_4) - 2(p_1\cdot p_4)(p_2\cdot p_3) \; . \tag{8.83}$$

Assembling the ingredients for the spin-averaged squared amplitude finally results in

$$\langle|\mathcal{M}|^2\rangle = 64G_\mathrm{F}^2\cos^2\theta_\mathrm{C}(p_1\cdot p_2)(p_3\cdot p_4) \; . \tag{8.84}$$

This can be expressed using the centre-of-mass energy squared of the neutrino-quark system

$$\hat{s} = E_\mathrm{cm}^2 = (p_1+p_2)^2 = (p_3+p_4)^2 \; , \tag{8.85}$$

with

$$(p_1+p_2)^2 = p_1^2+p_2^2+2p_1\cdot p_2 = m_\nu^2+m_d^2+2p_1\cdot p_2 \approx 2p_1\cdot p_2 \tag{8.86}$$

$$(p_3+p_4)^2 = p_3^2+p_4^2+2p_3\cdot p_4 \approx m_\mu^2+2p_3\cdot p_4 \; , \tag{8.87}$$

where we have neglected the masses of neutrinos and quarks but we retain for now the mass of the muon. Using the resulting expressions for $p_1\cdot p_2$ and $p_3\cdot p_4$ in Eq. (8.84) gives

$$\langle|\mathcal{M}|^2\rangle = 16G_\mathrm{F}^2\cos^2\theta_\mathrm{C}\hat{s}(\hat{s}-m_\mu^2) \; , \tag{8.88}$$

which can then be used in Eq. (7.34) for the differential cross section. This requires the initial and final state momenta, which are found to be

$$|\boldsymbol{p}_i| = \frac{E_{\rm cm}}{2} , \tag{8.89}$$

$$|\boldsymbol{p}_f| = \frac{E_{\rm cm}^2 - m_\mu^2}{2E_{\rm cm}} . \tag{8.90}$$

Assembling the ingredients gives the differential cross section for $\nu_\mu d \to \mu^- u$ in the centre-of-mass frame,

$$\frac{d\sigma}{d\Omega} = \frac{G_{\rm F}^2 \cos^2\theta_{\rm C}}{4\pi^2} \frac{(\hat{s} - m_\mu^2)^2}{\hat{s}} \approx \frac{G_{\rm F}^2 \cos^2\theta_{\rm C} \hat{s}}{4\pi^2} , \tag{8.91}$$

where the final approximation holds for $E_{\rm cm} \gg m_\mu$. The cross section is thus independent of scattering angle in the centre-of-mass frame.

To find the total cross section we integrate $d\sigma/d\Omega$ over all angles to find

$$\sigma(\nu_\mu d \to \mu^- u) = \int \frac{d\sigma}{d\Omega}\, d\Omega = 4\pi \frac{d\sigma}{d\Omega} = \frac{G_{\rm F}^2 \cos^2\theta_{\rm C} \hat{s}}{\pi} \qquad (\hat{s} \gg m_\mu^2) . \tag{8.92}$$

To express this in terms of the lab-frame incident neutrino energy E_ν we can use $\hat{s} = 2m_d E_\nu$, which is a valid approximation since $\hat{s} \gg m_d^2$ in practice. This gives

$$\sigma(\nu_\mu d \to \mu^- u) = \frac{2G_{\rm F}^2 \cos^2\theta_{\rm C} m_d E_\nu}{\pi} . \tag{8.93}$$

That is, the total cross section grows directly in proportion to the lab-frame energy of the neutrino.

Consider now the corresponding antineutrino reaction $\overline{\nu}_\mu u \to \mu^+ d$, as shown in the Feynman diagram of Fig. 8.11.

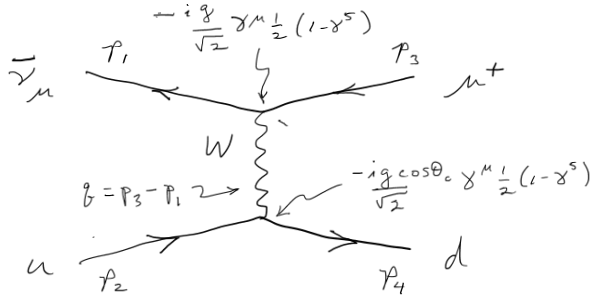

Figure 8.11: Feynman diagram for $\overline{\nu}_\mu u \to \mu^+ d$.

Application of the Feynman rules gives the amplitude

$$\mathcal{M} = -i\frac{G_{\rm F}\cos\theta_{\rm C}}{\sqrt{2}} \left[\overline{v}(p_1)\gamma_\mu(1-\gamma^5)v(p_3)\right] \left[\overline{u}(p_4)\gamma^\mu(1-\gamma^5)u(p_2)\right] . \tag{8.94}$$

Carrying out the corresponding set of steps as before gives the centre-of-mass differential cross section

$$\frac{d\sigma}{d\Omega} = \frac{G_{\rm F}^2 \cos^2\theta_{\rm C} \hat{s}}{4\pi^2} \left(\frac{1+\cos\theta}{2} \right)^2 , \tag{8.95}$$

where θ is the angle between the incoming antineutrino and outgoing muon. Thus in contrast to neutrino scattering, for the antineutrino case, the outgoing μ^+ prefers to follow the direction of the incoming $\overline{\nu}_\mu$. Integrating Eq. (8.95) over the outgoing angles gives the total cross section (for $\hat{s} \gg m_\mu^2$)

$$\sigma(\overline{\nu}_\mu u \to \mu^+ d) = \frac{G_{\rm F}^2 \cos^2\theta_{\rm C} \hat{s}}{3\pi} . \tag{8.96}$$

For an isoscalar target (equal numbers of neutrons and protons and hence equal numbers of u and d quarks) one therefore expects the ratio of antineutrino-nucleon to neutrino-nucleon total cross sections

$$\frac{\sigma(\overline{\nu}N)}{\sigma(\nu N)} = \frac{1}{3} . \tag{8.97}$$

Furthermore, for both neutrino and antineutrino reactions one expects the cross section to increase in proportion to the lab-frame (anti)neutrino energy.

Measurements of the neutrino and antineutrino scattering cross sections are shown in Fig. 8.12 [19]. These show the ratio of the cross section over the neutrino energy, σ/E_ν, as a function of E_ν. These ratios are close to being constant, as predicted, which confirms the picture of the neutrino colliding with a point-like scattering centre. The ratio of neutrino to antineutrino cross sections is closer to 1/2, however, rather than the predicted value of 1/3. This is evidence for the presence of antiquarks in the nucleon. We will return to this reaction when we look in greater detail at the parton content of the nucleon in Ch. 11.

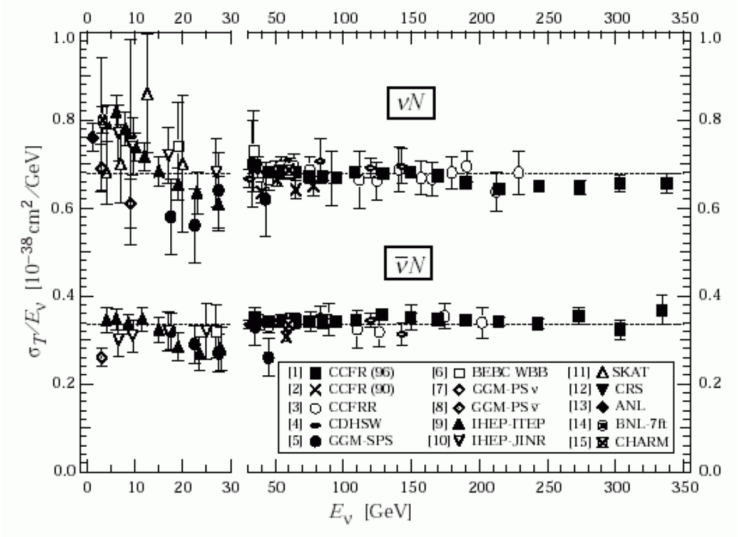

Figure 8.12: The ratio of the cross section to incident neutrino energy for neutrino and antineutrino scattering [19].

Chapter 9

The Electroweak Standard Model

By 1957 the the parity-violating $V - A$ theory of weak interactions was complete and in 1963 it was modified to include Cabibbo's theory of quark flavour mixing, now described through the CKM matrix. There did not exist at this point any experimental results that stood in contradiction with its predictions. There was no direct evidence for the $W^{\pm}$ boson and no known processes that would require a neutral Z boson. Nevertheless, there were theoretical problems with the $V - A$ theory such as the violation of unitarity and renormalizability, as mentioned in Sec. 8.1. The key idea to circumvent these theoretical difficulties was *gauge symmetry*, a known symmetry of electromagnetism. This was extended to a unified "electroweak Standard Model" that preserved the successes of the $V - A$ theory, solved the theoretical issues, and in addition predicted a neutral Z that was subsequently discovered. The model we will see in this chapter should only work for massless particles, but of course we observe particles with nonzero masses. In Chapter 10 we will see how masses can be be brought into the theory while maintaining the gauge symmetry.

9.1 Local gauge symmetry for electromagnetism

We will start by seeing how the electromagnetic interaction possesses what is called U(1) local gauge symmetry. This will provide the basic pattern for the gauge symmetry of the electroweak Standard Model. Consider first the Dirac equation for a free particle,

$$(i\gamma_\mu \partial^\mu - m)\psi(x) = 0 \,, \tag{9.1}$$

and suppose the solution $\psi(x)$ is transformed by multiplying by a constant complex phase,

$$\psi'(x) = e^{i\alpha}\psi(x) \,. \tag{9.2}$$

Because α is a constant (independent of space or time), this is called a *global* U(1) (unitary 1-dimensional) transformation. If $\psi(x)$ is a solution, then $\psi'(x)$ is as well.

Now suppose that α depends on space and time. Without loss of generality let us write the transformation as

$$\psi'(x) = e^{iq\alpha(x)}\psi(x) \ , \tag{9.3}$$

where q is a constant that we will identify as the charge of the particle and $\alpha(x)$ is an arbitrary function of space and time. Substituting this into the Dirac equation gives on the left-hand side

$$[i\gamma_\mu(\partial^\mu + iq\partial^\mu\alpha) - m]\,\psi \ . \tag{9.4}$$

But if ψ solves the free-particle Dirac equation (9.1), then the expression (9.4) does not in general equal zero because of the extra term $iq\partial^\mu\alpha$.

Recall, however, from Sec. 4.5 that the Dirac equation (4.59) for a particle of charge q in an electromagnetic potential $A^\mu(x)$ is

$$(i\gamma_\mu\partial^\mu - m)\psi(x) = q\gamma_\mu A^\mu(x)\psi(x) \ . \tag{9.5}$$

Suppose now that the transformation not only changes $\psi(x)$ according to Eq. (9.3), but we modify the potential $A^\mu(x)$ to be

$$A'^\mu(x) = A^\mu(x) - \partial^\mu\alpha(x) \ . \tag{9.6}$$

In this way the extra $-\partial^\mu\alpha$ cancels the unwanted term in Eq. (9.4) and the pair of transformed quantities, ψ' and A'^μ, together are a solution to the Dirac equation (9.5). Recall from Sec. 3.1 that Maxwell's equations are such that a shift in the four-vector potential according to Eq. (9.6) does not lead to any changes in the $\boldsymbol{E}$ or $\boldsymbol{B}$ fields.

We can restate how we carry out the gauge transformation by defining the *(gauge) covariant derivative*[1] as

$$D^\mu = \partial^\mu + iqA^\mu \ , \tag{9.7}$$

so that the quantity $D^\mu\psi$ transforms as

$$\begin{aligned} D^\mu\psi \to (D^\mu\psi)' &= (\partial^\mu + iq(A^\mu - \partial^\mu\alpha))e^{iq\alpha}\psi \\ &= e^{iq\alpha}\,\partial^\mu\psi + iq(\partial^\mu\alpha)\,e^{iq\alpha}\psi + iqA^\mu e^{iq\alpha}\psi - iq(\partial^\mu\alpha)\,e^{iq\alpha}\psi \\ &= e^{iq\alpha}(\partial^\mu + iqA^\mu)\psi \ , \end{aligned} \tag{9.8}$$

i.e., $D^\mu\psi$ changes under a gauge transformation in the same manner as ψ. Since the gauge field A^μ is contained within the covariant derivative, the Dirac equation then resembles that of a free particle,

$$(i\gamma_\mu D^\mu - m)\psi(x) = 0 \ . \tag{9.9}$$

[1]Here the word covariant does not refer to whether Lorentz indices are written as upper or lower but rather to the modified space-time derivative that includes A^μ.

And since ψ and $D^\mu\psi$ transform in the same way, it maintains its form under a gauge transformation.

The transformations of ψ and A^μ together are called a *local* gauge transformation and the Dirac equation for a particle in an electromagnetic field is said to possess a local U(1) gauge symmetry. That is, one is allowed to change the phase of ψ by an amount that can vary arbitrarily as a function of x but only if there exists an electromagnetic potential A^μ and its value is modified such that the change induced by the transformation of ψ is canceled by the shift in A^μ.

If one had wanted to insist that $\psi(x)$ has a local U(1) gauge, symmetry, it would have been necessary in a sense to predict the existence of the photon. Of course when the Dirac equation was proposed, the laws of electromagnetism and its gauge symmetry were already known. But as a guide to extending the $V - A$ theory of weak interactions, we can guess that an analogous symmetry might exist and we will see that this holds only if additional particles are introduced into the theory, namely, the $W^\pm$ and Z. This symmetry fixes the couplings of the new "gauge bosons" to the fermions and furthermore it results in a theory that is renormalisable, so that higher-order corrections result in well-defined finite predictions.

9.2 Yang-Mills gauge theories

The local gauge symmetry exhibited by electromagnetism can be viewed as a special case of a more general class of theory developed by Yang and Mills in 1954 [30]. Consider a wave equation of the same form as Eq. (9.9), $(i\gamma^\mu D_\mu - m)\psi = 0$, with a covariant derivative D_μ to be defined below. In a Yang-Mills theory, we suppose that the gauge transformation for ψ is more general than in electromagnetism and has the form

$$\psi(x) \to \psi'(x) = U(x)\psi(x) \,, \tag{9.10}$$

where

$$U(x) = \exp\left[ig\alpha^a(x)T^a\right] \tag{9.11}$$

is an $N \times N$ unitary matrix, g is a constant called the gauge coupling, $\alpha^a(x)$ are a set of n arbitrary functions of space and time, T^a are matrices described below, and summation is implied over the repeated index a. Here ψ is a multicomponent field that can be viewed as

$$\psi(x) = \begin{pmatrix} \psi_1(x) \\ \psi_2(x) \\ \vdots \\ \psi_N(x) \end{pmatrix} \,, \tag{9.12}$$

where each of the $\psi_i(x)$ is a four-component Dirac spinor. That is, ψ carries both gauge and spinor indices, and the transformation U acts only on the gauge indices.

The set of all possible transformations given by Eq. (9.10) constitutes an N-dimensional representation of the *gauge group*. Some additional information on group theory is given in

Appendix A. For now what we need to know is that the set of gauge transformations are a representation of what is called a *Lie group*, which is characterised by a set of Hermitian matrices $T^1, \ldots, T^n$ called *generators*. For a Lie group, the commutator $[T^a, T^b]$ is always a linear combination of the generators, which can be expressed as

$$[T^a, T^b] = if^{abc}T^c \ . \tag{9.13}$$

This relation defines a Lie algebra and the f^{abc} are called the structure constants. The generators also obey a normalisation condition chosen by convention to be

$$\mathrm{Tr}(T^a T^b) = \frac{1}{2}\delta^{ab} \ . \tag{9.14}$$

If the generators do not commute, i.e., at least some of the structure constants are nonzero, the group is said to be non-Abelian.

As an example, for the group $SU(2)$ (special unitary group in two dimensions), the generators T^1, T^2, T^3 are related to the Pauli matrices $T^i = \frac{1}{2}\sigma_i$, $i = 1, 2, 3$. They have the Lie algebra

$$[T^i, T^j] = i\epsilon_{ijk}T^k \ , \tag{9.15}$$

i.e., for $SU(2)$ the structure constants are given by the antisymmetric Levi-Civita symbol ϵ_{ijk}. For the group $SU(N)$ there are $n = N^2 - 1$ generators.

In the wave equation for ψ, the covariant derivative D^μ is defined as

$$D^\mu = \partial^\mu + igT^a A^{\mu,a}(x) \ . \tag{9.16}$$

That is, we introduce one gauge field $A^{\mu,a}(x)$ for each of the generators of the gauge group, and from these we define the combined gauge field

$$A^\mu = A^{\mu,a}T^a \ . \tag{9.17}$$

The gauge fields are assumed to change under a gauge transformation as

$$A^\mu \to A'^\mu = UA^\mu U^{-1} + \frac{i}{g}(\partial^\mu U)U^{-1} \ . \tag{9.18}$$

The covariant derivative (9.16) operating on ψ transforms as

$$\begin{aligned}
(D^\mu\psi)' &= (\partial^\mu + igA'^\mu)(U\psi) \\
&= (\partial^\mu U)\psi + U\partial^\mu\psi + igA'^\mu U\psi \\
&= (\partial^\mu U)\psi + U\partial^\mu\psi + ig\left[UA^\mu U^{-1} + \frac{i}{g}(\partial^\mu U)U^{-1}\right]U\psi \\
&= U(\partial^\mu + igA^\mu)\psi \ .
\end{aligned} \tag{9.19}$$

As in the case of electromagnetism, $D^\mu\psi$ is found to transform in the same manner as ψ, and as a result the theory is invariant under the combined transformation of ψ and the gauge fields $A^{\mu,a}$.

If the $\alpha^a(x)$ are small, then we can approximate $U(x) \approx 1+ig\alpha^a(x)T^a$, $U^{-1} \approx 1-ig\alpha^a(x)T^a$, and thus the transformation rule for the fields $A^{\mu,a}$ becomes

$$A^{\mu,a} \to A'^{\,a}_\mu = A^{\mu,a} - \partial^\mu\alpha^a + gf^{abc}\alpha^b A^{\mu,c} \; . \tag{9.20}$$

Notice that the gauge transformation for the fields (9.20) differs in general from the corresponding formula for QED (9.6) through the presence of terms $gf^{abc}\alpha^b A^{\mu,c}$. These are present when the gauge group is non-Abelian, and as we will see below, they lead to interactions between gauge bosons.

Once we say that our theory should respect a symmetry of a certain gauge group, the Yang-Mills formalism then tells us what new gauge bosons must be included and from the corresponding covariant derivative we obtain the Feynman rules for amplitudes. In the following section we will apply this framework to construct the electroweak Standard Model (also called the Glashow-Weinberg-Salam or GWS model) using the gauge group $SU(2)_L \times U(1)$. In 1971 it was shown by 't Hooft that Yang-Mills theories with gauge groups in a broad class, which includes that of the GWS model, are renormalisable [31]. In Chapter 11 we will construct Quantum Chromodynamics as a Yang-Mills theory based on the gauge group $SU(3)$.

9.3 Electroweak gauge symmetry

Our goal is to construct a gauge theory of the Yang-Mills type to reproduce the features of the weak interactions that we have seen. For an appropriate choice of gauge group we will find gauge bosons corresponding to the $W^\pm$, which give the usual "charged current" weak interactions such as beta decay. In addition, the new theory contains the photon, acting as in QED, and it predicts a new neutral vector boson, the Z, with "neutral-current" interactions such as $Z \to \nu\overline{\nu}$.

This model solves two of the important theoretical issues that plagued the V-A theory: it is found to be renormalisable, and the intermediate vector bosons prevent cross sections from violating the unitarity bound at high energy. Furthermore, it "unifies" the electromagnetic and weak interactions, which are seen to result from a particular gauge symmetry. An important complication emerges, however, as the symmetry on which the theory is based is broken if one tries to assign nonzero particle masses. The charged fermions have, however, measured nonzero masses, and the weak intermediate vector bosons must also be massive to explain the low rates of weak interactions with an effective coupling $G_{\rm F} \sim g^2/M_W^2$. We will nevertheless treat all particles has massless for now, and we will use the Higgs mechanism in Ch. 10 to reintroduce masses while maintaining the gauge symmetry.

Will will take as the fundamental fermions of the theory the three lepton families and six quarks that are known today, although not all of these had been discovered when the original electroweak model was proposed. As we have seen in the previous section, to construct a Yang-Mills theory, we place the various fermion fields into an N-component multiplet such as in Eq. (9.12). The gauge transformations that act on the components of the multiplets constitute a representation of a gauge group. In the case of the electroweak model, this is the direct product of two groups: $SU(2) \times U(1)$.

The group $SU(2)$ is defined by the set of unitary 2×2 matrices with determinant equal to $+1$. This group has three traceless Hermitian generators $\boldsymbol{T} = (T_1, T_2, T_3)$, called (weak) isospin operators, which satisfy the Lie algebra $[T_i, T_j] = i\epsilon_{ijk}T_k$. The fermion fields thus transform according to $\psi' = U_T\psi$ with

$$U_T = \exp\left[ig\boldsymbol{\alpha}(x) \cdot \boldsymbol{T}\right] \ , \tag{9.21}$$

where g is the gauge coupling constant, $\boldsymbol{\alpha} = (\alpha_1, \alpha_2, \alpha_3)$ are arbitrary functions of space and time, and the T_i correspond to some representation of the generators.

In the electroweak model, the left- and right-chiral components of the fermions transform under different representations of $SU(2)$. The left-chiral components of the leptons and quarks are placed into $SU(2)$ doublets:

$$\begin{pmatrix} \nu_e \\ e^- \end{pmatrix}_L \ , \quad \begin{pmatrix} \nu_\mu \\ \nu^- \end{pmatrix}_L \ , \quad \begin{pmatrix} \nu_\tau \\ \tau^- \end{pmatrix}_L \ , \tag{9.22}$$

$$\begin{pmatrix} u \\ d' \end{pmatrix}_L \ , \quad \begin{pmatrix} c \\ s' \end{pmatrix}_L \ , \quad \begin{pmatrix} t \\ b' \end{pmatrix}_L \ . \tag{9.23}$$

Here for the down-type quarks one uses the CKM-rotated versions, i.e., the weak eigenstates d', s' and b'. The doublets transform under the fundamental (two-dimensional) representation of $SU(2)$, for which the generators can be taken as $T_i = \frac{1}{2}\tau_i$, $i = 1, 2, 3$, where τ_i are the Pauli matrices:

$$\tau_1 = \begin{pmatrix} 0 & 1 \\ 1 & 0 \end{pmatrix} \ , \quad \tau_2 = \begin{pmatrix} 0 & -i \\ i & 0 \end{pmatrix} \ , \quad \tau_3 = \begin{pmatrix} 1 & 0 \\ 0 & -1 \end{pmatrix} \ . \tag{9.24}$$

Here these are usually called τ rather than σ to emphasise that they act on the two-component isospin doublets, not on spin. The right-chiral components transform under the singlet (trivial) representation of $SU(2)$. This means $T_i = 0$, $i = 1, 2, 3$, and thus the transformation corresponds to multiplication by unity.

The choice of the group $SU(2)$ is constrained by the need to preserve the normalisation of the states, from which U_T should be unitary,

$$U_T U_T^\dagger = U_T^\dagger U_T = I \ . \tag{9.25}$$

From this requirement we have $\det(U_T U_T^\dagger) = |\det U_T|^2 = 1$, and therefore $\det U_T = e^{i\theta}$ for some constant phase θ. Without loss of generality we can take $\theta = 0$, i.e., $\det U_T = 1$, and therefore the transformation is an element of the group $SU(2)$. This will result in mixing of the upper and lower components of the isospin doublets and this will lead to the various transitions between fermion types that are observed.

The fermions also transform under the gauge group $U(1)$, the group of 1×1 unitary matrices. This is equivalent to multiplication by a complex phase factor, which can depend in general on

the spacetime coordinates. The group $U(1)$ has a single generator, which is simply a scalar (a 1×1 matrix) called the (weak) hypercharge Y, and so the group is sometimes called $U(1)_Y$. The fermion fields transform as $\psi' = U_Y \psi$ with

$$U_Y = \exp\left[i \frac{g'}{2} Y \beta(x) \right] , \tag{9.26}$$

where g' is another gauge coupling constant and $\beta(x)$ is an arbitrary function of x. The hypercharge Y is related to a particle's charge Q and the eigenvalue t_3 of the third component of isospin[2]

$$Q = t_3 + \frac{Y}{2} . \tag{9.27}$$

The left-handed isospin doublets have $t_3 = +1/2$ for the up-type and $-1/2$ for the down type; the right-handed singlets are assigned $t_3 = 0$. Recall the up-type quarks have charge $Q = +2/3$ and the down-type $Q = -1/3$. This results in the hypercharge values:

$$Y = \begin{cases} -1 & \nu_{\ell,L}, \ell_L, \quad \ell = e,\ \mu,\ \tau, \\ -2 & e_R, \mu_R, \tau_R, \\ +1/3 & u_L,\ c_L,\ t_L,\ d'_L,\ s'_L,\ b'_L, \\ +4/3 & u_R,\ c_R,\ t_R, \\ -2/3 & d_R,\ s_R,\ b_R. \end{cases} \tag{9.28}$$

For the $SU(2)_L \times U(1)_Y$ gauge symmetry to hold, we need to replace the Dirac equation by one that includes a covariant derivative D^μ, analogous to that of Eq. (9.7) for QED. One might try, for example, something like

$$(i\gamma_\mu D^\mu - M)\psi = 0 \tag{9.29}$$

for a particle of mass M. But because the left- and right-chiral components have different gauge transformations, the mass term breaks the gauge symmetry. For the moment, therefore, we will omit M and treat the particles as massless. The masses will be resurrected in Chapter 10 in a way that preserves the gauge symmetry using the Higgs mechanism.

In analogy with QED one finds the needed covariant derivative D^μ to be

$$D^\mu = \partial^\mu + ig\boldsymbol{T} \cdot \boldsymbol{W}^\mu + i\frac{g'}{2} Y B^\mu , \tag{9.30}$$

where g and g' are the coupling strengths corresponding to the $\mathrm{SU}(2)_L$ and U(1) gauge transformations, the weak isospin operator $\boldsymbol{T}$ is

$$\boldsymbol{T} = \begin{cases} \frac{\boldsymbol{\tau}}{2} & \text{for isospin doublets (left-handed)} , \\ 0 & \text{for isospin singlets (right-handed)} , \end{cases} \tag{9.31}$$

[2]Provided the difference is clear from context, the symbol T_3 is sometimes used to denote both the generator as well as its eigenvalue.

and $\boldsymbol{W}^\mu = (W_1^\mu, W_2^\mu, W_3^\mu)$ and B^μ are gauge fields. We will see below that mixtures of these emerge as four gauge bosons: $W^\pm$, Z and the photon γ.

9.4 Gauge interactions and the weak mixing angle

In this section we will see how using the covariant derivative (9.30) leads to specific combinations of the gauge fields being interpreted as the $W^\pm$, photon and Z bosons, and how it determines the couplings of these to the fermions.

9.4.1 The $W^\pm$ and its couplings to fermions

To see how the $\mathrm{SU}(2)_L \times \mathrm{U}(1)_Y$ gauge transformation introduced above results in the interactions that we want, we can first look separately at the left-handed leptons. For these, the covariant derivative (9.30) includes the term $\boldsymbol{\tau} \cdot \boldsymbol{W}^\mu$, which we can write as

$$\boldsymbol{\tau} \cdot \boldsymbol{W}^\mu = \sqrt{2} \left[\tau_+ W^{(+)\mu} + \tau_- W^{(-)\mu} \right] + \tau_3 W_3^\mu \,, \tag{9.32}$$

where

$$\tau_+ = \tfrac{1}{2}(\tau_1 + i\tau_2) = \begin{pmatrix} 0 & 1 \\ 0 & 0 \end{pmatrix} \,, \qquad \tau_- = \tfrac{1}{2}(\tau_1 - i\tau_2) = \begin{pmatrix} 0 & 0 \\ 1 & 0 \end{pmatrix} \tag{9.33}$$

are the isospin raising and lowering operators and

$$W^{(\pm)\mu} = \frac{1}{\sqrt{2}}(W_1^\mu \mp i W_2^\mu) \,. \tag{9.34}$$

The raising and lowering operators have have the expected properties, e.g., the wave function for an left-handed electron contains

$$\psi_{e,L} \sim \begin{pmatrix} 0 \\ 1 \end{pmatrix} \,, \tag{9.35}$$

and application of the raising operator changes this to a neutrino:

$$\tau^+ \psi_{e,L} \sim \begin{pmatrix} 0 & 1 \\ 0 & 0 \end{pmatrix} \begin{pmatrix} 0 \\ 1 \end{pmatrix} = \begin{pmatrix} 1 \\ 0 \end{pmatrix} \sim \psi_{\nu,L} \,. \tag{9.36}$$

For the left-handed leptons one has hypercharge $Y = -1$, so the covariant derivative (9.30) can be written

$$D^\mu = \partial^\mu + i\frac{g}{\sqrt{2}} \left(\tau_+ W^{(+)\mu} + \tau_- W^{(-)\mu} \right) + i\frac{g}{2}\tau_3 W_3^\mu - i\frac{g'}{2} B^\mu \,. \tag{9.37}$$

At this point it is useful to recall what was done when solving the Dirac equation for a particle of charge q in an electromagnetic potential,

$$\gamma_\mu D^\mu \psi = 0 \ , \tag{9.38}$$

with $D^\mu = \partial^\mu + iqA^\mu$, here with the mass set to zero. We wrote this earlier with the source term on on the right-hand side,

$$\gamma_\mu \partial^\mu \psi = -iq\gamma_\mu A^\mu \psi \ , \tag{9.39}$$

and the solution was expressed as a power series in the coupling strength q, or for the electron $e = -q$. The terms that entered into amplitudes involved integrals over the initial and final state wave functions and A^μ, namely,

$$S_{fi}^{(1)} = q \int d^4x' \, \overline{\phi}_f(x') \not{A} \phi_i(x') \ . \tag{9.40}$$

Carrying out these integrals led to the Feynman rules for QED. When we go through the same procedure using the covariant derivative (9.37), the terms that enter the integrals are now those that appear in the covariant derivative (9.30) to the right of the ∂^μ (times -1 since the source term of the non-homogeneous Dirac equation was put on the right-hand side),

$$-ig\boldsymbol{T} \cdot \boldsymbol{W}^\mu - i\frac{g'}{2} Y B^\mu \ . \tag{9.41}$$

These are bracketed by isospin singlets or doublets of Dirac spinors for the desired initial and final states. The fields $\boldsymbol{W}^\mu$ come multiplied by 2×2 matrices that, as we saw above, can change a lower component to an upper one and vice versa. So an amplitude will contain terms such as

$$\mathcal{M} \sim -i\frac{g}{\sqrt{2}} \overline{\nu}_L \gamma_\mu \tau_+ e_L W^{(+)\mu} \ . \tag{9.42}$$

where here and below we are using the name of the particle to represent both its Dirac spinor and isospin components. The isospin doublets corresponding to the neutrino and electron are on either side of the raising operator τ_+, giving

$$\begin{pmatrix} 1 & 0 \end{pmatrix} \begin{pmatrix} 0 & 1 \\ 0 & 0 \end{pmatrix} \begin{pmatrix} 0 \\ 1 \end{pmatrix} = 1 \ . \tag{9.43}$$

This multiplies the term that contains the Dirac spinors and gamma matrix $\overline{u}_L \gamma^\mu u_L$, which are contracted separately. We see from the amplitude that the interaction changes an electron into a neutrino, and thus must be accompanied by absorption of a W^+. Thus the combinations of W_1^μ and W_2^μ shown in Eq. (9.34) are identified with the $W^\pm$ boson.

Consider, for example, the reaction $\nu_\mu e^- \to \mu^- \nu_e$ as shown in Fig. 9.1. Generalising the Feynman rules to this diagram gives the amplitude

$$\mathcal{M} = \frac{g^2}{8M_W^2} \left[\overline{\mu} \gamma_\mu \tfrac{1}{2}(1 - \gamma^5) \tau_- \nu_\mu \right] \left[\overline{\nu}_e \gamma^\mu \tfrac{1}{2}(1 - \gamma^5) \tau_+ e \right] \ , \tag{9.44}$$

where the propagator for the W was taken as $ig^{\mu\nu}/M_W^2$, which follows from Eq. (8.6) assuming $|q^2| \ll M_W^2$. Here for the fermions we have omitted the subscript L and included instead explicitly the left-chiral projection operators $\frac{1}{2}(1-\gamma^5)$, and as above the particle name represents both the Dirac spinor and the isospin doublet.

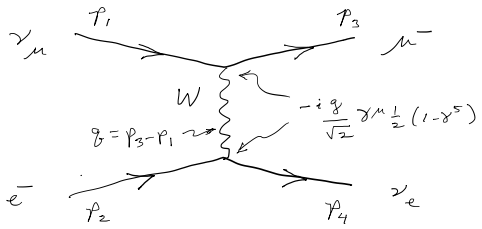

Figure 9.1: Feynman diagram for $\nu_\mu e^- \to \mu^- \nu_e$.

In the $V-A$ theory, the amplitude corresponding to Eq. (9.44) would have the same currents multiplied by factor of $G_{\rm F}/\sqrt{2}$. Thus we recover the correspondence seen earlier,

$$G_{\rm F} = \frac{\sqrt{2}g^2}{8M_W^2} \,. \tag{9.45}$$

In this way one finds that the the same coupling between the W boson and all of leptons, the up-type quarks u, c, t, and the CKM-rotated down-type quarks d', s' and b'. The vertex factor is $-i\frac{g}{\sqrt{2}}\gamma^\mu\frac{1}{2}(1-\gamma^5)$, which only allows the left-chiral component to participate.

The interaction always involves a transition of fermions with $t_3 = 1/2$ and $-1/2$ within the same family. Couplings such as $W^- \to \overline{u}s'$ are zero. If one expresses the flavour eigenstates in terms of the mass eigenstates according to Eq. (8.70), then the vertex for up-type quark i and down-type quark j includes the CKM matrix element V_{ij}, i.e.,

$$-i\frac{g}{\sqrt{2}}V_{ij}\gamma^\mu\tfrac{1}{2}(1-\gamma^5) \,. \tag{9.46}$$

9.4.2 The Z boson and photon and the weak mixing angle

Consider first a neutral-current interaction involving neutrinos. The terms that would appear in the amplitude are of the form

$$-i\frac{g}{2}\overline{\nu}_L\gamma_\mu\tau_3\nu_L W_3^\mu \quad \text{and} \quad i\frac{g'}{2}\overline{\nu}_L\gamma_\mu\nu_L B^\mu \,. \tag{9.47}$$

Here we can use $\tau_3\nu_L = \nu_L$, i.e., the neutrino is in the upper row of the isospin doublet. We cannot identify the photon field A^μ with W_3^μ or B^μ because we do not want the neutrino to couple to photons. Nevertheless we can form a linear combination of W_3^μ and B^μ whose coefficients conspire to give a zero coupling for neutrinos, and we identify this as the photon field, i.e.,

$$A^\mu = aW_3^\mu + bB^\mu \,. \tag{9.48}$$

In an amplitude, the coefficients a and b get combined with the gauge couplings g and g' to form the coupling to A^μ, which we want to be equal to zero:

$$a\left(-\frac{g}{2}\right) + b\frac{g'}{2} = 0 \; . \tag{9.49}$$

To preserve the normalisation we also require $a^2 + b^2 = 1$. We therefore find

$$a = \frac{g'}{\sqrt{g^2 + g'^2}} \; , \qquad b = \frac{g}{\sqrt{g^2 + g'^2}} \; . \tag{9.50}$$

The normalisation condition is automatically satisfied by defining the weak mixing angle $\theta_{\rm W}$ through

$$\cos\theta_{\rm W} = \frac{g}{\sqrt{g^2 + g'^2}} \; , \qquad \sin\theta_{\rm W} = \frac{g'}{\sqrt{g^2 + g'^2}} \; . \tag{9.51}$$

The combination of W_3^μ and B^μ that has zero coupling to the neutrino is then identified as the photon field,

$$A^\mu = \cos\theta_{\rm W} B^\mu + \sin\theta_{\rm W} W_3^\mu \; , \tag{9.52}$$

and the orthogonal combination is the Z boson,

$$Z^\mu = -\sin\theta_{\rm W} B^\mu + \cos\theta_{\rm W} W_3^\mu \; . \tag{9.53}$$

The original fields are therefore

$$B^\mu = \cos\theta_{\rm W} A^\mu - \sin\theta_{\rm W} Z^\mu \; , \tag{9.54}$$

$$W_3^\mu = \sin\theta_{\rm W} A^\mu + \cos\theta_{\rm W} Z^\mu \; . \tag{9.55}$$

A neutral-current amplitude for the neutrino contains both parts shown in Eq. (9.47), which gives

$$\begin{aligned} -i\frac{g}{2}\overline{\nu}_L\gamma_\mu\nu_L W_3^\mu + i\frac{g'}{2}\overline{\nu}_L\gamma_\mu\nu_L B^\mu &= \frac{i}{2}(-g\sin\theta_{\rm W} + g'\cos\theta_{\rm W})\overline{\nu}_L\gamma_\mu\nu_L A^\mu \\ &- \frac{i}{2}(g\cos\theta_{\rm W} + g'\sin\theta_{\rm W})\overline{\nu}_L\gamma_\mu\nu_L Z^\mu \; . \end{aligned} \tag{9.56}$$

The first term on the right vanishes because by construction $-g\sin\theta_{\rm W} + g'\cos\theta_{\rm W} = 0$. The second term is multiplied by

$$g\cos\theta_{\rm w} + g'\sin\theta_{\rm W} = \sqrt{g^2 + g'^2} = \frac{g}{\cos\theta_{\rm W}} \; . \tag{9.57}$$

The coupling for the neutral current to a neutrino is therefore

$$-i\frac{g}{2\cos\theta_{\rm W}}\overline{\nu}\gamma_\mu\tfrac{1}{2}(1-\gamma^5)\nu\ . \tag{9.58}$$

In an analogous manner one finds the coupling of the photon field A^μ to an electron is

$$g'\cos\theta_{\rm W} = g\sin\theta_{\rm W} \equiv e\ . \tag{9.59}$$

For the coupling of an electron to Z^μ the amplitudes are found to contain

$$-\frac{ig}{2\cos\theta_{\rm W}}\overline{u}\gamma_\mu(c_{V,e}-c_{A,e}\gamma^5)uZ^\mu\ , \tag{9.60}$$

where

$$c_{V,e} = -1/2+2\sin^2\theta_{\rm W}\ , \tag{9.61}$$

$$c_{A,e} = -1/2\ , \tag{9.62}$$

are called the vector- and axial-vector couplings of the electron to the Z. These are the same couplings for all three families e, μ and τ.

9.4.3 Summary of couplings of gauge bosons to fermions

The couplings of fermions to a photon are the same as in QED: the vertex factor for particle of charge q is $iq\gamma^\mu$. The couplings of fermions to the W are also easy to summarise: the coupling strength $g/\sqrt{2}$ for the left-chiral components and zero otherwise. More precisely, a W-fermion vertex in a Feynman diagram contains

$$-i\frac{g}{\sqrt{2}}\gamma^\mu\tfrac{1}{2}(1-\gamma^5)\ . \tag{9.63}$$

This is the same as in the $V-A$ theory of the weak interaction where g, M_W and $G_{\rm F}$ are related by Eq. (9.45). For coupling of an up-type quark i to down-type j, the vertex includes the CKM matrix element V_{ij} (or V_{ij}^* for a an antiquark).

For the coupling of a Z boson to a fermion pair, the vertex factor is given in terms of the vector- and axial-vector couplings by

$$-i\frac{g}{2\cos\theta_{\rm W}}\gamma^\mu(c_{V,f}-c_{A,f}\gamma^5) \tag{9.64}$$

The couplings can be expressed in an equivalent way by writing $\gamma_\mu(c_{V,f}-c_{A,f}\gamma^5)$ as

$$\gamma_\mu(c_{V,f}-c_{A,f}\gamma^5) = \gamma_\mu[c_{L,f}(1-\gamma^5)+c_{R,f}(1+\gamma^5)] \tag{9.65}$$

with $c_{L,f}=\frac{1}{2}(c_{V,f}+c_{A,f})$ and $c_{R,f}=\frac{1}{2}(c_{V,f}-c_{A,f})$. One can summarise all the couplings of a fermion pair to the Z boson as:

$$c_{V,f} = t_{3,f} - 2Q_f \sin^2\theta_{\rm W} \ , \tag{9.66}$$

$$c_{A,f} = t_{3,f} \ , \tag{9.67}$$

$$c_{L,f} = t_{3,f} - Q_f \sin^2\theta_{\rm W} \ , \tag{9.68}$$

$$c_{R,f} = -Q_f \sin^2\theta_{\rm W} \ . \tag{9.69}$$

The couplings for the Z boson are summarised in Table 9.1.

Table 9.1: Z boson couplings to fermions.

Fermion	t_3	Q_f	$c_{V,f}$	$c_{A,f}$	$c_{L,f}$	$c_{R,f}$
ν_e, ν_μ, ν_τ	$+\frac{1}{2}$	0	$\frac{1}{2}$	$\frac{1}{2}$	$\frac{1}{2}$	0
$e^-, \mu^-\tau^-$	$-\frac{1}{2}$	-1	$-\frac{1}{2} + 2\sin^2\theta_W$	$-\frac{1}{2}$	$-\frac{1}{2} + \sin^2\theta_W$	$\sin^2\theta_W$
u, c, t	$+\frac{1}{2}$	$+\frac{2}{3}$	$\frac{1}{2} - \frac{4}{3}\sin^2\theta_W$	$\frac{1}{2}$	$\frac{1}{2} - \frac{2}{3}\sin^2\theta_W$	$-\frac{2}{3}\sin^2\theta_W$
d, s, b	$-\frac{1}{2}$	$-\frac{1}{3}$	$-\frac{1}{2} + \frac{2}{3}\sin^2\theta_W$	$-\frac{1}{2}$	$-\frac{1}{2} + \frac{1}{3}\sin^2\theta_W$	$\frac{1}{3}\sin^2\theta_W$

9.5 Discovery of neutral-current processes

The Glashow-Weinberg-Salam model predicts a neutral intermediate vector boson, the Z. But when it was proposed in the 1960s, there was no experimental evidence of weak processes that would result from a neutral boson. This changed in 1973 with the discovery of "weak neutral currents" in the Gargamelle bubble chamber at CERN [32]. In this experiment, a beam of muon-type neutrinos was produced by first creating beams of π^+ and π^-, which then decay as $\pi^- \to \mu^-\overline{\nu}_\mu$ and $\pi^+ \to \mu^+\nu_\mu$. The muons and any remaining hadrons are then absorbed in a thick earth absorber and only the ν_μ or $\overline{\nu}_\mu$ make it as far as the bubble chamber.

The Gargamelle bubble chamber was filled with freon, a dense liquid, in which hadrons either interact or are absorbed. Only muons are sufficiently penetrating to leave a long track in the chamber. In the event shown in Fig. 9.2, for example, one sees a neutrino interaction producing a number of hadrons and in addition a muon which exits the chamber to the right. The Gargamelle group also observed events where hadrons were produced but without muons, as shown in Fig. 9.3.

These two kinds of events can be interpreted with Feynman diagrams such as the ones shown in Fig. 9.4. In Fig. 9.4(a), the neutrino emits a charged W boson and is converted into a muon. The W is absorbed by a d quark in the nucleon and changes into a u quark, which is kicked out at a large angle. The quarks produce a system of hadrons consisting of at least one nucleon (to conserve baryon number) and a number of mesons. Since the charge of the lepton is changed, these are called a *charged current* (CC) events. In Fig. 9.4(b), the neutrino exchanges a neutral Z with the nucleon and it stays a neutrino; no muon is produced. In the bubble chamber one only sees the tracks from the hadrons. These are *neutral current* (NC) events.

(a)

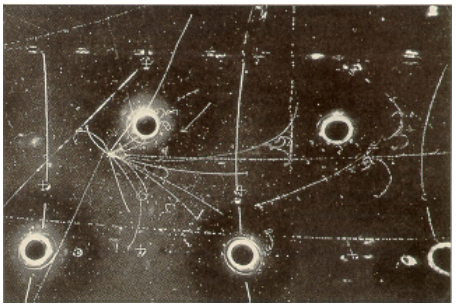

(b)

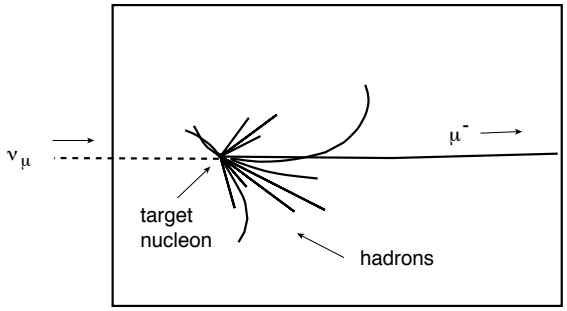

Figure 9.2: Bubble chamber photograph (left) and its interpretation (right) showing the reaction $\nu_\mu \mathrm{N} \to \mu^- +$ hadrons, where N is a nucleon (from D. Perkins in [33], p. 428). The neutrino enters from the left and the muon exits to the right.

(a)

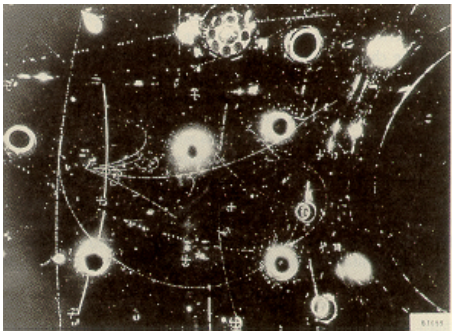

(b)

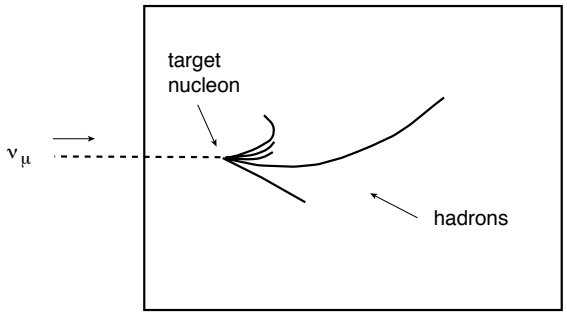

Figure 9.3: Bubble chamber photograph (left) and its interpretation (right) showing the reaction $\nu_\mu \mathrm{N} \to \nu_\mu +$ hadrons (from D. Perkins in [33], p. 428). The neutrino enters from the left. All of the final state particles are identified as hadrons.

The cross sections for charged current and neutral current events depend on the coupling strengths of the W and Z to the quarks and leptons involved. In the GWS electroweak theory, these couplings depend on the value of the weak mixing angle θ_W. From the observed ratio of charged current to neutral current events, the Gargamelle group was able to conclude that $\sin^2\theta_\mathrm{W}$ was around 0.3 to 0.4. More recent measurements give $\sin^2\theta_\mathrm{W} = 0.23$. Much more important than the measured values of the couplings was simply the observation of weak neutral current events, which indicated that something like the Z boson must exist.

The $W^\pm$ and Z bosons were eventually discovered at CERN in 1983 by the UA1 Experiment [34, 35] and found to have masses

$$M_W = 80.4\,\mathrm{GeV}\,, \tag{9.70}$$

$$M_Z = 91.2\,\mathrm{GeV}\,. \tag{9.71}$$

Further information on the discoveries and subsequent tests of the Standard Model can be found e.g. in Refs. [33, 36].

Figure 9.4: Feynman diagrams for (a) a charged current and (b) a neutral current neutrino scattering event.

9.6 Decay rate of the Z boson

As an example of an electroweak process we will derive the decay rate of a Z boson in to a fermion-antifermion pair. Doing so at this point requires some cheating as we have assumed in finding the electroweak couplings that all the particles are massless, otherwise the gauge symmetry would be violated. Will will show in Ch. 10 how gauge symmetry can be maintained with massive particles by means of the Higgs mechanism. We will therefore use the couplings from the previous section and suppose a Z mass $M_Z = 91.2\,\text{GeV}$, and we will also make use of a relation to be derived in Ch. 10 between the masses of the W and Z, namely, $M_W = M_Z \cos\theta_W$.

Suppose a Z boson with four-momentum p and polarisation vector ε^μ decays into a fermion-antifermion pair with four-momenta and spins k_1, s_1 and k_2, s_2, as shown in the Feynman diagram in Fig. 9.5.

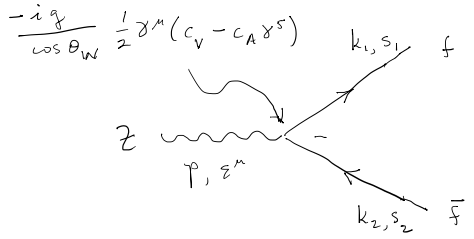

Figure 9.5: Feynman diagram for the decay $Z \to f\overline{f}$.

Using the coupling for a Z to fermion-antifermion pair from Eq. (9.64), the amplitude is found to be

$$\begin{aligned}\mathcal{M} &= \overline{u}(k_1, s_1)\left(\frac{-ig}{2\cos\theta_W}\gamma^\mu(c_V - c_A\gamma^5)\right)v(k_2, s_2)\varepsilon_\mu \\ &= \frac{-ig}{2\cos\theta_W}\overline{u}\not{\varepsilon}(c_V - c_A\gamma^5)v\,, \end{aligned} \tag{9.72}$$

where in the second line, the dependence of $\overline{u}$ and v on the momentum and spin have been suppressed to simplify the notation. The vector an axial vector couplings c_V and c_A are given in Table 9.1 for the different fermion types.

Suppose we do not measure the spin of the final-state fermions so we are interested in knowing the decay rate summed over spins. Using the Casimir trick of Eq. 7.57 gives

$$\begin{aligned}\sum_{s_1,s_2}|\mathcal{M}|^2 &= \sum_{s_1,s_2}\frac{g^2}{4\cos^2\theta_W}\left[\overline{u}\gamma^\mu(c_V-c_A\gamma^5)v\right]\left[\overline{u}\gamma^\nu(c_V-c_A\gamma^5)v\right]^*\varepsilon_\mu\varepsilon_\nu^* \\ &= \frac{g^2}{4\cos^2\theta_W}\mathrm{Tr}\left[\gamma^\mu(c_V-c_A\gamma^5)\not{k}_2\overline{\gamma^\nu(c_V-c_A\gamma^5)}\not{k}_1\right]\varepsilon_\mu\varepsilon_\nu^* \,. \end{aligned} \tag{9.73}$$

Using the properties of gamma matrices seen in Sec. 7.5 we find $\overline{\gamma^\nu(c_V-c_A\gamma^5)}=\gamma^\nu(c_V-c_A\gamma^5)$. Moving the second factor of $(c_V-c_A\gamma^5)$ to the left past $\not{k}_2\gamma^\nu$ gives two sign changes to the γ^5 term that cancel, after which we obtain

$$(c_V-c_A\gamma^5)^2 = c_V^2-2c_Vc_A\gamma^5+c_A^2(\gamma^5)^2 = c_V^2+c_A^2-2c_Vc_A\gamma^5 \,, \tag{9.74}$$

where we used $(\gamma^5)^2=1$. The spin-summed amplitude squared is therefore

$$\sum_{s_1,s_2}|\mathcal{M}|^2 = \frac{g^2}{4\cos^2\theta_W}\mathrm{Tr}\left[(c_V^2+c_A^2+2c_Vc_A\gamma^5)\not{\varepsilon}\not{k}_2\not{\varepsilon}^*\not{k}_1\right] \,. \tag{9.75}$$

The trace can be evaluated using Eqs. (7.61) and (7.63) to give

$$\begin{aligned}\sum_{s_1,s_2}|\mathcal{M}|^2 &= \frac{g^2}{\cos^2\theta_W}\Big[(c_V^2+c_A^2)\left((\varepsilon\cdot k_2)(\varepsilon^*\cdot k_1)+(\varepsilon\cdot k_1)(\varepsilon^*\cdot k_2)-(\varepsilon\cdot\varepsilon^*)(k_1\cdot k_2)\right) \\ &- 2c_Vc_Ai\epsilon_{\mu\nu\rho\sigma}\varepsilon^\mu k_2^\nu\varepsilon^{\rho*}k_1^\sigma\Big] \,. \end{aligned} \tag{9.76}$$

Now suppose that the Z is polarised along the z-axis with with $\varepsilon^\mu=(0,0,0,1)$, so that $\varepsilon^*=\varepsilon$. Then the combination of factors $\varepsilon^\mu k_2^\nu\varepsilon^{\rho*}k_1^\sigma$ is symmetric under interchange of μ and ρ. The antisymmetric tensor $\epsilon_{\mu\nu\rho\sigma}$ with which it is contracted is antisymmetric under $\mu\leftrightarrow\rho$, and so the term containing c_Vc_A gives zero. Furthermore, for our choice of the polarisation vector one has $\varepsilon\cdot k_1=\varepsilon^*\cdot k_1$, $\varepsilon\cdot k_2=\varepsilon^*\cdot k_2$, $\varepsilon\cdot\varepsilon^*=\varepsilon_\mu\varepsilon^\mu=-1$. Therefore the spin-summed amplitude squared becomes

$$\sum_{s_1,s_2}|\mathcal{M}|^2 = \frac{g^2(c_V^2+c_A^2)}{\cos^2\theta_W}\Big[2(\varepsilon\cdot k_1)(\varepsilon\cdot k_2)+k_1\cdot k_2\Big] \,. \tag{9.77}$$

If we now consider the decay in the rest frame of the Z, the four-momenta k_1 and k_2 are

$$k_1 = \frac{M_Z}{2}(1,\sin\theta,0,\cos\theta) \,, \tag{9.78}$$

$$k_2 = \frac{M_Z}{2}(1,-\sin\theta,0,-\cos\theta) \,, \tag{9.79}$$

where θ is the polar angle of the outgoing fermion with respect to the z axis. Here we are assuming that the fermion masses are much less than $M_Z = 91.2\,\text{GeV}$ and can be neglected, which is a good approximation for all fermions except the top quark. An on-shell Z cannot decay into a $t\bar{t}$ pair since $m_t = 174\,\text{GeV}$. Using Eqs. (9.78) and (9.79), the spin-summed amplitude squared becomes

$$\sum_{s_1,s_2} |\mathcal{M}|^2 = \frac{g^2(c_V^2 + c_A^2)M_Z^2}{2\cos^2\theta_W} \sin^2\theta \; . \tag{9.80}$$

This can now be used in the formula (7.26) for the differential decay rate where we replace $|\mathcal{M}|^2$ by the corresponding spin-summed quantity:

$$d\Gamma = \frac{1}{32\pi^2 M^2} \sum_{s_1,s_2} |\mathcal{M}|^2 p^* \, d\Omega \; . \tag{9.81}$$

Here $p^* = |\boldsymbol{k}_1| \approx M_Z/2$ is the momentum of either of the outgoing fermions, which is approximately $M_Z/2$ if we neglect its rest mass. The amplitude is independent of the azimuthal angle ϕ, so for the solid angle element $d\Omega$ we can use $2\pi d\cos\theta$. We therefore find the differential decay rate for Z boson polarised along the z axis,

$$\frac{d\Gamma}{d\cos\theta} = \frac{g^2(c_V^2 + c_A^2)M_Z}{64\pi\cos^2\theta_W} \sin^2\theta \; . \tag{9.82}$$

To find the total decay rate we integrate Eq. (9.82) over $\cos\theta$ from -1 to 1 (use, e.g., $x = \cos\theta$ so $\sin^2\theta = 1 - x^2$, $\int_{-1}^{1}(1 - x^2)\,dx = 4/3$) to find

$$\Gamma(Z \to f\overline{f}) = \frac{g^2(c_V^2 + c_A^2)M_Z}{48\pi\cos^2\theta_W} \; . \tag{9.83}$$

Because the direction of the z axis is arbitrary, Eq. (9.83) gives the total decay rate for a Z boson with its spin in any direction (i.e., for an unpolarised Z).

To express the final result in more convenient form we can use a relation between the W and Z masses that emerges from the Higgs mechanism, which we will see in Ch. (10), namely, $M_W = M_Z\cos\theta_W$. Using this, we can express the weak coupling g in terms of the Fermi constant with

$$G_\text{F} = \frac{\sqrt{2}}{8}\frac{g^2}{M_W^2} = \frac{\sqrt{2}}{8}\frac{g^2}{M_Z^2\cos^2\theta_W^2} \tag{9.84}$$

so that the decay rate of a Z boson to a fermion-antifermion pair is

$$\Gamma(Z \to f\overline{f}) = \frac{G_\text{F} M_Z^3(c_V^2 + c_A^2)}{6\pi\sqrt{2}} \; . \tag{9.85}$$

Using measured values values for the parameters

$$\begin{aligned} M_Z &= 91.2\,\text{GeV} \\ G_\text{F} &= 1.166 \times 10^{-5}\,\text{GeV}^{-2} \\ \sin^2\theta_W &= 0.233 \end{aligned} \tag{9.86}$$

results in values for the first family (ν_e, e^-, u, d):

$$\begin{aligned} \Gamma(Z \to \nu_e \overline{\nu}_e) &= 166\,\text{MeV} \\ \Gamma(Z \to e^+ e^-) &= 83.9\,\text{MeV} \\ \Gamma(Z \to u\overline{u}) &= 96.6\,\text{MeV} \\ \Gamma(Z \to d\overline{d}) &= 124\,\text{MeV} \end{aligned} \tag{9.87}$$

To find the total decay rate we need to sum over all the possible fermion types, excluding the top quark as it is too massive for the decay $Z \to t\bar{t}$. Furthermore we need to include a number of colours $N_c = 3$ for all of the quark types, which will be discussed further in Ch. 11. This gives a predicted value for the total decay rate

$$\Gamma_Z = N_\nu \Gamma(Z \to \nu_e \overline{\nu}_e) + 3\Gamma(Z \to e^+ e^-) + 2N_C \Gamma(Z \to u\overline{u}) + 3N_C \Gamma(Z \to d\overline{d}) = 2.44\,\text{GeV}\ , \tag{9.88}$$

where N_ν is the number of neutrino types. When using $N_\nu = 3$, accounting for fermion masses and including higher-order electroweak and QCD corrections, the prediction becomes $\Gamma_Z = 2.4940 \pm 0.0009\,\text{GeV}$, which is excellent agreement with the experimentally measured value of $2.4955 \pm 0.0023\,\text{GeV}$ [19]. This provides an important confirmation of the hypothesis of $N_c = 3$ colours and $N_\nu = 3$ neutrino families.

9.7 Self interaction of gauge bosons

As a consequence of the non-Abelian nature of the gauge group $SU(2)$, the gauge bosons $W^\pm$, Z and γ interact with each other. This is in contrast to the situation in pure QED, where the gauge group $U(1)$ is Abelian and therefore the photon has no direct coupling to other photons. In this section we will briefly mention the origin of the gauge boson self-couplings and quote the main results without detailed derivation.

In the case of electromagnetism, the wave equation for the field strength tensor is $\partial_\mu F^{\mu\nu} = j^\nu$ (cf. Eq. (3.12)). The corresponding tensor for the fields $\boldsymbol{W}_\mu = (W^1_\mu, W^2_\mu, W^3_\mu)$ is

$$F^a_{\mu\nu} = \partial_\mu W^a_\nu - \partial_\nu W^a_\mu - g\epsilon_{abc} W^b_\mu W^c_\nu\ , \tag{9.89}$$

where g is the gauge coupling and the antisymmetric tensor ϵ_{abc} are the structure constants of $SU(2)$. The wave equation for the gauge bosons are then

$$\partial_\nu F^{\mu\nu,a} - g\epsilon_{abc} W^b_\nu F^{\mu\nu,c} = J^{\mu,a} \,, \tag{9.90}$$

where $J^{\mu,a}$ represents the source current from fermion and Higgs fields. Even if these are absent, there is still an effective current $g\epsilon_{abc} W^b_\nu F^{\mu\nu,c}$ that represents the gauge boson self interaction. When using perturbation theory as in Ch. 6 to compute amplitudes, these involve an interaction Hamiltonian that contains a product of the gauge field and the self-interaction current:

$$H_{\rm int} \sim g\epsilon_{abc} W^a_\mu W^b_\nu F^{\mu\nu,c} \,. \tag{9.91}$$

Since $F^{\mu\nu,c}$ contains terms with one power of the field (through its derivatives), it combines with the other two factors $W^a_\mu W^b_\nu$ to give a coupling of three gauge bosons with a strength of g. And the term in $F^{\mu\nu,c}$ proportional to g that contains two powers of the field combines with the factors $W^a_\mu W^b_\nu$ to give a coupling of four gauge bosons of strength g^2. The possible vertices are shown in Fig. 9.6. There are none with only Z bosons and/or photons.

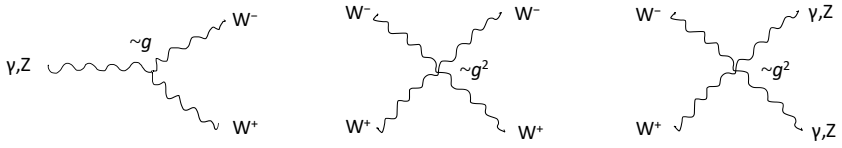

Figure 9.6: Triple and quartic gauge boson vertices in the electroweak Standard Model.

The triple gauge couplings provide a specific testable prediction of the electroweak Standard Model. These were first probed at the LEP Collider at CERN through investigation of the reaction $e^+e^- \to W^+W^-$. This proceeds at leading order trough the three Feynman diagrams shown in Fig. 9.7, two of which contain a triple gauge vertex.

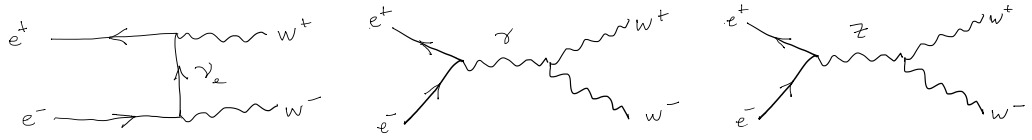

Figure 9.7: Feynman diagrams for $\mathrm{e^+e^- \to W^+W^-}$.

The cross section $\sigma(\mathrm{e^+e^- \to W^+W^-})$ measured at different centre-of-mass energies is shown in Fig. 9.8 [37]. The solid curve represents the Standard Model's prediction evaluated at $M_{\rm W} = 80.4$ GeV. Also shown in Fig. 9.8 are the predicted cross sections if one omits the amplitude with the ZWW vertex or if one takes only the $\nu_{\rm e}$ exchange graph (see Figs. 9.7). The triple-gauge coupling diagrams interfere destructively with the ν_e exchange, so removing them results in a prediction that is far above the experimental data, thus providing an important confirmation of their presence in the Standard Model.

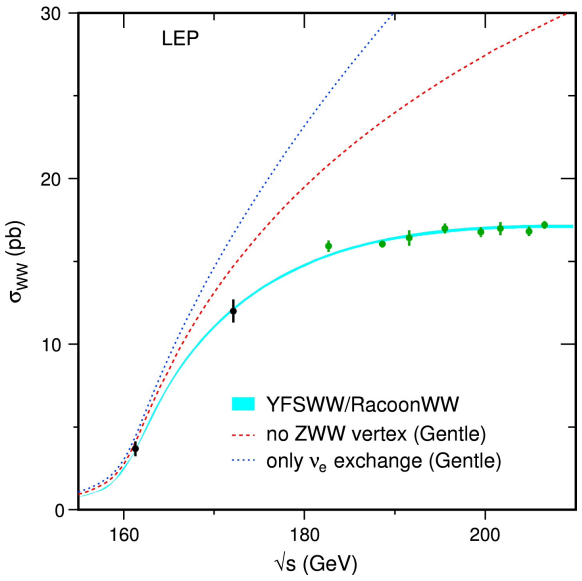

Figure 9.8: The cross section $\sigma(e^+e^- \to W^+W^-)$ measured by the LEP experiments and shown with the Standard Model prediction [37].

Chapter 10

The Higgs Mechanism

In the previous chapter we saw how the electroweak theory was constructed using local gauge symmetry as the guiding principle, but this only held when all the particles had zero mass. Of course the particles of Nature are observed to have nonzero masses, so this cannot be completely correct. In this chapter we will see how the theory can be modified so as to preserve the gauge symmetry for nonzero masses using the Higgs mechanism, which leads to the prediction of an additional particle, the Higgs boson.

The Higgs mechanism was proposed by a number of physicists in the early 1960s, including Anderson [42], Brout and Englert [43], Higgs [44], Guralnik, Hagan and Kibble [45] and first put into the electroweak Standard Model by Weinberg [46]. Although we have managed to construct most of the Standard Model thus far without the complicated machinery of Quantum Field Theory (QFT), we will find it useful to briefly introduce this in Sec. 10.1. We will then explore the mechanism in a simplified model in Sec. 10.2 and then in the full electroweak Standard Model in Secs. 10.3 through 10.5.

10.1 A brief introduction to quantum field theory

In this section we recap the Lagrangian approach to classical mechanics and indicate how this corresponds to a classical field theory in the limit where the number of particles in the system becomes large. We then describe in very rough terms the changes that are made in converting the classical to a quantum field theory. Finally we list the Lagrangian densities for several important theories. A complete introduction to QFT and be found in the texts by Peskin and Schroeder [38] or Zee [39].

10.1.1 The Lagrangian formalism for field theory

For a classical system of particles with generalised coordinates $\boldsymbol{q} = (q_1, \ldots, q_N)$ and velocities $\dot{\boldsymbol{q}} = (\dot{q}_1, \ldots, \dot{q}_N)$, which evolves from time t_1 to t_2, one defines the action S as

$$S = \int_{t_1}^{t_2} L(\boldsymbol{q}, \dot{\boldsymbol{q}})\, dt \ , \tag{10.1}$$

where the Lagrangian $L = T - V$ is the difference between the system's kinetic and potential energies at each point in time. The coordinates and velocities are found to be those $\boldsymbol{q}(t)$ and $\dot{\boldsymbol{q}}(t)$ that minimize the action, i.e., $\delta S = 0$. As a consequence, the equations of motion are found from the Euler-Lagrange equations

$$\frac{\partial L}{\partial q_i} - \frac{d}{dt}\left(\frac{\partial L}{\partial \dot{q}_i}\right) = 0 \,, \qquad i = 1, \ldots, N \,. \tag{10.2}$$

Consider now a system of a large number of masses δm separated by distances δx connected by springs of spring constant k as shown in Fig. 10.1. The coordinate q_i corresponds to the displacement of the ith mass from its equilibrium position. The Lagrangian is

$$\begin{aligned} L &= \sum_{i=1}^{N} \left(\tfrac{1}{2}\delta m\, \dot{q}_i^2 - \tfrac{1}{2}k(q_{i+1} - q_i)^2\right) \\ &= \sum_{i=1}^{N} \frac{\delta x}{2}\left[\left(\frac{\delta m}{\delta x}\right)\dot{q}_i^2 - k\,\delta x\left(\frac{q_{i+1} - q_i}{\delta x}\right)^2\right] \\ &= \sum_{i=1}^{N} \delta x\, L_i \,, \end{aligned} \tag{10.3}$$

where L_i is Lagrangian density with respect to length.

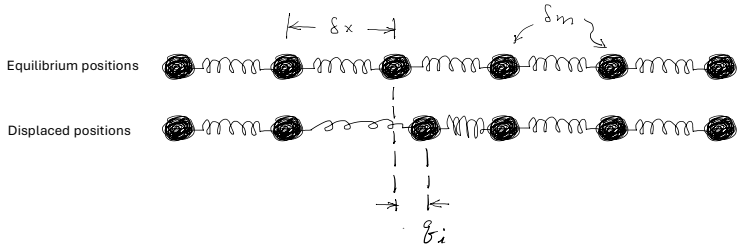

Figure 10.1: Masses δm with spacing δx connected by springs. The displacement of the ith mass from its equilibrium position is q_i.

Now consider the limit where the number of masses N becomes very large and δm and δx go to zero, such that the mass per unit length $\delta m/\delta x$ approaches a constant. In this limit, the index i measures the x coordinate of the ith mass and the displacement $q_i \equiv \phi(x)$ becomes a function of the continuous variable x, i.e., it is a *field*. The ratio $\delta m/\delta x \to \rho$ approaches a constant (linear) density, and as we reduce the length of each spring its spring constant increases inversely with its length such that $k\,\delta x \to \tau$ becomes a constant tension. The index i gets replaced by the continuous variable x that measures the position along the string of masses and the displacement q_i is replaced by a continuous *field* $\phi(x)$, which represents the displacement of the mass at x from its equilibrium. The Lagrangian becomes

$$L \to \int dx\, \frac{1}{2}\left[\rho\dot{\phi}^2(x) - \tau\left(\frac{\partial \phi}{\partial x}\right)^2\right] \equiv \int dx\, \mathcal{L}(x) \,, \tag{10.4}$$

where $\mathcal{L}(x)$ is the Lagrangian density. The Euler-Lagrange equations for the field become

$$\frac{\partial \mathcal{L}}{\partial \phi(x)} - \frac{d}{dt}\left(\frac{\partial \mathcal{L}}{\partial \dot{\phi}(x)}\right) = 0 \,. \tag{10.5}$$

for which we find

$$\tau\left(\frac{\partial^2 \phi}{\partial x^2}\right) - \rho\left(\frac{\partial^2 \phi}{\partial t^2}\right) = 0 \,. \tag{10.6}$$

We recognise this as a wave equation corresponding to a propagation speed $v = \sqrt{\tau/\rho}$.

If we now consider a more general field to be a function of position in a three-dimensional space and time, then $\phi \to \phi(x)$ where x is the usual space-time four-vector. The action can be written

$$S = \int_{t_1}^{t_2} dt \int d^3x \, \mathcal{L}(\phi, \partial_\mu \phi) \,, \tag{10.7}$$

where $\mathcal{L}$ is the Lagrangian density. (In the following, we will focus almost exclusively on the Lagrangian density rather than the Lagrangian itself, and so for brevity will often drop the word density.) To make the theory consistent with Lorentz invariance we will allow the Lagrangian to depend in general on the field and on its derivatives with respect to space and time. The Euler-Lagrange equation (10.5) becomes

$$\frac{\partial \mathcal{L}}{\partial \phi} - \partial_\mu \frac{\partial \mathcal{L}}{\partial(\partial_\mu \phi)} = 0 \,. \tag{10.8}$$

10.1.2 From classical to quantum field theory

The Lagrange formalism described above corresponds to a classical field theory viewed as the limit of a large number of particles. If the particles obey quantum mechanics, then the resulting Quantum Field Theory takes on a number of characteristics that we mention here only briefly.

In a quantum theory, the small masses described above behave like coupled quantum harmonic oscillators. A wave-like collective excitation of the oscillators moving along the line of masses can be characterised by a certain energy and momentum and corresponds to a particle. When generalised to three dimensions, the string of masses is analogous to a lattice of atoms.

One of the primary reasons to introduce QFT is that we need a quantum theory that can describe particles being created and destroyed. A given quantum state can be characterised by some number of particles n with momenta $\boldsymbol{p}_1, \ldots, \boldsymbol{p}_n$. The direct sum of the Hilbert spaces for all n is called a Fock space. In QFT, the wave functions ϕ, ψ, A^μ, etc., become operators. The Fourier transforms of the fields are expressed as creation and annihilation operators that operate on the state vectors in the Fock space to create and destroy particles of different momenta.

For the individual quantum oscillators in the string of masses, the position q_i and momentum and $p_i = \partial L/\partial \dot{q}_i$ become operators $\hat{q}_i$ and $\hat{p}_i$ that follow commutation relations $[\hat{q}_i, \hat{p}_j] = i\delta_{ij}$. When we take the limit where the number of oscillators becomes infinite, these are replaced

by commutators for the field operators. The momentum density operator is found from the Lagrangian density,

$$\pi(x,t) = \frac{\partial \mathcal{L}}{\partial \dot{\phi}} \; , \tag{10.9}$$

and the equal-time commutation relation for ϕ and π becomes

$$[\phi(\boldsymbol{x},t), \pi(\boldsymbol{x}',t)] = i\delta^3(\boldsymbol{x}-\boldsymbol{x}') \; . \tag{10.10}$$

If the particles are fermions described by a Dirac field ψ, then the corresponding relation involves the equal-time component-wise anticommutator between ψ and its adjoint $\psi^\dagger$:

$$\{\psi_\alpha(\boldsymbol{x},t), \psi^\dagger_\beta(\boldsymbol{x}',t)\} = \delta_{\alpha\beta}\delta^3(\boldsymbol{x}-\boldsymbol{x}') \; . \tag{10.11}$$

These relations lead to the rules followed in creating and annihilating particles. For fermions, the anticommutator results in antisymmetric states thus enforcing the Pauli exclusion principle.

10.1.3 Lagrangian densities for some important field theories

The simplest Lagrangian density is for a free scalar field $\phi(x)$:

$$\mathcal{L} = \frac{1}{2}(\partial_\mu\phi)(\partial^\mu\phi) - \frac{1}{2}m^2\phi^2 \; . \tag{10.12}$$

The factor of $1/2$ does not affect the resulting equation of motion but is included to give correct normalisation to the energy density. Applying the Euler-Lagrange equation (10.8) gives

$$(\partial_\mu\partial^\mu + m^2)\phi = 0 \; , \tag{10.13}$$

which we recognise as the Klein-Gordon equation for a particle of mass m.

Given two real scalar fields $\phi_1(x)$ and $\phi_2(x)$ one can define a complex scalar field ϕ as

$$\phi = \frac{\phi_1 + i\phi_2}{\sqrt{2}} \; . \tag{10.14}$$

The field ϕ and its complex conjugate ϕ^* can be taken as two independent fields with the Lagrangian density

$$\mathcal{L} = (\partial_\mu\phi)(\partial^\mu\phi)^* - m^2\phi\phi^* \; . \tag{10.15}$$

The Euler-Lagrange equations result in

$$(\partial_\mu\partial^\mu + m^2)\phi = 0 \; , \tag{10.16}$$

$$(\partial_\mu\partial^\mu + m^2)\phi^* = 0 \; . \tag{10.17}$$

That is, both ϕ and ϕ^* obey the Klein-Gordon equation.

The Lagrangian for Quantum Electrodynamics includes the Dirac field ψ describing a electron with mass m and charge $-e$ and the photon field A^μ and can be written

$$\mathcal{L} = -\frac{1}{4}F_{\mu\nu}F^{\mu\nu} + \overline{\psi}(i\gamma_\mu D^\mu - m)\psi \; . \tag{10.18}$$

Here

$$F^{\mu\nu} = \partial^\mu A^\nu - \partial^\nu A^\mu \tag{10.19}$$

is the field-strength tensor and

$$D^\mu = \partial^\mu - ieA^\mu \tag{10.20}$$

is the covariant derivative. Treating ψ, $\overline{\psi}$ and A^μ as the independent fields, the Euler-Lagrange equations give the Dirac equation,

$$(i\gamma_\mu \partial^\mu - m)\psi = -e\gamma_\mu A^\mu \psi \; . \tag{10.21}$$

The Lagrangian for a massive vector field B^μ is

$$\mathcal{L} = -\frac{1}{4}F_{\mu\nu}F^{\mu\nu} + \frac{1}{2}M^2 B_\mu B^\mu \; , \tag{10.22}$$

where $F_{\mu\nu} = \partial_\mu B_\nu - \partial_\nu B_\mu$. The Euler-Lagrange equation gives

$$(\partial_\nu \partial^\nu + M^2)B^\mu - \partial^\mu(\partial_\nu B^\nu) = 0 \; , \tag{10.23}$$

which is the Proca equation.

10.1.4 Relating the Lagrangian to properties of the theory

The usual point of view in Quantum Field Theory is that the Lagrangian is not derived, rather it defines the theory, and any Lagrangian that leads to the same equations of motion is equivalent. It is relatively straightforward to see directly from the Lagrangian the form of the interactions and the corresponding Feynman rules for a given theory. If there is a term in the Lagrangian that has a product of fields or their derivatives, then there will be vertices that create and destroy particles of those types. For example, using the covariant derivative (10.20) in the QED Lagrangian of Eq. (10.18) gives an interaction term

$$\mathcal{L}_{\rm int} = e\overline{\psi}\gamma_\mu \psi A^\mu \; . \tag{10.24}$$

This corresponds to a vertex joining two fermion lines and a photon. The vertex factor can be read off as i times whatever coefficient multiplies the product of the fields, i.e., $ie\gamma_\mu$. If the vertex involves N identical particles, then one must include a symmetry factor of $N!$, i.e.,

$$\text{vertex factor} = i \times \text{ coefficient of fields } \times \text{ symmetry factor } N! \,. \tag{10.25}$$

We can also read off the particle masses from the Lagrangian from the coefficient of the terms that contain two factors of the field. For a scalar particle, for example, in the Lagrangian of a scalar field Eq. (10.12) the mass m is read off of the term $-\frac{1}{2}m^2\phi^2$, from the vector boson Lagrangian (10.22) the mass term is $\frac{1}{2}M^2B_\mu B^\mu$, and from the QED Lagrangian (10.18) it is $-m\overline{\psi}\psi$.

Notice that the power of m in the mass terms is different for fermions and bosons, and from this one can see that the dimension of the fields is different. Since the action S is dimensionless and it is obtained from the Lagrangian density by integrating over d^4x, the Lagrangian density must have dimension of x^{-4}, or E^4 in energy units with $\hbar = c = 1$. We therefore see that boson fields have units of E and fermions have $E^{3/2}$. Boson and fermion fields are said to be dimension 1 and 3/2 operators, respectively.

Finally, it is easy in the Lagrangian formalism to identify a symmetry of the theory as a transformation that leaves the action invariant. In the important cases of Lorentz and gauge invariant theories, the Lagrangian density $\mathcal{L}$ itself is invariant, but in general $\mathcal{L}$ could change by a total derivative provided the action does not change. This is equivalent to and in a way simpler than the formulation of a symmetry using the equations of motion, which are said to be covariant under a certain transformation if the equations maintain the same form and the wave functions transform according to a given rule. With the Lagrangian formalism, for example, it is easy to see that a theory is Lorentz invariant if its Lagrangian is constructed from bilinear covariants that are contracted so as to give a Lorentz scalar.

10.2 Higgs mechanism for a U(1) local gauge symmetry

Before seeing the Higgs mechanism in the full electroweak Standard Model it is useful to first look at a theory with a single vector field B^μ with the Lagrangian

$$\mathcal{L} = -\frac{1}{4}F_{\mu\nu}F^{\mu\nu} \,, \tag{10.26}$$

where $F_{\mu\nu} = \partial_\mu B_\nu - \partial_\nu B_\mu$. It is easy to verify that $\mathcal{L}$ is invariant under a local gauge transformation

$$B^\mu(x) \to B'^\mu(x) = B^\mu(x) - \partial^\mu\alpha(x) \,. \tag{10.27}$$

If, however, we were to assign a mass term $\frac{1}{2}M^2B_\mu B^\mu$ as in the Proca Lagrangian (10.22), then the gauge symmetry is broken, since the transformation results in extra terms:

$$\frac{1}{2}M^2B_\mu B^\mu \to \frac{1}{2}M^2B'_\mu B'^\mu = \frac{1}{2}M^2B_\mu B^\mu - M^2\partial_\mu\alpha(x)B^\mu + \frac{1}{2}M^2(\partial_\mu\alpha)(\partial^\mu\alpha) \,. \tag{10.28}$$

Our approach in this section will be to extend the theory by including a complex scalar field and then by a suitable redefinition of the fields we will wind up with a mass for B_μ in a

manner that preserves gauge symmetry. As a consequence the theory will contain a massive scalar particle. This is the *Higgs mechanism*, and when we apply it to the full electroweak Standard Model, we will obtain masses for the $W^{\pm}$ and Z bosons and massive scalar particle, the Higgs boson.

Let us include a complex scalar field $\phi = (\phi_1 + i\phi_2)/\sqrt{2}$, and suppose we want the theory to have a U(1) local gauge symmetry, i.e., it should be invariant under the transformation

$$\phi(x) \to \phi'(x) = e^{iq\alpha(x)}\phi(x) \ , \tag{10.29}$$

where $\alpha(x)$ is an arbitrary function of space and time, and the gauge coupling constant q will turn out to be related to the mass of the field B^μ.

As seen in Eq. (10.15), the Lagrangian acquires a kinetic term $(\partial_\mu\phi)(\partial^\mu\phi)^*$, and one can verify that by itself this term is not invariant under the gauge transformation. It can be made gauge invariant, however, by following the usual Yang-Mills procedure from Sec. 9.2, where we replace ∂_μ by the covariant derivative

$$D_\mu = \partial_\mu + iqB_\mu \ . \tag{10.30}$$

One can then show that the modified kinetic term $(D_\mu\phi)(D^\mu\phi)^*$ is invariant under the full gauge transformation where ϕ changes according to (10.29) and B^μ according to (10.27).

This still does not supply a mass for the gauge field B_μ. To provide this without violating the gauge symmetry, we further modify the Lagrangian to read

$$\mathcal{L} = -\frac{1}{4}F_{\mu\nu}F^{\mu\nu} + (D_\mu\phi)(D^\mu\phi)^* - V(\phi) \ . \tag{10.31}$$

Here $V(\phi)$ is the Higgs potential,

$$V(\phi) = \mu^2\phi^*\phi + \lambda(\phi^*\phi)^2 \ , \tag{10.32}$$

where μ^2 and λ are parameters discussed below. The potential enters the Lagrangian with a minus sign so that the Hamiltonian (energy) density $\mathcal{H} = \pi\dot{\phi} - \mathcal{L}$ is positive. The potential is invariant under Lorentz and U(1) gauge transformations and thus can be included in the Lagrangian without violating any of its required symmetries.

If we regard ϕ for the moment as a classical field that takes on a numerical value, we must have $\lambda > 0$ for V to have a finite minimum. If $\mu^2 > 0$, then the minimum of $V(\phi)$ is at $\phi = 0$, as shown in Fig. 10.2(a). In this case the parameter μ corresponds to the particle mass for the field. If, however, $\mu^2 < 0$,[1] then the potential has the "Mexican hat" shape of Fig. 10.2(b). It is minimised for

$$\phi_1^2 + \phi_2^2 = \frac{-\mu^2}{\lambda} \equiv v^2 \ , \tag{10.33}$$

and is said to have a nonzero *vacuum expectation value* v.

[1] We do not need to think of μ^2 as the square of anything; it is simply a parameter that can take on positive or negative values.

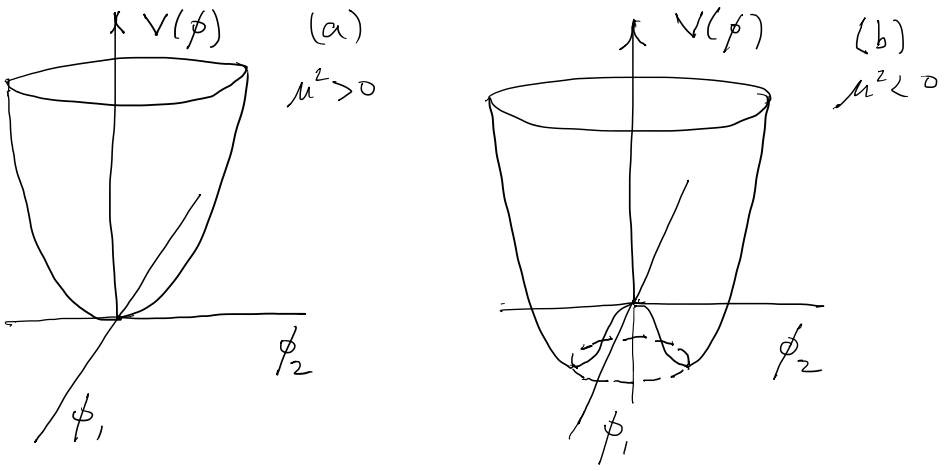

Figure 10.2: Potential $V(\phi)$ for (a) $\mu^2 > 0$ and (b) $\mu^2 < 0$.

There are an infinite number of degenerate vacuum states corresponding to all values of ϕ_1 and ϕ_2 where $\phi_1^2 + \phi_2^2 = v^2$, only one of which is realised. The Lagrangian is invariant under a transformation of the fields that leaves $\phi_1^2+\phi_2^2$ unchanged, but the vacuum state does not respect the symmetry, which is therefore said to be *spontaneously broken*. Without loss of generality we can choose the vacuum state to have $(\phi_1, \phi_2) = (v, 0)$ and define $\phi_1(x) = \eta(x) + v$ and $\phi_2(x) = \xi(x)$, i.e.,

$$\phi = \frac{1}{\sqrt{2}}(\eta + v + i\xi) \tag{10.34}$$

In terms of the new fields the Lagrangian (10.31) is

$$\begin{aligned} \mathcal{L} &= -\frac{1}{4}F_{\mu\nu}F^{\mu\nu} + \mu^2\eta^2 + \frac{1}{4}\mu^2 v^2 \\ &+ \frac{1}{2}\left[(\partial_\mu + iqB_\mu)(v + \eta + i\xi)\right]\left[(\partial^\mu - iqB^\mu)(v + \eta - i\xi)\right] \\ &+ \text{ interaction terms.} \end{aligned} \tag{10.35}$$

The term $\frac{1}{4}\mu^2 v^2$ is a constant and thus plays no role and can be dropped. The interaction terms contain higher powers of η and ξ and for the moment are not of primary interest. Multiplying out the terms in square brackets gives

$$\begin{aligned} \mathcal{L} &= -\frac{1}{4}F_{\mu\nu}F^{\mu\nu} + \frac{1}{2}q^2 v^2 B_\mu B^\mu + qvB_\mu(\partial^\mu\xi) \\ &+ \frac{1}{2}(\partial_\mu\eta)(\partial^\mu\eta) + \mu^2\eta^2 + \frac{1}{2}(\partial_\mu\xi)(\partial^\mu\xi) + \text{ interaction terms .} \end{aligned} \tag{10.36}$$

Looking at the terms in the Lagrangian we see that the field B^μ has acquired a term proportional to $B_\mu B^\mu$, i.e., a mass of $m_B = qv$. The field η is a real scalar field with mass $m_\eta = \sqrt{-2\mu^2}$ and the field ξ has the usual kinetic term for a scalar field but no mass term; it is called a Goldstone boson. Furthermore the term $qvB_\mu(\partial^\mu\xi)$ appears to couple the fields B_μ and ξ.

Both this coupling and the massless Goldstone boson do not, however, represent physically meaningful terms. To see this, we can write the terms involving B_μ and ξ as

$$\frac{1}{2}(\partial_\mu\xi)(\partial^\mu\xi) + \frac{1}{2}q^2v^2B_\mu B^\mu + qvB_\mu(\partial^\mu\xi) = \frac{1}{2}q^2v^2\left(B_\mu + \frac{1}{qv}\partial_\mu\xi\right)\left(B^\mu + \frac{1}{qv}\partial^\mu\xi\right) . \quad (10.37)$$

By including the complex scalar field with the covariant derivative D_μ, the Lagrangian (10.31) is invariant under the transformation of both B_μ and ϕ according to Eqs. (10.27) and (10.29), respectively. We can therefore carry out a gauge transformation using $\alpha = -\xi/qv$,

$$B'^\mu = B^\mu + \partial^\mu\left(\frac{\xi}{qv}\right) , \quad (10.38)$$

$$\phi' = e^{-i\xi/v}\phi , \quad (10.39)$$

which gives what is called the unitary gauge. As we are treating η and ξ as perturbations about the vacuum state, we can regard their original definition equivalently as

$$\phi(x) = \frac{1}{\sqrt{2}}(v + \eta + i\xi) \approx \frac{1}{\sqrt{2}}(v + \eta)e^{i\xi/v} . \quad (10.40)$$

In this way, under the gauge transformation the field ϕ becomes

$$\phi \to \phi' = e^{-i\xi/v}\frac{1}{\sqrt{2}}(v + \eta)e^{i\xi/v} = \frac{1}{\sqrt{2}}(v + \eta) . \quad (10.41)$$

That is, after transformation to the unitary gauge, the field ξ disappears, and ϕ emerges as a purely real scalar field η, which corresponds to the Higgs boson. The Lagrangian is

$$\mathcal{L} = -\frac{1}{4}F_{\mu\nu}F^{\mu\nu} + \frac{1}{2}m_B^2B_\mu B^\mu + \frac{1}{2}(\partial_\mu\eta)(\partial^\mu\eta) - \frac{1}{2}m_\eta^2\eta^2 + \text{ interaction terms} , \quad (10.42)$$

where $m_B = qv$ and $m_\eta = \sqrt{-2\mu^2} = \sqrt{2\lambda}v$.

Although it may seem that we have lost a physical degree of freedom through a redefinition of the fields, this is not the case. Before including the field ϕ, B^μ appeared as massless and thus only had two independent degrees of freedom, since a massless vector particle has two transverse and no longitudinal polarisation states. Adding in the two components ϕ_1 and ϕ_2 meant we then had four degrees of freedom. After rewriting ϕ_1 and ϕ_2 in terms of η and ξ and transforming to the unitary gauge, the degree of freedom corresponding to the massless Goldstone boson ξ is said to be "eaten" by the field B^μ, which appears as massive. The complex scalar field is replaced by a real scalar field η, losing one degree of freedom, and the field B^μ gains a degree of freedom because of its mass and the corresponding longitudinal polarisation state.

10.3 The Higgs mechanism in the electroweak Standard Model

When we introduced the electroweak Standard Model in Ch. 9, we needed to treat all of the particles as massless to keep from breaking the gauge symmetry. We know, however, that the SM particles, in particular the $W^{\pm}$ and Z bosons, have nonzero masses. To bring this into the theory while maintaining gauge invariance we will generalise the U(1) Higgs mechanism seen in the previous section to the $\mathrm{SU(2)_L} \times \mathrm{U(1)}$ gauge symmetry of electroweak Standard Model.

Since the Standard Model has three massive gauge bosons that were initially treated as massless, we need to supply three degrees of freedom from massless Goldstone bosons that can be recast as the longitudinal polarisation components of the $W^{\pm}$ and Z. To do this we need therefore more than one complex scalar field ϕ and in the minimal Standard Model this is achieved by a doublet of complex scalars, one charged and one neutral, i.e., four independent fields:

$$\phi = \begin{pmatrix} \phi^+ \\ \phi^0 \end{pmatrix} = \frac{1}{\sqrt{2}} \begin{pmatrix} \phi_1 + i\phi_2 \\ \phi_3 + i\phi_4 \end{pmatrix} \ . \tag{10.43}$$

Leaving aside for the moment the kinetic terms and fermion fields, the SM Lagrangian contains terms corresponding to the new doublet ϕ:

$$\mathcal{L}_{\mathrm{H}} = (D_\mu \phi)(D^\mu \phi)^\dagger - V(\phi) \ , \tag{10.44}$$

where the Higgs potential is

$$V(\phi) = \mu^2 \phi^\dagger \phi + \lambda (\phi^\dagger \phi)^2 \ , \tag{10.45}$$

with $\lambda > 0$ and $\mu^2 < 0$. The potential is minimum for any ϕ_i, $i = 1, \ldots, 4$ where $\phi^\dagger \phi \equiv v^2/2 = -\mu^2/2\lambda$. The covariant derivative D_μ is the same as Eq. (9.30), namely,

$$D_\mu = \partial_\mu + ig\boldsymbol{T} \cdot \boldsymbol{W}_\mu + i\frac{g'}{2} Y B_\mu \ . \tag{10.46}$$

We assume that under the SU(2) part of the gauge transformation, ϕ behaves like a weak isospin doublet, i.e., $T = 1/2$. That is, the charged scalar ϕ^+ has $T_3 = 1/2$ and the neutral ϕ^0 has $T_3 = 1/2$. For the $U(1)_Y$ part of the gauge transformation we therefore have weak hypercharge $Y = 2(Q - T_3) = 1$.

We took one of the complex fields as neutral and the other charged, which will allow us to generate longitudinal components for the neutral Z and charged $W^{\pm}$. But we do not want to generate a mass term for the photon, which will interact with the charged component ϕ^+. Therefore we choose the vacuum state to correspond to $\phi_1 = \phi_2 = \phi_4 = 0$ and $\phi_3 = v$, i.e., only the neutral scalar ϕ^0 acquires a nonzero vacuum expectation value:

$$\langle 0|\phi|0\rangle = \frac{1}{\sqrt{2}} \begin{pmatrix} 0 \\ v \end{pmatrix} \ . \tag{10.47}$$

In analogy with Eq. (10.34) we can expand the fields about this minimum as

$$\phi = \frac{1}{\sqrt{2}} \begin{pmatrix} \phi_1(x) + i\phi_2(x) \\ v + \eta(x) + i\phi_4(x) \end{pmatrix} . \tag{10.48}$$

Again in analogy with the U(1) gauge theory of Sec. 10.2, after transformation to the unitary gauge the fields ϕ_1 and ϕ_2 and ϕ_4 will be "eaten" by the $W^{\pm}$ and Z fields, and correspond to their longitudinal polarisation components. The field $\eta(x)$ is a real scalar field that we will rename $h(x)$ and call the Higgs boson. The doublet ϕ will then appear as

$$\phi = \frac{1}{\sqrt{2}} \begin{pmatrix} 0 \\ v + h(x) \end{pmatrix} . \tag{10.49}$$

To express the Lagrangian with this replacement for ϕ we need the term

$$D_\mu \phi = \left(\partial_\mu + ig\boldsymbol{T} \cdot \boldsymbol{W}_\mu + i\frac{g'}{2} Y B_\mu \right) \frac{1}{\sqrt{2}} \begin{pmatrix} 0 \\ v + h(x) \end{pmatrix} . \tag{10.50}$$

Using the SU(2) generators $\boldsymbol{T} = \frac{1}{2}\boldsymbol{\tau}$ and hypercharge $Y = 1$ and substituting the ingredients into the Lagrangian (10.44) together with the transformed ϕ of Eq. (10.49) in the Higgs potential gives

$$\begin{aligned} \mathcal{L}_{\rm H} &= \tfrac{1}{2}\big(\partial_\mu h\big)\big(\partial^\mu h\big) + \tfrac{1}{8} g^2 \big(W_{1,\mu} + iW_{2,\mu}\big)\big(W_1^\mu - iW_2^\mu\big)(v+h)^2 \\ &+ \tfrac{1}{8}\big(gW_\mu 3, -g'B_\mu\big)\big(gW_3^\mu - g'B^\mu\big)(v+h)^2 \\ &- \frac{\mu^2}{2}(v+h)^2 - \frac{\lambda}{4}(v+h)^4 . \end{aligned} \tag{10.51}$$

Having identified in Sec. 9.4.1 the combinations $W^{(\pm)\mu} = \frac{1}{\sqrt{2}}(W_1^\mu \mp iW_2^\mu)$ as the charged W boson, we can express

$$\big(W_{1,\mu} + iW_{2,\mu}\big)\big(W_1^\mu - iW_2^\mu\big) = |W_\mu^+|^2 + |W_\mu^-|^2 , \tag{10.52}$$

where $|W_\mu^\pm|^2 \equiv (W_\mu^\pm)(W^{\pm,\mu})^*$. Therefore we see that the term in $\mathcal{L}_{\rm H}$

$$\tfrac{1}{8} g^2 \big(W_{1,\mu} + iW_{2,\mu}\big)\big(W_1^\mu - iW_2^\mu\big)v^2 = \frac{1}{2} M_W^2 \left(|W_\mu^+|^2 + |W_\mu^-|^2 \right) \tag{10.53}$$

corresponds to its mass term (cf. Eq. (10.22)) with the mass of the W given by

$$M_W = \frac{gv}{2} . \tag{10.54}$$

We had also identified the combinations of $W_\mu^{(3)}$ and B_μ (see Eqs. (9.52) and (9.53))

$$A^\mu = \cos\theta_{\rm W} B^\mu + \sin\theta_{\rm W} W_3^\mu = \left(gB^\mu + g' W_3^\mu\right)/\sqrt{g^2+g'^2}\,, \tag{10.55}$$

$$Z^\mu = -\sin\theta_{\rm W} B^\mu + \cos\theta_{\rm W} W_3^\mu = \left(-g' B^\mu + g W_3^\mu\right)/\sqrt{g^2+g'^2} \tag{10.56}$$

as the photon and Z boson, respectively. Therefore the term in $\mathcal{L}_{\rm H}$

$$\tfrac{1}{8}\left(gW_{3,\mu} - g'B_\mu\right)\left(gW_3^\mu - g'B^\mu\right) = \tfrac{1}{2}M_Z^2 Z_\mu Z^\mu \tag{10.57}$$

corresponds to the mass of the Z with

$$M_Z = \tfrac{1}{2}v\sqrt{g^2+g'^2} = \frac{gv}{2\cos\theta_{\rm W}}\,. \tag{10.58}$$

We therefore obtain a predicted relation between the masses of the W and Z bosons, namely,

$$\frac{M_W}{M_Z} = \cos\theta_{\rm W}\,. \tag{10.59}$$

Furthermore, the Lagrangian (10.51) contains no term that would correspond to the mass of the combination $gB^\mu + g'W_3^\mu$, so as we wanted, the photon remains massless.

The relation (10.59) between M_W and M_Z is one of the most important predictions of the Standard Model. Recall from Eq. (9.59) that $\cos\theta_W$ is determined by the two couplings g and g' or equivalently g and e as

$$\cos\theta_W = \sqrt{1 - \frac{e^2}{g^2}}\,. \tag{10.60}$$

Thus the Higgs mechanism makes a testable prediction between the strengths of the electromagnetic and weak couplings and the masses of the W and Z bosons.

In the form $M_W = M_Z\sqrt{1-e^2/g^2}$, the relation does not provide a very sensitive test because the coupling strength g is not measured to high accuracy. This is because all low energy weak processes such as muon decay depend only on the ratio $g^2/M_{\rm W}^2$. This is equivalent to the Fermi constant $G_{\rm F} = \sqrt{2}g^2/8M_{\rm W}^2$, which is known to much higher accuracy. In order to provide a more sensitive test, we can rewrite the relations to give $M_{\rm W}$ as a function of e (or α), $G_{\rm F}$ and $M_{\rm Z}$, or an even more accurate prediction is obtained from a global fit of observables related to electroweak physics [40]. This yields a predicted value for the W mass of

$$M_{\rm W} = 80.3545 \pm 0.0057\ {\rm GeV}\,, \tag{10.61}$$

which is in very good agreement with most of the values measured values, although there is significant tension with a recent measurement by the CDF Experiment as shown in Fig. 10.3.

By multiplying out the part of the Lagrangian (10.51)

$$-\frac{\mu^2}{2}(v+h)^2 - \frac{\lambda}{4}(v+h)^4 \tag{10.62}$$

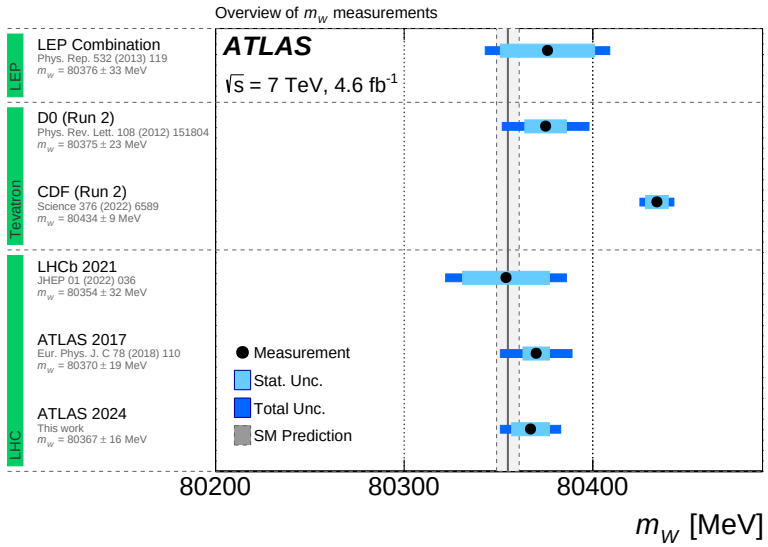

Figure 10.3: Measurements of the mass of the W boson with the prediction of the Standard Model (from [41]).

one obtains the quadratic term

$$-\frac{1}{2}\left(\mu^2 + 3\lambda v^2\right) h^2 = -\frac{1}{2} m_{\mathrm{H}}^2 h^2 \,, \tag{10.63}$$

from which we can identify the mass of the Higgs boson to be

$$m_{\mathrm{H}} = \sqrt{2\lambda} v = \sqrt{-2\mu^2} \,. \tag{10.64}$$

Although the vacuum expectation value $v = 2M_W/g = 246\,\mathrm{GeV}$ is determined from low-energy measurements (it is fixed by G_{F}), the parameter λ was not known until the Higgs boson itself was discovered in 2012 and its mass determined to be 125 GeV.

Because of the success in providing a renormalisable gauge-invariant theory, the Higgs mechanism found broad acceptance in the decade or so after it was proposed. This interest increased substantially in 1983 after the discovery of the W and Z bosons [34, 35] and measurement of their masses, which confirmed the prediction $M_W/M_Z = \cos\theta_{\mathrm{W}}$.

Another important success will only be mentioned here briefly: in the Standard Model without the Higgs boson, the cross section for scattering of massive longitudinally polarised W bosons grows with E_{cm}^2 and exceeds the unitarity limit at energies of around 1 TeV. By including the Higgs boson, Feynman diagrams that involve Higgs exchange interfere destructively with the rest, cancelling the E_{cm}^2 increase and keeping the cross section below the unitarity limit. More information can be found in standard texts such as Refs. [4, 3].

Thus for several decades, most physicists were convinced that the Higgs boson, or something like it, must exist but, it had not been experimentally observed and its mass was not known. All of the experiments from the 1980s onwards able to look for the Higgs boson did so, and it was finally found in 2012 at by the ATLAS [47] and CMS [48] experiments at the Large Hadron Collider (LHC) at CERN. Its mass has been measured to be [19]

$$m_H = 125.11 \pm 0.20\,\mathrm{GeV} \,. \tag{10.65}$$

10.4 Couplings of the Higgs boson

In this section we will expand out the portion of the Lagrangian (10.51) that results in interactions between Higgs bosons and other particles. This will give us the vertex factors that will permit us to compute production cross sections and decay rates of the Higgs.

10.4.1 Coupling of the Higgs boson to gauge bosons

By multiplying out the term $(v+h)^2$ and $(v+h)^4$ in Eq. (10.51) for $\mathcal{L}_{\rm H}$ and expressing $W_1^\mu, W_2^\mu, W_3^\mu$ and B^μ in terms of $W^{(\pm),\mu}$, Z^μ and A^μ, one finds the mass terms seen above as well as terms corresponding to interactions of gauge and Higgs bosons. These include, for example,

$$\tfrac{1}{2}g^2 v W_\mu^{(-)} W^{(+)\mu} h + \tfrac{1}{4}g^2 W_\mu^{(-)} W^{(+)\mu} h^2 \; . \tag{10.66}$$

The first term represents coupling of two W bosons and a Higgs, as shown in Fig. 10.4(a). The coefficient of $W_\mu^{(-)} W^{(+)\mu} h$ is $\frac{1}{2}g^2 v$ which can be written $g M_W$ by using Eq. (10.54). Following the rules of Sec. 10.1.4, the vertex factor in the Feynman diagram is therefore $ig M_W$. One must also include a factor of $g^{\mu\nu}$ to match the Lorentz indices of the fields W_μ and W_ν. The second term above contains $W_\mu^{(-)} W^{(+)\mu} hh$ with a coefficient of $\frac{1}{4}g^2$. There are two identical particles in the diagram so the vertex factor is multiplied by $i2!$ and also by $g^{\mu\nu}$ to match the Lorentz indices of the W fields, to give $ig^2 g^{\mu\nu}/2$ as shown in Fig. 10.4(b). The corresponding term with couplings between a pair of Z bosons and one or two Higgs bosons has the same vertex factors as for a W pair except with g replaced by $g/\cos\theta_{\rm W}$, or equivalently M_W replaced by M_Z, as shown in Fig. 10.4(c) and (d).

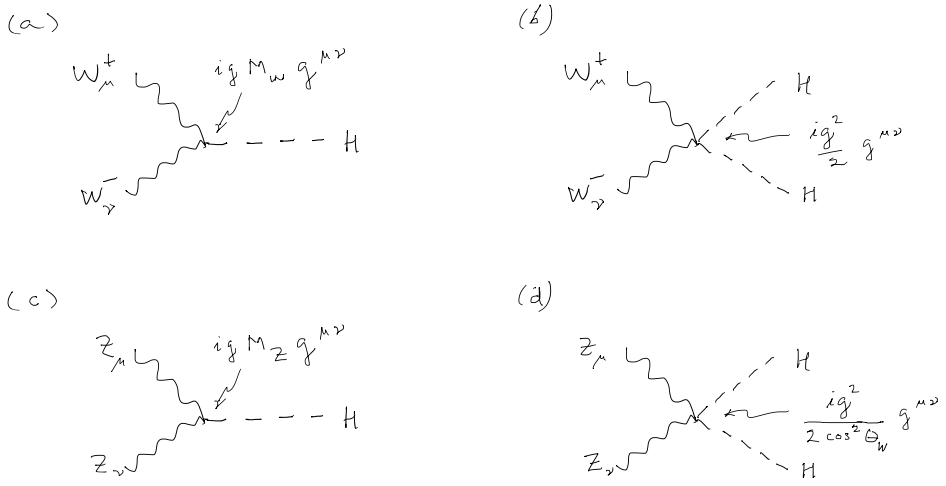

Figure 10.4: Feynman diagrams for coupling of (a) WWh, (b) WWhh, (c) ZZH and (d) ZZhh shown with the corresponding vertex factors.

Thus for both the a the WWh and ZZh, the vertex factor is proportional to the mass of the particle to which the Higgs couples. There is no term in the Lagrangian of the form $A_\mu A_\nu h$, i.e.,

there is no direct coupling between the photon and the Higgs. The decay $H \to \gamma\gamma$ does occur, however, but only via an intermediate loop of massive particles.

10.4.2 Coupling of the Higgs boson to fermions

The portion of the Lagrangian we have written out so far does not supply masses for fermions. These can also be included with the Higgs mechanism in a manner that preserves gauge invariance. We will regard for now the neutrinos as massless and let us consider the charged leptons. First, consider the mass term for a Dirac fermion $-m\overline{\psi}\psi$. We can write $\psi = \psi_L + \psi_R$ where ψ_L and ψ_R are the left- and right-chiral components, i.e., $\psi_L = P_L\psi = \frac{1}{2}(1-\gamma^5)\psi$, $\psi_R = P_R\psi = \frac{1}{2}(1+\gamma^5)\psi$. Notice that because $\gamma^0\gamma^5 = -\gamma^5\gamma^0$ we have $\gamma^0 P_L = P_R\gamma^0$ and $\gamma^0 P_R = P_L\gamma^0$. Furthermore $(\gamma^5)^\dagger = \gamma^5$ and so $P_L = P_L^\dagger$ and $P_R = P_R^\dagger$. Therefore

$$\overline{\psi}_L = (P_L\psi)^\dagger\gamma^0 = \psi^\dagger\gamma^0 P_R = \overline{\psi}P_R \,, \tag{10.67}$$

and similarly $\overline{\psi}_R = \overline{\psi}P_L$. When we construct the mass term $-m\overline{\psi}\psi$ with $\psi = \psi_L + \psi_R$ we therefore find that $\overline{\psi}_L\psi_L = \overline{\psi}P_R P_L\psi = 0$ and also $\overline{\psi}_R\psi_R = 0$. The only terms that survive are

$$-m\overline{\psi}\psi = -m(\overline{\psi}_L\psi_R + \overline{\psi}_R\psi_L) \,. \tag{10.68}$$

Because the $SU(2)_L \times U(1)$ gauge transformation is different for the left- and right-chiral components, it appears that a mass term of the form of Eq. (10.68) would break the symmetry.

Despite this obstacle, we can make use of the properties of the gauge transformation and hypercharge assignments to construct a combination of the fermion and Higgs fields that is gauge invariant, and from this we will be able to generate fermion masses. In the Higgs mechanism, an SU(2) gauge transformation of the complex doublet ϕ of Eq. (10.43) is

$$\phi' = U_T\phi \,, \tag{10.69}$$

where $U_T = \exp[ig\boldsymbol{\alpha}(x)\cdot\boldsymbol{T}]$. Let us use the name of the lepton to stand for its wave function, e.g., $\ell = \psi_\ell$, and define the isospin doublet of left-chiral leptons

$$L = \begin{pmatrix} \nu_\ell \\ \ell \end{pmatrix}_L \,. \tag{10.70}$$

Under the $SU(2)_L$ gauge transformation the left-chiral components become

$$L' = U_T L \,, \tag{10.71}$$

$$\overline{L}' = (U_T L)^\dagger\gamma^0 = L^\dagger\gamma^0 U_T^\dagger = \overline{L}U_T^\dagger \,, \tag{10.72}$$

where γ^0 is understood to multiply both components of the isospin doublet. Because both L and ϕ transform in the same way and U_T is unitary, the combination $\overline{L}\phi$ is invariant under SU(2).

The right-chiral components of the charged leptons are isospin singlets $R = \psi_{\ell,R}$; they are assigned $T_3 = 0$ and do not change under $SU(2)_L$. Under $U(1)_Y$, they transforms as $R' = U_Y R$ with $U_Y = e^{iY\theta}$ where $\theta \equiv g'\beta(x)$. The hypercharge values $Y = 2(Q - T_3)$ give $Y_\phi = 1$, $Y_L = -1$ and $Y_R = -2$. Under $U(1)_Y$ the terms in $(\overline{L}\phi)R$ transform as

$$\overline{L} = L^\dagger\gamma^0 \quad \rightarrow \quad \overline{L}' = (e^{-i\theta}L)^\dagger\gamma^0 = \overline{L}e^{i\theta} \tag{10.73}$$

$$\phi \quad \rightarrow \quad \phi' = e^{i\theta}\phi \tag{10.74}$$

$$R \quad \rightarrow \quad R' = e^{-2i\theta}R\,, \tag{10.75}$$

Therefore the combination $(\overline{L}\phi)R$ is invariant under $U(1)_Y$, and since R does not change under $SU(2)$, $(\overline{L}\phi)R$ is invariant under the full $SU(2)\times U(1)_Y$ gauge transformation. We can therefore add to the Lagrangian

$$\mathcal{L}_\ell \;=\; -y_\ell\left[\overline{L}\phi R + (\overline{L}\phi R)^\dagger\right]\,, \tag{10.76}$$

where y_ℓ is a constant called the Yukawa coupling discussed further below and the Hermitian conjugate $(\overline{L}\phi R)^\dagger$ is included to ensure that the full Lagrangian is real.

After repeating the spontaneous symmetry breaking procedure and transforming to the unitary gauge as in Sec. 10.3, the field ϕ becomes

$$\phi(x) = \frac{1}{\sqrt{2}}\begin{pmatrix} 0 \\ v + h(x) \end{pmatrix}\,. \tag{10.77}$$

Because the upper component of ϕ is zero, the terms in Eq. (10.76) involving the neutrino vanish and one obtains

$$\mathcal{L}_\ell = -\frac{y_\ell}{\sqrt{2}}v(\overline{\ell}_L\ell_R + \overline{\ell}_R\ell_L) - \frac{y_\ell}{\sqrt{2}}h(\overline{\ell}_L\ell_R + \overline{\ell}_R\ell_L)\,. \tag{10.78}$$

We can identify the first term as a mass term $-m_\ell\overline{\psi}\psi$ with the lepton's mass

$$m_\ell = \frac{y_\ell v}{\sqrt{2}}\,. \tag{10.79}$$

The constant y_ℓ is called the Yukawa coupling and its value is adjusted to give the value of m_ℓ observed experimentally. Thus we obtain the masses without violating gauge symmetry, but there is no predicted relation between the masses, rather we must introduce an adjustable parameter for each one, to which we assign the value $y_\ell = \sqrt{2}m_\ell/v$.

The second term in $\mathcal{L}_\ell$ from Eq. (10.78) is an interaction term between a lepton pair and a Higgs boson, for which we identify the vertex factor $-iy_\ell/\sqrt{2} = -im_\ell/v$. Thus just as for the gauge bosons, the coupling strength of charged leptons, and in fact all fermions, to the Higgs is proportional to the mass of the particle with which the Higgs couples.

Because the charged component of the doublet ϕ is assigned a vacuum expectation value of zero, we can not use this mechanism to generate masses for neutrinos. Although the observation of neutrino oscillations tells us that neutrinos cannot (all) be massless, there are a number of choices for bringing them into a gauge invariant theory which go outside the scope of this course. A brief description of the problem and possible solutions can be found, e.g., in Ref. [3].

The zero expectation value for ϕ^+ therefore means that we cannot use exactly the same scheme for the up-type quarks as we did with charged leptons. Nevertheless, one can exploit a property of the SU(2) transformation to show that the recipe for up- and also down-type quarks gives exactly the same result as we found for the leptons (for further details see, e.g., Ref. [3]). Therefore for all Dirac fermions f we introduce a Yukawa coupling y_f and assign its value from the observed mass:

$$y_f = \sqrt{2}\frac{m_f}{v} \,, \tag{10.80}$$

where $v = 2M_W/g = 246\,\text{GeV}$ is the vacuum expectation value of the neutral component ϕ^0. The Higgs couples to fermion pairs according to the Feynman diagram shown in Fig.10.5 with the vertex factor $-im_f/v$.

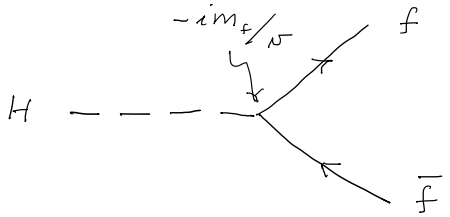

Figure 10.5: Feynman diagram for the coupling of a fermion pair to the Higgs boson.

10.4.3 Self-coupling of the Higgs boson

Multiplying out the part of the Higgs Lagrangian (10.51) that contains $-(\lambda/4)(v+h)^4$ gives the terms

$$-\lambda v h^3 - \frac{\lambda}{4}h^4 \,. \tag{10.81}$$

These represent couplings of three and four Higgs bosons, respectively, as shown in Fig. 10.6.

For the triple-Higgs coupling, the factor multiplying h^3 in the Lagrangian is $-\lambda v$, and there are $N = 3$ identical particles at the vertex. Including the symmetry factor $N! = 6$, one finds the vertex factor

$$-6i\lambda v = -\frac{3im_{\text{H}}^2}{v} = -\frac{3igm_{\text{H}}^2}{2M_W} \,. \tag{10.82}$$

For the quartic coupling there are $N = 4$ identical particles giving

$$-6i\lambda = -\frac{3im_{\text{H}}^2}{v^2} = -\frac{3ig^2m_{\text{H}}^2}{4M_W^2} \,. \tag{10.83}$$

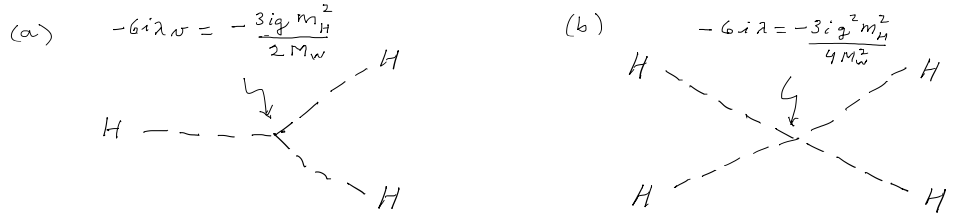

Figure 10.6: Feynman diagrams for (a) triple and (b) quartic Higgs couplings shown with the corresponding vertex factors.

Measurement of proton-proton collision events with two Higgs bosons in the final state would be sensitive to the triple-Higgs coupling and thus provide an important test of this prediction.

10.5 Higgs boson properties

A complete survey of the properties of the Higgs boson goes beyond the scope of this course, but we will show here some illustrative highlights. As an example that uses the couplings that we have just derived, we can compute the rate for the decay of a Higgs boson to fermion-antifermion pairs. The diagram is shown in Fig. 10.5 above. Let us take the four-momenta of the fermion and antifermion to be p_1 and p_2, respectively.

The diagram has an initial scalar particle and two outgoing fermions. The Feynman rule for an external scalar is that the amplitude simply gets a factor of unity. This can be at least roughly understood by analogy with an external fermion, where a wave function $\psi(x) = u(p)e^{ip\cdot x}$ results in a factor $u(p)$ in the amplitude. The wave function of a scalar particle is just $\phi(x) = e^{ip\cdot x}$, and the amplitude thus only picks up a factor of 1. As derived above, the vertex factor is $-im_f/v$. The amplitude is therefore

$$\mathcal{M} = -\frac{im_f}{v}\overline{u}(p_1)v(p_2) \ . \tag{10.84}$$

After squaring the amplitude we need to sum over the final state spins using the Casimir trick, which gives

$$\langle|\mathcal{M}|^2\rangle = \frac{m_f^2}{v^2}\mathrm{Tr}\left[(\not{p}_1 + m_f)(\not{p}_2 - m_f)\right] \ . \tag{10.85}$$

The trace includes two terms with a single factor of the momentum which give zero since they contain an odd number of gamma matrices. Further, we have $\mathrm{Tr}(\not{p}_1\not{p}_2) = 4p_1 \cdot p_2$ and $\mathrm{Tr}I_4 = 4$, so we find

$$\langle|\mathcal{M}|^2\rangle = \frac{m_f^2}{v^2}(4p_1 \cdot p_2 - 4m_f^2) \ . \tag{10.86}$$

The centre-of-mass energy squared is $m_\mathrm{H}^2 = (p_1 + p_2)^2 = 2m_f^2 + 2p_1 \cdot p_2$ so the amplitude squared becomes

$$\langle|\mathcal{M}|^2\rangle = \frac{2m_f^2 m_{\rm H}^2}{v^2}\left(1-\frac{4m_f^2}{m_{\rm H}^2}\right) . \tag{10.87}$$

In the rest frame of the Higgs, the momentum of either of the two outgoing fermions is given by

$$p^* = \frac{m_{\rm H}}{2}\left(1-\frac{4m_f^2}{m_{\rm H}^2}\right)^{1/2} . \tag{10.88}$$

We can then use Eq. (7.27) for an isotropic two-body decay rate in the c.m. system to find

$$\Gamma(H\to f\overline{f}) = \frac{p^*}{8\pi m_{\rm H}^2}\langle|\mathcal{M}|^2\rangle = \frac{m_f^2 m_{\rm H}}{8\pi v^2}\left(1-\frac{4m_f^2}{m_{\rm H}^2}\right)^{3/2} . \tag{10.89}$$

The formula does not hold for the top quark, since a Higgs with $m_{\rm H} = 125\,\text{GeV}$ cannot decay into a $t\bar{t}$ pair with a mass of $2\times 173\,\text{GeV}$. For the lighter fermions, the factor involving $4m_f^2/m_{\rm H}^2$ can for most purposes be ignored (it is less than one percent for the b quark). For quarks, we need to include a factor of $N_C = 3$ for the three possible colours. The most important feature in the formula for the decay rate is that it is proportional to the square of the mass of the fermion, and therefore the rates to b, c, τ and μ are found to be in the ratios

$$\Gamma_{bb} \,:\, \Gamma_{cc} \,:\, \Gamma_{\tau\tau} \,:\, \Gamma_{\mu\mu} = 3m_b^2 \,:\, 3m_c^2 \,:\, m_\tau^2 \,:\, m_\mu^2 . \tag{10.90}$$

For the Higgs decay to a pair of vector bosons, the calculations are more involved, in particular because with $M_W = 80.4\,\text{GeV}$, $M_Z = 91.2\,\text{GeV}$ and $m = 125\,\text{GeV}$, the Higgs is not massive enough to decay into a pair of on-shell W or Z bosons. The decay can only occur if at least one of the final state bosons is virtual. Taking mass effects and higher-order corrections into account, the branching ratios for the Higgs to decay to all of the relevant final states is shown in Fig. 10.7(a) as a function of the Higgs mass $m_{\rm H}$. From the sum of the kinematically allowed partial decay rates one can find the total decay rate shown versus $m_{\rm H}$ in 10.7(b).

The plots in Fig. 10.7 were particularly relevant before the actual mass of the Higgs boson was known. At the currently known mass of 125 GeV, the total rate is predicted to be

$$\Gamma_{\rm H} = 4.1\,\text{MeV} . \tag{10.91}$$

Although this is significantly below the resolution needed for a direct measurement, the decay rate can be estimated indirectly by exploiting interference effects in decays of the Higgs to ZZ and subsequent decays of the Z bosons to leptons. The ATLAS Experiment has reported a measured value of $\Gamma_{\rm H} = 4.5^{+3.0}_{-2.2}\,\text{MeV}$ in good agreement with the prediction [50].

Looking at the branching ratios in Fig. 10.7(b), it is interesting to note that for a mass of 125 GeV, the Higgs has measurable decay fractions into a fairly wide variety of final states, allowing for a number of important tests of the predicted rates. The rates are often quantified using the coupling strength parameters κ_f and κ_V for fermions and vector bosons, respectively, defined as dimensionless factors that modify the corresponding Higgs couplings relative to the SM values. A measure of the coupling can then be given with the so-called reduced values,

(a) (b)

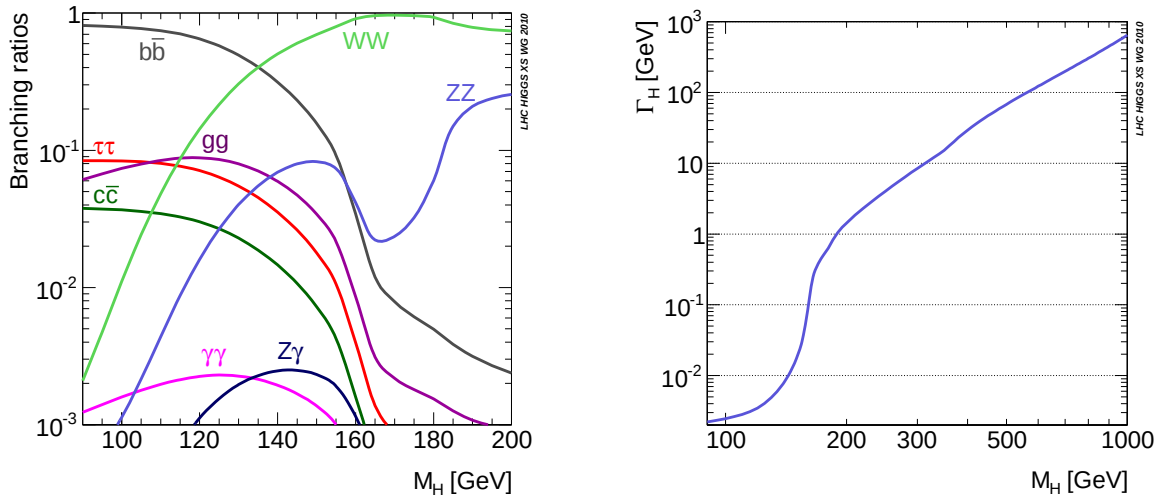

Figure 10.7: (a) Higgs branching ratios and (b) the total Higgs decay width versus the Higgs mass (from [49]).

defined as $\kappa_f m_f/v$ for fermions ($f = t, b, \tau, \mu$) and $\sqrt{\kappa_V} M_V/v$ for vector bosons $V = W, Z$, as a function of their masses m_f and M_V. Measured values are shown with the SM prediction in Fig. 10.8 as a function of the mass of the particle to which the Higgs couples. This shows spectacular agreement between data and observation over many orders of magnitude in coupling strength.

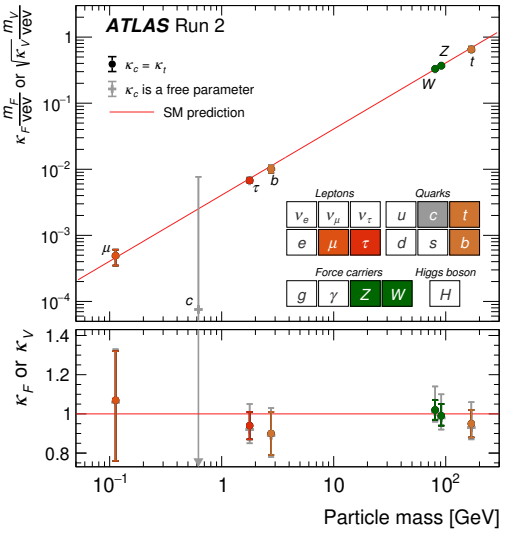

Figure 10.8: Measurements of the coupling strength modifiers (see text) of the Higgs boson to different particles as as function of the particle's mass. (from [51]).

Chapter 11

Quantum Chromodynamics

In this chapter we will look at the fundamental theory of strong interactions based on an SU(3) gauge theory of quarks and gluons: Quantum Chromodynamics or QCD. An introduction to the ideas behind QCD can be found in Chapter 10 of the PH3520 Lecture Notes [1], and to make these notes self-contained some of that material is included here.

11.1 Evidence for colour

Ever since it was realized that an atomic nucleus consists of protons and neutrons, it was clear that there must exist a nuclear or 'strong' force, capable of binding them together. Attempts to construct a theory of strong interactions based on the exchange of a massive particle, such as Yukawa's theory of pion exchange, were not very successful. Once electron–proton scattering experiments indicated that nucleons are themselves not elementary particles, the question of strong interactions turned to their constituents, namely, quarks. In the 5 to 10 years following the introduction of the quark model, there emerged evidence that quarks possess an additional property which was called *colour*. Important clues came from the symmetry properties of baryon wave functions, the total hadronic cross section in e^+e^- annihilation, and the π^0 lifetime.

Almost immediately after the quark model was introduced, Greenberg pointed out that it is impossible to construct from it certain baryon wave functions with symmetry properties consistent with the Pauli exclusion principle [52]. The Δ^{++}, for example, is a resonance created in π^+p scattering. It consists of three u quarks, and from the angular distribution observed in the reaction $\pi^+p \to \pi^+p$ it must have spin $J = 3/2$. Furthermore, the Δ^{++} is the lowest mass combination of three u quarks, and any reasonable model of hadrons predicts that the lowest mass state must have orbital angular momentum of zero. This means that the spatial part of the wave function is symmetric upon interchange of any of the two quarks, and to form a $J = 3/2$ state the three quark spins must be aligned parallel, so the spin part of the wave function is symmetric as well.

The rules of quantum mechanics, however, require a system of identical fermions to be described by an antisymmetric wave function, i.e., it must change sign upon interchange of any pair. Greenberg proposed that if the quarks were to possess an additional quantum number, which later was called colour, then the three u quarks need not be in the same state and the exclusion principle would not be violated. One can show that at least three colours are needed

in order to construct an antisymmetric wave function for the Δ^{++}. Other than that, it was not clear from these considerations how many colours there should be or what colour means in any larger context.

The next piece of evidence for colour came from the reaction $e^+e^- \to$ hadrons. In the quark model, hadronic final states are assumed to result from the reaction $e^+e^- \to q\overline{q}$, where q represents a quark of any of the possible flavours. The transformation of the quark and antiquark into ordinary hadrons such as pions and kaons was not – and still is not – understood in detail, but could be assumed to occur with unit probability. In this model, therefore, the total cross section for $e^+e^- \to$ hadrons was simply taken as the sum of the cross sections to produce a quark–antiquark pair for all of the kinematically accessible flavours, i.e., those with masses $m_q < E_{\rm cm}/2$.

Let us consider this reaction first at centre-of-mass energies significantly less than the mass of the Z, so that to first approximation the amplitude is given by the diagram with an intermediate photon, as shown in Fig. 11.1(a). This is essentially the same diagram as for $e^+e^- \to \mu^+\mu^-$ in Fig. 11.1(b), the main difference being that the coupling strength for the $q\overline{q}\gamma$ vertex is $\frac{2}{3}e$ for up-type quarks and $\frac{1}{3}e$ for down-type quarks, whereas it is e for the $\mu^+\mu^-\gamma$ vertex. The only other difference in the amplitudes stems from the different masses of the final state particles, but as long as these are much smaller than the centre-of-mass energy, they will not have a significant influence on the cross section.

Figure 11.1: Lowest order Feynman diagrams for (a) $e^+e^- \to q\overline{q}$ and (b) $e^+e^- \to \mu^+\mu^-$.

Neglecting effects due to the masses of final state particles and using the Feynman diagrams of Fig. 11.1, the total cross sections were found in Sec. 7.6 to be

$$\sigma(e^+e^- \to q\overline{q}) = \frac{4\pi\alpha^2 Q_q^2}{3E_{\rm cm}^2}\,, \tag{11.1}$$

$$\sigma(e^+e^- \to \mu^+\mu^-) = \frac{4\pi\alpha^2}{3E_{\rm cm}^2}\,, \tag{11.2}$$

where $\alpha = e^2/4\pi$ and Q_q is the quark's charge in units of e, i.e., $\frac{2}{3}$ for u, c and t, and $-\frac{1}{3}$ for d, s and b.

The total hadronic cross section is given by the sum of the cross sections for the kinematically accessible quark flavours. For experiments carried out at the PETRA e^+e^- ring with $E_{\rm cm}$ between 14 and 44 GeV, this meant the five flavours u, d, s, c and b. One usually defines R as the ratio of the cross sections for production of hadrons to that for $\mu^+\mu^-$. Using the cross sections above and including all flavours except top we find

$$R = \frac{\sigma(\mathrm{e^+e^-} \to \text{ hadrons})}{\sigma(\mathrm{e^+e^-} \to \mu^+\mu^-)}$$
$$= \sum_{q=u,d,s,c,b} Q_q^2 = 2 \times \left(\frac{2}{3}\right)^2 + 3 \times \left(\frac{-1}{3}\right)^2 = \frac{11}{9} \,. \tag{11.3}$$

Measurements of R, however, indicated a value closer to 4, as seen in Fig. 11.2. Again we are rescued by the concept of colour. Suppose that a quark can come in one of N_c possible colour states, and that an antiquark can carry one of the corresponding 'anticolours'. Furthermore suppose that colour is conserved when the virtual photon decays into the $q\overline{q}$ pair, so that we can get, e.g., red-antired, blue-antiblue, etc., but not red-antiblue. The prediction for R then becomes

$$R = N_\mathrm{c} \sum_q Q_q^2 \,. \tag{11.4}$$

The best agreement with the data is found for $N_\mathrm{c} = 3$, for which the prediction is $R = 11/3 \approx 3.7$. We will return later and show how QCD even explains why the measured value of R is slightly larger than this.

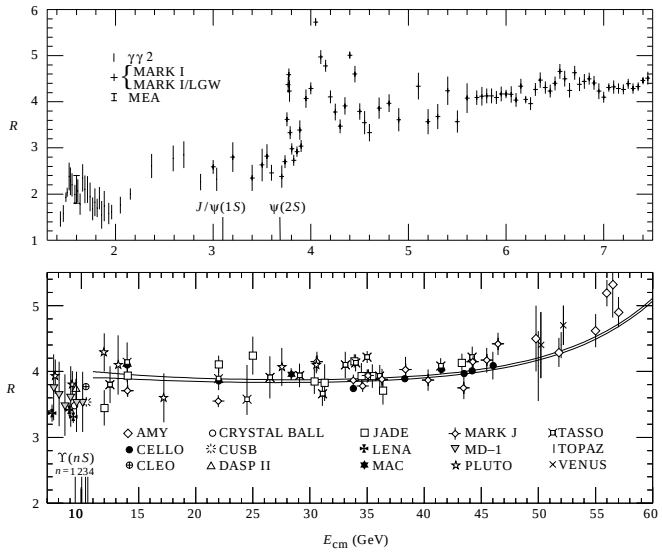

Figure 11.2: Measurements of R, the ratio of $\sigma(\mathrm{e^+e^-} \to \text{ hadrons})$ to $\sigma(\mathrm{e^+e^-} \to \mu^+\mu^-)$ as a function of the centre-of-mass energy [19].

Additional evidence for the assignment $N_\mathrm{c} = 3$ comes from the decay rate of the neutral pion. Here one finds that the π^0 decay rate is proportional to N_c^2, and for $N_\mathrm{c} = 3$ the prediction is $\Gamma(\pi^0 \to \gamma\gamma) = 7.6$ eV [53]. The measured decay rate is $\Gamma(\pi^0 \to \gamma\gamma) = 7.7 \pm 0.6$ eV [19], in good agreement with $N_\mathrm{c} = 3$ and not in agreement with any other integer value.

11.2 QCD as an SU(3) gauge theory

Given the evidence for colour, it was natural to build this into a theory of strong interactions patterned after QED or more generally a non-Abelian Yang-Mills theory of the type used for

the electroweak model. Such a theory was proposed by Gell-Mann and Fritzsch [54] based on the gauge group SU(3). In this model, quarks of any flavour are characterised by a colour index and grouped into a triplet,

$$q = \begin{pmatrix} q_1 \\ q_2 \\ q_3 \end{pmatrix} , \tag{11.5}$$

where each of the q_i is a four-component Dirac wave function (or field). The quark triplets are assumed to change under an SU(3) gauge transformation,

$$q \to q' = U_c q \, . \tag{11.6}$$

Here U_c is an element of the fundamental representation of SU(3), i.e., it is a 3×3 unitary matrix with unit determinant. The most general matrix with this property can be written

$$U_c = e^{ig_s \alpha^a(x) T^a} \, , \tag{11.7}$$

where g_s is the gauge coupling (s for "strong"), $\alpha^a(x)$ are arbitrary functions of x, T^a are the generators of SU(3) and summation over the index a is implied. The number of generators of the group SU(N) is $N^2 - 1$ so for SU(3), a runs from 1 to 8. The transformation has determinant unity, which means the generators are traceless, and for it to be unitary the generators must be Hermitian. The conventional choice that satisfies these requirements is

$$T^a_{ij} = \frac{\lambda^a_{ij}}{2} \, , \quad a = 1, \ldots, 8, \tag{11.8}$$

where the Gell-Mann matrices λ^a are

$$\lambda^1 = \begin{pmatrix} 0 & 1 & 0 \\ 1 & 0 & 0 \\ 0 & 0 & 0 \end{pmatrix} , \quad \lambda^2 = \begin{pmatrix} 0 & -i & 0 \\ i & 0 & 0 \\ 0 & 0 & 0 \end{pmatrix} , \quad \lambda^3 = \begin{pmatrix} 1 & 0 & 0 \\ 0 & -1 & 0 \\ 0 & 0 & 0 \end{pmatrix} , \quad \lambda^4 = \begin{pmatrix} 0 & 0 & 1 \\ 0 & 0 & 0 \\ 1 & 0 & 0 \end{pmatrix} ,$$

$$\lambda^5 = \begin{pmatrix} 0 & 0 & -i \\ 0 & 0 & 0 \\ i & 0 & 0 \end{pmatrix} , \quad \lambda^6 = \begin{pmatrix} 0 & 0 & 0 \\ 0 & 0 & 1 \\ 0 & 1 & 0 \end{pmatrix} , \quad \lambda^7 = \begin{pmatrix} 0 & 0 & 0 \\ 0 & 0 & -i \\ 0 & i & 0 \end{pmatrix} , \quad \lambda^8 = \frac{1}{\sqrt{3}} \begin{pmatrix} 1 & 0 & 0 \\ 0 & 1 & 0 \\ 0 & 0 & -2 \end{pmatrix} . \tag{11.9}$$

The generators are normalised such that

$$\mathrm{Tr}(T^a T^b) = \frac{1}{2} \delta^{ab} \, . \tag{11.10}$$

As we saw from the discussion of Yang-Mills theories in Sec. 9.2, the gauge symmetry is only possible if one introduces a gauge field G^a_μ (the gluon field) for each generator, which for an infinitesimal transformation (cf. Eq. (9.20)) changes as

$$G^a_\mu \to G'^a_\mu = G^a_\mu - \partial_\mu \alpha^a - g_{\rm s} f^{abc} \alpha^b G^c_\mu \; . \tag{11.11}$$

Here $g_{\rm s}$ is the strong coupling constant, often replaced by

$$\alpha_{\rm s} = \frac{g_{\rm s}^2}{4\pi} \; , \tag{11.12}$$

and f^{abc} are the completely antisymmetric structure constants of SU(3), defined by the commutation relation $[T^a, T^b] = i f^{abc} T^c$. These can be obtained starting from

$$\begin{aligned} & f^{123} = 1, \\ & f^{147} = f^{156} = f^{246} = f^{257} = f^{345} = f^{376} = \frac{1}{2}, \\ & f^{458} = f^{678} = \frac{\sqrt{3}}{2} \end{aligned}$$

with all other nonzero terms found using $f^{abc} = -f^{bac} = -f^{acb}$.

The QCD Lagrangian is invariant under the SU(3) gauge transformation by including the gauge fields, which is accomplished by writing it with the covariant derivative

$$D_\mu = \partial_\mu + i g_{\rm s} T^a G^a_\mu \; . \tag{11.13}$$

The Lagrangian is

$$\begin{aligned} \mathcal{L}_{\rm QCD} &= -\frac{1}{4} F^a_{\mu\nu} F^{a,\mu\nu} + \sum_q \overline{q} (i \not{D} - m_q) q \\ &= -\frac{1}{4} F^a_{\mu\nu} F^{a,\mu\nu} + \sum_q \sum_{j,k=1}^{3} \overline{q}_j \left[(i \not{\partial} - m_q) \delta_{jk} - g_{\rm s} \not{G}^a T^a_{jk} \right] q_k \; , \end{aligned} \tag{11.14}$$

where the sums over the colour indices j and k are from one to $N_{\rm c} = 3$, the sum over q includes all quark flavours, $q = u, c, t, d, s, b$, and the gluon field-strength tensor is

$$F^a_{\mu\nu} = \partial_\mu G^a_\nu - \partial_\nu G^a_\mu - g_{\rm s} f^{abc} G^b_\mu G^c_\nu \; . \tag{11.15}$$

Multiplying out the terms in the Lagrangian reveals the vertices shown in Fig. 11.3. The qqg and ggg vertices have a strength of $g_{\rm s}$ and the four-gluon vertex goes as $g_{\rm s}^2$.

11.3 Confinement

At the time QCD was proposed in 1972, the relevant data pertained in large part to the variety of hadron types observed in high-energy collisions. The majority of known hadrons are interpreted as baryons made of three quarks and mesons consisting of a quark-antiquark

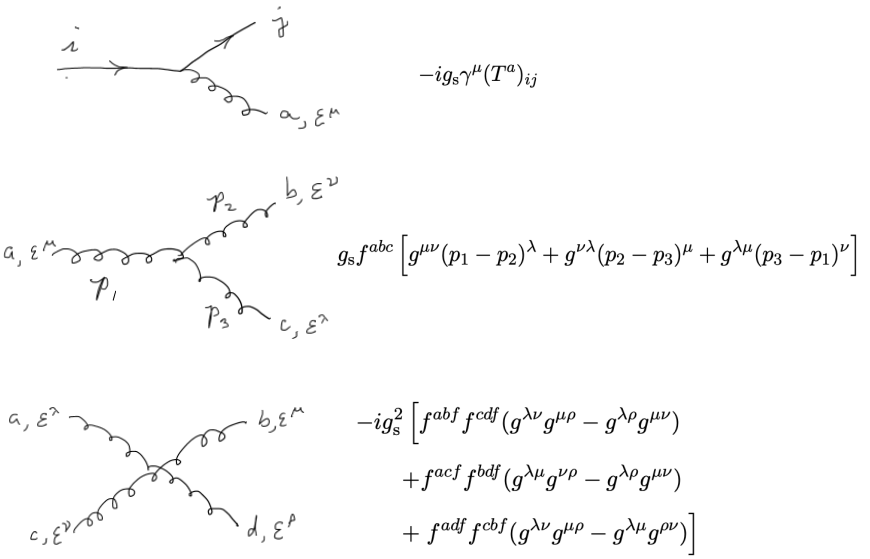

Figure 11.3: Possible quark and gluon interactions and their the vertex factors.

pair, supplemented more recently by a collection of more exotic objects are such as glueballs, tetraquarks or pentaquarks. What all of these hadron states have in common is that they are "colour neutral", which is to say they remain invariant under an SU(3) colour transformation.

If hadrons are modelled as consisting of quarks, one would naively expect free quarks to be liberated in high energy reactions. These would show up very visibly in experiments that measure tracks of charged particles based on their ionising power, which is proportional to the square of a particle's charge. Charge 1/3 or 2/3 particles should therefore give miniminum-ionising tracks with 1/9 or 4/9 of the ionisation seen for particles of unit charge. Despite many searches, no evidence for fractionally charged particles has been found.

In the 1960s, experiments on inelastic electron-nucleon scattering at large momentum transfer Q^2 (called Deep Inelastic Scattering or DIS) revealed evidence for the quark substructure of the nucleon. An analysis of the angles and energies of the scattered electrons indicated that in high Q^2 reactions, the target nucleons contained point-like scattering centres, and these behaved essentially like free particles.

In the early 1970s, electron-positron collisions were being studied at several accelerators including the SPEAR e^+e^- storage ring at the Stanford Linear Accelerator Center (SLAC). If one were to interpret the collisions that resulted in hadrons as coming from $e^+e^- \to q\overline{q}$, the question then arose as to what happened to the quark-antiquark pair. As mentioned in Sec. 11.1, one can assume that they convert somehow into colour-neutral hadrons, but in doing so one would expect them to retain some characteristics of the original quark and antiquark.

The possibility that a high-energy quark would lead to a "jet" or bundle of almost colinear hadrons had been proposed by Drell [55], Brodsky [56] and others and this was confirmed by the analysis of hadronic events from SPEAR [57] that became less spherical and more like back-to-back jets with increasing centre-of-mass energy. The two-jet structure of hadronic events in e^+e^- collisions becomes more visible at higher energies, such as the event from the ALEPH Experiment at the LEP Collider at $E_{\rm cm} = 91.2$ GeV shown in Fig. 11.4.

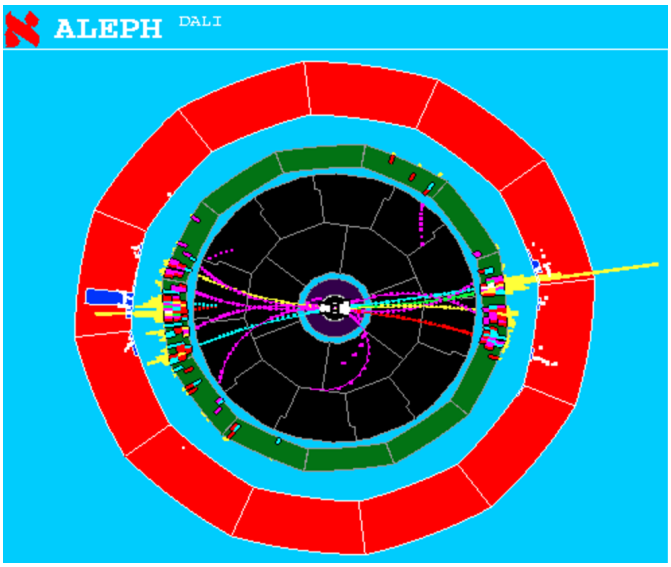

Figure 11.4: A two-jet event from an e^+e^- collision measured by the ALEPH Experiment at the LEP Collider (from [65]).

The production of back-to-back jets of hadrons from $e^+e^- \to q\overline{q}$ can be described with the "string" picture as illustrated in Fig. 11.5. The quark and antiquark are produced with high kinetic energies and recede away from each other. As they separate, they are slowed down by the attractive force and their kinetic energy goes into the energy of a flux tube or string. This field configuration can be motivated by QCD as a consequence of the gluon self-interaction, which results in a potential energy that grows linearly with distance. Thus the force between the quark and antiquark does not fall off with separation but rather remains constant.

The string can break by production of a second $q\overline{q}$ pair in its middle, resulting in two shorter and thus lower mass strings. This continues until what is left are small pieces of string which correspond to the mesons that make up the jets. The mesons from the ends of the original string have on average the highest momenta and those formed near the middle are almost at rest in the original string's rest frame.

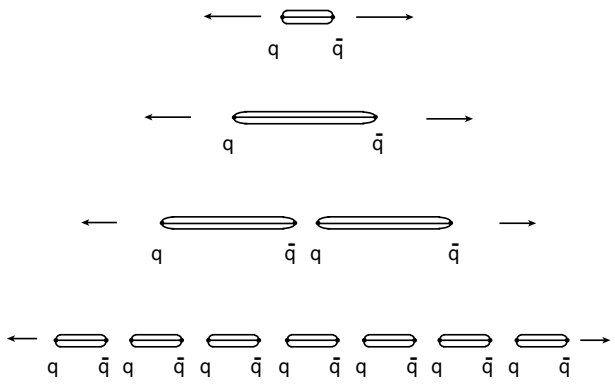

Figure 11.5: Hadron formation in the string model.

So on the one hand, quarks appeared to be quasi-free in high-Q^2 processes, but they are bound in hadrons as a consequence of the non-decreasing attractive force between particles with nonzero colour charge. This latter phenomenon is called *confinement* and one would hope to derive it directly from QCD. While this has not yet been proven rigorously, lattice QCD calculations indicate a linear potential and hence a constant attractive force, from which one

can understand how quarks cannot emerge as free particles.

What can be derived from QCD is that the effective coupling strength varies with the energy scale of the process in a manner that explains the results described above. That is, the effective value of $g_{\rm s}$ (or $\alpha_{\rm s}$) applicable for high-energy processes is low so that perturbation theory can be used. At low energies, the effective coupling becomes large, perturbation theory is not reliable, and quarks behave like confined particles. We will see how this comes about in greater detail in Sec. 11.4, and then look at how results can be extracted from QCD using perturbation theory.

11.4 The running of $\alpha_{\rm s}$

An important property of the Standard Model is that the coupling strengths depend on the energy scale of the reaction involved. The precise definition of the energy scale will depend on the process considered, but often it corresponds to the centre-of-mass energy and it is any case proportional to $E_{\rm cm}$. The couplings are said to 'run' with energy. This is seen most dramatically in QCD, where the strong coupling $\alpha_{\rm s}$ is found to decrease for increasing energy scale E as

$$\alpha_{\rm s}(E) = \frac{12\pi}{(33 - 2n_{\rm f})\log(E^2/\Lambda^2)} \; . \tag{11.16}$$

Here $n_{\rm f}$ is the number of quark flavours with masses less than E, and Λ is called the *QCD scale parameter*, which has a value of approximately 200 MeV. From equation (11.16) we can see that if the energy is equal to Λ, then the coupling strength becomes infinite. In fact, (11.16) is itself based on a perturbative expansion in $\alpha_{\rm s}$, which for large $\alpha_{\rm s}$ is no longer valid. The main message is, however, that for energies on the order of 1 GeV, the strong coupling becomes so large that quarks and gluons become bound into hadrons, i.e. states consisting of three quarks (baryons) or a quark and antiquark (mesons), which are colour neutral. This phenomenon of confinement is not well understood theoretically, since the coupling is too large to allow for reliable predictions using perturbation theory. For energies much larger than Λ, $\alpha_{\rm s}$ becomes small and perturbation theory can be used. This decrease in the coupling is known as *asymptotic freedom*.

The electromagnetic and weak couplings e and g also depend on the energy scale of the reaction. The weak coupling g decreases slightly and the electric charge e increases with energy. The behaviour of e can be understood qualitatively by considering an electric charge in a vacuum, as shown in Fig. 11.6. If a virtual $\mathrm{e}^-\mathrm{e}^+$ pair is created out of the vacuum, this would appear to violate conservation of energy. This is allowed by the uncertainty principle, however, as long as the virtual particles only live for a very short time before recombining. The result is that a certain amount of positive and negative charge is constantly swimming around in the vacuum, and in the presence of the negative point charge in Fig. 11.6, the vacuum becomes polarized. That is, the positrons are attracted towards the charge and electrons are repelled. This has the effect of partially screening some of the original negative charge, just as if it were in a dielectric medium.

If we consider the interaction of another charged particle with our original negative point charge, the effective coupling will be reduced because of the polarization of the vacuum. If, however, the incoming particle has a higher energy, then it will probe the target at a smaller distance scale and the screening effect will be reduced. Hence, the effective electric charge increases for increasing energies.

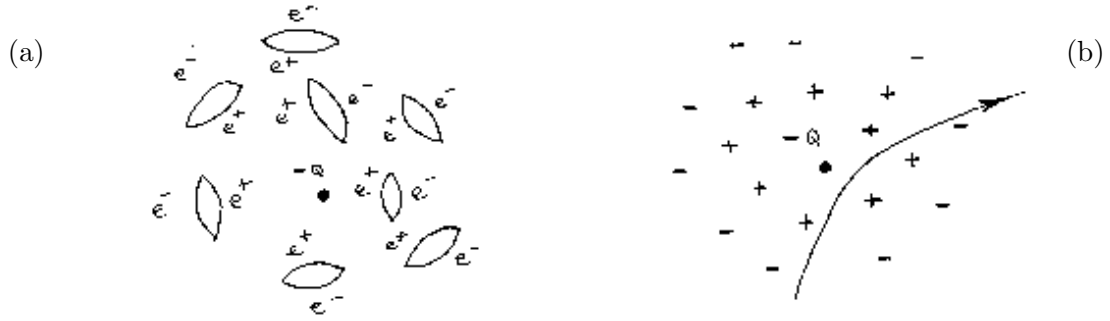

Figure 11.6: (a) A negative point charge in a vacuum surrounded by virtual e^+e^- pairs. (b) A high energy particle probes the point charge at short distances, penetrating past the screening of the e^+e^- pairs.

This type of reasoning leads to the correct qualitative picture, but it does not tell us, for example, why the QCD coupling decreases while the electromagnetic and weak couplings increase. To see this more quantitatively, one must use perturbation theory to compute interaction cross sections. As we have seen, the couplings (e, g, g_s) appear as expansion parameters in a power series. Higher order terms correspond to Feynman diagrams with more virtual particles, and hence more powers of the coupling, as shown in Fig. 11.7. An improved prediction for the total amplitude is obtained by summing the all diagrams with loops in the boson lines as shown in Fig. 11.7. One can show that the effect of summing this infinite set of loop diagrams is equivalent to replacing the usual constant coupling strengths by effective couplings that depend on the energy scale.

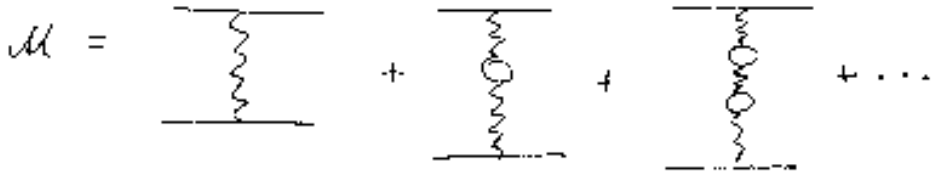

Figure 11.7: Some higher order corrections to a scattering amplitude.

Here the loops correspond to all of the different types of particles which can couple to the boson in question. If the exchanged particle in Fig. 11.7 is a photon, for example, then the loop could be any particle–antiparticle pair with electric charge, such as e^+e^-, $\mu^+\mu^-$, $q\bar{q}$, etc. The contribution of the diagram with the loop depends on the mass of the particle in the loop. To a good approximation, one can say that only particles with masses less than the energy scale of the reaction contribute. This leads to the dependence of α_s on the number of quark flavours n_f with masses less than the energy E, as seen in equation (11.16).

The decrease in the strong coupling for increasing energy is related to the fact that the gluon couples to itself (see Fig. 11.3), whereas the photon does not. That is, an exchanged gluon can have loops with quark–antiquark pairs as shown in Fig. 11.8(a), and also with a gluon pair as in Fig. 11.8(b). It turns out that the gluon loops contribute to the energy dependence with the opposite sign, i.e., they result in the decrease in the coupling for increasing energy.

Measurements of α_s from a number of different processes are shown in Fig. 11.9 [58]. Also shown on the plot is the QCD prediction, which is basically given by equation (11.16), except

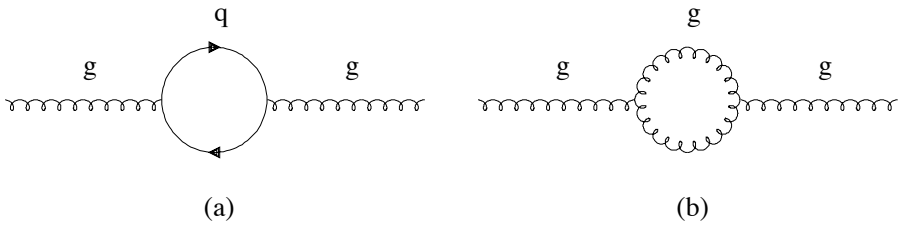

Figure 11.8: Higher order corrections to diagrams with exchanged gluons: (a) a quark–antiquark loop, (b) a gluon loop.

that higher order improvements have been included. The curve has been fitted to the data by adjusting Λ, which is equivalent to adjusting the value of α_s at a specified energy scale. Here the energy M_Z is used, since a number of important measurements of α_s are carried out using Z decays. From this analysis one finds $\alpha_s(M_Z) = 0.118 \pm 0.003$.

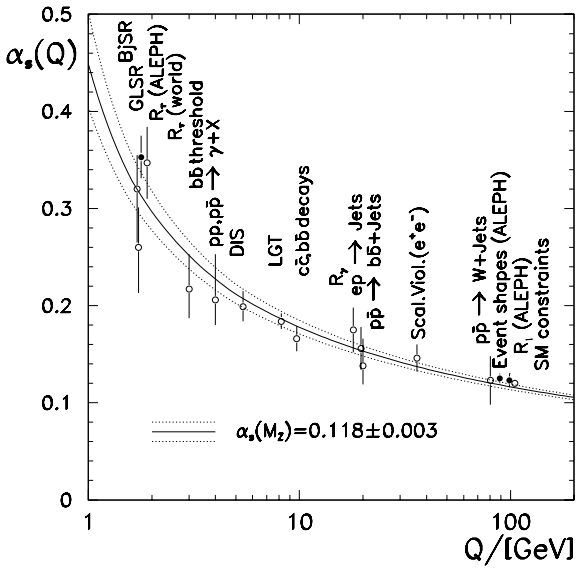

Figure 11.9: Measurements of α_s from different processes shown with the QCD prediction (from [58]).

The fact that the different measured values of α_s all lie reasonably close to the QCD curve (to within the estimated uncertainties) is one of the most encouraging confirmations of the theory. QCD is clearly not verified to the same level of precision as QED or even the electroweak part of the Standard Model, but nevertheless several of the measurements on Fig. 11.9 have accuracies at the level of several percent and these all lead to a consistent picture.

11.5 $e^+e^- \rightarrow$ hadrons

The reaction $e^+e^- \rightarrow$ hadrons provides a clean environment in which to study properties of QCD and to test its predictions. Annihilation of the e^+e^- pair into a γ/Z boson results in a $q\bar{q}$ pair. In Sec. 11.5.1 we will look the angular distribution of the $q\bar{q}$ axis as a probe of the spin of the quark. The $q\bar{q}$ pair can emit gluons, and in Sec. 11.5.2 we look at the lowest-order example

in which this occurs: $e^+e^- \to q\bar{q}g$. This provides another test of the QCD prediction and an opportunity to measure its coupling strength α_s.

11.5.1 $e^+e^- \to q\bar{q}$

One of the reactions that provides important information about QCD is $e^+e^- \to$ hadrons. To first approximation this proceeds by e^+e^- annihilation into a virtual photon or Z, which then dissociates into a quark–antiquark pair as in Fig. 11.1(a). In an e^+e^- storage ring where the electron and positron collide head-on, the total momentum of the system is zero and the quark and antiquark come off back-to-back, as shown in Fig. 11.10(a). What we see in the detector, however, are jets of hadrons, which are assumed to follow the directions of the quarks, as in Fig. 11.10(b). We have already seen two-jet events like this from the ALEPH detector at LEP in, e.g., Fig. 11.4.

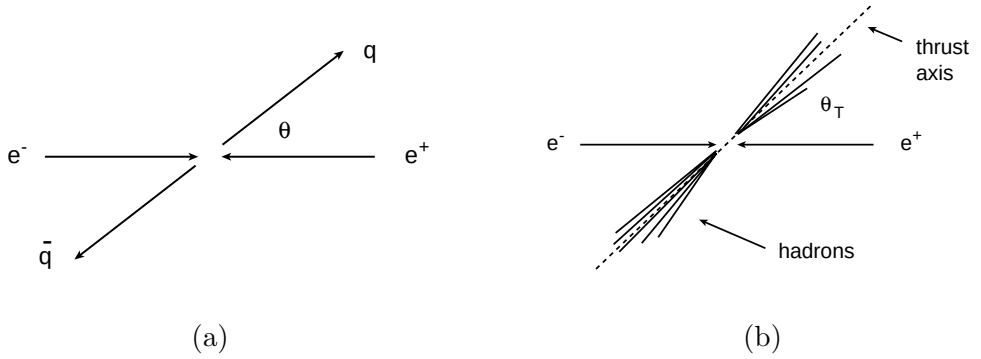

Figure 11.10: (a) Schematic illustration of the reaction $e^+e^- \to q\bar{q}$. (b) Jets of hadrons resulting from the quark and antiquark.

Any number of algorithms can be used to determine an axis that approximates the original $q\bar{q}$ direction. Often one takes the axis defined by the unit vector $\mathbf{n}_T$ such that the quantity

$$T = \frac{\sum_i |\mathbf{p}_i \cdot \mathbf{n}_T|}{\sum_i |\mathbf{p}_i|} \tag{11.17}$$

is a maximum. Here $\mathbf{p}_i$ is the momentum vector of the ith particle and the sums extend over all particles in the event. The unit vector that gives the maximum value for T defines the *thrust axis*, which will be at some angle θ_T relative to the beam line. It will point more or less along the direction of the two jets. The *thrust* is then defined as the value of T according to (11.17) using this axis. The thrust is close to 1 for an extreme two-jet like configuration, and it approaches 1/2 for an isotropically distributed set of final state particles.

The first thing we can look at with $e^+e^- \to$ hadrons is the distribution of the angle of the thrust axis relative to the beam line. This should basically follow the predicted angular distribution for the scattering angle θ of the quark relative to the direction of the e^-. In a two-jet event, however, it is difficult to know which jet came from the quark and which came from the antiquark. For a start we don't need to know this, however, and we simply look at the distribution of θ_T, which is defined such that $0 \le \theta_T \le \pi/2$. If we restrict ourselves to energies

where the forwards–backwards asymmetry $A_{\rm FB}$ is zero (this is true, e.g., at $E_{\rm cm} = M_{\rm Z}$), then the distribution of $\cos\theta_{\rm T}$ is given by

$$\frac{d\sigma}{d\cos\theta_{\rm T}} \propto 1 + \cos^2\theta_{\rm T} \; . \tag{11.18}$$

If we had modelled quarks as spin-zero rather than spin-$\frac{1}{2}$ particles, the prediction (11.18) would be proportional to $\sin^2\theta_{\rm T}$.

Figure 11.11 shows the distribution $d\sigma/d\cos\theta_{\rm T}$ from $\rm e^+e^- \to$ hadrons measured by the ALEPH detector at $E_{\rm cm} = M_{\rm Z}$ [58]. The two dotted curves show the predictions of the spin-zero and spin-$\frac{1}{2}$ hypotheses. The solid histograms are modified to include a number of additional effects, the most important of which comes from the fact that the detector does not cover the entire solid angle surrounding the interaction point. Because of this it is possible to measure the thrust axis accurately only if the jets have a certain minimum angle relative to the beam line. For the ALEPH detector this means $\cos\theta_{\rm T}$ less than around 0.8 ($\theta_{\rm T} > 36°$). Regardless of this technicality, the plot confirms clearly that jets follow the direction of spin-$\frac{1}{2}$ quarks.

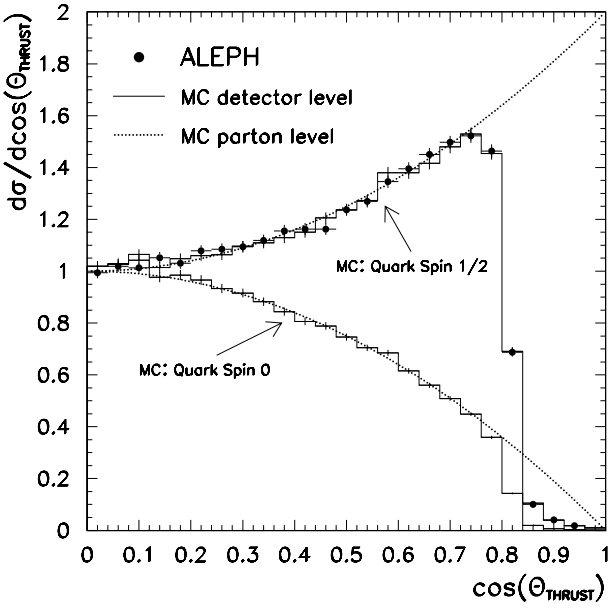

Figure 11.11: The distribution of $\cos\theta_{\rm T}$ for $\rm e^+e^- \to$ hadrons at $E_{\rm cm} = M_{\rm Z}$ measured by the ALEPH experiment [58].

11.5.2 $e^+e^- \to q\bar{q}g$

Since the reaction $\rm e^+e^- \to$ hadrons begins to first approximation by $\rm e^+e^- \to q\bar{q}$, it should be possible for the quark or antiquark to emit a gluon at a sufficiently large angle that it will produce a third jet. Such events were first observed at the PETRA $\rm e^+e^-$ ring in the late 1970s. Studies of these events provided the experimental discovery of the gluon, although of course neither free gluons nor free quarks have ever been observed. The three-jet structure becomes increasingly clear at higher energy accelerators such as LEP. An example from the ALEPH experiment at $E_{\rm cm} = 91.2$ GeV is shown in Fig. 11.12.

At the level of quarks and gluons, three-jet events are described to first approximation by the reaction $\rm e^+e^- \to q\bar{q}g$. At leading order in the strong coupling, the amplitude is given by the

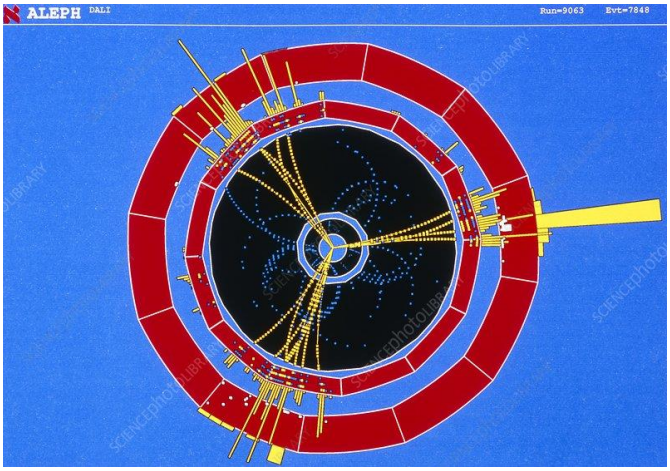

Figure 11.12: A three-jet event produced in e^+e^- collisions at $E_{cm} = 91.2$ GeV (from [65].

two Feynman diagrams shown in Fig. 11.13. The ratio of the $q\bar{q}g$ cross section to that for $q\bar{q}$ is thus proportional to α_s. We can therefore determine α_s by measuring the ratio of the number of three- to two-jet events. In practice this is done by defining *event-shape variables* such as thrust that characterize the jet structure of an event. The QCD predictions for the distributions of these variables depends on α_s, and one fits the prediction to the measurement by adjusting α_s to achieve the best level of agreement.

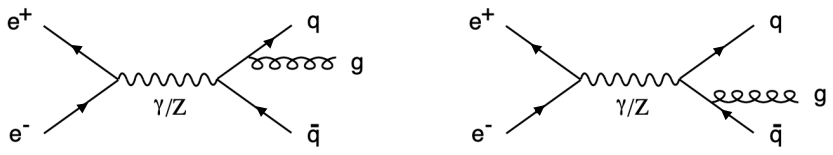

Figure 11.13: Leading-order Feynman diagrams for $e^+e^- \to q\bar{q}g$.

The predicted distribution of an event-shape variable is found by computing the amplitudes for multiparton events such as $q\bar{q}g$. The square of the amplitude gives the probability to produce this final state, which depends on the energies and angles of the quarks and gluons. This can be converted into the probability to find an event with a certain value of, say, the thrust, as defined by equation (11.17). Here it is important that the conversion of partons (quarks and gluons) into hadrons does not change the thrust of the event very much. For a number of event-shape variables like thrust one can show that this should hold, at least at sufficiently high centre-of-mass energies.

The distribution of a variable equivalent to thrust, namely, $L = -\ln(1-T)$, is shown in Fig. 11.14. The measurements from the ALEPH experiment [61] are shown as points, and the 'uncorrected' curve shows the prediction based on perturbative QCD for a final state consisting of quarks and gluons. The shaded band represents the prediction after corrections to account for hadronization. The form of the QCD prediction depends on the parameter α_s. If it were zero (or very small) then there would be no gluon emission and we would only see two-jet events near $T = 1$, i.e., at large values of $-\ln(1-T)$. A larger value of α_s increases the likelihood of gluon emission and hence the probability of low-thrust events.

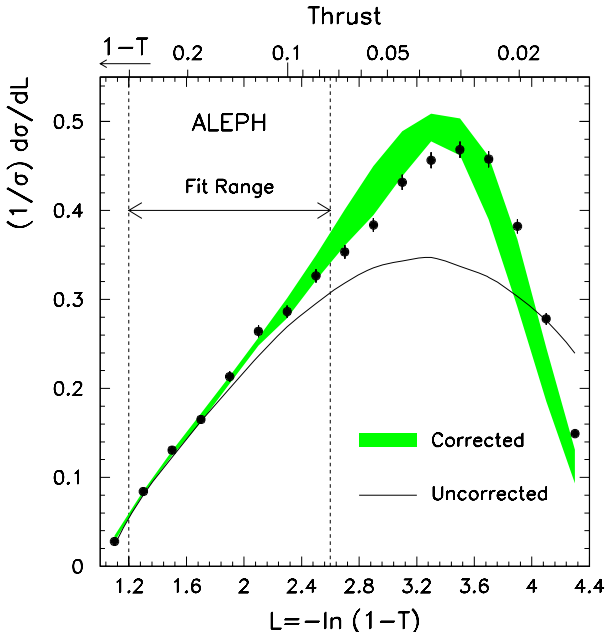

Figure 11.14: The distribution of the event-shape variable $-\ln(1-T)$, where T is the thrust. The QCD prediction (shaded band) has been fitted to the measured distribution (data points) by adjusting the value of α_s [61].

In Fig. 11.14, the value of α_s has been fitted to achieve the best agreement between the points and the curve in the indicated range. This gives $\alpha_s = 0.126 \pm 0.007$. Here the dominant uncertainty does not stem from the measurement accuracy but rather from the calculational difficulties in deriving the QCD curve. That is, the fitted thrust distribution is not the exact QCD prediction but is our best approximation based on an incomplete perturbation series and other corrections to account for hadronization. These uncertainties are reflected by the width of the band in Fig. 11.14. The thrust range for the determination of α_s has been restricted so that their impact is as small as possible.

The same procedure can be carried out using other variables sensitive to gluon emission, collectively called *event-shape variables*. One finds $\alpha_s(M_Z) \approx 0.12$ plus or minus around 3%, although the magnitude of the theoretical uncertainty is a subject of some controversy. These are represented as the data point labelled 'Event shapes (ALEPH)' in the plot of α_s versus energy shown in Fig. 11.9.

In addition to providing a measurement of α_s, distributions of event-shape variables provide an important test of QCD. This is because the QCD prediction contains in principle only a single free parameter, α_s, and we have many measured data points. In practice, however, there are additional parameters related to the modelling of the hadronization and there are uncertainties due to the incomplete perturbation series used to predict the distribution. At least for certain well-defined regions of the variables, however, these uncertainties are at the level of several percent or less, and to this degree of accuracy the QCD predictions are well confirmed.

11.5.3 Measuring α_s using $\sigma(e^+e^- \to \text{hadrons})$

An additional way to determine α_s is to measure its influence on the total cross section for the reaction $e^+e^- \to$ hadrons. In Section 11.1 we took this to be same as the sum of the cross sections $\sigma(e^+e^- \to q\bar{q})$ for all kinematically accessible quark flavours. If, however, the final state

is $q\bar{q}g$, then this will also lead to a hadronic event. The total cross section to produce hadrons is thus the sum of the cross sections for all of the possible final states consisting of quarks and gluons. (Remember that for different final states, one adds probabilities, i.e., cross sections, and not amplitudes.)

We can therefore express the total cross section as a perturbation series in α_s, for which the zeroth order term is given by the cross section for $e^+e^- \to q\bar{q}$. The correction to this at order α_s will include the cross section for $q\bar{q}g$, which we obtain by squaring the sum of the amplitudes in Fig. 11.13.

In addition, there will be corrections to amplitude for $e^+e^- \to q\bar{q}$ from the diagrams with virtual gluons as shown in Fig. 11.15. The total amplitude for $e^+e^- \to q\bar{q}$ is given by the sum of those with and without virtual gluons. The square of this amplitude will contain a term independent of α_s corresponding to the square of the diagram without virtual gluons. There will also be interference terms from the product of this diagram with those containing a virtual gluon, and these terms will be proportional to α_s.

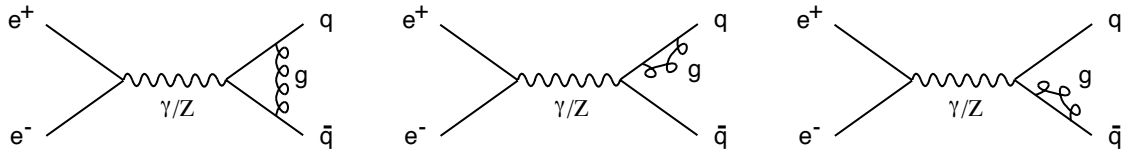

Figure 11.15: Higher order corrections to $e^+e^- \to q\bar{q}$ from virtual gluons.

The correction to the total hadronic cross section to first order in α_s thus consists of the $q\bar{q}g$ amplitude squared plus the correction to the amplitude for $q\bar{q}$ from the interference terms of order α_s. To obtain the total cross section, one must integrate over all possible momenta of the quarks and gluons involved. It turns out that in doing this, the cross section for $q\bar{q}g$ diverges; the QCD prediction to first order in perturbation theory for $q\bar{q}g$ is infinite. The infinities stem from configurations where the gluon's energy goes to zero (called an infrared divergence) and where the gluon and quark momenta are parallel (called a collinear divergence). This is not a problem with QCD; it is a deficiency of perturbation theory, which after all is only a mathematical approximation technique.

In computing the corrections to $\sigma(e^+e^- \to q\bar{q})$ also to order α_s, the Feynman rules also call for an integration over the possible momenta that can be carried by the virtual gluons. These integrals also diverge, but to negative infinity. By what seems like a minor miracle, the divergences in the cross sections for $\sigma(e^+e^- \to q\bar{q}g)$ and $\sigma(e^+e^- \to q\bar{q})$ almost cancel, leaving a small finite correction proportional to α_s. One finds

$$\sigma(e^+e^- \to q\bar{q}) + \sigma(e^+e^- \to q\bar{q}g) = \sigma_0 \left(1 + \frac{\alpha_s}{\pi}\right) , \tag{11.19}$$

where σ_0 is the cross section without QCD corrections given by equation (11.1). In fact, one can show that a similar miracle occurs at each order of perturbation theory. Negative infinities from virtual corrections cancel positive infinities from infrared and collinear gluons. What remain are finite corrections calculable at each order in perturbation theory.

Since to first approximation QCD does not affect the reaction $e^+e^- \to \mu^+\mu^-$, we can express the correction to the hadronic cross section as an equivalent modification to the quantity R, defined as the ratio of the hadronic to $\mu^+\mu^-$ cross sections. At each order in α_s the corrections become more difficult to compute. For R, the calculation has been carried out to order α_s^3,

$$R = R_0 \left[1 + \frac{\alpha_s}{\pi} + 1.411 \left(\frac{\alpha_s}{\pi}\right)^2 - 12.8 \left(\frac{\alpha_s}{\pi}\right)^3 + \ldots\right] , \tag{11.20}$$

where R_0 is the prediction without QCD corrections, i.e., to order α_s^0 [62].

This now explains why the value of R measured at $E_{cm} \approx 35$ GeV at PETRA was not 11/3 as we predicted in Section 11.1, but rather somewhat higher. Figure 11.9 shows that α_s at this energy is around 0.15. According to equation (11.20) this will increase the prediction for R from 11/3 to 3.85, which in reasonably good agreement with the measured values in Fig. 11.2. In fact, measurements of quantities closely related to R measured by the LEP experiments at E_{cm} close to M_Z allow for an accurate determination of α_s, yielding [19]

$$\alpha_s(M_Z) = 0.1200 \pm 0.0028 . \tag{11.21}$$

The fact that the total hadronic cross section, event-shape variables as well as a number of other processes all give consistent values of α_s is a convincing confirmation of QCD.

11.6 Quark-quark scattering

In this section we will look at the reaction $ud \to ud$, which is only one of a number of possible parton interactions in the collision of two protons. Assuming the strong interaction dominates over the electromagnetic and so ignoring photon exchange, it is described to lowest order by the single Feynman diagram in Fig. 11.16. (If we were to consider, e.g., $uu \to uu$ we would have the complication of an additional diagram with the momenta of the final-state quarks exchanged.) The indices i, j, k, l on the quarks refer to the colour state and take on values 1,2,3. The superscripts a and b on the generators T^a_{ji} and T^b_{lk} correspond to the colour state of the gluon that the quarks emit/absorb; they take on values from 1 to 8.

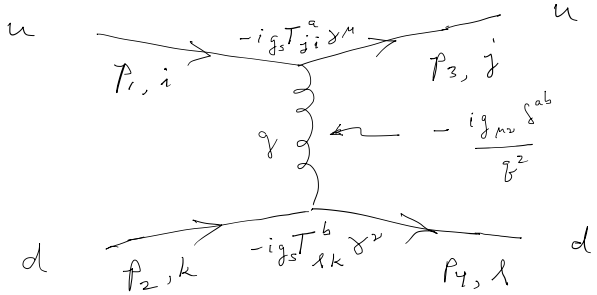

Figure 11.16: Feynman diagram for the reaction $ud \to ud$.

Using the Feynman rules from Fig. 11.3, the amplitude is found to be

$$\mathcal{M} = \left[\overline{u}_j(p_3)(-ig_s T^a_{ji}\gamma^\mu)u_i(p_1)\right] \left(\frac{-ig_{\mu\nu}\delta^{ab}}{q^2}\right) \left[\overline{u}_l(p_4)(-ig_s T^b_{lk}\gamma^\nu)u_k(p_2)\right] , \tag{11.22}$$

where the gluon's four-momentum is taken as $q = p_1 - p_3$, so in the gluon propagator $q^2 = (p_1 - p_3)^2 \equiv t$. Summing over the Lorentz index ν and the colour index b gives

$$\mathcal{M} = -\frac{g_s^2}{q^2} T^a_{ji} T^a_{lk} \left[\overline{u}_j(p_3)\gamma_\mu u_i(p_1)\right] \left[\overline{u}_l(p_4)\gamma^\mu u_k(p_2)\right] \ . \tag{11.23}$$

The part of the amplitude in the pair of square brackets is essentially the same as what is obtained from $e^-\mu^- \to e^-\mu^-$ with the exception of the replacement $e^2 \to g_s^2$ and the presence of the SU(3) generators $T^a_{ji}T^a_{lk} = \frac{1}{4}\lambda^a_{ji}\lambda^a_{lk}$.

The absolute square of the amplitude from Eq. (11.23) gives the probability for the initial-state colour indices i and j to result in the final-state indices k and l. We assume that the $N_c^2 = 9$ possible colour combinations of the incoming u and d quarks are equally probable and thus average over initial state and also sum over final state colour indices. We have already eliminated the colour index b using the δ^{ab} in the gluon propagator but still need to sum over a. The final result will therefore include a factor

$$C = \frac{1}{N_c^2} \sum_{i,j,k,l} \left| \sum_{a=1}^{8} T^a_{ji} T^a_{lk} \right|^2 \ , \tag{11.24}$$

where for clarity the sum over a is written explicitly. Using the fact that the generators are Hermitian so that e.g. $(T^b_{ji})^* = T^b_{ij}$, we can write the sum as

$$\begin{aligned}
\sum_{i,j,k,l} \left| \sum_a T^a_{ji} T^a_{lk} \right|^2 &= \sum_{i,j,k,l} \left(\sum_a T^a_{ji} T^a_{lk} \right) \left(\sum_b T^b_{ji} T^b_{lk} \right)^* \\
&= \sum_{i,j,k,l} \sum_{a,b} T^a_{ji} (T^b_{ji})^* T^a_{lk} (T^b_{lk})^* \\
&= \sum_{a,b} \left(\sum_{i,j} T^a_{ji} T^b_{ij} \right) \left(\sum_{k,l} T^a_{lk} T^b_{kl} \right) \\
&= \sum_{a,b} \Big[\mathrm{Tr}(T^a T^b) \Big]^2 \ .
\end{aligned} \tag{11.25}$$

We can then use the normalisation property of the SU(3) generators of Eq. (11.10),

$$\mathrm{Tr}(T^a T^b) = T_F \delta^{ab} \ , \tag{11.26}$$

where $T_F = 1/2$. The factor C from Eq. (11.24) thus becomes

$$C = \frac{1}{N_c^2} \sum_{a,b} \Big[\mathrm{Tr}(T^a T^b) \Big]^2 = \frac{T_F^2}{N_c^2} \sum_{a,b=1}^{8} (\delta^{ab})^2 = \frac{8 T_F^2}{N_c^2} = \frac{2}{9} \ , \tag{11.27}$$

where the numerical result holds for $N_c = 3$.

The amplitude squared summed over final-state and averaged over initial state spins for $ud \to ud$ is obtained using the usual trace techniques seen in Ch. 7. One finds

$$\langle |\mathcal{M}|^2 \rangle = 2C g_{\rm s}^4 \frac{s^2 + u^2}{t^2} \,, \tag{11.28}$$

where s, t and u are the Mandelstam variables introduced in Sec. (7.4), Eqs. (7.36)–(7.36). Finally, this can be used in Eq. (7.43) for the differential cross section with respect to t to find

$$\frac{d\sigma}{dt} = \frac{1}{16\pi s^2} \langle |\mathcal{M}|^2 \rangle = \frac{4\pi}{9} \frac{\alpha_{\rm s}^s}{s^2} \left(\frac{s^2 + u^2}{t^2} \right) \,. \tag{11.29}$$

The process $ud \to ud$ is only one of a number of parton-parton reactions that take place in proton-proton (or any hadron-hadron) collisions. The amplitudes squared for the relevant parton processes are shown in Tab. 11.1 (from Ref. [53]).

Table 11.1: The leading–order spin-averaged squared amplitudes for parton scattering processes (from [53]).

Process	$\langle \lvert\mathcal{M}\rvert^2 \rangle / g_{\rm s}^4$	$\theta^* = \pi/2$
$qq' \to qq'$	$\frac{4}{9} \frac{s^2+u^2}{t^2}$	2.22
$q\overline{q}' \to q\overline{q}'$	$\frac{4}{9} \frac{s^2+u^2}{t^2}$	2.22
$qq \to qq$	$\frac{4}{9} \left(\frac{s^2+u^2}{t^2} + \frac{s^2+t^2}{u^2} \right) - \frac{8}{27} \frac{s^2}{ut}$	3.26
$q\overline{q} \to q'\overline{q}'$	$\frac{4}{9} \frac{t^2+u^2}{s^2}$	0.22
$q\overline{q} \to q\overline{q}$	$\frac{4}{9} \left(\frac{s^2+u^2}{t^2} + \frac{t^2+u^2}{s^2} \right) - \frac{8}{27} \frac{u^2}{st}$	2.59
$q\overline{q} \to gg$	$\frac{32}{27} \frac{t^2+u^2}{tu} - \frac{8}{3} \frac{t^2+u^2}{s^2}$	1.04
$gg \to q\overline{q}$	$\frac{1}{6} \frac{t^2+u^2}{tu} - \frac{3}{8} \frac{t^2+u^2}{s^2}$	0.15
$gq \to gq$	$-\frac{4}{9} \frac{s^2+u^2}{su} + \frac{u^2+s^2}{t^2}$	6.11
$gg \to gg$	$\frac{9}{2} \left(3 - \frac{tu}{s^2} - \frac{su}{t^2} - \frac{st}{u^2} \right)$	30.4

Chapter 12

Partons and Collider Physics

Using the Standard Model as developed in the previous chapters we can calculate cross sections for processes involving quarks or gluons (collectively, *partons*) in the initial and/or final states. This is not enough, however, to give us a prediction for something that we can actually measure. Any partons in an initial state will be bound into hadrons such as protons. And high-energy partons produced in the final state will manifest themselves as groups of hadrons, mostly pions, called *jets*, with momenta in roughly the same direction. In this chapter we will quantify the parton content of hadrons with parton distribution functions (PDFs) in Sec. 12.1 and we will use these to describe Deep Inelastic Scattering (DIS), the inelastic scattering of a lepton by a nucleon, in Sec. 12.2. Section 12.3 describes the basic setup of hadron-hadron collisions; Sec. 12.4 illustrates this with production of lepton pairs (the Drell-Yan process); Sec. 12.5 gives a precise definition of a jet and finally in Sec. 12.6 we look at production of pairs of jets in proton-proton collisions.

12.1 Parton distribution functions

The basic idea of the quark model is that hadrons such as the proton are composed of quarks, and in particular the proton is the combination uud. Before the quark-model was widely accepted, Feynman proposed that at sufficiently high energy, the collision of an electron and a proton would involve scattering of the electron by point-like constituents, which he called "partons" [66]. After QCD was proposed a few years later, it became clear that the partons could be quarks, antiquarks or gluons. Let us therefore suppose that a hadron A with four-momentum p_A consists of partons of type $q, \overline{q}, g$ labeled by an index a, and we will suppose that a parton's four-momentum can be expressed as

$$p_a = x p_A \ . \tag{12.1}$$

That is, the variable x gives the fraction of the hadron's momentum carried by the parton. If we consider a reference frame where the proton is moving very fast, one might think that its three quarks should each carry fixed fractions of the total momentum, but this is not the case. A parton's value of x has a continuous probability distribution from 0 to 1 whose form depends on two important effects. First, the partons themselves are relativistic in the rest frame

of the proton, and second, we must consider QCD interactions. Because of the interactions, the effective momentum fraction of a parton that participates in an interaction depends on the distance scale probed, and thus on the four-momentum transfer.

Let us first neglect the effect of interactions and consider only the effect of relativity. In general the momentum fraction x carried by a parton of mass m inside a proton with mass M depends on the reference frame, and in a given frame, a parton could carry different fractions of the proton's momentum and energy. The value of x expressed as a four-momentum fraction as in Eq. (12.1) approaches a well-defined limit, however, if two criteria are satisfied, namely, the proton is highly relativistic, and also if the parton itself is highly relativistic in the rest frame of the proton. To see this, first consider a collection of partons in the rest frame of a proton, as shown in Fig. 12.1(a). A parton with mass m has energy E and is moving with an angle θ relative to the z axis. In this frame, the four-momentum of the proton is $p_A = (M, 0, 0, 0)$ and the parton has four momentum $p_a = (E_a, \boldsymbol{p}_a)$.

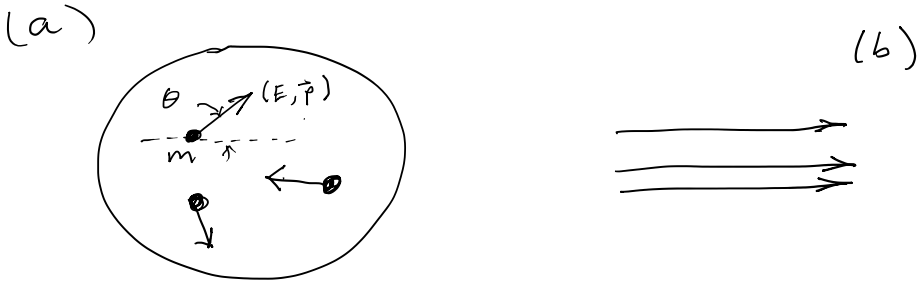

Figure 12.1: Partons in a proton (a) at rest and (b) in a reference frame in which the proton is highly relativistic.

Now consider the frame in which the proton is moving in the z direction with momentum $p'_{A,z} = \beta\gamma M$ where $\beta\gamma \gg 1$. In this frame, one has $E'_A \approx p'_{A,z}$ for the proton and $E'_a \approx p'_{a,z}$ for the parton, since the transverse components of parton's momenta $p'_{a,x}$ and $p'_{a,y}$ are small compared to $p'_{a,z}$. Since in the rest frame $E_A = M$ and $p_{A,z} = 0$, the fraction of the z-component of momentum carried by the parton in the primed frame is

$$x = \frac{p'_{a,z}}{p'_{A,z}} = \frac{\beta\gamma E_a + \gamma p_{a,z}}{\beta\gamma E_A + +\gamma p_{A,z}} = \frac{E_a + \sqrt{E_a^2 - m^2}\cos\theta/\beta}{M} \,, \tag{12.2}$$

where the numerator and denominator have been boosted to the primed frame with a Lorentz transformation. Suppose that for the boost $\gamma \gg 1$ and $\beta \approx 1$. In this approximation, the value x becomes

$$x \approx \frac{E_a + \sqrt{E_a^2 - m^2}\cos\theta}{M} \,, \tag{12.3}$$

where E_a and θ refer to rest-frame values. If the partons were nonrelativistic in the proton's rest frame then one would have $E_a \approx m$ and therefore $x \approx m/M$. So even in a highly boosted "infinite momentum" frame, the x would approach a fixed constant, independent of the random motion of the parton within the proton.

If, however, the partons are relativistic in the proton's rest frame, i.e., $E_a \gg m$, then one has

$$x \approx \frac{E_a}{M}(1 + \cos\theta) \; . \tag{12.4}$$

If $E_a \gg m$, then from momentum conservation the maximum energy of a parton in the proton's rest frame is $M/2$, and so $0 \leq x \leq 1$. The gluons are massless so of course these are relativistic. The u and d quarks also satisfy this criterion, since their rest masses are only $m_u \approx 2.2$ MeV and $m_d \approx 4.7$ MeV [19], much smaller than the proton mass of 938.3 MeV.

Thus for a given energy E_a and angle θ, the momentum fraction approaches a fixed limit when $\beta\gamma \gg 1$, and in the simple picture given here this fraction depends on the energy and direction of the parton in the proton's rest frame. Classically one would imagine that the partons in a proton are continually changing direction and exchanging energy, and so a parton's x at a random time should have some continuous distribution. For a parton of type a in a hadron this is given by the parton distribution function or PDF $f_a(x)$. More concretely, the PDF $f_a(x)\,dx$ represents the expected number of partons of type a with momentum fraction in the range $[x, x + dx]$ in the hadron.

QCD changes this picture because a parton's effective momentum fraction becomes dependent on the distance scale probed in the interaction. The relevant distance is inversely related to a four-momentum transfer (squared) Q^2, whose precise definition depends on the interaction in question. For example, for the electron-quark scattering that we will see in Sec. 12.2, $Q^2 = -q^2$, where q is the four-momentum of a photon exchanged between the electron and quark.

Roughly speaking one can see this as resulting from the virtual gluons and quark-antiquark pairs that arise from quantum fluctuations in the proton. If an exchanged photon has a very long wavelength, then the interaction has small Q^2 and the photon only senses the proton's total charge. At a smaller wavelength (higher Q^2) the photon sees individual quarks, and at even higher Q^2 the photon can resolve a quark that has emitted a virtual gluon and in doing so changes the momentum fraction that it carries.

Because the state of the particle resolved in the interaction depends on Q^2, the PDFs $f_a(x)$ are replaced by functions $f_a(x, Q^2)$. Although perturbative QCD cannot predict the PDFs themselves, it can say how the PDFs change as a function of Q^2. A careful treatment of this question is outside the scope of these notes but in the simplest approximation, the PDFs follow the Dokhshitzer-Gribov-Lipatov-Altarelli-Parisi (DGLAP) equations,

$$\frac{\partial f_a(x, Q^2)}{\partial \ln Q^2} = \sum_b \int_x^1 \frac{dz}{z} P_{ab}(z, \alpha_s(Q^2)) f_b\left(\frac{x}{z}, Q^2\right), \tag{12.5}$$

where $f_a(x, Q^2)$ is the PDF for parton type a and the functions $P_{ab}(z, \alpha_s(Q^2))$ are called the splitting kernels for splitting of parton type b into type a retaining a four-momentum fraction z, which can be derived from perturbative QCD. Further information can be found in texts such as [3]. In the following to simplify the notation we will usually write, e.g., $f_a(x)$ and it should be understood that the PDFs have been evolved to the appropriate Q^2 with the DGLAP equations.

The parton distribution functions obey a number of relations called "sum rules". For example, the proton is modeled as consisting of valence quarks *uud* plus virtual quark-antiquark pairs and gluons. Therefore one can impose the *baryon number sum rule*,

$$\int_0^1 \left[f_u(x) - f_{\overline{u}}(x)\right]\, dx \;=\; 2\,, \tag{12.6}$$

$$\int_0^1 \left[f_d(x) - f_{\overline{d}}(x)\right]\, dx \;=\; 1\,, \tag{12.7}$$

$$\int_0^1 \left[f_Q(x) - f_{\overline{Q}}(x)\right]\, dx \;=\; 0\,, \quad Q = s, c, \ldots\,. \tag{12.8}$$

Furthermore, the sum of the momentum fractions of all of the partons must equal unity, which leads to the *momentum sum rule*,

$$\int_0^1 x\left(\sum_q \left[f_q(x) + f_{\overline{q}}(x)\right] + f_g(x)\right)\, dx = 1\,. \tag{12.9}$$

The constraints implied by these and other sum rules are used in measurements of PDFs as described further in Sec. 12.2.1.

12.2 Deep inelastic scattering

Parton distribution functions are most easily measured using a scattering process of a single hadron such as a proton and a point-like fermion such as an electron. The proton is broken apart, i.e., the reaction is inelastic, and we denote the final-state system of hadrons by X. The basic kinematics of the reaction are illustrated in Fig. 12.2. It is dominated by exchange of a single photon with four-momentum $q = k - k'$, where $k = (E, \boldsymbol{k})$ and $k' = (E', \boldsymbol{k}')$ are the four-momenta of the incoming and outgoing electron, respectively. The four-momentum transfer q^2 is

$$\begin{aligned} q^2 \;&=\; (k-k')^2 = k^2 + k'^2 - 2k\cdot k' = 2m_e^2 - 2EE' + 2\boldsymbol{k}\cdot\boldsymbol{k}' \\ &\approx\; -2EE'(1-\cos\theta) = -4EE'\sin^2\frac{\theta}{2}\,, \end{aligned} \tag{12.10}$$

where the approximation of the second line holds in the high-energy limit where we can neglect the electron mass, and θ is scattering angle of the electron. Since q^2 is negative, for convenience one defines $Q^2 = -q^2$. We will be interested in large Q^2, where the scattering is said to be "deep".

From the Feynman diagram of Fig. 12.2 one finds the amplitude

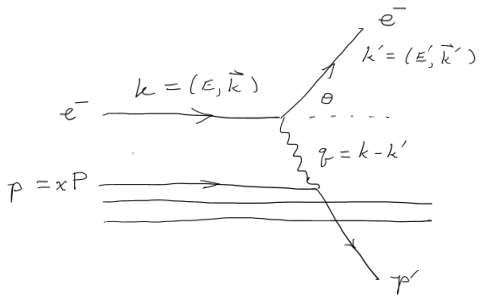

Figure 12.2: Feynman diagram for the reaction $e^- + p \to e^- + X$.

$$\begin{aligned} \mathcal{M} &= \left[\overline{u}(k')(ie\gamma_\mu)u(k)\right]\left(\frac{-ig^{\mu\nu}}{q^2}\right)\left[\overline{u}(p')(-ieQ_q\gamma_\nu)u(p)\right] \\ &= \frac{-e^2Q_q}{q^2}\left[\overline{u}(k')\gamma_\mu u(k)\right]\left[\overline{u}(p')\gamma^\mu u(p)\right] \ , \end{aligned} \tag{12.11}$$

where $Q_q = 2/3$ for up-type and $-1/3$ for down-type quarks. Using the tools of Ch. 7 to square the amplitude, average over initial spins and sum over final spins, one finds

$$\langle|\mathcal{M}|^2\rangle = 32\pi^2\alpha^2Q_q^2\frac{(2\hat{s}^2 + 2\hat{s}q^2 + q^4)}{q^4} \ , \tag{12.12}$$

where $\hat{s} = (k+p)^2$ is the invariant mass squared of the initial electron-quark system and we are supposing the energies are sufficiently high that we can neglect the electron and quark masses. Using this in Eq. 7.43 for the differential cross section with respect to the Mandelstam variable $t = (k-k')^2 = q^2$ gives

$$\frac{d\sigma}{dq^2} = \frac{2\pi\alpha^2Q_q^2}{q^4}\left[1 + \left(1 + \frac{q^2}{\hat{s}}\right)^2\right] \ . \tag{12.13}$$

Here $\hat{s} = (k+p)^2$ is the centre-of-mass energy squared of the electron-quark system,

$$\hat{s} = (k+p)^2 = (k+xP)^2 = m_e^2 + x^2M^2 + 2xk\cdot P \approx 2xk\cdot P \ . \tag{12.14}$$

Here we are using $p = xP$ where x is the four-momentum fraction of the proton carried by the struck parton and the approximation holds for energies high enough that we can neglect the electron and proton masses m_e and M. The centre-of-mass energy squared of the electron-proton system is

$$s = (k+P)^2 = m_e^2 + M^2 + 2k\cdot P \approx 2k\cdot P \ . \tag{12.15}$$

Therefore we find the relation between s, $\hat{s}$ and x valid for high energies,

$$\hat{s} = xs \ . \tag{12.16}$$

The momentum fraction x can be directly measured from the energy and scattering angle of the electron. To see how this is done, we can use conservation of the four-momenta of the struck quark plus that of the virtual photon and the outgoing quark, i.e., $xP + q = p'$ and therefore

$$(xP + q)^2 = p'^2 \,, \tag{12.17}$$

which is to say

$$(xP)^2 + 2xP \cdot q + q^2 = m_q^2 \,, \tag{12.18}$$

where m_q is the mass of the struck quark. But on the left-hand side we have $(xP)^2 = p^2 = m_q^2$, so we find $2xP \cdot q + q^2 = 0$ or

$$x = \frac{-q^2}{2P \cdot q} = \frac{Q^2}{2P \cdot q} \,. \tag{12.19}$$

Equation (12.19) defines a measurable quantity called the Bjorken x variable, which we interpret as the momentum fraction of the struck quark. In the rest frame of the proton (the lab frame), $P = (M, 0, 0, 0)$ and so

$$P \cdot q = P \cdot (k - k') = M(E - E') = M\nu \,. \tag{12.20}$$

Here $\nu \equiv P \cdot q/M$ is a Lorentz invariant quantity, which in the lab frame is the energy lost by the electron: $\nu = E - E'$. So we can measure both Q^2 and x as

$$Q^2 = 4EE' \sin^2 \frac{\theta}{2} \,, \tag{12.21}$$

$$x = \frac{Q^2}{2M\nu} \,. \tag{12.22}$$

Using $Q^2 = -q^2$ and $\hat{s} = xs$, We can rewrite the differential cross section from Eq. (12.13) as

$$\frac{d\sigma}{dQ^2} = \frac{2\pi\alpha^2 Q_q^2}{Q^4} \left[1 + \left(1 - \frac{Q^2}{xs} \right)^2 \right] \,. \tag{12.23}$$

This is the differential cross section for a single target quark with four-momentum $p = xP$. We cannot, however, fix the momentum fraction x in advance, rather it will vary randomly from collision to collision. The number of targets of quark type q with x in the range $[x, x + dx]$ is given by the parton distribution function as $f_q(x)\, dx$. Furthermore, if the proton contains antiquarks with PDF $f_{\bar{q}}(x)$, then these contribute to the scattering with the same cross section formula. We can therefore write the double differential cross section with respect to Q^2 and x as

$$\frac{d^2\sigma}{dx\,dQ^2} = \sum_q \frac{2\pi\alpha^2 Q_q^2}{Q^4}\left[1+\left(1-\frac{Q^2}{xs}\right)^2\right]\left[f_q(x)+f_{\overline{q}}(x)\right]\ , \tag{12.24}$$

where the sum is over all quark types.

A very high-Q^2 event from the H1 detector at the HERA collider at DESY (Hamburg) is shown in Fig. 12.3(a) [67]. The event is actually a positron–proton collision, where the incident positron with an energy of 27.5 GeV enters from the left and scatters off an 820 GeV proton entering from the right. (From a standpoint of investigating the proton's structure, e^-p and e^+p collisions provide essentially the same information.) The positron is scattered back to the lower left, and a large number of hadrons from the collision can be seen to the upper left. Figure 12.3(b) shows a scatter plot of x and Q^2 from the Zeus experiment, also at the HERA collider [68]. The density of points in this plane translates directly into a measurement of the cross section $\frac{d^2\sigma}{dx\,dQ^2}$.

(a)

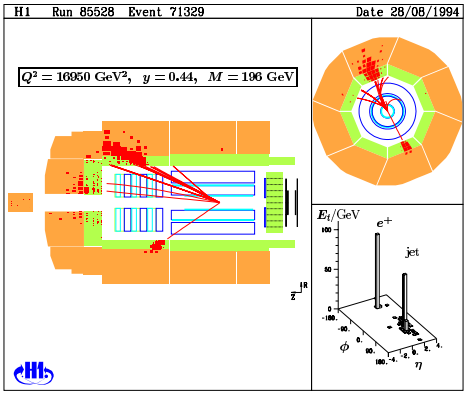

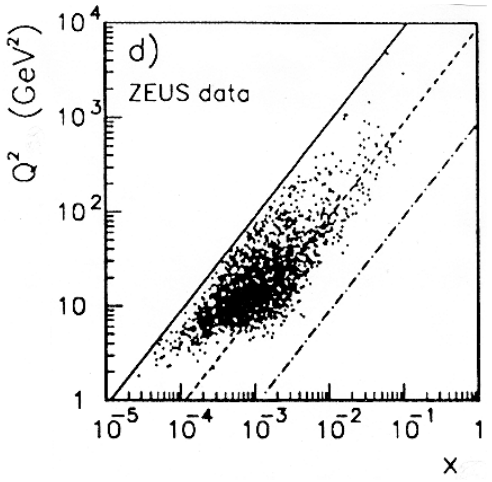

(b)

Figure 12.3: (a) A very high-Q^2 positron–proton collision from the H1 detector at the HERA collider (from [67]). (b) A scatter plot of Q^2 vs. x measured by the Zeus detector (from [68]).

12.2.1 Measuring PDFs

As can be seen from Eq. (12.24), a measurement of $\frac{d^2\sigma}{dx\,dQ^2}$ provides information on the sum of the PDFs for quarks and antiquarks. To disentangle quarks, antiquarks and the relative contributions of different flavours, one can make use of other processes such as neutrino deep inelastic scattering, which we saw in Sec. 8.7. Recall we found the total cross sections

$$\sigma(\nu_\mu d \to \mu^- u) \;=\; \sigma(\nu_\mu \overline{u} \to \mu^- \overline{d}) = \frac{G_{\rm F}^2 \cos^2\theta_{\rm C}\hat{s}}{\pi}\ , \tag{12.25}$$

$$\sigma(\overline{\nu}_\mu u \to \mu^+ d) \;=\; \sigma(\overline{\nu}_\mu \overline{d} \to \mu^+ \overline{u}) = \frac{G_{\rm F}^2 \cos^2\theta_{\rm C}\hat{s}}{3\pi}\ . \tag{12.26}$$

The kinematics of these processes is essentially the same as for electron-proton scattering, namely, $\hat{s} = sx$ gives the centre-of-mass energy where x is the momentum fraction carried

by the struck quark. To determine x from Eqs. (12.21) and (12.22) we need the outgoing muon energy E' and scattering angle θ, which are relatively easy to measure. But a neutrino beam has significant spread in the energies of the incident neutrinos, so to better estimate E on an event-by-event basis one can measure the energy of the hadrons produced and use $E = E_\mu + E_{\rm had}$. Thus for every event one can measure x and their distribution gives the differential cross section $d\sigma/dx$. From the cross sections (12.25) and (12.26) one can relate these to the u and d quark and antiquark PDFs as

$$\frac{d\sigma}{dx}(\nu_\mu p \to \mu^- + X) = \frac{G_{\rm F}^2 \cos^2\theta_{\rm C} sx}{\pi}\left[f_d(x) + f_{\overline{u}}(x)\right] , \tag{12.27}$$

$$\frac{d\sigma}{dx}(\overline{\nu}_\mu p \to \mu^+ + X) = \frac{G_{\rm F}^2 \cos^2\theta_{\rm C} sx}{3\pi}\left[f_u(x) + f_{\overline{d}}(x)\right] . \tag{12.28}$$

A complete determination of parton densities combines many different measured cross sections including the electron and neutrino deep inelastic scattering, $pp \to \mu^+\mu^- + X$ (the Drell-Yan process), $pp \to Z/W + X$ and others. These are used together with the DGLAP equations to relate processes at different Q^2 scales and the sum rules mentioned in Sec. 12.1. The PDFs can be parametrized in a manner that yields the PDFs for different parton types for collisions at different Q^2 scales. Examples from the CTEQ Collaboration are shown in Fig. 12.4. The PDFs are then assumed to be universal in the sense that they describe the parton content of a hadron regardless of the type of collision process. We can therefore use the PDFs measured in deep inelastic scattering to make predictions for cross sections for proton-proton scattering, which we will see below in Sec. 12.3.

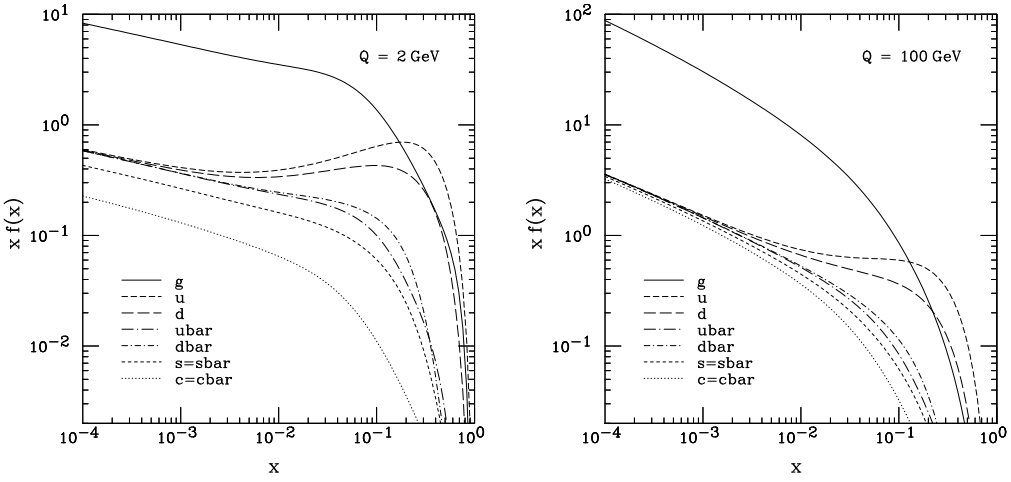

Figure 12.4: Measurements of parton distribution functions at $Q = 2$ and $Q = 100\,\text{GeV}$ (CTEQ6M, Ref. [69]).

12.3 Hadron-collider physics

The differential cross section for the collision of hadrons A and B resulting in a final state X can be written

$$\frac{d^2\sigma}{dx_1\,dx_2}(AB \to X) = \sum_{a,b} \sigma(ab \to X|\hat{s} = x_1x_2s) f_{A,a}(x_1, Q^2) f_{B,b}(x_2, Q^2) \;, \tag{12.29}$$

where x_1 and x_2 are the four-momentum fractions of the colliding partons, s is the centre-of-mass energy squared of the two hadrons, and $\sigma(a, b \to X|\hat{s} = x_1x_2s)$ is the parton-level cross section at a centre-of-mass energy of the parton-parton system $\hat{s}$. The PDFs $f_{A,a}(x_1, Q^2)$ and $f_{B,b}(x_2, Q^2)$ give the number of partons with four-momentum fractions x_1 and x_2 at Q^2 characteristic of the parton-level collision (the "hard scale"), usually taken equal to $\hat{s}$. The product of these terms is summed over all possible parton combinations that could result in the final state X. Here we will focus on proton-proton collisions and since the colliding hadrons are both protons we can write the PDFs without the subscripts A or B. Note, however, that the indices of the PDFs have been written a and b, and these are summed over all of the relevant parton types. The momentum fractions have been written x_1 and x_2, since these will be quantities that we can measure for each event regardless of the parton types that collide.

To predict the total cross section for the hadron-level process, we integrate Eq. (12.29) over x_1 and x_2 from 0 to 1. Often instead we will want to find a differential cross section with respect to one or two other variables, generically, u and v. Then the differential cross section for with respect to the new variables can be found in the usual manner using

$$\frac{d^2\sigma}{du\,dv} = |J| \frac{d^2\sigma}{dx_1\,dx_2} \tag{12.30}$$

where $|J|$ is the absolute value of the Jacobian determinant for the transformation. Alternatively, the transformed cross section can be found from

$$\frac{d^2\sigma}{du\,dv} = \int\int \frac{d^2\sigma}{dx_1\,dx_2} \delta(u - u(x_1, x_2)) \delta(v - v(x_1, x_2))\, dx_1\, dx_2 \;. \tag{12.31}$$

These methods will be used in Sections 12.4 and 12.6 below.

Before we confront theoretical predictions with experiment we need to introduce several concepts and variables that are used to characterise events in a hadron collider like the LHC. A coordinate system is established with the origin at the collision point and the z axis along one of the two beam directions (for the ATLAS detector, this is towards Geneva), the y axis points up and the x axis towards the centre of the LHC. The LHC has been run with a centre-of-mass energy $E_{\rm cm}$ up to 13.6 TeV, i.e., much greater than the proton's mass, so we can approximate the four-momenta of the two incoming particles as

$$p_A = (E_p, 0, 0, E_p) \;, \tag{12.32}$$

$$p_B = (E_p, 0, 0, -E_p) \;, \tag{12.33}$$

where $E_p = E_{\rm cm}/2$ is the energy of each proton.

The parton-level cross section in Eq. (12.29) depends on the centre-of-mass energy squared of the parton-parton system, which depends on that of the proton-proton system and on the

momentum fractions carried by the partons. Comparing the proton-proton centre-of-mass energy squared $s = (p_A + p_B)^2$ to that of the partons, $\hat{s} = (x_1 p_A + x_2 p_B)^2$, and neglecting rest-mass terms, one finds

$$\hat{s} = x_1 x_2 s \; . \tag{12.34}$$

In the lab frame, the total z component of momentum and energy of the colliding partons are

$$p_z = x_1 p_{A,z} + x_2 p_{B,z} = E_p(x_1 - x_2) \; , \tag{12.35}$$

$$E = E_p(x_1 + x_2) \; . \tag{12.36}$$

The rapidity y of the two-parton system is therefore

$$y = \frac{1}{2} \ln \left(\frac{E + p_z}{E - p_z} \right) = \frac{1}{2} \ln \left(\frac{x_1}{x_2} \right) \; . \tag{12.37}$$

Using $\tau = \hat{s}/s = x_1 x_2$, it is often convenient to express x_1 and x_2 as

$$x_1 = \sqrt{\tau} e^{y} \; , \tag{12.38}$$

$$x_2 = \sqrt{\tau} e^{-y} \; . \tag{12.39}$$

An individual particle emerging from the collision point has a direction characterised by the usual angles θ and ϕ, and energy E and momentum vector $\boldsymbol{p}$. From these quantities one defines the rapidity y in the same way as given by the first equality of Eq. (12.37). For ultra-relativistic particles this becomes

$$\eta = - \ln \tan \frac{\theta}{2} \; , \tag{12.40}$$

called the *pseudorapidity*, which is usually used in place of the polar angle θ. A useful equivalent relation is $\cos\theta = \tanh\eta$. One can easily show that differences in rapidity are invariant under boosts along the z axis. The transverse momentum p_T of a particle is the component transverse to the z axis, i.e.,

$$p_T = \sqrt{p_x^2 + p_y^2} \; , \tag{12.41}$$

which is invariant under boosts along the z axis. The three components of momentum $\boldsymbol{p}$ of a particle can be equivalently given by reporting p_T, η and ϕ. Usually individual particles are highly relativistic so that their rest mass can be neglected.

When two protons collide, the "hard scattering" process involves only one parton in each of the protons. The partons that do not participate in the hard scattering are called the proton remnant. They continue along the beam direction, but as they are no longer in a colour-neutral state they cannot directly appear as final-state particles. Rather, they form two jets of

hadrons that continue in the direction of the beams. These particles constitute what is called the *underlying event*, as illustrated in Fig. 12.5. These particles are emitted at low angles relative to the z axis and most do not enter the sensitive volume of the detector. When we talk about the final state particles of a proton-proton collision, unless otherwise stated we are referring to the particles emitted from the hard scattering of two partons, excluding the underlying event.

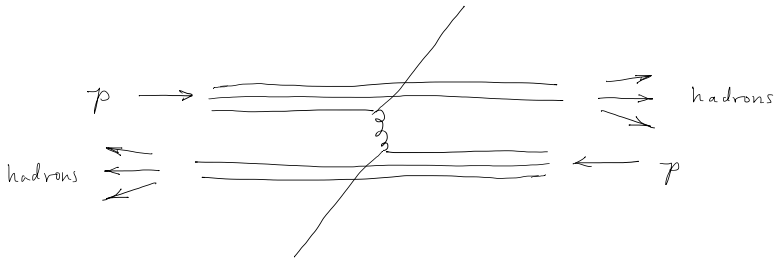

Figure 12.5: Illustration of the underlying event in a pp collision created from the two proton remnants.

Suppose two partons with momentum fractions x_1 and x_2 collide, giving two outgoing particles. From Eqs. (12.34) and (12.37), the final-state system has invariant mass squared $\hat{s} = x_1 x_2 s$ and rapidity $y = \frac{1}{2}\ln(x_1/x_2)$. In the partons' c.m. frame the particles emerge back-to-back, with angles θ_1^* and $\theta_2^* = \pi - \theta_1^*$, corresponding to pseudorapidities $\eta_1^* = -\ln\tan(\theta_1^*/2)$ and $\eta_2^* = -\eta_1^*$, as shown in Fig. 12.6(a). The rapidities of the outgoing particles in the lab frame are found from

$$\eta_1 = \eta_1^* + y \,, \tag{12.42}$$

$$\eta_2 = \eta_2^* + y \,. \tag{12.43}$$

Thus one sees that the difference of two rapidity values is invariant under a boost along the z axis. The transverse momenta of the outgoing particles are invariant under a boost along the z axis and so are the same in the parton's c.m. frame and in the lab frame. The configuration of particles shown in Fig. 12.6 is found for any scattering event that results in two particles in the final state in addition to the underlying event.

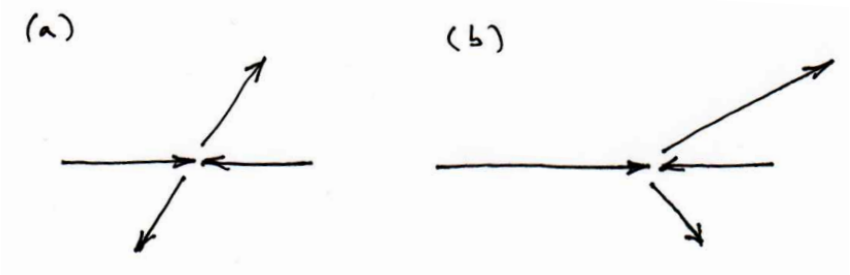

Figure 12.6: Configuration of a two-to-two scattering event (a) in the parton c.m. frame and (b) in the lab frame.

12.4 The Drell-Yan process

An important reaction at hadron colliders is the production of an oppositely-signed lepton pair such as $\mu^+\mu^-$, called the Drell-Yan process. At lowest order this proceeds through $q\bar{q}$ annihilation

into a virtual photon or Z, which then decays to $\mu^+\mu^-$ and so is similar to $e^+e^- \to \mu^+\mu^-$. If the c.m. energy of the colliding quarks is much less than the mass of the Z, then by comparing with Eq. (7.81) we find the cross section

$$\sigma(q\overline{q} \to \mu^+\mu^-) = \frac{4\pi\alpha^2 Q_q^2}{3N_c\hat{s}} \ . \tag{12.44}$$

Here Q_q is the charge of the quark in units of e and the factor of N_c reflects the fraction of colour-anticolour combinations that can annihilate into the colour-neutral photon. As usual, $\hat{s} = x_1x_2s$ where x_1 and x_2 are the momentum fractions of the colliding partons.

Collisions of a quark and antiquark of course take place in a proton-antiproton collider such as the Tevatron at Fermilab (Chicago), but it is also found in a proton-proton collider like the LHC because of virtual antiquarks in the proton. For the case of pp collisions, the differential cross section with respect to x_1 and x_2 is

$$\frac{d^2\sigma}{dx_1dx_2}(pp \to \mu^+\mu^-X) = \frac{4\pi\alpha^2}{9sx_1x_2}\sum_q Q_q^2\left[f_q(x_1)f_{\overline{q}}(x_2) + f_{\overline{q}}(x_1)f_q(x_2)\right] \ , \tag{12.45}$$

where f_q and $f_{\overline{q}}$ are the PDFs of q and $\overline{q}$ in the proton and we have substituted $N_c = 3$. The sum is in principle over all quark flavours, but u and d dominate first because they are present as valence quarks and also because of their lower mass. To describe proton-antiproton collisions, we can exploit the symmetry between quarks in a proton and antiquarks in an antiproton, namely, $f_{p,q}(x) = f_{\overline{p},\overline{q}}(x)$ and $f_{p,\overline{q}}(x) = f_{\overline{p},q}(x)$, so that

$$\frac{d^2\sigma}{dx_1dx_2}(p\overline{p} \to \mu^+\mu^-X) = \frac{4\pi\alpha^2}{9sx_1x_2}\sum_q Q_q^2\left[f_q(x_1)f_q(x_2) + f_{\overline{q}}(x_1)f_{\overline{q}}(x_2)\right] \ , \tag{12.46}$$

where the PDFs here all refer to the proton. This can be converted into a differential cross section with respect to invariant mass $m_{\mu\mu} = \sqrt{x_1x_2s}$ and rapidity $y = \frac{1}{2}\ln(x_1/x_2)$ of the $\mu^+\mu^-$ system using the Jacobian,

$$J = \begin{vmatrix} \frac{\partial x_1}{\partial m_{\mu\mu}} & \frac{\partial x_1}{\partial y} \\ \frac{\partial x_2}{\partial m_{\mu\mu}} & \frac{\partial x_2}{\partial y} \end{vmatrix} = -\frac{2m_{\mu\mu}}{s} \ . \tag{12.47}$$

which gives for the pp case,

$$\begin{aligned} \frac{d^2\sigma}{dm_{\mu\mu}dy}(pp \to \mu^+\mu^-X) &= \frac{8\pi\alpha^2}{9sm_{\mu\mu}}\sum_q Q_q^2\left[f_q\left(\frac{m_{\mu\mu}}{\sqrt{s}}e^y\right)f_{\overline{q}}\left(\frac{m_{\mu\mu}}{\sqrt{s}}e^{-y}\right)\right. \\ &+ \left. f_{\overline{q}}\left(\frac{m_{\mu\mu}}{\sqrt{s}}e^y\right)f_q\left(\frac{m_{\mu\mu}}{\sqrt{s}}e^{-y}\right)\right] \ . \end{aligned} \tag{12.48}$$

To find the differential distribution with respect to $m_{\mu\mu}$ alone, Eq. (12.48) can be integrated over y between limits $y_{\min}$ and $y_{\max}$, which are set by the requirement that the momentum fractions

satisfy $x_1 \leq 1$, $x_2 \leq 1$ and also $x_1 x_2 = m_{\mu\mu}^2/s$. Therefore the maximum rapidity of the $\mu^+\mu^-$ system is found when

$$y_{\max} = \frac{1}{2} \ln \frac{x_{1,\max}}{x_2} = \frac{1}{2} \ln \frac{1}{(m_{\mu\mu}^2/s)} = -\ln(m_{\mu\mu}/\sqrt{s}) \,, \tag{12.49}$$

and by symmetry $y_{\min} = -y_{\max}$.

A measurement of the Drell-Yan cross section $\sigma(pp \to \mu^+\mu^- X)$ by the ATLAS Experiment is shown in Fig. 12.7. As the mass of the muon pair can easily equal and exceed the mass of the Z, one must include in the prediction annihilation of the $q\overline{q}$ pair both into a photon and a Z. This leads to the resonance peak seen at $m_{\mu\mu} = M_Z$. If Nature were to include another Z-like particle (a Z') at a higher mass, then one should see an additional peak in the Drell-Yan mass distribution. The absence of such a peak allows one to exclude the existence of a Z' for masses up to 4.1 TeV [76].

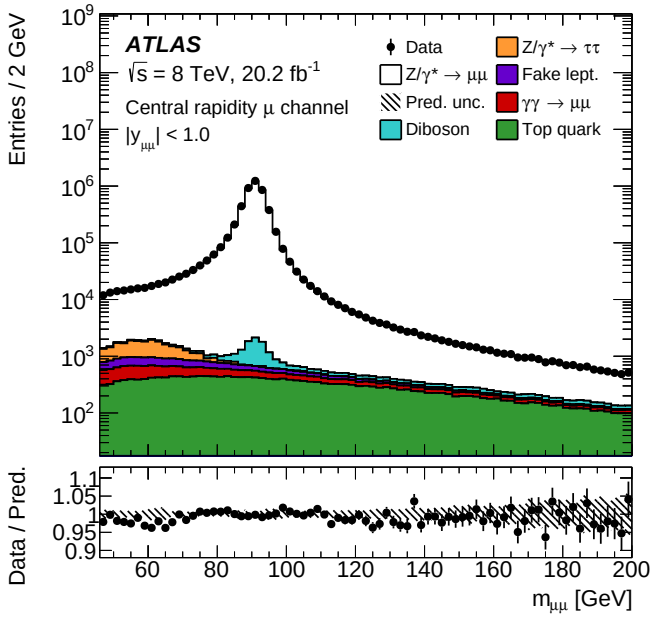

Figure 12.7: The differential cross section $d\sigma/dm_{\mu\mu}$ for the of the Drell-Yan process $pp \to \mu^+\mu^- X$ [75].

12.5 Jets

Using the parton distribution functions can calculate how often a collision of hadrons should result in collisions of their constituent partons to produce two outgoing partons, e.g., $ud \to ud$. But this does not quite give a prediction for something we can measure, since we do not see the outgoing quarks. Rather, we see events with jets of particles as shown in Fig. 12.8.

The two "jets" of particles seen in the event contain tens or hundreds of particles, mainly pions and photons from the decays $\pi^0 \to \gamma\gamma$ as well as kaons and other particles. As seen earlier in e^+e^- collisions, we assume that these jets are initiated by a high-energy parton such as a quark or a gluon. It is difficult to distinguish quark- from gluon-produced jets and so what is usually measured is the cross section for jets produced by either of the two. Thus all of the subprocesses shown in Tab. 11.1 contribute to the production of events with two jets.

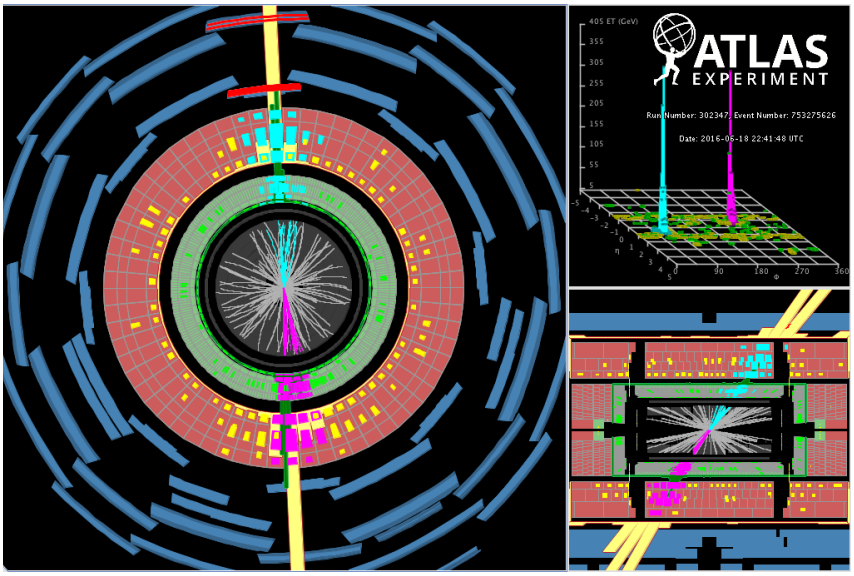

Figure 12.8: A dijet event recorded by the ATLAS Detector at the LHC [70].

Before we can make a prediction for the cross section of events contain jets we must define a jet more precisely. Here we will give the definition usually used for jets produced in proton-proton collisions like at the LHC. Suppose we start with an event containing N particles with momenta $\boldsymbol{p}_1, \ldots, \boldsymbol{p}_N$, where a particle could be a measured hadron or a theoretically predicted parton. For any pair of particles i and j we define a measure of their angular separation as

$$\Delta R_{ij} = \sqrt{(\eta_i - \eta_j)^2 + (\phi_i - \phi_j)^2} \,, \tag{12.50}$$

where η is the pseudorapidity and ϕ is the azimuthal angle.

A "clustering" jet-finding algorithm begins by calculating for each pair of particles i and j a measure of their distance from each other, usually taken as

$$d_{ij} = \min\left(p_{T,i}^{2p}, p_{T,j}^{2p}\right) \frac{(\Delta R_{ij})^2}{R^2} \,, \tag{12.51}$$

where p and R are numbers that we will set below. We also find the "distance" of each particle relative to the beam direction through its transverse momentum squared:

$$d_{iB} = p_{T,i}^{2p} \,. \tag{12.52}$$

Starting from all N particles, one calculates the set of all distances d_{ij} and d_{iB} and finds the smallest one. If it is for a pair of particles i and j, then these two particles are merged by adding their four-momenta, and the new "pseudo-particle" replaces them in the list. If the minimum distance is for a particle and the beam direction, then the particle is labeled as a "jet" and it is removed from the list. This is then iterated until all (pseudo-)particles are labeled as jets.

Different values of the parameter p give different algorithms. Taking $p = 1$ gives what is called the k_T algorithm [71]. The minimum distance values are found for the lowest p_T particles,

and so these get clustered together first. Taking $p = 0$ (the Cambridge/Aachen algorithm [72]) clusters the particles based solely on their direction without consideration of their energies, and taking $p = -1$ gives what is called the "anti-k_T" algorithm [73]. It tends to cluster the most energetic particles first, and results in jets that are roughly circular in the (η, ϕ) plane. It is the default algorithm used by most analyses at the LHC.

The parameter R is called the cone size, with typical values in the range $R \sim 0.4$ to 1.0. The larger values allow "fatter" jets, since more particles will be clustered together before they are labeled as jets. In the limit where $R \to 0$, all of the initial particles would be called jets. Thus a given event could be classified has having a different number of events depending on the value chosen for R.

12.6 Dijet production in pp collisions

Using the ingredients from above we are finally in a position to confront QCD predictions with measurements at the LHC. In Sec. 11.6 we derived the differential cross section $d\sigma/dt$ for quark-quark scattering. The quark pair in the final state will produce two jets whose energy and momentum closely follow those of the quarks. First, we can write the cross section from Eq. (11.29) as $d\sigma/dQ^2$ where $Q^2 = -q^2 = -t$,

$$\frac{d\hat{\sigma}}{dQ^2} = \frac{4\pi}{9}\frac{\alpha_s^2}{Q^4}\left[1 + \left(1 - \frac{Q^2}{\hat{s}}\right)^2\right] , \tag{12.53}$$

where we made us of the relation $\hat{s} + \hat{t} + \hat{u} = 0$ in the high-energy limit to eliminate $\hat{u}$, and variables that refer to the parton system have now been written with hats. Using $\hat{s} = x_1 x_2 s$, the triple-differential cross section with respect to Q^2, x_1 and x_2 for $pp \to ud$ becomes

$$\frac{d^3\sigma}{dQ^2 dx_1 dx_2} = \left.\frac{d\hat{\sigma}}{dQ^2}\right|_{\hat{s}=x_1 x_2 s} 2 f_u(x_1) f_d(x_2) , \tag{12.54}$$

where the factor of 2 enters because the u quark could be in either proton with the d quark in the other. We can first transform from the variables x_1, x_2 and Q^2 to the dijet invariant mass m_{jj}, the rapidity y of the parton system in the lab frame and the scattering angle θ^* or equivalently the pseudorapidity η^* of the back-to-back outgoing partons in their c.m.. The momentum fractions are related to the mass and rapidity by

$$x_{1,2} = \frac{m_{jj}}{\sqrt{s}} e^{\pm y} . \tag{12.55}$$

Further, $Q^2 = -(p_1 - p_3)^2 \approx 2p_1 \cdot p_3 = \hat{s}(1 - \cos\theta^*)/2$, and one from the definition of pseudorapidity (12.40) one finds $\cos\theta^* = \tanh\eta^*$. The Jacobian for the transformation is therefore

$$J = \begin{vmatrix} \frac{\partial x_1}{\partial m_{jj}} & \frac{\partial x_1}{\partial y} & \frac{\partial x_1}{\partial \eta^*} \\ \frac{\partial x_2}{\partial m_{jj}} & \frac{\partial x_2}{\partial y} & \frac{\partial x_2}{\partial \eta^*} \\ \frac{\partial Q^2}{\partial m_{jj}} & \frac{\partial Q^2}{\partial y} & \frac{\partial Q^2}{\partial \eta^*} \end{vmatrix} = \frac{m_{jj}^3}{s}(1 - \tanh^2\eta^*) . \tag{12.56}$$

Using x_1 and x_2 from Eq. (12.55) we therefore have

$$\frac{d^3\sigma}{dm_{jj}d\eta^* dy} = \frac{4\pi}{9}\frac{\alpha_s^2}{Q^4}\left[1+\left(1-\frac{Q^2}{m_{jj}^2}\right)^2\right]\frac{m_{jj}^3}{s}(1-\tanh^2\eta^*)f_u\left(\frac{m_{jj}}{\sqrt{s}}e^{y}\right)f_d\left(\frac{m_{jj}}{\sqrt{s}}e^{-y}\right)\ , \tag{12.57}$$

where $Q^2 = \frac{m_{jj}^2}{2}(1-\tanh\eta^*)$. To find the differential distribution with respect to only m_{jj} and η^*, Eq. (12.57) can be integrated over y between the same limits $y_{\min}$ and $y_{\max}$ as found from Eq. (12.49) with $m_{\mu\mu} \to m_{jj}$.

The process $ud \to ud$ is only one of a number of parton-parton scattering processes that leads to two jets in the final state. Using Table 11.1 we can find all of the relevant cross sections and transform them into the desired form in the same way as done above for $ud \to ud$. The final assembly of ingredients and any integration over variables is thus a nontrivial calculation done in practice on a computer.

Figure 12.9 shows the measurement by the ATLAS Experiment of the differential cross section for events with two jets ("dijet events") as a function of the invariant mass of the dijet pair, for different regions of (positive) rapidity y^*, here equivalent to $|\eta^*|$, which corresponds to the scattering angle of the back-to-back jets in the partonic c.m. frame [74]. The agreement between data and prediction is all the more impressive considering that the cross sections span many orders of magnitude.

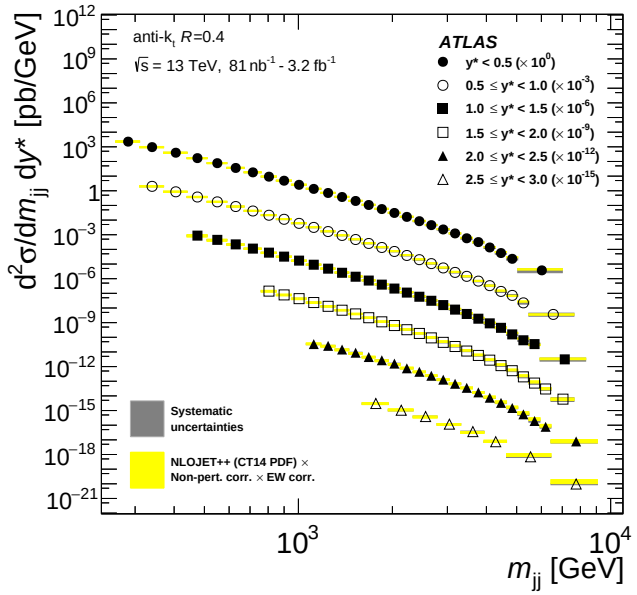

Figure 12.9: Dijet differential cross sections measured by the ATLAS Collaboration with the QCD predictions [74].

Appendix A

Introduction to Group Theory

In this section we review some basic concepts of group theory. This will prove useful in describing the symmetries of particle physics, most importantly Lorentz (and Poincaré) symmetry and gauge symmetry.

A.1 Definition of a group

A group G is defined by a set of elements $a, b, c, \ldots$ together with a composition rule (often called multiplication) which can be written, e.g., ab (or sometimes $a \circ b$). The set is said to be a group if the following properties hold:

1. For all elements a, b in G, the combination (product) ab is also an element of G.
2. Group multiplication is associative, i.e, $(ab)c = a(bc)$.
3. The group contains an identity element we can call I such that $Ia = aI = a$ for all a in G.
4. For every element a in G there exists an inverse element we can call a^{-1} such that $aa^{-1} = a^{-1}a = I$.

If the product of any two elements of the group is the same independent of the order, i.e., $ab = ba$ for all $a, b \in G$, then the group is said to be Abelian, otherwise it is non-Abelian.

A simple example of a group is the set of all integers with the composition rule given by addition. The set is closed under addition, addition is associative, the identity element is 0 and the inverse of any integer n is $-n$. The same set is not a group if the combination rule is multiplication, since the inverses are not members of the set.

A subgroup H of a group G is a subset of G for which the elements also satisfy the defining properties of a group. For example, the set of integers is a subgroup of the set of real numbers with the composition rule given by addition.

The group itself is an abstract entity defined by the multiplication table of its elements. In physics we are most often interested in sets of $n \times n$ matrices with matrix multiplication used as the composition rule. These are used to define a transformation on an n-dimensional vector

space. If their multiplication table is the same as that of a group G, they are said to form an n-dimensional matrix representation of G. That is, all elements $g_1, g_2, \ldots$ in G, correspond to a matrix M such that

$$M(g_i)M(g_j) = M(g_i g_j) \tag{A.1}$$

for all $g_i \in G$.

As an example, consider the set of 2×2 matrices that rotate a two-dimensional vector $\begin{pmatrix} x_1 \\ x_2 \end{pmatrix}$. The elements of this group can be parametrised by an angle θ as

$$R(\theta) = \begin{pmatrix} \cos\theta & -\sin\theta \\ \sin\theta & \cos\theta \end{pmatrix} . \tag{A.2}$$

As can be readily verified, the matrices R are orthogonal ($RR^T = R^T R = I$) and they have a determinant $\det R = 1$. They define the group $SO(2)$, the special orthogonal group in two dimensions, where "special" means the determinant is equal to unity. Here the matrices define the group and are said to be the fundamental representation. Some properties of these and several other groups are summarised in Sec. A.3.

A.2 Lie groups

The number of elements of a group can be finite or infinite. We will be particularly interested in *Lie groups*,[1] which have an infinite number of elements that can be labeled by one or more continuous parameters, and furthermore, the rules for the composition and inverse of elements are given by analytic functions of the parameters. Examples include the groups of Lorentz and gauge transformations.

The properties of Lie groups can be fully determined by examining those elements that differ infinitesimally from the identity. For example, suppose the elements of a Lie group $g(\boldsymbol{\theta})$ are labeled by an r-dimensional vector of real parameters $\boldsymbol{\theta} = (\theta_1, \ldots, \theta_r)$ such that $g(0) = I$. For an infinitesimal $\delta\boldsymbol{\theta}$, the group element $g(\delta\boldsymbol{\theta})$ is therefore to first order

$$g(\delta\boldsymbol{\theta}) = g(0) + \sum_{a=1}^{r} \delta\theta_a \frac{dg}{d\theta_a}\bigg|_{\theta=0} \equiv I - i\delta\theta_a T^a , \tag{A.3}$$

where

$$T^a = i\frac{dg}{d\theta_a}\bigg|_{\boldsymbol{\theta}=0} \tag{A.4}$$

with $a = 1, \ldots, r$ and summation over repeated indices implied. The T^a are called the infinitesimal generators of the group. The group element corresponding to a finite parameter value $\boldsymbol{\theta}$ can be found by expressing $\theta_a = N\delta\theta_a$ and combining the group element N times:

[1] Sophus Lie, 1842-1899, Norwegian mathematician.

$$g(\boldsymbol{\theta}) = \prod_{j=1}^{N} g(\delta\boldsymbol{\theta}) = \prod_{j=1}^{N} \left(I - i\frac{\theta_a T^a}{N} \right)^N \to e^{-i\theta_a T^a} \,, \tag{A.5}$$

where the final exponential expression results from the limit $N \to \infty$. By including the factor of i in the definition of the generators in Eqs. (A.3) and (A.4), one ensures that if the T^a are Hermitian then the group elements g are unitary.

An important aspect of Lie groups involves the commutator of the generators $[T^a, T^b] = T^a T^b - T^b T^a$. One can show that the commutator for any pair of generators of a Lie group is a linear combination of the generators themselves. The set of all the commutators,

$$[T^a, T^b] = i f^{abc} T^c \,, \tag{A.6}$$

defines a *Lie algebra*, where f^{cab} are complex numbers called the structure constants.

An example of a Lie group is given by the set of unitary transformations on a two-dimensional vector space with determinant of unity. These define the group SU(2). The group elements can be written

$$R(\boldsymbol{\alpha}) = \exp\left[-i \sum_{i=1}^{3} \alpha_i S^i \right] \,, \tag{A.7}$$

with parameters $\boldsymbol{\alpha} = (\alpha_1, \alpha_2, \alpha_3)$ and generators $\boldsymbol{S} = (S^1, S^2, S^3)$ that are related to the Pauli matrices,

$$S^1 = \tfrac{1}{2}\sigma_1 = \tfrac{1}{2}\begin{pmatrix} 0 & 1 \\ 1 & 0 \end{pmatrix} \,, \qquad S^2 = \tfrac{1}{2}\sigma_2 = \tfrac{1}{2}\begin{pmatrix} 0 & -i \\ i & 0 \end{pmatrix} \,, \qquad S^3 = \tfrac{1}{2}\sigma_3 = \tfrac{1}{2}\begin{pmatrix} 1 & 0 \\ 0 & -1 \end{pmatrix} \,. \tag{A.8}$$

The factor of i is included in Eq. (A.7) so that a unitary matrix R is obtained from the usual Hermitian spin operators $\boldsymbol{S} = \frac{1}{2}\boldsymbol{\sigma}$. The Lie algebra is the usual set of commutation relations for angular momentum,

$$[S^i, S^j] = i\epsilon_{ijk} S^k \,, \tag{A.9}$$

where ϵ_{ijk} is the fully antisymmetric Levi-Cevita symbol. One can show that the Lie algebra of SU(2) is the same as that of the group of proper rotations in a three-dimensional space SO(3).

A.3 Summary of some important groups

Some important groups in Particle Physics include:

- $O(n)$, the set of orthogonal $n \times n$ matrices;
- $SO(n)$, the set of orthogonal $n \times n$ matrices with determinant equal to unity;
- $U(n)$, the set of unitary $n \times n$ matrices;
- $SU(n)$, the set of unitary $n \times n$ matrices with determinant equal to unity.

Table A.1: Basic properties of some Lie groups used in Particle Physics. Here R is a real $n \times n$ matrix; U is a complex $n \times n$ matrix; I is the $n \times n$ identity matrix.

Group	Defining property	Parameters
$O(n)$	$R^T R = I$	$n(n-1)/2$
$SO(n)$	$R^T R = I,\ \det R = +1$	$n(n-1)/2$
$U(n)$	$U^\dagger U = I$	n^2
$SU(n)$	$U^\dagger U = I,\ \det U = 1$	$n^2 - 1$

Their properties are summarised in Table A.1.

In Particle Physics the generators of $SU(n)$, T^a with $a = 1, \ldots, n^2 - 1$, are defined so as to satisfy the normalisation condition

$$\mathrm{Tr}(T^a T^b) = \frac{1}{2}\delta^{ab} \equiv T_F \delta^{ab} \,, \tag{A.10}$$

which is to say, $T_F = \frac{1}{2}$. The "Casimir eigenvalues" (colour factors) C_F and C_A are defined by

$$(T^a T^a)_{ij} = C_F \delta_{ij} \quad \to \quad C_F = \frac{n^2 - 1}{2n} \,, \tag{A.11}$$

$$f^{acd} f^{bcd} = C_A \delta^{ab} \quad \to \quad C_A = n \,. \tag{A.12}$$

For the important case of the gauge group of QCD $SU(3)$ one has $C_F = 4/3$ and $C_A = 3$. The completeness relation for the generators of $SU(n)$ is found to be

$$(T^a)_{ij} (T^b)_{kl} = T_F \left(\delta_{il}\delta_{jk} - \frac{1}{n}\delta_{ij}\delta_{kl} \right) \,. \tag{A.13}$$

Here for convenience we give again the generators for $SU(3)$ seen in Ch. 11. They can be defined as $T^a_{ij} = \frac{1}{2}\lambda^a_{ij}$, $a = 1, \ldots, 8$, where the Gell-Mann matrices λ^a are

$$\lambda^1 = \begin{pmatrix} 0 & 1 & 0 \\ 1 & 0 & 0 \\ 0 & 0 & 0 \end{pmatrix}, \quad \lambda^2 = \begin{pmatrix} 0 & -i & 0 \\ i & 0 & 0 \\ 0 & 0 & 0 \end{pmatrix}, \quad \lambda^3 = \begin{pmatrix} 1 & 0 & 0 \\ 0 & -1 & 0 \\ 0 & 0 & 0 \end{pmatrix}, \quad \lambda^4 = \begin{pmatrix} 0 & 0 & 1 \\ 0 & 0 & 0 \\ 1 & 0 & 0 \end{pmatrix},$$

$$\lambda^5 = \begin{pmatrix} 0 & 0 & -i \\ 0 & 0 & 0 \\ i & 0 & 0 \end{pmatrix}, \quad \lambda^6 = \begin{pmatrix} 0 & 0 & 0 \\ 0 & 0 & 1 \\ 0 & 1 & 0 \end{pmatrix}, \quad \lambda^7 = \begin{pmatrix} 0 & 0 & 0 \\ 0 & 0 & -i \\ 0 & i & 0 \end{pmatrix}, \quad \lambda^8 = \frac{1}{\sqrt{3}} \begin{pmatrix} 1 & 0 & 0 \\ 0 & 1 & 0 \\ 0 & 0 & -2 \end{pmatrix}. \tag{A.14}$$

Appendix B

Introduction to Green Functions

Green functions provide a general method for solving nonhomogeneous differential equations. They can be applied to multivariable problems but for simplicity here we will only talk about the single variable case. Suppose we have a nonhomogeneous ordinary differential equation for a function $u(x)$,

$$\mathcal{L}u(x) = f(x) \,, \tag{B.1}$$

where $\mathcal{L}$ is a linear differential operator and the nonhomogeneous term $f(x)$ is a given function called the source term.

To solve Eq. (B.1), first consider the related equation

$$\mathcal{L}G(x, x') = \delta(x - x') \,, \tag{B.2}$$

where $\delta(x - x')$ is the Dirac delta function. The solution to this equation, $G(x, x')$, is called the Green function corresponding to the differential operator $\mathcal{L}$. For the Green function we will suppose homogeneous boundary conditions, i.e., it should go to zero at the ends of the interval on which x is defined (in the example below at $x \to \pm\infty$). If we can find $G(x, x')$, then using it we can write the solution to the original equation (B.1) as

$$u(x) = \int G(x, x') f(x') \, dx' \,, \tag{B.3}$$

where here and throughout this section, integrals without the limits specified are understood to be over all allowed values of the variable (e.g., $-\infty < x' < \infty$).

We can easily verify that Eq. (B.3) is a solution by substituting it into (B.1), which gives

$$\begin{aligned}
\mathcal{L}u(x) &= \mathcal{L}\int G(x,x')f(x')\,dx' \\
&= \int \mathcal{L}G(x,x')f(x')\,dx' \\
&= \int \delta(x-x')f(x')\,dx' \\
&= f(x)\,. \qquad \text{(B.4)}
\end{aligned}$$

Notice that we are integrating over x', but the operator $\mathcal{L}$ contains derivatives with respect to x. Therefore we can bring $\mathcal{L}$ inside the integral where it only operates on the Green function, not on $f(x')$. To arrive at the final line of Eq. (B.4) we used the usual sifting property of the delta function and also the fact that $\delta(x-x') = \delta(x'-x)$.

Once we have found the Green function corresponding to a given combination of operator, we can use it with any source function $f(x)$ to solve for $u(x)$. Note that because the operator $\mathcal{L}$ is linear, we are allowed to add a solution to the homogeneous equation $\mathcal{L}u_0(x) = 0$ to $u(x)$ and it will still be a solution, i.e.,

$$\mathcal{L}(u(x)+u_0(x)) = \mathcal{L}u(x) + \mathcal{L}u_0(x) = f(x)\,. \qquad \text{(B.5)}$$

Appendix C

Introduction to Complex Integration

Suppose we want to compute an integral

$$I = \int_{-\infty}^{\infty} f(x)\, dx \;, \tag{C.1}$$

where x is real and f in general can take on complex values. First, note we can be express I as

$$I = \lim_{R\to\infty} \int_{-R}^{R} f(x)\, dx \;. \tag{C.2}$$

Next, we replace the real-valued x by a complex variable $z = x + iy$. We will then form a closed contour in the complex plane, part of which runs along the real axis. The portion of the integral along the real axis can be identified with (C.2). By using the *residue theorem* (introduced below) we can relate the desired integral (C.1) to properties of the function f (its *residues*) that can usually be found easily.

More concretely, consider the contour C in the complex z plane shown on the left of Fig. C.1. It proceeds from $-R$ to R along the real axis and then connects back to $-R$ by following a circular arc in the upper half-plane of radius R. By default the orientation of the contour is anticlockwise, as indicated by the arrow.

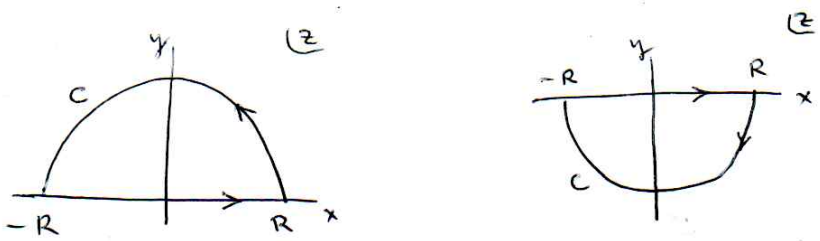

Figure C.1: Integration contours that close in the upper half (left) and the lower half (right) of the complex z plane.

Suppose the function $f(z)$ diverges at points z_j, $j = 1, 2, \ldots$ in the complex plane; these divergent points are called *poles*. According to the *residue theorem* (see, e.g., Ref. [78]), an integral around a closed contour in the complex plane is equal to $2\pi i$ times the sum of the *residues* of the poles that are inside the contour. That is,

$$I_C = \int_C f(z)\, dz = 2\pi i \sum_j \mathrm{Res}(f, z_j) \; . \tag{C.3}$$

It is important to note that the sum only includes poles that are inside the contour C. If, for example, C contains no poles, then the integral is zero. Suppose the function $f(z)$ can be written in the form

$$f(z) = \frac{g(z)}{h(z)} \; , \tag{C.4}$$

where $g(z)$ is finite but $h(z)$ has zeros at the points z_j, corresponding to the poles of $f(z)$. In this case the formula for the residue is

$$\mathrm{Res}(f, z_j) = \frac{g(z_j)}{h'(z_j)} \; . \tag{C.5}$$

For example, $f(z)$ is said to have a *simple pole* if

$$f(z) = \frac{g(z_j)}{z - z_j} \; , \tag{C.6}$$

and in this case one finds $\mathrm{Res}(f, z_j) = g(z_j)$. The functions $g(z)$ and $h(z)$ must satisfy certain properties for the formulas above to apply; more information can be found in standard references such as [78].

The method of contour integration is useful provided the integral along the part of the path in the upper half-plane goes to zero for $R \to \infty$. Suppose, for example, $f(z)$ contains an exponential term like e^{iz}. As $y = \mathrm{Im}(z)$ is positive in the upper half-plane, terms like $e^{i(x+iy)}$ go as e^{-y} and are exponentially suppressed. If, however, $f(z)$ contains a term like e^{-iz}, then this becomes large in the upper half-plane but small in the lower half-plane, as shown for the contour on the right of Fig. C.1. In this case the orientation of the contour is opposite that the one that closes in the upper half-plane, and the resulting integral around C acquires a minus sign.

The precise conditions under which the arc-shaped portion of the integral goes to zero are discussed in standard references such as [78]. Provided we can neglect this portion of the integral, we can find our final answer as

$$\int_{-\infty}^{\infty} f(x)\, dx = 2\pi i \sum_j \mathrm{Res}(f, z_j) \; , \tag{C.7}$$

where the sum only includes residues of poles that are inside the contour C.

Appendix D

Feynman Rules for the Standard Model

Feynman rules for $-i\mathcal{M}$

External particles:

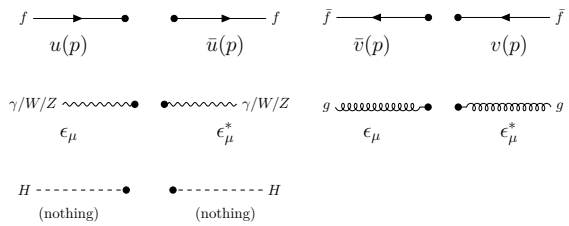

Propagators:

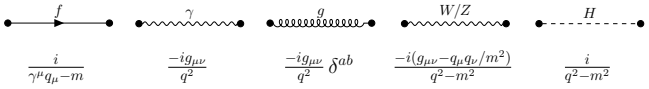

Three-point vertices:

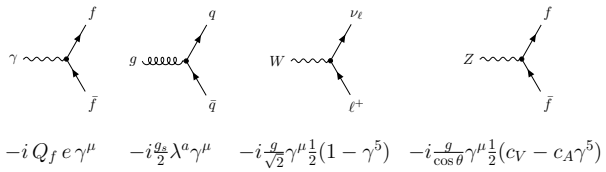

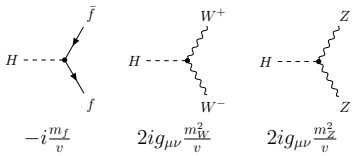

Bibliography

[1] Glen D. Cowan and Veronique Boisvert, *Lecture Notes on Particle Physics*, RHUL Physics (2023).

[2] Peter Schmüser, *Feynman-Graphen und Eichtheorien für Experimentalhysiker*, 2nd ed., Springer, 1995.

[3] Mark, Thomson, *Modern Particle Physics*, CUP, 2013.

[4] Ian J.R. Aitchison and Anthony J.G. Hey, *Gauge Theories in Particle Physics*, 4th edition, CRC Press, 2021; `https://doi.org/10.1201/9781315275253` (Open Access).

[5] Richard Feynman, Robert B. Leighton, Matthew Sands, *The Feynman Lectures on Physics*, Addison-Wesley, 1964; `feynmanlectures.caltech.edu`.

[6] John David Jackson, *Classical Electrodynamics*, 3rd edition, Wiley, 1999.

[7] Paul Adrien Maurice Dirac, *The Quantum Theory of the Electron*, Proceedings of the Royal Society A, Volume 117, Issue 778 (1928).

[8] Herbert Goldstein, Charles Poole and John Safko, *Classical Mechanics*, 3rd edition, Addison Wesley, 2002.

[9] G.E. Uhlenbeck and S. Goudsmit, *Electron Spin and Proton Spin in the Hydrogen and Hydrogen-Like Atomic Systems*, Naturwissenschaften 13(47) (1925) 953.

[10] X. Fan, T.G. Myers, B.A.D. Sukra, and G. Gabrielse, *Measurement of the Electron Magnetic Moment*, Phys. Rev. Letters 130, 071801 (2023).

[11] S.S. Schweber, *An Introduction to Relativistic Quantum Field Theory*, Row, Peterson and Company, New York, 1961.

[12] E.C.G. Stückelberg, *La Mécanique du point matériel en théorie de relativité et en théorie des quanta*, Helv. Phys. Acta 15 (1942), pp. 23-37.

[13] R.P. Feynman, *The Theory of Positrons*, Phys. Rev. 76, 749 (1949).

[14] R.P. Feynman, *Space-Time Approach to Quantum Electrodynamics*, Phys. Rev. 76, 769 (1949).

[15] F.J. Dyson, *The Radiation Theories of Tomonaga, Schwinger, and Feynman*, Phys. Rev. 75, 486 (1949).

[16] S. Bethke and A. Wagner, *The JADE experiment at the PETRA e^+e^- collider: history, achievements and revival*, Eur. Phys. J. H (2022) 47:16; e-print: arxiv:2208.11076.

[17] Wolfgang Pauli, letter to Lise Meitner, 4 December 1930, Pauli Archive, CERN, `https://cds.cern.ch/record/83282`.

[18] Enrico Fermi, *Versuch einer Theorie der β-Strahlen. I*, Zeitschrift für Physik A, 88, 3–4 (1934) 161–177.

[19] S. Navas et al. (Particle Data Group), Phys. Rev. D 110, 030001 (2024).

[20] C.S. Wu *et al.*, Phys. Rev. **105** (1957) 1413.

[21] T.D. Lee and C.N. Yang, Phys. Rev. **104** (1956) 254.

[22] R.P. Feynman and M. Gell-Mann, *Theory of the Fermi Interaction*, Phys. Rev. 109 (1958) 193.

[23] E.C.G. Sudarshan and R.E. Marshak, *Chirality Invariance and the Universal Fermi Interaction*, Phys. Rev. 109 (1958) 1860.

[24] Murray Gell-Mann, *A Schematic Model of Baryons and Mesons*, Physics Letters 8 (1964) 214–215.

[25] George Zweig, *An SU(3) Model for Strong Interaction Symmetry and its Breaking*, CERN Report CERN-TH-401 (1964).

[26] M. Kobayashi and T. Maskawa, Prog. Theor. Phys. **49** (1973) 652.

[27] L. Wolfenstein, Phys. Rev. Let. **51** (1983) 1945.

[28] J. Steinberger, *Experiments with High-Energy Neutrino Beams*, 1988 Nobel Lecture, Rev. Mod. Phys. 61, 3 (1989).

[29] W.-D. Schlatter, *Highlights from High Energy Neutrino Experiments at CERN*, Adv. Ser. Dir. High Energy Phys. 23 (2015) 185-203.

[30] C.N. Yang and R.L. Mills, *Conservation of Isotopic Spin and Isotopic Gauge Invariance*, Phys. Rev. 96, 1 (1954) 191–195.

[31] G. 't Hooft, *Renormalization of massless Yang-Mills fields*, Nucl. Phys. B 33 (1971) 173.

[32] F.J. Hasert *et al.*, Phys. Lett. **46B** (1973) 138.

[33] L. Hoddeson, L Brown, M. Riordan and M. Dresden (eds.), *The Rise of the Standard Model*, Cambridge University Press, 1997.

[34] G. Arnison *et al.* (UA1 Collaboration), Phys. Lett. **122B** (1983) 103.

[35] G. Arnison *et al.* (UA1 Collaboration), Phys. Lett. **126B** (1983) 398.

[36] Robert Cahn and Gerson Goldhaber, *The Experimental Foundations of Particle Physics*, Cambridge University Press, 2009.

[37] The ALEPH, DELPHI, L3 and OPAL Collaborations and the LEP Electroweak Working Group, *Electroweak measurements in electron–positron collisions at W-boson-pair energies at LEP*, Phys. Rept., vol. 532, pp. 119–244 (2013).

[38] Michael E. Peskin and Daniel V. Schroeder, *An Introduction To Quantum Field Theory*, CRC Press, 1995.

[39] Anthony Zee, *Quantum Field Theory in a Nutshell*, 2nd edition, Princeton University Press, 2010.

[40] J. de Blas et al., *Global analysis of electroweak data in the Standard Model*, Phys. Rev. D 106 (2022) 033003; e-print arXiv:2112.07274.

[41] G. Aad et al. (ATLAS Collaboration), *Measurement of the W-boson mass and width with the ATLAS detector using proton-proton collisions at* $\sqrt{s} = 7$ *TeV*, accepted by EPJC, arXiv:2403.15085 (2024).

[42] P.W. Anderson, *Plasmons, Gauge Invariance, and Mass*, Physical Review, 130(1), 439–442 (1963), DOI: 10.1103/PhysRev.130.439.

[43] F. Englert and R. Brout, *Broken Symmetry and the Mass of Gauge Vector Mesons*, Physical Review Letters, 13(9), 321–323 (1964), DOI: 10.1103/PhysRevLett.13.321.

[44] Peter Higgs, *Broken Symmetries and the Masses of Gauge Bosons*, Physical Review Letters, 13(16), 508–509 (1964), DOI: 10.1103/PhysRevLett.13.508.

[45] G.S. Guralnik, C.R. Hagen and T.W.B. Kibble, *Global Conservation Laws and Massless Particles*, Physical Review Letters, 13(20), 585–587 (1964). DOI: 10.1103/PhysRevLett.13.585.

[46] S. Weinberg, *A Model of Leptons*, Physical Review Letters, 19(21), 1264–1266 (1967), DOI: 10.1103/PhysRevLett.19.1264.

[47] G. Aad et al. (ATLAS Collaboration), *Observation of a new particle in the search for the Standard Model Higgs boson with the ATLAS detector at the LHC* Physics Letters B, 716(1), 1–29 (2012), DOI: 10.1016/j.physletb.2012.08.020.

[48] S. Chatrchyan et al. (CMS Collaboration), *Observation of a new boson at a mass of 125 GeV with the CMS experiment at the LHC*, Physics Letters B, 716(1), 30–61 (2012), DOI: 10.1016/j.physletb.2012.08.021

[49] S. Dittmaier et al. (LHC Higgs Cross Section Working Group), *Handbook of LHC Higgs Cross Sections: 1. Inclusive Observables*, CERN-2011-002, arXiv:1101.0593 (2011).

[50] G. Aad et al. (ATLAS Collaboration), *Evidence of off-shell Higgs boson production from ZZ leptonic decay channels and constraints on its total width with the ATLAS detector*, Physics Letters B Volume 846, 10 November 2023, 138223.

[51] G. Aad et al. (ATLAS Collaboration), *A detailed map of Higgs boson interactions by the ATLAS experiment ten years after the discovery*, Nature volume 607, pages52–59 (2022).

[52] O.W. Greenberg, Phys. Rev Lett. **13** (1964) 585.

[53] R.K. Ellis, W.J. Stirling and B.R. Webber, *QCD and Collider Physics*, Cambridge University Press, 1996.

[54] Harald Fritzsch and Murray Gell-Mann, *Current Algebra: Quarks and What Else?*, eConfC720906V2:135-165,1972; e-print: arXiv:hep-ph/0208010.

[55] S.D. Drell, D.J. Levy, T.-M. Yan, *Theory of Deep-Inelastic Lepton-Nucleon Scattering and Lepton-Pair Annihilation Processes I*, Phys. Rev. 187, 2159 (1969).

[56] J.D. Bjorken and S.J. Brodsky, *Statistical Model for Electron-Positron Annihilation into Hadrons*, Phys. Rev. D 1, 1416 (1970).

[57] G. Hanson et al., *Evidence for Jet Structure in Hadron Production by e^+e^- Annihilation*, Phys. Rev. Lett. 35, 1609 (1975).

[58] R. Barate *et al.* (ALEPH Collaboration), Physics Reports **294** (1998) 1.

[59] J. Ellis, M.K. Gaillard, G.G. Ross, *Search for Gluons in e^+e^- Annihilation*, Nucl. Phys. B 111, 253 (1976).

[60] P. Söding, *On the discovery of the gluon*, Eur. Phys. J. H 35, 3–28 (2010).

[61] D. Decamp *et al.* (ALEPH Collaboration), Phys. Lett. B **284** (1992) 163.

[62] S.G. Gorishny, A. Kataev and S.A. Larin, Phys. Lett. **B259** (1991) 114; L.R. Surguladze and M.A. Samuel, Phys. Rev. Lett. **66** (1991) 560.

[63] Gïther Dissertori, Ian G. Knowles, and Michael Schmelling, *Quantum Chromodynamics: High Energy Experiments and Theory*, Oxford University Press, 2009.

[64] Vernon D. Barger and Roger J.N. Phillips, *Collider Physics*, Westview Press, 1991.

[65] Website of the ALEPH Collaboration, ALEPH Event Displays, `https://aleph.web.cern.ch/aleph/aleph/Public.html`.

[66] R.P. Feynman, "The Behavior of Hadron Collisions at Extreme Energies", in High Energy Collisions: Third International Conference at Stony Brook, N.Y. Gordon & Breach, 1969, pp. 237–249.

[67] Web site of the H1 experiment, `www-h1.desy.de`.

[68] John F. Martin, *Report from the ZEUS Collaboration at HERA*, in Persis Drell and David Rubin (eds.), *Proceedings of the XVI International Symposium on Lepton and Photon Interactions*, AIP, New York, 1994.

[69] J. Pumplin et al. (CTEQ Collaboration), *New Generation of Parton Distributions with Uncertainties from Global QCD Analysis*, JHEP 0207:012,2002.

[70] The ATLAS Collaboration, ATLAS events at 13 TeV - 2016 conferences, CERN Document Server, `https://cds.cern.ch/record/2202818`

[71] S. Catani, Y. L. Dokshitzer, M. H. Seymour and B. R. Webber, Nucl. Phys. B 406 (1993) 187.

[72] Y. L. Dokshitzer, G. D. Leder, S. Moretti and B. R. Webber, JHEP 9708, 001 (1997).

[73] Matteo Cacciari, Gavin P. Salam, Gregory Soyez, *The anti-k_t jet clustering algorithm*, JHEP 0804:063,2008; e-print arXiv:0802.1189.

[74] M. Aaboud et al. (ATLAS Collaboration), *Measurement of inclusive jet and dijet cross-sections in proton-proton collisions at $\sqrt{s} = 13$ TeV with the ATLAS detector*, JHEP 05 (2018) 195; e-print arXiv:1711.02692.

[75] M. Aaboud et al. (ATLAS Collaboration), *Measurement of the Drell-Yan triple-differential cross section in pp collisions at $\sqrt{s} = 8$ TeV*, JHEP 12 (2017) 059.

[76] M. Aaboud et al. (ATLAS Collaboration), *Search for new high-mass phenomena in the dilepton final state using 36 fb^{-1} of proton-proton collision data at $\sqrt{s} = 13$ TeV with the ATLAS detector*, JHEP 10 (2017) 182.

[77] Glen Cowan, *Lecture Notes on Mathematical Methods*, RHUL Physics, 2016.

[78] K.F. Riley, M.P. Hobson and S.J. Bence, *Mathematical Methods for Physics and Engineering*, Cambridge University Press, 2006.

[79] Michael E. Peskin, Concepts of Elementary Particle Physics, OUP, 2019.